

Thesis submitted for the degree of  
Doctor of Philosophy  
at the University of Leicester

by

**Yiyang Sun BSc MRes (China)**

**Biocentre**

**Department of Biochemistry**

**University of Leicester**

Oct 2007

UMI Number: U492223

All rights reserved

INFORMATION TO ALL USERS

The quality of this reproduction is dependent upon the quality of the copy submitted.

In the unlikely event that the author did not send a complete manuscript and there are missing pages, these will be noted. Also, if material had to be removed, a note will indicate the deletion.



UMI U492223

Published by ProQuest LLC 2013. Copyright in the Dissertation held by the Author.  
Microform Edition © ProQuest LLC.

All rights reserved. This work is protected against  
unauthorized copying under Title 17, United States Code.



ProQuest LLC  
789 East Eisenhower Parkway  
P.O. Box 1346  
Ann Arbor, MI 48106-1346

## ***ABSTRACT***

### **STATs signalling in human bladder cancer: Potential chemopreventive role for indoles**

**Yiyang Sun**

While the transcription factors, signal transducers and activators of transcription (STATs) have been implicated in the development of cancer in a variety of tissues, no such information exists for bladder cancer. In patient tissues, STAT1, STAT3 and STAT5 were observed in normal bladder epithelium, while expression of phosphorylated proteins was essentially absent. In contrast, phospho-STAT3 in superficial tumours and phospho-STAT1, 3 and 5 in muscle invasive tumours were present. Thus their increased expression, activation and nuclear localisation, may be associated with bladder tumour progression. Three epithelial bladder cancer lines (RT112, RT4, HT1376) had constitutive phospho-STAT5, while three mesenchymal lines (J82, T24, UMUC3) had activated STAT3. Constitutive expression and activation of STATs was EGF-independent. Specific knockdown of STAT3 in J82 cells increased STAT1 expression and phosphorylation. STAT1 and/or STAT3 knockdown led to inhibition of cell-matrix adhesion to fibronectin or collagen and suppression of cell migration. The dietary molecules, Indole-3-carbinol (I3C) ( $\geq 100\mu\text{M}$ ) or 3, 3'-diindolylmethane (DIM) ( $\geq 50\mu\text{M}$ ) induced apoptosis in J82 and RT112 cells by 48 hours. DIM-induced apoptosis in J82 cells was accompanied by downregulation of STAT1, 5a and 5b and inhibition of phospho-STAT1 and phospho-STAT3. In RT112 cells, DIM inhibited STAT5a, 5b and phospho-STAT5, but had no effect on STAT3. DIM ( $\geq 10\mu\text{M}$ ) inhibited J82 cell adhesion to fibronectin and collagen, accompanied by decreased N-cadherin, P-cadherin and  $\beta$ -catenin expression. Furthermore, DIM ( $1\mu\text{M}$ ) was able to significantly decrease cell adhesion following STAT1 and/or STAT3 knockdown, suggesting inhibition of cell adhesion by DIM may involve the STAT pathway. This investigation *in vivo* and *in vitro* has provided an indication that phosphorylated STATs may be a potential marker of invasiveness in human bladder cancer. Elucidation of the effects of indoles and DIM in particular, at a molecular level has given an insight as to how these dietary agents may be useful in the therapy and/or prevention of bladder tumours.

## ***ACKNOWLEDGEMENTS***

First of all, I would like to express my gratitude to my supervisor Professor Maggie Manson, for her constant encouragement, support, and invaluable suggestions throughout this study, and for financial support from MRC and ORSAS to make my PhD study possible in UK. I would also like to thank my co-supervisor Dr Marina Kriajevska for her continuous guidance and excellent advice which has made a deep impression on me.

I am grateful to Dr Mai-Kim Cheng for her contribution to one part of this project, and Richard and Jenny Edwards who prepared tissue sections for this study. I am thankful to Mr Leyshon Griffiths for his assistance in the grading of muscle-invasive tissue sections, and also would like to thank Professor Kilian Mellon for reviewing part of my thesis and providing valuable feedback. My sincere thanks go to my committee member, Dr. Catrin Pritchard for her time and suggestions during the last two and half years, and Dr. Katherine Clark who offered her generous help and support with the adhesion studies.

A special thanks goes to Xiaoming, Hailan, Lorenza, Hasan and Richard V for their friendship and help, which gave me the feeling of being at home and taught me to be 'brave'. I am thankful to Mr Jakob Mejlvang for providing A431/sip model and useful suggestions. I would also like to thank everyone in the Biocentre and the Hodgkin Building who shared experiences and knowledge during the time of study.

Lastly, I am deeply indebted to my husband for his constant support, understanding and patience during my study in Leicester.

**I wish to dedicate this thesis to my beloved father and mother, and greatly thank them for all that they have done.**

# CONTENTS

<b>ABSTRACT</b>	<b>I</b>
<b>ACKNOWLEDGEMENT</b>	<b>II</b>
<b>LIST OF FIGURES</b>	<b>VIII</b>
<b>LIST OF TABLES</b>	<b>XIII</b>
<b>ABBREVIATIONS</b>	<b>XV</b>
<b>CHAPTER 1 INTRODUCTION</b>	<b>1</b>
<b>1.1 Bladder cancer</b>	<b>2</b>
<b>1.2 Signal Transducers and Activators of Transcription (STATs)</b>	<b>7</b>
<i>1.2.1 The STAT family of proteins</i>	<i>7</i>
<i>1.2.2 Structures of STATs</i>	<i>7</i>
<i>1.2.3 Activation mechanisms of STATs</i>	<i>8</i>
<i>1.2.4 Normal physiological role of STATs</i>	<i>10</i>
<i>1.2.5 STAT activation in oncogenesis</i>	<i>12</i>
<i>1.2.6 Role of STAT signalling in oncogenesis</i>	<i>15</i>
<i>1.2.7 Regulation of STAT signalling</i>	<i>16</i>
<b>1.3 STATs in bladder cancer</b>	<b>18</b>
<b>1.4 Cell cycle</b>	<b>18</b>
<b>1.5 Apoptosis</b>	<b>22</b>
<b>1.6 Metastasis</b>	<b>25</b>
<b>1.7 Cancer chemoprevention</b>	<b>31</b>
<b>1.8 Indoles</b>	<b>34</b>
<i>1.8.1 Chemistry of I3C and DIM</i>	<i>34</i>
<i>1.8.2 Indoles and chemoprevention</i>	<i>35</i>
<i>1.8.3 Dietary agents and bladder cancer</i>	<i>41</i>
<i>1.8.4 Bioavailability of Indoles</i>	<i>42</i>
<b>AIMS</b>	<b>43</b>

<b>CHAPTER 2 MATERIALS AND METHODS</b>	<b>44</b>
<b>2.1 Materials</b>	<b>45</b>
<b>2.1.1 Chemicals</b>	<b>45</b>
<b>2.1.2 Antibodies</b>	<b>46</b>
<b>2.1.3 Plasmids and oligos</b>	<b>47</b>
<b>2.1.4 Suppliers addresses</b>	<b>47</b>
<b>2.2 Buffers</b>	<b>48</b>
<b>2.3 Cell lines</b>	<b>51</b>
<b>2.3.1 Maintenance of cell lines</b>	<b>52</b>
<b>2.3.1.1 Passaging of cells</b>	<b>52</b>
<b>2.3.2 Treatment of cells</b>	<b>52</b>
<b>2.3.2.1 Treatment of cells with serum starvation or EGF/serum stimulation</b>	<b>52</b>
<b>2.3.2.2 Treatment of cells with indoles or inhibitors</b>	<b>52</b>
<b>2.4 Preparation of cell fractions</b>	<b>53</b>
<b>2.4.1 Whole cell lysates</b>	<b>53</b>
<b>2.4.2 Nuclear protein</b>	<b>53</b>
<b>2.4.3 BCA protein assay</b>	<b>53</b>
<b>2.5 Western blotting</b>	<b>54</b>
<b>2.5.1 Antibody binding</b>	<b>55</b>
<b>2.5.2 Immunoprecipitation of STAT proteins</b>	<b>57</b>
<b>2.6 Assessment of cell proliferation and cell death</b>	<b>57</b>
<b>2.6.1 Cell cycle analysis</b>	<b>57</b>
<b>2.6.2 Annexin V staining for apoptosis</b>	<b>58</b>
<b>2.6.3 Hoechst 33258 staining for apoptosis</b>	<b>58</b>
<b>2.6.4 Caspase3/7 assay</b>	<b>59</b>
<b>2.7 Assessment of cell motility</b>	<b>60</b>
<b>2.7.1 Adhesion assay</b>	<b>60</b>
<b>2.7.2 Treatment of cells for adhesion assay</b>	<b>60</b>
<b>2.7.3 Transwell migration assay</b>	<b>60</b>
<b>2.8 Immunohistochemistry</b>	<b>61</b>
<b>2.8.1 Ethical approval</b>	<b>61</b>
<b>2.8.2 Tissue preparation and staining</b>	<b>61</b>
<b>2.9 Immunocytochemistry</b>	<b>63</b>

<b>2.10 Preparation and transfection of plasmid DNA and siRNAs</b>	<b>64</b>
<b>2.10.1 Plasmids and siRNAs</b>	<b>64</b>
<b>2.10.2 Transformation of competent bacteria</b>	<b>65</b>
<b>2.10.3 Preparation of plasmid DNA</b>	<b>66</b>
<b>2.10.4 Transient transfection of plasmid DNA and siRNAs into cells</b>	<b>67</b>
<b>2.10.4.1 Electroporation of J82 cells</b>	<b>67</b>
<b>2.10.4.2 Nucleofection of RT112 cells</b>	<b>67</b>
<b>2.10.5 Reporter gene assays</b>	<b>67</b>
<b>2.10.5.1 Measurement of <math>\beta</math>-galactosidase activity</b>	<b>67</b>
<b>2.10.5.2 Measurement of luciferase activity</b>	<b>68</b>
<b>2.11 Statistical analysis</b>	<b>68</b>

## **CHAPTER 3 EXPRESSION OF STATS AND CADHERINS**

### **IN THE HUMAN BLADDER TISSUES**

**69**

<b>3.1 Human bladder specimens</b>	<b>72</b>
<b>3.2 Determination of STATs status in normal bladder epithelium</b>	<b>72</b>
<b>3.3 Determination of STATs status in superficial bladder tumours</b>	<b>75</b>
<b>3.4 Determination of STATs status in muscle invasive bladder tumours</b>	<b>81</b>
<b>3.5 Relationship between STATs expression and stage of bladder tumours</b>	<b>90</b>
<b>3.6 Determination of cadherin status in superficial bladder tumours</b>	<b>92</b>
<b>3.7 Determination of cadherin status in muscle invasive bladder tumours</b>	<b>96</b>
<b>3.8 Relationship between cadherins expression and stage of bladder tumours</b>	<b>99</b>
<b>3.9 Relationship between STATs and cadherins expression in bladder tumours</b>	<b>100</b>

## **CHAPTER 4 STATS SIGNALLING IN BLADDER CANCER CELLS**

**110**

<b>4.1 Determination of STATs status in a panel of human bladder cell lines</b>	<b>113</b>
<b>4.1.1 Basal levels of total STAT1 and STAT3 under normal growth condition</b>	<b>113</b>
<b>4.1.2 Effect of serum starvation on STAT1 and STAT3 protein levels</b>	<b>113</b>
<b>4.1.3 Effect of EGF stimulation on STAT1, 3 and 5 protein expression and activity</b>	<b>115</b>
<b>4.2 Localisation of STATs in bladder cancer cells</b>	<b>120</b>
<b>4.3 Transcriptional activity of STATs</b>	<b>123</b>
<b>4.4 Inhibition of STATs activity</b>	<b>125</b>

4.4.1 <i>Effect of AG490 on STATs phosphorylation and cell cycle</i>	125
4.4.2 <i>Effect of piceatannol on STAT and cadherin expression</i>	132
4.4.3 <i>Effect of PP2 on STATs phosphorylation</i>	133
4.5 <b>Inhibition of STAT expression in RT112 and J82 cells using siRNAs to STATs</b>	137
4.5.1 <i>Establishment of RT112 nucleofection</i>	137
4.5.2 <i>Establishment of STAT transfection in J82 cells</i>	139
4.5.3 <i>Effect of individual STATs knockdown on other STATs protein levels and phosphorylation status in J82 cells</i>	139
4.6 <b>Effect of STAT1 and/or STAT3 knockdown on cell adhesion and migration in J82 cells</b>	144
4.6.1 <i>Effect of STAT1 and/or STAT3 knockdown on cell adhesion in J82 cells</i>	146
4.6.2 <i>Effect of STAT1 and/or STAT3 knockdown on migration</i>	148
4.7 <b>STATs phosphorylation status in A431/sip model of EMT</b>	149
<b>CHAPTER 5 EFFECTS OF INDOLES ON THE STAT</b>	
<b>SIGNALLING PATHWAY</b>	<b>157</b>
5.1 <b>Effect of indoles on STATs protein levels and phosphorylation status</b>	160
5.1.1 <i>Effect of I3C on STAT3 protein levels and phosphorylation status</i>	160
5.1.2 <i>Effect of DIM on STATs protein levels and phosphorylation status</i>	161
5.2 <b>Effect of indoles on ERK and Akt protein levels and phosphorylation status in J82 cells</b>	165
5.3 <b>Effect of indoles on cell proliferation and apoptosis</b>	169
5.3.1 <i>Cell cycle analysis following treatment with DIM</i>	169
5.3.2 <i>Assessment of apoptosis in response to indoles</i>	173
5.3.2.1 <i>Assessment of apoptosis by annexin V staining in response to indoles</i>	173
5.3.2.2 <i>Assessment of apoptosis by caspase3/7 activity in response to DIM</i>	178
5.3.2.3 <i>Assessment of apoptosis by PARP cleavage in response to DIM</i>	179
5.4 <b>Effect of DIM on cell adhesion in J82 cells</b>	181
5.4.1 <i>Effect on adhesion molecules in J82 cells following low concentration DIM treatment</i>	181
5.4.2 <i>Effect on cell adhesion in J82 cells following DIM treatment</i>	184

<i>5.4.3 Effect on cell adhesion in STAT1 and/or 3 knockdown J82 cells following DIM treatment</i>	189
<b>CHAPTER 6 GENERAL DISCUSSION</b>	<b>197</b>
<b>REFERENCES</b>	<b>202</b>
<b>APPENDICES</b>	<b>240</b>
<b>Appendix 1 Immunohistochemistry of bladder cancers</b>	<b>241</b>
<b>Appendix 2 Meeting presentation</b>	<b>250</b>

## **LIST OF FIGURES**

<b>1.1 Diagram showing the relationship between the location and depth of the tumour and the stage</b>	<b>3</b>
<b>1.2 Model for bladder cancer progression and showing important genetic events associated with tumourigenesis</b>	<b>4</b>
<b>1.3 Generic structures of STAT molecules</b>	<b>8</b>
<b>1.4 Activation mechanisms and downstream targets of STAT proteins</b>	<b>10</b>
<b>1.5 Stages of the cell cycle</b>	<b>21</b>
<b>1.6 Induction of apoptosis by mitochondrial and death receptor pathways</b>	<b>23</b>
<b>1.7 The main steps in the formation of metastasis</b>	<b>26</b>
<b>1.8 Model for cell migration and the main molecules involved</b>	<b>28</b>
<b>1.9 Chemoprevention during carcinogenesis</b>	<b>32</b>
<b>1.10 Molecular targets of dietary agents</b>	<b>33</b>
<b>1.11 Chemical structure of glucobrassicins</b>	<b>34</b>
<b>1.12 Chemical structures of I3C and its acid condensation product DIM</b>	<b>35</b>
<b>2.1 Cleavage of the non-fluorescent caspase substrate Z-DEVD-R110 by caspase-3/7 to create the fluorescent rhodamin 110</b>	<b>59</b>
<b>2.2 Plasmid maps</b>	<b>65</b>
<b>3.1 Expression of STAT (1, 3, 5) in normal bladder epithelium</b>	<b>74</b>
<b>3.2 Expression of STAT3 and pSTAT3 in superficial bladder tumours</b>	<b>76</b>
<b>3.3 Expression of STAT5b in superficial bladder tumours</b>	<b>78</b>
<b>3.4 Expression of STAT5a and pSTAT5 in superficial bladder tumours</b>	<b>79</b>
<b>3.5 Expression of STAT1 and pSTAT1 in superficial bladder tumours</b>	<b>80</b>
<b>3.6 Expression of STAT3 in muscle invasive bladder tumours</b>	<b>82</b>
<b>3.7 Expression of pSTAT3 in muscle invasive bladder tumours</b>	<b>83-84</b>
<b>3.8 Expression of STAT5 in muscle invasive bladder tumours</b>	<b>86</b>
<b>3.9 Expression of pSTAT5 in muscle invasive bladder tumours</b>	<b>87</b>
<b>3.10 Expression of STAT1 in muscle invasive bladder tumours</b>	<b>89</b>
<b>3.11 Expression of pSTAT1 in muscle invasive bladder tumours</b>	<b>90</b>

<b>3.12 Expression of E-cadherin in superficial bladder tumours</b>	<b>93</b>
<b>3.13 Expression of N-cadherin in superficial bladder tumours</b>	<b>94</b>
<b>3.14 Expression of P-cadherin in superficial bladder tumours</b>	<b>95</b>
<b>3.15 Expression of E-cadherin in muscle invasive bladder tumours</b>	<b>97</b>
<b>3.16 Expression of N-cadherin in muscle invasive bladder tumours</b>	<b>98</b>
<b>3.17 Expression of P-cadherin in muscle invasive bladder tumours</b>	<b>99</b>
<b>3.18 Expression of E-cadherin and pSTAT (3 and 5) in superficial bladder tumours</b>	<b>101</b>
<b>3.19 Expression of E and N-cadherin and pSTAT (3 and 5) in muscle invasive bladder tumours</b>	<b>103</b>
<b>3.20 Expression of E and N-cadherin and pSTAT (3 and 5) in muscle invasive bladder tumours</b>	<b>104</b>
<b>4.1 Effect of serum starvation and re-stimulation on total STAT1 and STAT3 expression levels in 6 bladder cell lines</b>	<b>114</b>
<b>4.2 Effect of EGF stimulation on STAT1 and STAT3 phosphorylation status in A431 cells</b>	<b>115</b>
<b>4.3 Effect of EGF stimulation on EGFR expression and phosphorylation in bladder cancer cells</b>	<b>115</b>
<b>4.4 Effects of serum starvation or EGF stimulation on total and phosphorylated STAT1 in bladder cell lines</b>	<b>117</b>
<b>4.5 Effects of serum starvation or EGF stimulation on total and phosphorylated STAT3 in bladder cell lines</b>	<b>118</b>
<b>4.6 Effects of serum starvation or EGF stimulation on total and phosphorylated STAT5 in bladder cell lines</b>	<b>119</b>
<b>4.7 Western blots showing STATs localisation in J82 and RT112 cell lines</b>	<b>120</b>
<b>4.8 Determination of STATs localisation in J82 cells by immunofluorescence</b>	<b>121</b>
<b>4.9 Determination of STATs localisation in RT112 cells by immunofluorescence</b>	<b>122</b>
<b>4.10 Correlation of pGRR5-Luc reporter with luciferase activity</b>	<b>123</b>
<b>4.11 Effect of STAT3C on STAT transactivation in J82 cells</b>	<b>124</b>
<b>4.12 Effect of STAT3C on STAT transactivation in RT112 cells</b>	<b>124</b>
<b>4.13 Effect of STAT3C on STAT transactivation in A431/sip cells</b>	<b>125</b>

<b>4.14 Effect of AG490 on phosphorylated STAT3 levels in J82 cells</b>	<b>126</b>
<b>4.15a Effect of AG490 upon cell cycle in J82 cells</b>	<b>127</b>
<b>4.15b Flow cytometric analysis of J82 cells following AG490 treatment</b>	<b>128</b>
<b>4.16 Effect of AG490 on total and phosphorylated STAT5 levels in RT112 cells</b>	<b>129</b>
<b>4.17a Effect of AG490 upon cell cycle in RT112 cells</b>	<b>130</b>
<b>4.17b Flow cytometric analysis of RT112 cells following AG490 treatment</b>	<b>131</b>
<b>4.18 Effect of piceatannol alone or with AG490 on STAT5 protein levels in RT112 cells</b>	<b>132</b>
<b>4.19 Effect of piceatannol on N-cadherin expression in J82 cells</b>	<b>133</b>
<b>4.20 Effect of PP2 on STATs levels in J82 cells</b>	<b>134</b>
<b>4.21 Effect of PP2 on cell aggregation and morphological appearance in J82 cells</b>	<b>135</b>
<b>4.22 Effect of PP2 on total and phosphorylated STAT5 levels in RT112 cells</b>	<b>136</b>
<b>4.23 GFP fluorescence showing efficiency of RT112 nucleofection</b>	<b>138</b>
<b>4.24 Efficiency of STAT3 knockdown in RT112 cells</b>	<b>138</b>
<b>4.25 Efficiency of STAT5 knockdown in RT112 cells</b>	<b>139</b>
<b>4.26 Efficiency of STAT3 knockdown in J82 cells</b>	<b>140</b>
<b>4.27a Efficiency of STATs knockdown in J82 cells</b>	<b>141</b>
<b>4.27b Histograms showing efficiency of STATs knockdown in J82 cells</b>	<b>142</b>
<b>4.28 Effect of siRNAs on STAT transactivation in J82 cells</b>	<b>143</b>
<b>4.29 Immunoprecipitation showing complex formation among STAT1, 3 and 5 in J82 cells</b>	<b>143</b>
<b>4.30 Effect on cyclin D1, caspase 3 and survivin expression in STATs knockdown J82 cells</b>	<b>144</b>
<b>4.31 Efficiency of STAT1 and/or STAT3 knockdown in J82 cells</b>	<b>145</b>
<b>4.32 Quantitation of J82 cell adhesion to fibronectin or collagen I</b>	<b>146</b>
<b>4.33 Effect on J82 cell adhesion in the presence of anti-<math>\beta</math>1-integrin antibody</b>	<b>147</b>
<b>4.34 Effect on cell adhesion in STAT1 and/or STAT3 knockdown J82 cells</b>	<b>148</b>
<b>4.35 Effect on cell migration in STAT1 and/or STAT3 knockdown J82 cells</b>	<b>149</b>
<b>4.36 STATs phosphorylation status in A431/sip model of EMT</b>	<b>150</b>
<b>5.1a Effect of I3C on total and phosphorylated STAT3 levels in J82, T24</b>	

<i>and RT112 cells</i>	160
<i>5.1b Histograms showing effect of I3C on phosphorylated STAT3 in J82 and T24 cells</i>	161
<i>5.2 Effect of DIM on total and phosphorylated STAT3 levels in T24 cells</i>	162
<i>5.3a Effect of DIM on total and phosphorylated STAT levels in J82 cells</i>	162
<i>5.3b Histograms showing effect of DIM on total and phosphorylated STAT levels in J82 cells</i>	163
<i>5.4a Effect of DIM on total and phosphorylated STAT levels in RT112 cells</i>	164
<i>5.4b Histograms showing effect of DIM on total and phosphorylated STAT levels in RT112 cells</i>	165
<i>5.5 Effect of I3C or DIM on total and phosphorylated ERK and Akt levels in J82 cells</i>	166
<i>5.6a Histograms showing effect of I3C on total and phosphorylated ERK and Akt in J82 cells</i>	167
<i>5.6b Histograms showing effect of DIM on total and phosphorylated ERK and Akt in J82 cells</i>	168
<i>5.7 Flow cytometric analysis of prodium iodide stained RT112 and J82 cells following DIM treatment</i>	170
<i>5.8 Effect of DIM on cell cycle in J82 and RT112 cells</i>	171
<i>5.9 Effect of DIM on Cyclin D1 and survivin levels in J82 and RT112 cells</i>	172
<i>5.10 Effect of I3C or DIM on apoptosis in RT112 cells</i>	174
<i>5.11 Plots showing effect of I3C or DIM on apoptosis in RT112 cells</i>	175
<i>5.12 Effect of I3C or DIM on apoptosis in J82 cells</i>	176
<i>5.13 Plots showing effect of I3C or DIM on apoptosis in J82 cells</i>	177
<i>5.14 Plots showing effect of I3C or DIM on apoptosis in RT4 cells</i>	178
<i>5.15 Effect of DIM on caspase3/7 activity in J82, RT112 and RT4 cells</i>	180
<i>5.16 Hoechst staining and caspase3 levels in DIM treated J82 cells</i>	181
<i>5.17 Effect of DIM on PARP cleavage in J82, RT112 and RT4 cells</i>	182
<i>5.18 Effect of DIM on cadherins and <math>\beta</math>-catenin levels in J82 cells</i>	183
<i>5.19 Immunostaining showing effect of DIM on N-cadherin, <math>\beta</math>-catenin and</i>	

<i>tubulin distribution in J82 cells</i>	<i>184</i>
<i>5.20 Effect of DIM on J82 cell adhesion to fibronectin and collagen I</i>	<i>185</i>
<i>5.21 Effect of DIM on cell viability in J82 cells</i>	<i>186</i>
<i>5.22 Effect on cell adhesion to fibronectin and collagen I in the presence of DIM</i>	<i>187</i>
<i>5.23 Effect of DIM on cell adhesion in presence of anti-fibronectin antibody</i>	<i>188</i>
<i>5.24 Effect of DIM on cell adhesion in STAT1 and/or 3 knockdown J82 cells</i>	<i>190</i>

## **LIST OF TABLES**

<b>1.1 Oncogenes and tumour-suppressor genes relevant to bladder cancer</b>	<b>6</b>
<b>1.2 Main features of STATs</b>	<b>9</b>
<b>1.3 STAT activation in human tumours and cell lines</b>	<b>14</b>
<b>1.4 Cyclin-CDK complexes are activated at specific points of the cell cycle</b>	<b>20</b>
<b>1.5 Summary of studies using I3C and DIM as cancer chemopreventive agents</b>	<b>37</b>
<b>1.6 Summary of cell signalling components modulated by I3C and DIM</b>	<b>39</b>
<b>1.7 Summary of studies indicating I3C as a tumour promoter</b>	<b>40</b>
<b>2.1 Information on bladder cell lines</b>	<b>51</b>
<b>2.2 Antibodies: conditions for use</b>	<b>55</b>
<b>2.3 Antibodies: dilution for use</b>	<b>62</b>
<b>2.4 Antibodies/binding protein: dilution for use</b>	<b>63</b>
<b>3.1 Grade and stage of human bladder tumour tissues</b>	<b>73</b>
<b>3.2 Pattern of staining in superficial tumours for STAT3 and pSTAT3</b>	<b>75</b>
<b>3.3 Pattern of staining in superficial tumours for STAT5 and pSTAT5</b>	<b>77</b>
<b>3.4 Pattern of staining in superficial tumours for STAT1 and pSTAT1</b>	<b>79</b>
<b>3.5 Pattern of staining in muscle invasive tumours for STAT3 and pSTAT3</b>	<b>81</b>
<b>3.6 Pattern of staining in muscle invasive tumours for STAT5 and pSTAT5</b>	<b>85</b>
<b>3.7 Pattern of staining in muscle invasive tumours for STAT1 and pSTAT1</b>	<b>88</b>
<b>3.8 Difference of STATs staining between superficial and muscle invasive bladder tumours</b>	<b>91</b>
<b>3.9 Pattern of staining in superficial tumours for cadherins</b>	<b>92</b>
<b>3.10 Pattern of staining in muscle invasive tumours for cadherins</b>	<b>96</b>
<b>3.11 Difference of cadherins staining between superficial and muscle invasive bladder tumours</b>	<b>100</b>
<b>3.12 Coexpression of phosphorylated STATs and cadherins in superficial and muscle invasive bladder tumours</b>	<b>101</b>
<b>4.1 Nucleofection buffer and programme tested for RT112 nucleofection</b>	<b>137</b>
<b>4.2 Some characteristics of bladder cells (J82 and RT112) and A431/sip cells</b>	<b>152</b>

<b><i>5.1 Effect of DIM on cell cycle in the RT112 and J82 cell lines</i></b>	<b>169</b>
<b><i>5.2 J82 and RT112 cell lines expressing different cadherin/catenin profiles</i></b>	<b>194</b>

## ***ABBREVIATIONS***

<b>Abl</b>	<b>Abelson leukaemia protein</b>
<b>ANOVA</b>	<b>Analysis of variance</b>
<b>Apaf-1</b>	<b>Apoptosis protease activating factor-1</b>
<b>AR</b>	<b>Androgen receptor</b>
<b>Bcl-x<sub>L</sub></b>	<b>B-cell lymphoma/leukaemia</b>
<b>BSA</b>	<b>Bovine serum albumin</b>
<b>CAK</b>	<b>CDK activating kinase</b>
<b>Caspase</b>	<b>Cysteine aspartate specific protease</b>
<b>CAT</b>	<b>Chloramphenicol acetyltransferase</b>
<b>CDK</b>	<b>Cyclin-dependent kinase</b>
<b>CKI</b>	<b>Cyclin-dependent kinase inhibitor</b>
<b>CIS</b>	<b>Carcinoma in situ</b>
<b>CSF-1</b>	<b>Colony-stimulating factor-1</b>
<b>DAPI</b>	<b>4', 6-diamidino-2-phenyl-indole, dihydrochloride</b>
<b>DAPK-1</b>	<b>Death-associated protein kinase-1</b>
<b>DIM</b>	<b>3, 3'-diindolylmethane</b>
<b>DMEM</b>	<b>Dulbecco's modified Eagle's medium</b>
<b>DMSO</b>	<b>Dimethylsulphoxide</b>
<b>ECM</b>	<b>Extracellular matrix</b>
<b>EDTA</b>	<b>Ethylenediaminetetraacetic acid</b>
<b>EGCG</b>	<b>(-) - epigallocatechin-3-gallate</b>
<b>EGF</b>	<b>Epidermal growth factor</b>
<b>EGFR</b>	<b>Epidermal growth factor receptor</b>
<b>EMT</b>	<b>Epithelial-mesenchymal transition</b>
<b>EPO</b>	<b>Erythropoietin</b>
<b>ER</b>	<b>Estrogen receptor</b>
<b>ERK</b>	<b>Extracellular signal regulated kinase</b>
<b>FAK</b>	<b>Focal adhesion kinase</b>
<b>FasL</b>	<b>Fas ligand</b>
<b>FCS</b>	<b>Fetal calf serum</b>
<b>FGFR</b>	<b>Fibroblast growth factor receptor</b>

FITC	Fluorescein isothiocyanate
FRA-1	Fos-related antigen 1
G <sub>1</sub>	Gap 1 phase of the cell cycle
G <sub>2</sub>	Gap 2 phase of the cell cycle
GAS	$\gamma$ -interferon-activated sequence
GH	Growth hormone
GRR	IFN- $\gamma$ response region
GST	Glutathione <i>S</i> -transferase
HGF	Hepatocyte growth factor
HIF1	Hypoxia-inducible factor 1
I3C	Indole-3-carbinol
IAP	Inhibitor of apoptosis
IFN	Interferon
IL	Interleukin
ILK	Integrin-linked kinase
ISRE	IFN-stimulated response elements
JAK	Janus kinase
KDa	Kilodalton
LOH	Loss of heterozygosity
M	Mitosis phase of the cell cycle
MAPK	Mitogen activated protein kinase
MCL1	Myeloid cell leukemia sequence 1
MEFs	Mouse embryonic fibroblasts
MMP	Matrix metalloproteinase
NF- $\kappa$ B	Nuclear factor- $\kappa$ B
NK	Natural killer
ONPG	Ortho-nitrophenyl- $\beta$ -galactosidase
PARP	Poly (ADP ribose) polymerase
PBS	Phosphate buffered saline
PDGF	Platelet-derived growth factor
PI	Propidium iodide
PI3K	Phosphoinositide-3-kinase
PIAS	Protein inhibitor of activated STAT
PRL	Prolactin

PS	Phosphatidylserine
PVDF	Polyvinylidene difluoride
RASSF1A	RAS association domain family 1A
Rb	Retinoblastoma
ROS	Reactive oxygen species
RPMI	Roswell Park Memorial Institute
SDS	Sodium dodecyl sulphate
SH2	Src-homology 2
SHP-1	SH2-domain phosphatase-1
SIP1	Smad interacting protein-1
SOCS	Suppressor of cytokine signaling
STAT	Signal transducer and activator of transcription
TAD	Transactivation domain
TAE	Tris acetate EDTA
tBid	Truncated bid
TBST	Tris buffered saline-tween
TCC	Transitional cell carcinoma
T/E	Tris/EDTA
TEMED	Tetramethyl ethylene diamine
TK	Tyrosine kinase
TNF	Tumor necrosis factor
TRAIL	TNF-related apoptosis inducing ligand
UV	Ultra violet
VEGF	Vascular endothelial growth factor
XIAP	X chromosome-linked inhibitor of apoptosis
ZO-1	Zonula occludens-1

## **CHAPTER 1**

### **INTRODUCTION**

## **1.1 Bladder cancer**

Bladder cancer is the fifth most common cancer in North America, Northern and Western Europe, and other developed countries ([www.who.int/cancer/resources/incidences/en/](http://www.who.int/cancer/resources/incidences/en/), Li *et al.*, 2005). In the UK, bladder cancer is the fourth most common cancer in men and the ninth most common cancer in women, affecting around 10,000 people each year (based on [www.bupa.co.uk](http://www.bupa.co.uk)).

Studies (Brandau and Bohle, 2001; Feng *et al.*, 2002) have found that the risk factors for developing bladder cancer include tobacco, occupation in the rubber, chemical and leather industries, certain parasitic infections and exposure to arsenic. In addition, the median age at diagnosis of bladder cancer is 70, and men are two to three times more likely than women to develop bladder cancer (Hayat *et al.*, 2007).

The common symptoms of bladder cancer include blood in the urine, pain during urination and frequent urination. Tumours are staged according to how far they have spread within the bladder, to nearby tissues and to other organs (based on [www.cancerhelp.org.uk](http://www.cancerhelp.org.uk), *figure 1.1*).

The wall of the bladder is lined with transitional and squamous cells. More than 90% of bladder cancers begin in transitional cells and are therefore called transitional cell carcinomas (TCCs), whereas only 8% are squamous cell carcinomas. Noninvasive transitional cell carcinomas of the bladder have two distinct forms. Papillary transitional cell carcinomas, accounting for approximately 70-80% of bladder cancers, often tend to recur locally, but rarely progress to the muscle-invasive and metastatic stages, whereas flat carcinoma in situ, a more dangerous lesion, is known to frequently progress to invasive disease (Knowles, 2001).

Clinical data indicate that invasive transitional cell carcinomas may develop either from superficial papillary tumours, which progress relatively infrequently, or from carcinoma in situ (CIS), which may act as the major precursor (Spruck III *et al.*, 1994). Williams and Stein (2004) reported that more than 50% of the muscle-invasive transitional cell carcinomas that grow through the lining and into the muscular wall of bladder eventually metastasise to distant organs. The major progression of bladder cancer is shown in *figure 1.2*.

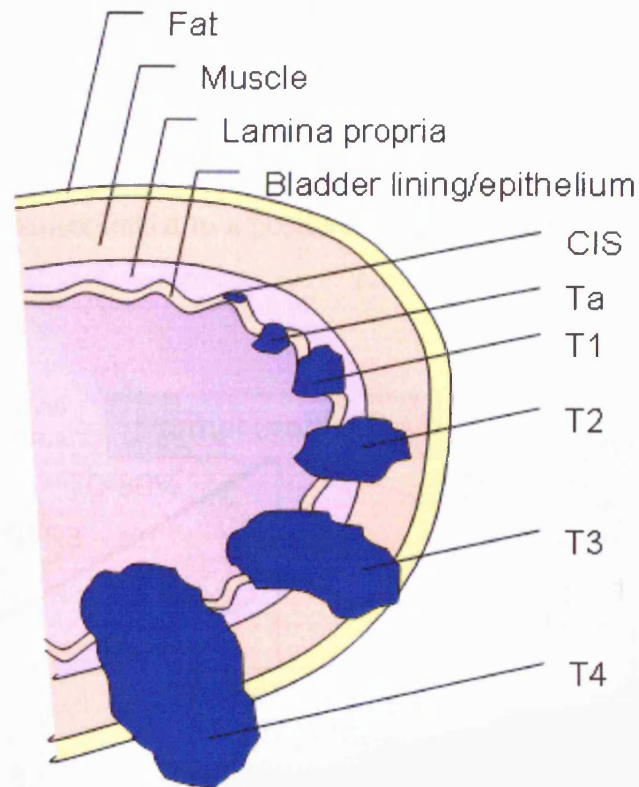


**Figure 1.1** Diagram showing the relationship between the location and depth of the tumour and the stage.

*Ta: non-invasive papillary carcinoma*

*Tis: carcinoma in situ (CIS); non-invasive flat carcinoma*

*T1: tumour invades lamina propria but not as deep as the muscle tissue*

*T2: tumour invades muscle*

*T3: tumour invades fatty tissue that surrounds the bladder*

*T4: tumour invades prostate, uterus, vagina, pelvic wall or abdominal wall*

Tumour progression is thought to occur through the accumulation of multistep genetic alterations, including constitutive activation of oncogenes, loss of tumour suppressor genes and distinct chromosomal regions (Chatterjee *et al.*, 2004a). Many genetic alterations that are currently believed to be important for bladder cancer development and progression have been reported (figure 1.2, Wolff *et al.*, 2005; Mo *et al.*, 2007).

As several studies have shown (Cappellen *et al.*, 1999; Bakkar *et al.*, 2003; van Rhijn *et al.*, 2004; Wolff *et al.*, 2005), activating mutations in the gene occur in approximately 70-85% of the low grade, noninvasive papillary TCCs (stage Ta). These mutations are also found in 21% and 16% of lamina propria TCCs (stage T1) and muscle invasive TCCs (stage T2-T4), respectively, but not in CIS tumours, indicating that, although the progression of noninvasive

papillary tumours occurs infrequently, when it happens, it goes through a different pathway than CIS (Billerey *et al.*, 2001). FGFR3 and Ras gene mutations, which possibly affect the same pathway, are discovered to be mutually exclusive (Jebar *et al.*, 2005). Bladder tumours with FGFR3 mutations show a lower rate of recurrence than those without, which enables FGFR3 to be the first marker linked to a positive prognosis for bladder cancer (van Rhijn *et al.*, 2004).

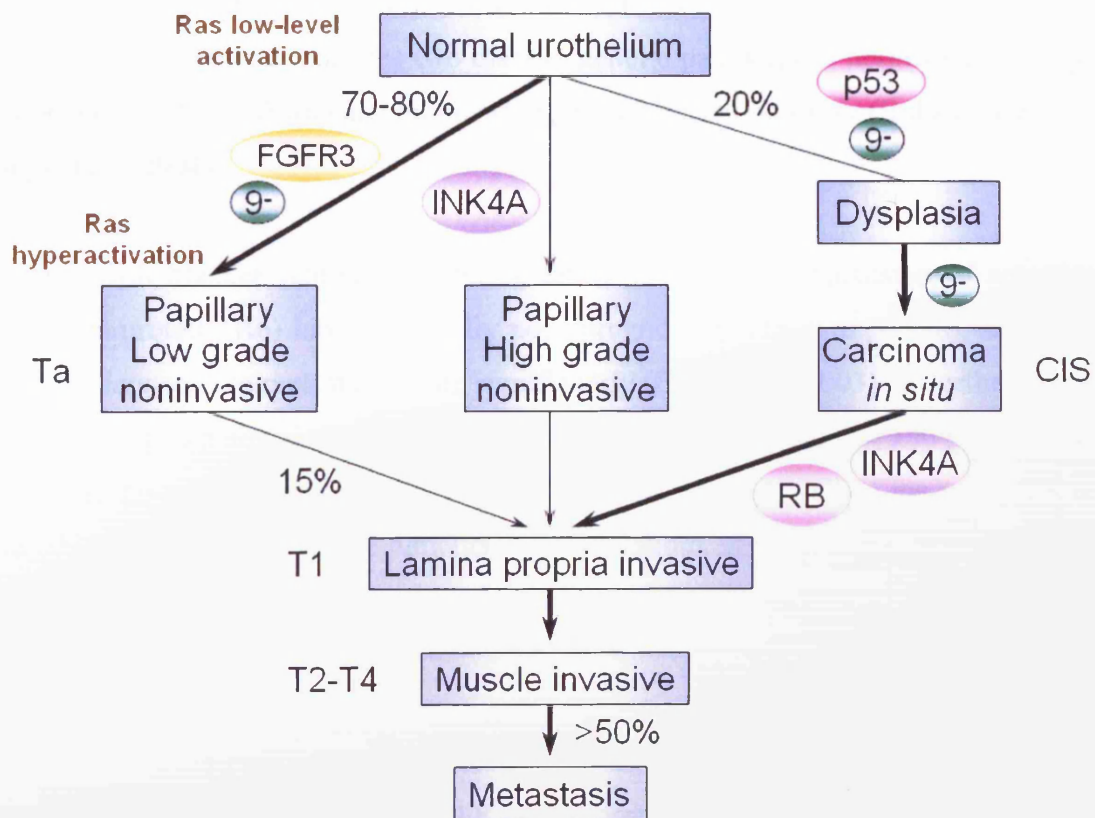


**Figure 1.2 Model for bladder cancer progression showing important genetic events associated with tumourigenesis.** Values for bladder cancer progression frequencies are obtained from Dinney *et al.*, 2004, Knowles, 2001, Williams and Stein, 2004. FGFR3, fibroblast growth factor receptor 3; Rb, retinoblastoma; INK4A, encoding p14 and p16; 9-, deletion of part or all of chromosome 9.

The most common genetic change in human tumours is mutation in the TP53 gene (Hollstein *et al.*, 1991). Mutations in p53 are frequently found in invasive and high grade superficial TCCs including CIS, but rarely in low grade papillary lesions (Bakkar *et al.*, 2003). It has been reported that p53 mutation is observed in 51% (25 out of 49) of muscle invasive tumours and 65% (15 out of 23) of dysplasias and CIS, compared to only 3% (1 out of 36) of Ta

tumours (Spruck III *et al.*, 1994). Point mutations of p53 result in an altered protein, resistant to degradation by ubiquitin (Dowell *et al.*, 1994), which enables accumulation of p53 in the nucleus, which can be detected by immunohistochemistry (Esrig *et al.*, 1993; Cordon-Cardo *et al.*, 1994).

Alterations in FGFR3 and p53 describe almost 80% of urothelial cell carcinomas. However, they concur in only 5.7%, revealing that these two markers are almost always mutually exclusive (van Rhijn *et al.*, 2004). In addition, the clinical outcome linked to each of these two molecular markers indicates two distinct genetic pathways: a noninvasive and papillary, FGFR3-associated pathway and an invasive p53-associated pathway (Bakkar *et al.*, 2003; van Rhijn *et al.*, 2004).

Patients with bladder tumours exhibiting either loss or overexpression of retinoblastoma-associated protein (Rb) have an equally poor prognosis (Cote *et al.*, 1998), as tumours with Rb alterations tend to metastasise more significantly (Cote *et al.*, 2003). Together alterations in both Rb and p53 pathways and loss of the *INK4A* locus (encoding p14 and p16) are associated with a greater risk of recurrence (Orlow *et al.*, 1999). On the basis of the combined p53, pRb and p21 status, patients whose tumours have alterations in any two or all three determinants show 57% and 93% recurrence rates (Chatterjee *et al.*, 2004a), indicating a synergistic effect of tumourigenesis among these proteins.

The epidermal growth factor receptor (EGFR) is a member of the tyrosine kinase family encoded by *c-erbB* oncogenes. EGFR is the protein product of *c-erbB-1*, one of the four known *c-erbB* oncogenes, and *c-erbB-1* protooncogene has been reported to be associated with poor prognosis in patients with bladder cancer (Nicholson *et al.*, 2001). Colquhoun and Mellon (2002) have reviewed that many studies show overexpressed EGFR in bladder cancer which is associated with high tumour stage, tumour progression and poor prognosis. However, the mechanism of the association between EGFR expression and poor clinical outcome is still not clear.

Molecular epidemiological studies in different races and tumour stages/grades have shown that activated HRAS is observed in up to 84% of bladder TCCs (Hong *et al.*, 1996; Vageli *et al.*, 1996; Saito *et al.*, 1997; Przybojewska *et al.*, 2000), and more than 50% of human bladder tumours overexpress RAS mRNA and protein (Vageli *et al.*, 1996). A recent study has shown

that hyperactivation of HRAS is necessary and sufficient to initiate bladder tumourigenesis (Mo *et al.*, 2007), and the latency of RAS-induced bladder tumours is significantly shortened by the loss of p53 (Gao *et al.*, 2004).

**Table 1.1 Oncogenes and tumour-suppressor genes relevant to bladder cancer**

<b>Genes</b>	<b>Alterations</b>	<b>Excludes</b>	<b>Clinical association with bladder tumours</b>
<b>Oncogenes</b>			
FGFR3	Activating mutation	HRAS TP53	Ta and low grade, low recurrence of Ta
HRAS	Activating mutation or overexpression	FGFR3	None
E2F	Gene amplification and overexpression		Higher stage and grade
<b>Tumour-suppressor genes</b>			
RASSF1A	Hypermethylation		Higher stage
Rb	Deletion or hyperphosphorylation		Higher stage and grade
TP53	Inactivating mutation or deletion	FGFR3	T1s and high stage and high grade
p14/p16	Homozygous deletion or hypermethylation		Higher stage and grade

*Adapted from Wolff et al., 2005*

Another common event occurring early on in bladder tumourigenesis is deletion of part or all of chromosome 9 (Hartmann *et al.*, 2002). The loss of heterozygosity (LOH) of chromosome 9 is observed in 34% of low and high grade papillary tumours compared to 12% in CIS and dysplasias, whereas loss of a chromosome allele is detected in 59% of invasive tumours (Spruck III *et al.*, 1994). The genetic alterations and clinical association of oncogenes and tumour-suppressor genes relevant to bladder cancer are shown in *table 1.1*.

Therefore, urothelial cell carcinomas are described by a number of specific genetic defects, including mutations in FGFR3, alterations in p53 and Rb tumour-suppressor genes, frequent LOH, and constitutive activation of RAS-MAPK pathway (Wolff *et al.*, 2005).

## **1.2 Signal Transducers and Activators of Transcription (STATs)**

### **1.2.1 The STAT family of proteins**

When cytokines and growth factors bind to their cognate receptors on the cell surface, they trigger specific intracellular events which transmit critical biological signals through the cytoplasm to the nucleus. STAT proteins are at the centre of these signal transduction pathways, activated by many cytokines and growth factors. As their name suggests, STATs serve a dual function of signal transduction and gene regulation (Catlett-Falcone *et al.*, 1999a).

Since their identification 15 years ago (Schindler *et al.*, 1992), STATs have been recognised as latent cytoplasmic transcription factors required for cell growth, survival, differentiation, and motility. This family now has seven different members, designated as STAT1, STAT2, STAT3, STAT4, STAT5a, STAT5b and STAT6. In addition, two variants ( $\alpha$  and  $\beta$ ) of STATs 1 and 3 have been identified (Darnell, 1997).

### **1.2.2 Structures of STATs**

Currently, the seven different STAT proteins are known to be encoded in three chromosomal clusters in mammals. *Stat1* and *Stat4* map to the proximal region of mouse chromosome 1 (human chromosome 2q32.2-q32.3), *Stat2* and *Stat6* map to the distal region of mouse chromosome 10 (human chromosome 12q13), and *Stat3*, *Stat5a* and *Stat5b* map to the distal region of mouse chromosome 11 (human chromosome 17q21.31, 17q11.2) (Copeland *et al.*, 1995).

Each STAT molecule contains a central DNA binding domain, a src-homology 2 (SH2) domain critical for homo- or heterodimerisation, and a transactivation domain (TAD) containing a conserved tyrosine residue necessary for tyrosine phosphorylation. Some STAT proteins also have a conserved serine residue in their transactivation domain in the C-terminal region, which is required for the maximal transcriptional activity (Catlett-Falcone *et al.*, 1999a).

As previous studies have shown, STAT1, 3, 4, 5a and 5b are 750~795 amino acids long, and, STAT2 and 6 are ~850 amino acids long (Schindler and Darnell, 1995; Hou *et al.*, 1994) (Figure 1.3).

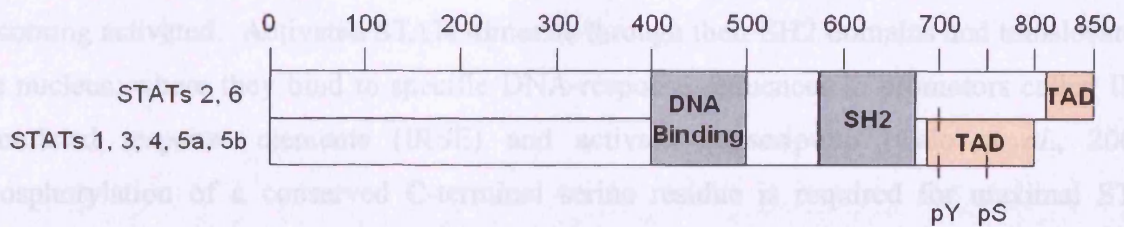


**Figure 1.3 Generic structures of STAT molecules.** The diagram illustrates common functional regions shared by STAT family members. The site of phosphotyrosine (pY) is contained in all activated STATs, whereas, the site of phosphoserine (pS) which is located in the C-terminal TAD is only contained in activated STATs 1, 3, 4, 5a and 5b (Darnell, 1997).

### 1.2.3 Activation mechanisms of STATs

STATs are ligand-induced transcriptional factors. So far, it is known that more than 35 different polypeptide ligands can activate one or more different STATs, which indicates the STAT family participates in a range of biological events (Darnell, 1997). According to their response to different ligands, STATs can be divided into two groups. One group includes STATs 2, 4 and 6, which has a narrow activation profile, only activated by interferon- $\alpha$  (IFN $\alpha$ ) and a few interleukins (ILs) (Schindler and Darnell, 1995; Hou *et al.*, 1994; Cho *et al.*, 1996). In contrast, STATs 1, 3 and 5 are activated by a series of ligands and are involved in a broad range of biological processes, including embryogenesis, apoptosis and development (Bromberg, 2002). Some activating cytokines and phosphorylation sites of each STAT member are shown in *table 1.2*.

The latter group of STAT proteins becomes activated by tyrosine phosphorylation induced by cytokine receptors, receptor tyrosine kinases (TK), or non-receptor tyrosine kinases. Growth factor receptors, such as epidermal growth factor (EGF), hepatocyte growth factor (HGF), platelet-derived growth factor (PDGF) and colony-stimulating factor-1 (CSF-1) receptors, which possess intrinsic tyrosine kinase activity, can activate STAT proteins either directly or indirectly, by means of Janus Kinase (JAK) proteins. In contrast, phosphorylation of STAT proteins by cytokine receptors, which have no intrinsic enzymatic activity, must depend on receptor-associated tyrosine kinases JAK. The JAK family of cytoplasmic tyrosine kinases consists of four members: JAK1, JAK2, JAK3 and TYK2, which can be activated by dimerisation or oligomerisation of receptors. Activation of these tyrosine kinases results in phosphorylation on the receptor cytoplasmic tails to provide docking sites for the recruitment

of monomeric STATs. Once recruited, STATs are subsequently phosphorylated, thus becoming activated. Activated STATs dimerise through their SH2 domains and translocate to the nucleus, where they bind to specific DNA-response sequences in promoters called IFN-stimulated response elements (IRSE) and activate transcription (Calo *et al.*, 2003). Phosphorylation of a conserved C-terminal serine residue is required for maximal STAT transcriptional activity by increasing interaction with some important proteins in STAT-mediated transcription (Decker and Kovarik, 2000).

**Table 1.2 Main features of STATs**

<b>STAT</b>	<b>Activated by</b>	<b>Phosphorylation sites</b>	<b>Functions</b>
STAT1	IFNs, IL-6, GF	Tyr 701, Ser 727	Response to type I and II IFNs, IL-2, IL-6, EGF, PDGF, GM-CSF
STAT2	IFNs	Tyr 690	Response to type I IFN
STAT3	IL-6 family, PRL, GH, GF, Src	Tyr 705, Ser 727	Embryogenesis, involution of the post-lactating mammary gland
STAT4	IL-12, IFN	Tyr 722, Ser 721	Response to IL-12 for the development of type I T-helper cells
STAT5a	PRL, EPO, GH, GF	Tyr 694, Ser 726	Development of the mammary gland and lactogenesis
STAT5b	PRL, EPO, GH, GF	Tyr 694, Ser 731	Response to the GH, regulation of sexual dimorphism and development of NK cells
STAT6	IL-4, IL-13	Tyr 641	Response to IL-4 and IL-13 for the development of type II T-helper cells

*IFN, interferon; IL, interleukin; GF, growth factors; GH, growth hormone; PRL, prolactin; EPO, erythropoietin; NK, natural killer (adapted from Calo et al., 2003).*

Unlike receptor TKs, non-receptor tyrosine kinases, such as src and bcr-abl (a fusion of the breakpoint-cluster region and abl (Abelson leukaemia protein) proteins), can also activate STAT proteins independently of receptor engagement. A close correlation between STAT3 activation and the oncogenic transformation of src has been reported (Turkson *et al.*, 1998). STAT3 is constitutively activated in mammalian cells transformed by oncogenic src, and the

transforming ability of src can be blocked by dominant-negative forms of STAT3. *Figure 1.4* shows the activation mechanisms and downstream targets of STATs.

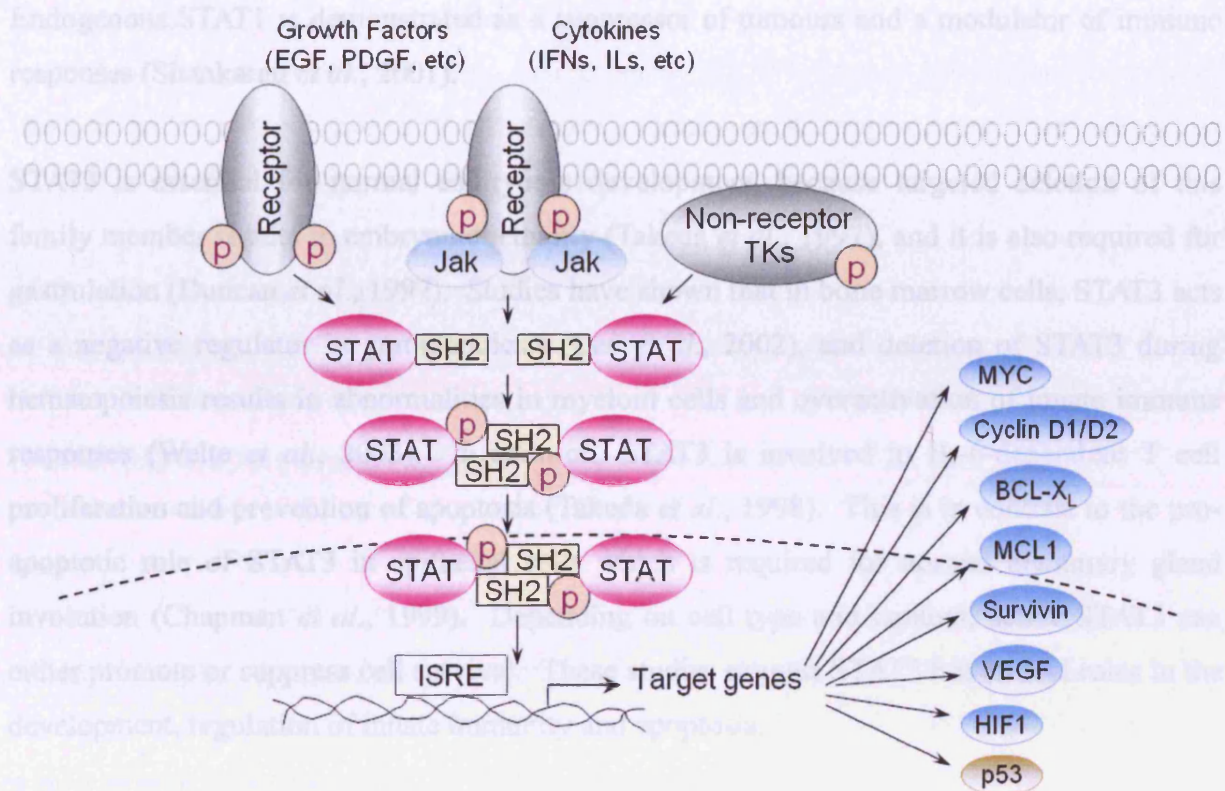


**Figure 1.4 Activation mechanisms and downstream targets of STAT proteins.**

Downstream targets shown in brown are downregulated by STATs, whereas those in blue are upregulated (these molecules are targets of mainly STAT1, 3 and 5) (Yu and Jove, 2004).

Abbreviations: Bcl-x<sub>L</sub>, B-cell lymphoma/leukaemia; MCL1, Myeloid cell leukemia sequence 1; VEGF, Vascular endothelial growth factor; HIF1, Hypoxia-inducible factor 1.

#### 1.2.4 Normal physiological role of STATs

The role of individual STAT proteins under normal physiological conditions has been defined by using *Stat* knockout mice.

*Stat1*-deficient mice show no gross developmental defects, but display a lack of responsiveness to IFN $\gamma$  which has growth inhibitory effects (Durbin *et al.*, 1996; Meraz *et al.*, 1996). Also, these mice develop tumours more rapidly and with greater frequencies compared with wild-type mice (Kaplan *et al.*, 1998). Lymphocytes derived from *Stat1*<sup>-/-</sup> mice display increased proliferation and reduced apoptosis *in vitro*, revealing an essential role of STAT1 in lymphocyte survival (Lee *et al.*, 2000). In colon carcinoma HT29 cells, targeted

disruption of *STAT1* leads to the reduction of the growth inhibitory effect of IL-4, whereas reconstitution of STAT1 can restore this effect. Additionally, dominant negative-STAT1 expressing HT29 cells lose the growth inhibition in response to IL-4 (Chang *et al.*, 2000). Endogenous STAT1 is demonstrated as a suppressor of tumours and a modulator of immune responses (Shankaran *et al.*, 2001).

STAT3 is essential for normal embryonic development, because targeted deletion of this family member results in embryonic lethality (Takeda *et al.*, 1997), and it is also required for gastrulation (Duncan *et al.*, 1997). Studies have shown that in bone marrow cells, STAT3 acts as a negative regulator in granulopoiesis (Lee *et al.*, 2002), and deletion of STAT3 during hematopoiesis results in abnormalities in myeloid cells and overactivation of innate immune responses (Welte *et al.*, 2003). In addition, STAT3 is involved in IL-6-dependent T cell proliferation and prevention of apoptosis (Takeda *et al.*, 1998). This is in contrast to the pro-apoptotic role of STAT3 in epithelial cells which is required for normal mammary gland involution (Chapman *et al.*, 1999). Depending on cell type and context, active STAT3 can either promote or suppress cell survival. These studies suggest STAT3 has critical roles in the development, regulation of innate immunity and apoptosis.

STAT5a and STAT5b are encoded by different genes which are chromosomally linked. *Stat5a* knockout female mice have no ability to develop normal breast tissue or to lactate. *Stat5b* is not able to compensate for the absence of *Stat5a*, although these two proteins have more than 90% identity in amino acid sequences (Liu *et al.*, 1997). However, *Stat5b*<sup>-/-</sup> female mice still can lactate, and *Stat5b*<sup>-/-</sup> males have serum levels of liver-produced proteins, characteristic of female mice (Udy *et al.*, 1997). Also, *Stat5b*<sup>-/-</sup> mice have decreased numbers of NK cells which mediate proliferation and cytolytic activity (Imada *et al.*, 1998). Consistent with the phenotype of mice lacking either *Stat5a* or *Stat5b*, mice doubly deficient in both *Stat5a* and *Stat5b* have defective immune system function and impaired mammary gland development (Ivashkiv and Hu, 2004).

So far, studies have shown that *Stat2* deficient mice display increased susceptibility to viral infections (Park *et al.*, 2000), and *Stat4* deficiency results in impaired T helper (Th) 1 cell function (Kaplan *et al.*, 1996) whereas *Stat6*-null mice exhibit defective Th2 cell function (Shimoda *et al.*, 1996).

Overall, these findings have demonstrated that STAT is critical for normal cellular processes, including growth, apoptosis, immune function, embryonic and mammary development. *Table 1.2* shows the main function of each individual STAT.

In normal physiological conditions, activation of STAT proteins is a tightly regulated, transient process which normally lasts a few minutes, up to several hours. Therefore, the persistent STATs expression could be associated with oncogenesis.

#### ***1.2.5 STAT activation in oncogenesis***

Increasing evidence has shown that STATs are frequently constitutively activated in a wide range of human cancers (Turkson and Jove, 2000; Catlett-Falcone *et al.*, 1999a; Bowman *et al.*, 2000). As shown in *table 1.3*, STAT3, STAT5 and to a lesser extent, STAT1 are found to be overactive in a variety of human tumours and cell lines.

Enhanced tyrosine-kinase activity is closely linked to many proliferative diseases, such as cancer (Levitzki, 1999). Oncogenic tyrosine kinases, including src, EGFR, JAK and many others, are often persistently activated due to genetic or epigenetic alterations in tumours. STATs become constitutively activated as a result of one or more overactive upstream tyrosine kinases (Buettner *et al.*, 2002). The role of STATs in oncogenesis is mediated through the expression of genes involved in apoptosis, such as Mcl-1 (Epling-Burnette *et al.*, 2001), Bcl-x<sub>L</sub> (Zushi *et al.*, 1998) and survivin (Aoki *et al.*, 2003); proliferation, such as c-myc (Bowman *et al.*, 2001) and cyclin D1 (Masuda *et al.*, 2002); invasion, such as matrix metalloproteinase-9 (MMP-9) (Dechow *et al.*, 2004) and angiogenesis, such as VEGF (Niu *et al.*, 2002).

As noted previously, depending on the different stimulus and cell type, STATs can act either as suppressors or promoters of apoptosis. In general, STAT3 and STAT5 are important for transducing anti-apoptotic signals, whereas STAT1 has been implicated in suppressing cell survival under most circumstances. The first finding showing a direct link between STATs and human cancer was that inhibition of constitutively activated STAT3 in myeloma cells decreased expression of the anti-apoptotic gene Bcl-x<sub>L</sub> and induced apoptosis (Catlett-Falcone *et al.*, 1999b). Blocking either STAT3 or STAT5 resulted in downregulation of Mcl-1 and induction of apoptosis in lymphocytes (Epling-Burnette *et al.*, 2001). Consistently, expression of survivin, a member of the inhibitor of apoptosis family, is induced by activated STAT3 (Aoki *et al.*, 2003). Also, a constitutively activated mutant form, Stat3C has been

shown to transform fibroblasts and allow them to form tumours in mice (Bromberg *et al.*, 1999).

Recent studies have indicated that STAT1 can regulate apoptosis either through a transcriptional mechanism, by activating genes which encode proteins that mediate or initiate the cell death process, as caspases, cell death receptors and their ligands, or via a non-transcriptional mechanism by inhibiting anti-apoptotic proteins, such as NF- $\kappa$ B (Battle and Frank, 2002). The findings of gene targeting experiments have shown that the primary role of STAT1 *in vivo* is regulating IFN signalling (Durbin *et al.*, 1996; Meraz *et al.*, 1996). IFN- $\alpha$  and  $\gamma$  have been known to delay human neutrophil apoptosis, accompanied by activation of STAT1 and STAT3 (Sakamoto *et al.*, 2005), and also in human lymphocytes decreased cell proliferation and phosphorylated STAT1 was observed in response to IFN- $\alpha$  treatment (Cousens *et al.*, 2005).

In contrast, both STAT3 and STAT5 induce the expression of c-myc, a regulator of cell proliferation. Transformation by src is dependent upon STAT3-induced c-myc expression in normal cells (Bowman *et al.*, 2001). Moreover, constitutive activation of STAT3 and STAT5 has been shown to accelerate cell cycle progress by promoting the expression of cyclin D1/D2 (Martino *et al.*, 2001; Masuda *et al.*, 2002).

Mutations in p53 are considered to be the most common event in cancer (Hollstein *et al.*, 1991). However, they mostly occur at a late stage in tumour development, and many clinically detectable cancers exhibit reduction of p53 expression without mutations. STAT3 is involved in downregulation of p53 in normal growth and oncogenic signalling pathways via inhibiting p53 promoter activity, and inhibition of STAT3 can restore p53 function in some cancer cells (Niu *et al.*, 2005). Townsend *et al.*, (2004) have shown that STAT1 interacts with p53 directly which enhances DNA damage induced apoptosis. Correspondingly, both basal p53 levels and the induction of those p53 responsive genes, such as Bax and Fas were reduced in cells lacking STAT1.

Dechow *et al.*, (2004) have demonstrated that the activity of MMP-9 is required for STAT3C-mediated transformation of immortalised human mammary epithelial cells, and a positive correlation between MMP-9 expression and activated STAT3 has been shown in breast cancer specimens. The most potent signalling molecule involved in angiogenesis is VEGF which

binds to transmembrane receptor tyrosine kinases of endothelial cells (Plate *et al.*, 1992). In cancer cells, endothelial cell migration and proliferation, which is required for the formation of new blood vessels, is activated by increased levels of VEGF (Veikkola *et al.*, 2000).

**Table 1.3 STAT activation in human tumours and cell lines**

Cancer type	Activated STATs	References
Breast cancer (tumours)	STAT1, STAT3	Watson <i>et al.</i> , 1995
	STAT5a	Cotarla <i>et al.</i> , 2004
Breast cancer (cell lines)	STAT3	Garcia <i>et al.</i> , 1997
		Sartor <i>et al.</i> , 1997
Brain cancer (tumours)	STAT1, STAT3	Schaefer <i>et al.</i> , 2002
Colon cancer (tumours)	STAT3	Ma <i>et al.</i> , 2004
Head and neck cancer (cell lines)	STAT1, STAT3	Grandis <i>et al.</i> , 1998
Leukemia	STAT1, STAT3	Migone <i>et al.</i> , 1995
	STAT5	Gouilleux-Gruart <i>et al.</i> , 1996
		Shuai <i>et al.</i> , 1996
		Liu <i>et al.</i> , 1999
Lung cancer (cell lines)	STAT3, STAT5	Liby <i>et al.</i> , 2006
Lymphoma	STAT1, STAT3	Weber-Nordt <i>et al.</i> , 1996
	STAT5	Yu <i>et al.</i> , 1997
		Lund <i>et al.</i> , 1999
Mutiple myeloma (cell lines)	STAT1, STAT3	Catlett-Falcone <i>et al.</i> , 1999b
	STAT5	Hodge <i>et al.</i> , 2004
		Liby <i>et al.</i> , 2006
Nasopharyngeal cancer (tumours)	STAT3, STAT5	Hsiao <i>et al.</i> , 2003
Ovarian cancer (tumours)	STAT3, STAT5	Chen <i>et al.</i> , 2004
Pancreatic cancer	STAT3	Calo <i>et al.</i> , 2003
Prostate cancer (tumours)	STAT3	Ni <i>et al.</i> , 2002
	STAT6 (selectively)	Mora <i>et al.</i> , 2002
Prostate cancer (cell lines)	STAT3	Mora <i>et al.</i> , 2002
Thyroid cancer (papillary tumours)	STAT3	Trovato <i>et al.</i> , 2003

Additionally, constitutively activated STAT3 has been shown to increase VEGF expression and induce angiogenesis (Niu *et al.*, 2002), and blocking of STAT3 signalling in endothelial cells results in inhibition of migration and proliferation (Yahata *et al.*, 2003).

Furthermore, STAT3 has been shown to inhibit inflammation in various immune cells. In *Stat3*<sup>-/-</sup> macrophages and neutrophils, the expression of pro-inflammatory mediators is significantly upregulated (Takeda *et al.*, 1999). Overproduction of inflammatory cytokines and expansion of myeloid cells result from the loss of STAT3 in bone marrow cells during haematopoiesis (Welte *et al.*, 2003). Consistently, persistent STAT3 signalling decreases the production of pro-inflammatory mediators in tumour cells (Wang *et al.*, 2004). These data indicate that constitutively activated STAT3 leads to the promotion of immune evasion.

#### **1.2.6 Role of STAT signalling in oncogenesis**

STATs are activated by cytokine/growth factor interactions with their cognate receptors, and increasing evidence has shown that activation of STATs may be mediated by JAK and Src family members following ligand stimulation.

Constitutively activated STAT3 has been found in cell lines transformed with v-src and v-abl (Garcia *et al.*, 1997), such as in a human gallbladder adenocarcinoma cell line (Murakami *et al.*, 1998) and in mammary epithelial cells (Smith and Crompton, 1998). In addition, it has been demonstrated that JAK1 and PDGF receptor are required for maximal STAT3 activation in v-src transformed fibroblasts (Zhang *et al.*, 2000). Moreover, the transforming potential of v-src can be increased by wild-type STAT3 and reduced by dominant negative mutants, which suggests a critical role of STAT3 in cell transformation by v-src (Turkson *et al.*, 1998). Both during src transformation and following PDGF-induced mitogenesis, STAT3 promotes the expression of c-myc and exhibits oncogenic potential (Bowman *et al.*, 2001).

In breast cancer cells, the activation of HGF transcription, which promotes survival and growth during progression and metastasis, is induced by co-operatively activated src and STAT3 (Hung and Elliott, 2001). Furthermore, EGF stimulation further increases STAT DNA-binding activity, and biological effects of src and JAK family tyrosine kinases are transmitted at least partially via STAT3 signalling in mammary tumour cells (Garcia *et al.*, 2001).

Similar to STAT3, STAT5a/b can also be constitutively activated by JAK, or bcr-abl (Shuai *et al.*, 1996). Aberrant JAK activation, induced by TEL (translocation-ETS-leukemia) /JAK fusion oncoproteins, dramatically activates STAT5 and causes fatal myelo- and lymphoproliferative diseases (Schwaller *et al.*, 1998). In addition to STAT3, STAT5 has been found to play a role in cell transformation by bcr-abl in leukemia cells, and the use of dominant negative mutants of STAT5 reduces the expression of Bcl-x<sub>L</sub> and suppresses cell growth (de Groot *et al.*, 1999). In line with the fact that STAT1 is generally considered a tumour suppressor, it has been shown that this family member can reduce the expression of c-myc in response to IFNs and PDGF (Ramana *et al.*, 2000).

Based on the above studies, high levels of constitutive STAT3 and 5 activation appear to be important for maintaining malignant properties. The data imply that blocking STAT signalling will not only suppress tumour growth, but may also increase the tumour response to radiotherapy and chemotherapy.

### **1.2.7 Regulation of STAT signalling**

As described in *section 1.2.4*, STAT proteins play an important role in normal cellular processes such as cell growth, apoptosis, differentiation and embryonic development. Nevertheless, aberrant activation of STATs has been found in a large number of human cancers. In this case, disruption of aberrant JAK/STAT signalling exhibits minimal effects on normal cell growth (Turkson *et al.*, 1998; Bromberg *et al.*, 1998), which suggests that STATs and STAT-signalling could represent effective molecular targets for therapeutic intervention.

Tyrosine kinases involved in aberrant activation of STAT, such as JAK, src and bcr-abl, can be considered as possible targets for interrupting STAT signalling in human cancers. Tyrosine phosphatases are known to regulate JAK/STAT pathway by reversing the activity of the JAKs. One of the most detailed studies of phosphatases is SH2-domain phosphatase-1 (SHP-1) which has been shown to directly associate with and dephosphorylate JAK2, and the mechanism by which SHP-1 is also thought to function by binding directly to cytokine receptors to dephosphorylate signaling components (Jiao *et al.*, 1996). Other tyrosine phosphatases, such as CD45, appear to interact with JAKs thus regulating JAK/STAT signalling. Upon IL-3 stimulation, JAK2 is hyperphosphorylated in the absence of CD45 with enhanced JAK2 kinase activity. Consistently, *in vitro* studies showed that CD45 could directly dephosphorylate JAK2 (Greenhalgh and Hilton, 2001).

The suppressor of cytokine signalling (SOCS) family now comprises eight proteins, SOCS-1 to SOCS-7 and cytokine inducible SH2-containing protein (Greenhalgh and Hilton, 2001). Expression of SOCS proteins is induced in response to cellular activation, and SOCSs then inhibit cytokine signalling through a negative feedback loop (Chen *et al.*, 2000). SOCS-1 has been shown to bind to activated JAKs and inhibit their catalytic activity, and SOCS-3 also inhibits JAK activity by binding to the activated receptors. A kinase inhibitor region, which is essential for JAK inhibition, is located in the N-terminal region of both SOCS-1 and SOCS-3 (Chen *et al.*, 2004). Furthermore, the tyrphostin AG490, a JAK2 inhibitor, inhibits cell growth and induces apoptosis by blocking the STAT3 pathway in leukemias (Meydan *et al.*, 1996).

Cytokines or growth factors which bring about STAT activation could also be therapeutic targets. Sant7, an IL-6 antagonist, which is structurally similar to the physiological ligand, but has greater affinity for the receptor, can inhibit STAT3 activation and suppress tumour growth (Dalton and Jove, 1999). Therapeutic antibodies, anti-EGFR (C225) or anti-HER2 (Herceptin) are now used to neutralise specific epitopes on receptors, thus inhibiting interaction with their physiological ligand (Baselga, 2000a, 2000b). Furthermore, ZD1839, also known as Iressa, an orally active, selective EGFR-tyrosine kinase inhibitor, has antitumour activity (Baselga and Averbuch, 2000).

In addition, another effective way is negative regulation of STAT proteins. Phosphorylation and dimerisation of STATs are critical for STAT activation and function. Small phosphotyrosyl-peptides have been reported to block STAT phosphorylation and dimerisation by interacting with SH2 domain of STAT3 (Turkson *et al.*, 2001). Other negative regulators, such as the protein inhibitor of activated STAT (PIAS) family, appear to specifically associate with STAT molecules, thus blocking DNA binding activity (Betz *et al.*, 2001). PIAS proteins possibly function either by interfering with STAT dimerisation, or causing dissociation of activated STAT dimers. Furthermore, cytokine inducible SH2-containing protein, a member of the SOCS family, can compete with STAT5 for binding to the receptors by interacting with phosphorylated receptors (Matsumoto *et al.*, 1997).

Given the important central role of STATs in diverse human cancers and biological processes, increasing attention has focused on negative regulation of STAT signalling pathway. Receptors, JAKs and STATs, are three intermediates in STAT signalling considered as sites for therapeutic intervention.

### **1.3 STATs in bladder cancer**

Studies to date have shown that constitutive activation of STATs is frequently found in a wide variety of human primary tumours. However, none have investigated the status of STATs activation in bladder tumours. Only a few relevant studies have been published, as discussed below.

EGF stimulation can inhibit the growth of T24 human bladder cancer cells, probably via induction of p21<sup>waf1</sup> mediated by STAT1, but does not affect RT4 cells (Kawamata *et al.*, 1999). Itoh *et al.*, (2006) have recently demonstrated that STAT3 activation is required for MMP induction and malignant characteristics in T24 cells. It has been shown that STAT3, activated by EGF via phosphorylation, is then able to induce MMP1 transcription in T24 human bladder cancer cells. STAT3-deficient cells show an inhibition of cell migration and invasion with reduction of MMP (1, 10) levels. Furthermore, blocking of STAT3 with a dominant negative form significantly suppresses tumour formation in mice.

A very recent *in vivo* study has shown that during urothelial tumorigenesis, activation of STAT3 and STAT5 is detected in homozygous *Ink4a/Arf*<sup>-/-</sup> mice, which occurs via AKT signalling and is strongly associated with HRAS hyperactivation (Mo *et al.*, 2007).

Despite these studies, a role for STATs in human bladder cancer is not well established. The molecular changes occurring in TCCs lead to the loss of cell growth regulation, and STATs are known to mediate genes expression involved in cell proliferation. One particular interest in this thesis is the possible involvement of STAT signalling in cell cycle and apoptosis.

### **1.4 Cell cycle**

Cell division is a critical process in the development from a single-cell fertilised egg into a mature organism and in the renewal of some internal organs and cells. The series of events which take place during the formation and replication of a eukaryotic cell constitute the cell cycle. This consists of four distinct phases: G<sub>1</sub> (gap1), S (synthesis), G<sub>2</sub> (gap2) (collectively known as interphase, the interlude between two M phases) and M (mitosis) (Norbury and Nurse, 1992). In M phase, the cell's chromosomes and cytoplasm are divided between the two identical daughter cells. After M phase, each daughter cell begins a new cycle by

entering interphase, during which the cell is constantly producing RNA, synthesising protein and increasing in size. During S phase, all of the chromosomes are replicated. At the end of the G<sub>1</sub>, G<sub>2</sub> and the middle of M phase, checkpoints are designed to ensure that cells are ready to proceed to the next stage of cell division. When cells temporarily or permanently stop dividing, they will quit the cycle and enter a state of quiescence called G<sub>0</sub> phase.

Progression through the cell cycle is regulated by the complexes between cyclins and cyclin-dependent kinases (CDKs). Cyclins are the regulatory subunits and CDKs form the catalytic subunits of the heterodimers. Binding of cyclins to the well-conserved CDKs results in the phosphorylation of CDKs, and the active complexes subsequently activate the target proteins involved in cell cycle progression (Pine, 1995). In contrast to the rise and fall of cyclin protein levels, CDKs remain at stable levels and so far, six of nine identified CDKs are active during the cell cycle. The associations between three D-cyclins and CDK4 or CDK6 are required during G<sub>1</sub> phase. The complex between cyclin E and CDK2 can promote entry into S phase. Additionally, cyclin A in complex with CDK2 further regulates S phase. Driving progression of G<sub>2</sub> to M phase relies on cyclin A interaction with CDK1. The CDK1-cyclin B complex is essential for the entry and continuation through the M phase. Furthermore, transcriptional CDKs, including CDK7, a serine-threonine kinase known as the catalytic subunit of the CDK-activating kinase (CAK) complex, in association with cyclin H and CDK9 in complex with cyclin T, are constitutively expressed throughout the cell cycle (*table 1.4*) (reviewed in Vermeulen *et al.*, 2003; Shapiro, 2006).

The cell cycle is also regulated by the E2F transcription factors, Rb and Rb-associated proteins. As a nuclear phosphoprotein, Rb exists as a hypophosphorylated form in its resting state, and its deregulation is associated with tumourigenesis (Hickman *et al.*, 2002). The formation of CDK-cyclin complexes results in phosphorylation and inactivation of Rb, thus releasing the E2F family members which lead to complexing of cyclin E with CDK2. This complex is required to further phosphorylate Rb and fully activate E2F family members (Jones and Kazlauskas, 2001).

**Table 1.4 Cyclin-CDK complexes are activated at specific points of the cell cycle**

CDK	Cyclin	Cell cycle phase activity
CDK4	Cyclin D1, D2, D3	G <sub>1</sub> phase
CDK6	Cyclin D1, D2, D3	G <sub>1</sub> phase
CDK2	Cyclin E	G <sub>1</sub> /S phase transition
CDK2	Cyclin A	S phase
CDK1	Cyclin A, B	G <sub>2</sub> /M phase transition
CDK1	Cyclin B	Mitosis
CDK7	Cyclin H	CAK, all cell cycle phases
CDK9	Cyclin T	All cell cycle phases

CDKs can be inactivated by CDK inhibitors (CDI) which regulate CDK activity by either binding to CDK directly or binding to the CDK-cyclin complex. Two CDI families have been identified (reviewed in Vermeulen *et al.*, 2003). The INK4 family includes p15 (INK4b), p16 (INK4a), p18 (INK4c) and p19 (INK4d). This family complexes with CDK before cyclin binding and specially inactivates G<sub>1</sub> CDKs. The CIP/KIP family includes p21 (WAF1, CIP1), p27 (CIP2) and p57 (KIP2). In contrast with the INK4 family, these CDIs inactivate the CDK-cyclin complexes. The major cyclins, associated CDKs and their regulators are shown in *figure 1.5*.

The loss of normal cell cycle control is a consequence of alterations in various genes including inactivation of tumour suppressor genes such as pRb and p53 involved in cell division, and results in tumourigenesis via uncontrolled cell proliferation (Vermeulen *et al.*, 2003). Normal urothelium contains wild type p53, pRb, p21 and p27, whereas alterations in each of these four cell cycle regulators are observed in at least 34% of TCCs (Shariat *et al.*, 2007a). Those bladder cancers with alterations in pRb exhibit poor prognosis (Cote *et al.*, 1998). Moreover, the number of markers altered is associated with the increased risk of bladder cancer recurrence and progression, indicating that p53, pRb, p21 and p27 have a cooperative effect in bladder cancer and their combined status can be evaluated as prognostic markers (Shariat *et al.*, 2007b). One of the specific genetic defects in urothelial cell carcinoma is the loss of chromosome 9 where the *CDKN2A/ARF* gene is located and which encodes the p16 protein. It has been shown that p16 expression is statistically and inversely

associated with disease stage (Raspollini *et al.*, 2006). Patients with invasive bladder cancer exhibit significantly higher rate of p16 (INK4a) and p14 (ARF) methylation causing gene silencing than those with superficial bladder cancer (Kawamoto *et al.*, 2006).

In addition, p53 is closely linked with these pathways and plays an important role in proliferation control.

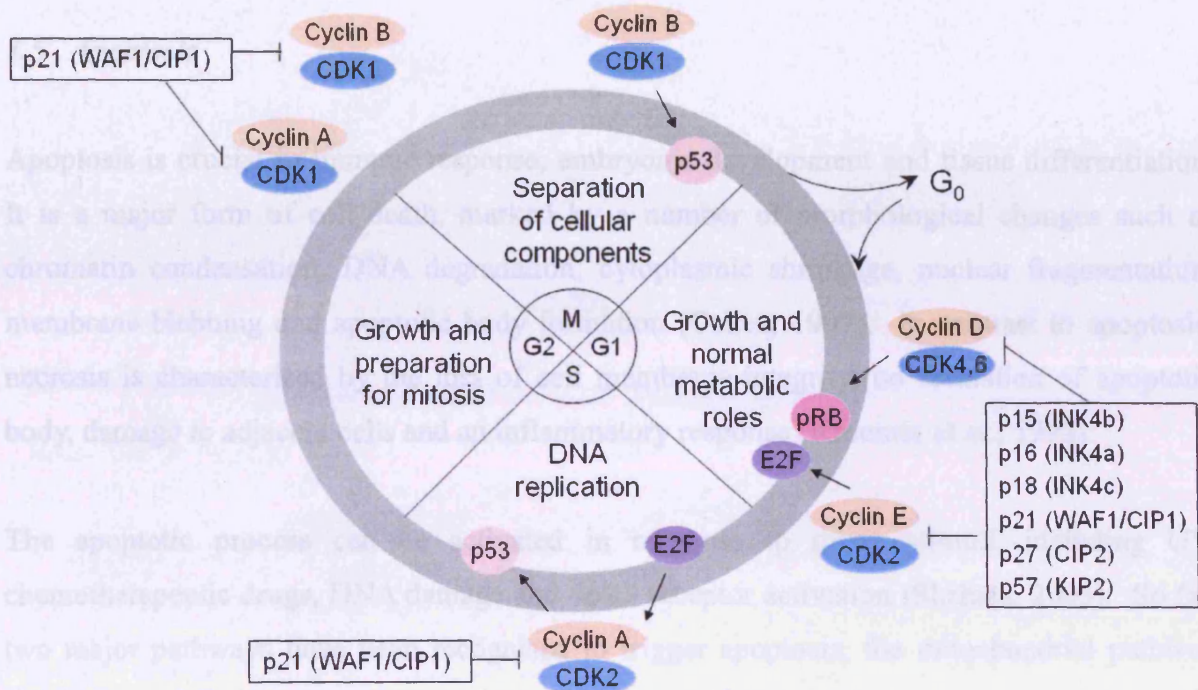


**Figure 1.5 Stages of the cell cycle.** The activation of phase-specific CDK-cyclin complexes and major regulators are indicated. The formation of CDK-cyclin complexes and the activation of CDKs by site specific phosphorylation trigger progression of the cell cycle. The active complexes subsequently activate target proteins involved in cell cycle progression, and the complexes can be inactivated by CDIs resulting in cell cycle arrest.

In addition, amplification of CDKs, cyclins, abnormal activity of CDK activating enzymes, inactivation of CDIs, as well as mutations in checkpoint proteins, have also been reported in cancer (McDonald and Deiry, 2000). Expression of cyclin D1 and E1 are significantly lower in specimens with advanced TCCs than in normal bladder urothelium. Low cyclin E1 (but not cyclin D1) expression is markedly associated with bladder cancer invasion, progression and metastasis (Shariat *et al.*, 2006). In contrast, overexpression of cyclin D1 has also been found in bladder cancer (Chatterjee *et al.*, 2004b). Recently, cyclin D3 overexpression was reported in Ta/T1 bladder cancers, correlated with larger tumour size and high proliferation rates (Lopez-Beltran *et al.*, 2006).

Cell studies have shown that convergence of many cellular signalling pathways ultimately provides the stimulus for cells to proliferate or die. Cell cycle and apoptosis are closely linked with these pathways and play an important role in proliferation control.

### ***1.5 Apoptosis***

Apoptosis is crucial in immune response, embryonic development and tissue differentiation. It is a major form of cell death, marked by a number of morphological changes such as chromatin condensation, DNA degradation, cytoplasmic shrinkage, nuclear fragmentation, membrane blebbing and apoptotic body formation (Cohen, 1997). In contrast to apoptosis, necrosis is characterised by the loss of cell membrane integrity, no formation of apoptotic body, damage to adjacent cells and an inflammatory response (Kroemer *et al.*, 1998).

The apoptotic process can be activated in response to many stimuli, including UV, chemotherapeutic drugs, DNA damage and death receptor activation (Shehata, 2005). So far, two major pathways have been recognised to trigger apoptosis, the mitochondrial pathway (intrinsic) and the death receptor pathway (extrinsic) (*figure 1.6*). Both pathways ultimately depend on the activation of members of the cysteine aspartate specific proteases (caspases) family (Bratton *et al.*, 2000). As key components in the apoptotic process, caspases consist of initiator caspases (such as caspases 8 and 9) and effector caspases (such as caspases 3, 6, 7) (Chen and Wang, 2002). The effector caspases can be activated by either an initiator caspase or an apoptosome complex between a pro-caspase and apoptosis protease activating factor-1 (Apaf-1) (Zhvivotovsky *et al.*, 1999). Caspases exist as inactive zymogens before they become fully activated. The pro-caspase zymogen contains an N-terminal prodomain, a large subunit and a small subunit. The zymogen requires cleaving at a specific aspartic site between large and small subunit to remove the prodomain for caspase activation. A fully active caspase protein exists as a tetramer containing two heterodimers each of which consists of one large and one small subunit (Cohen, 1997).

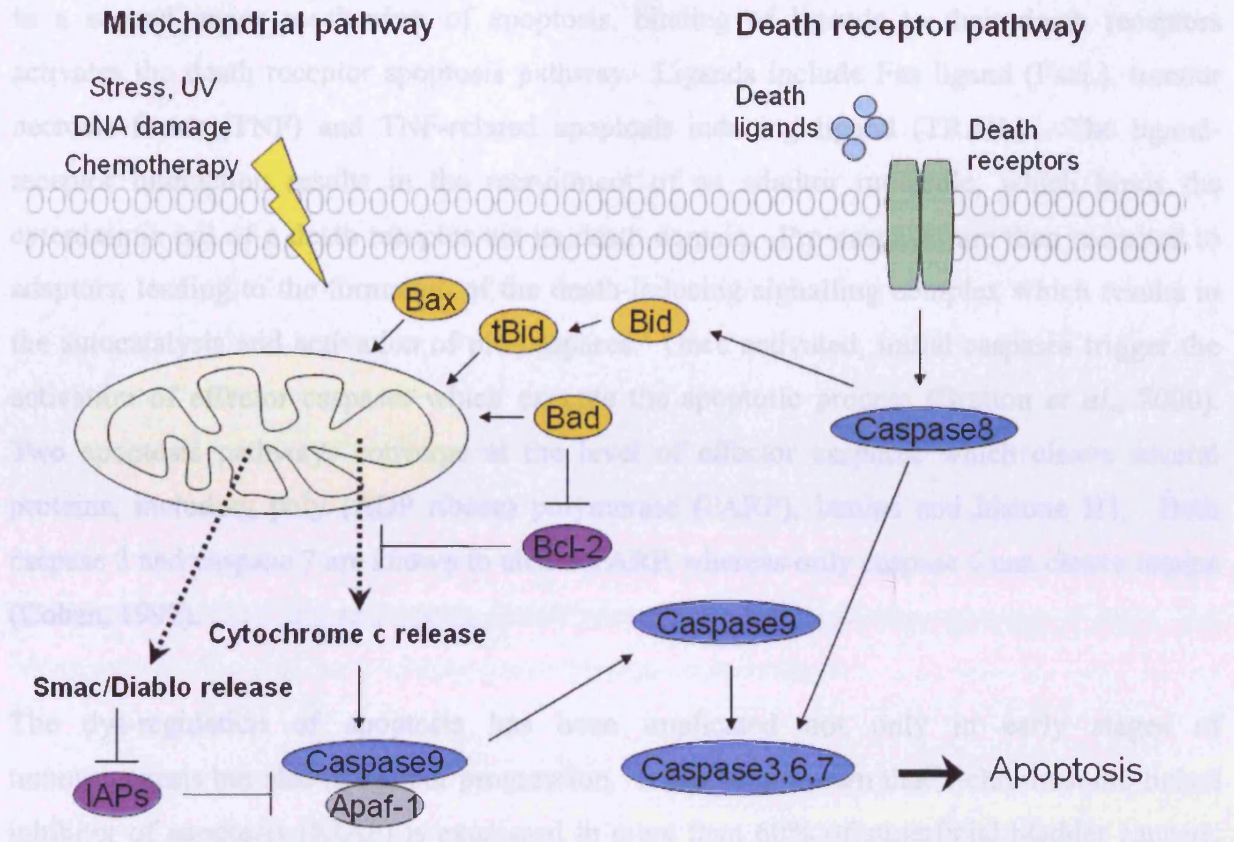


**Figure 1.6 Induction of apoptosis by mitochondrial and death receptor pathways.** In the mitochondrial pathway, cellular stress such as DNA damage causes the translocation of pro-apoptotic proteins (such as Bax, Bid, Bad) to the mitochondria where cytochrome c and Smac/Diablo are released. Cytochrome c then recruits and activates caspase 9. Once activated, caspase 9 triggers the activation of effector caspases. The release of Smac/Diablo can inhibit IAPs which counteract caspase 9. In the death receptor pathway, death ligands such as FasL, TNF and TRAIL bind to death receptors, thus recruiting and activating caspase 8. Active caspase 8 either signals to mitochondria through Bid cleavage or activates effector caspases leading to apoptosis.

The mitochondrial apoptosis pathway is induced by cellular stress such as DNA damage and cytotoxicity. These stimuli result in mitochondrial damage, leading to cytochrome c release into the cytosol. This is associated with the formation of an apoptosome complex by recruitment of pro-caspase via Apaf-1. The apoptosome complex activates pro-caspase into its mature form, in turn activating an effector caspase. The release of cytochrome c is regulated by Bcl-2 family members which consist of pro-apoptotic members (such as Bad, Bax and Bid) and anti-apoptotic members (such as Bcl-2, Bcl-x<sub>L</sub> and Bcl-W). Additionally, other molecules are released from damaged mitochondria, such as Smac/Diablo which counteracts the effect of inhibitor of apoptosis proteins (IAPs) (Bratton *et al.*, 2000).

In a second major mechanism of apoptosis, binding of ligands to their death receptors activates the death receptor apoptosis pathway. Ligands include Fas ligand (FasL), tumour necrosis factor (TNF) and TNF-related apoptosis inducing ligand (TRAIL). The ligand-receptor interaction results in the recruitment of an adaptor molecule, which binds the cytoplasmic tail of a death receptor via its death domain. Pro-caspases are then recruited to adaptors, leading to the formation of the death-inducing signalling complex which results in the autocatalysis and activation of pro-caspases. Once activated, initial caspases trigger the activation of effector caspases which execute the apoptotic process (Bratton *et al.*, 2000). Two apoptosis pathways converge at the level of effector caspases which cleave several proteins, including poly (ADP ribose) polymerase (PARP), lamins and histone H1. Both caspase 3 and caspase 7 are known to cleave PARP, whereas only caspase 6 can cleave lamins (Cohen, 1997).

The dys-regulation of apoptosis has been implicated not only in early stages of tumourigenesis but also in tumour progression. It has been shown that x chromosome-linked inhibitor of apoptosis (XIAP) is expressed in more than 60% of superficial bladder cancers, and its level apparently increases in poorly differentiated tumours (Li *et al.*, 2007). The methylation frequencies of Apaf-1 and death-associated protein kinase-1 (DAPK-1) in TCC of the bladder have recently been observed to be dramatically higher than those in normal bladder tissues (Christoph *et al.*, 2006). Alterations in Bcl-2, p53 and MDM2 have been observed in at least 37% of patients with muscle-invasive TCC of the bladder, and patients with all three markers aberrantly expressed have shown short-term survival (Maluf *et al.*, 2006).

Another molecular event associated with tumourigenesis and progression of bladder cancer is metastasis. The more deeply tumours spread within the bladder, the more aggressive and invasive the disease becomes.

## **1.6 Metastasis**

Metastasis is the spread to distant sites of malignant cells detached from the primary tumour, and is the major cause of death from cancer. Metastasis involves a series of discrete events occurring in sequence: cellular transformation and primary tumour growth is followed by extensive vascularisation, which supplies nutrients for cell expansion and establishes a capillary network as a migratory route from the primary tumour for cancer cells. Tumour cells then locally invade the host stroma, as well as blood vessels or lymphatics (intravasation), which have little resistance to penetration by tumour cells, thus providing the most common entry of tumour cells into the circulation. After surviving in the circulation, tumour cells arrest in capillaries, then either proliferate in these vessels or invade into adjacent organ parenchyma (extravasation) which completes the metastatic process (Gupta and Massague, 2006). *Figure 1.7* shows the main steps in metastasis.

Cell migration is essential for normal physiology such as embryonic development, homeostasis of the immune system and in response to pathological events like wound healing. Cell motility relies on the cell's ability to sense chemoattractants such as chemokines and growth factors. Such factors, in complex with their specific receptors on the cell membrane, activate pathways which alter the cell cytoskeleton and motility, thus regulating cell migration (Kedrin *et al.*, 2007).

To migrate, cells undergo a physically integrated molecular process, involving polarisation and elongation of cells; formation of cell protrusions (pseudopods) via membrane extension; attachment to the extracellular matrix (ECM) and the use of contractile forces and traction, leading to the gradual forward gliding of cells (Lauffenburger and Horwitz, 1996).

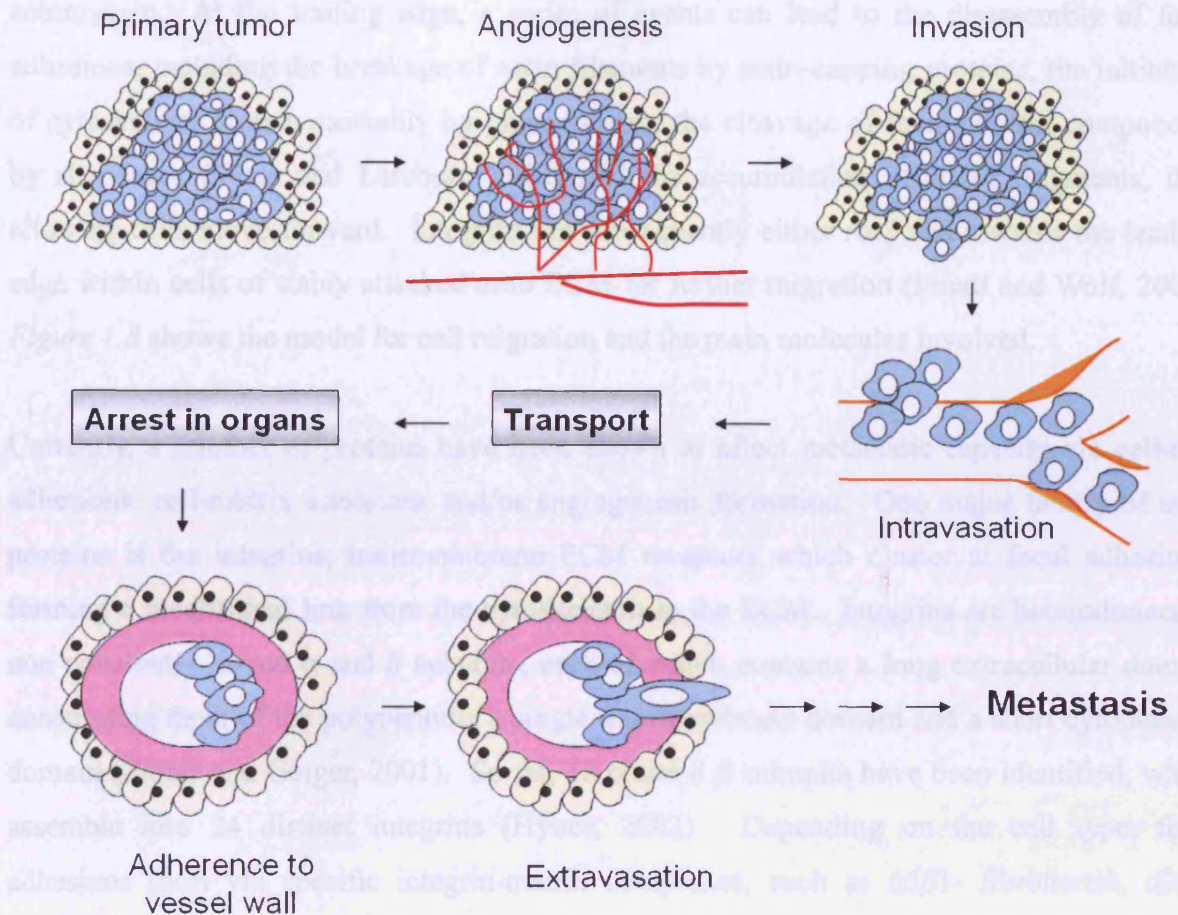


**Figure 1.7 The main steps in the formation of metastasis.** After extravasation, tumour cells must develop a micro-vascular network within the organ to continue growth, thus invading blood vessels, entering circulation and forming further metastasis (Fidler, 2003).

In both normal and cancer cells, cell extension is essential for the initiation and maintenance of cell motility. Cell protrusions, diverse in morphology and dynamics, can initiate ECM recognition and interaction. Actin polymerisation at filament ends leads to the propulsion and elongation of pseudopods. Cell protrusions then dynamically interact with ECM via the integrin family of adhesion molecules, which are clustered in the cell membrane. Integrins recruit actin-binding proteins, such as  $\alpha$ -actinin, talin, tensin and the focal adhesion kinase (FAK), via direct association with their intracellular domain, and vinculin and paxillin thus forming focal adhesions. In the vicinity of cell-ECM contacts, cleavage of ECM components by surface proteases induces the formation of active soluble MMPs which are able to further degrade small ECM fragments cleaved by MT1 (membrane-type) -MMP. Cell contraction is driven by actomyosin which is the complex between active myosin II and actin filaments.  $\text{Ca}^{2+}$ , calmodulin and the small G protein Rho have been reported to regulate the function of

actomyosin. At the trailing edge, a series of events can lead to the disassembly of focal adhesions, including the breakage of actin filaments by actin-capping proteins, the inhibition of cytoskeletal protein assembly by phosphatases, the cleavage of focal contact components by sheddases (Moss and Lambert, 2002) and the accumulation of ECM fragments, thus allowing cells move forward. Integrins are subsequently either recycled towards the leading edge within cells or stably attached onto ECM for further migration (Friedl and Wolf, 2003). *Figure 1.8* shows the model for cell migration and the main molecules involved.

Currently, a number of proteins have been shown to affect metastatic capacity via cell-cell adhesions, cell-matrix adhesions and/or angiogenesis formation. One major family of such proteins is the integrins, transmembrane ECM receptors which cluster at focal adhesions, forming a mechanical link from the cytoskeleton to the ECM. Integrins are heterodimers of non-covalently linked  $\alpha$  and  $\beta$  subunits, each of which contains a long extracellular domain constituting most of the polypeptide, a single transmembrane domain and a short cytoplasmic domain (Zamir and Geiger, 2001). So far, 18  $\alpha$  and 8  $\beta$  subunits have been identified, which assemble into 24 distinct integrins (Hynes, 2002). Depending on the cell type, focal adhesions form via specific integrin-matrix complexes, such as  $\alpha 5 \beta 1$ - fibronectin,  $\alpha 2 \beta 1$ - collagen,  $\alpha v \beta 3$ - fibronectin/vitronectin and  $\alpha 6 \beta 1 / \alpha 6 \beta 4$ - laminin (Friedl and Wolf, 2003). In a wide variety of cells, fibronectin is expressed and exists as a dimer consisting of two covalently linked, nearly identical subunits. There are 20 variants of human fibronectin due to the alternative splicing of a single pre-mRNA. Fibronectin is known to be a ligand for a twelve integrin receptors (reviewed in Pankov and Yamada, 2002). Collagens are triple helical proteins which exist throughout the body. Among 28 different types of collagens occurring in vertebrates, the majority are homotrimers. However, they can be heterotrimeric, such as collagen I containing two identical  $\alpha$  chains and a third different chain (reviewed in Kadler *et al.*, 2007).

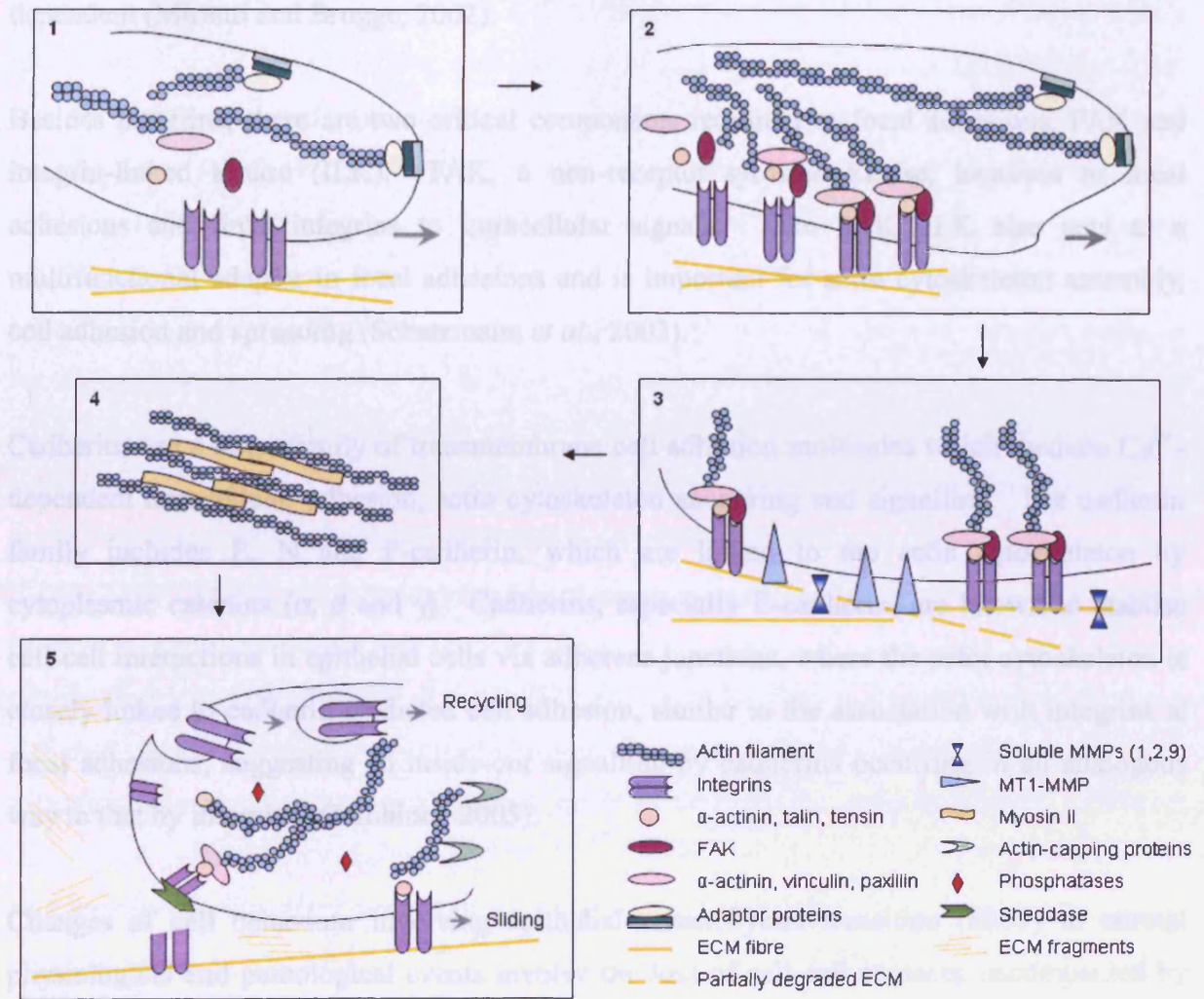


**Figure 1.8 Model for cell migration and the main molecules involved.** Step 1 – protrusion at the leading edge. Step 2 – formation of focal adhesions and interaction of cell-matrix. Step 3 – proteolysis of ECM components. Step 4 – contraction by actomyosin. Step 5 – release of the trailing edge (Friedl and Wolf, 2003).

Integrins occur as inactive molecules, neither binding ligands nor transducing signals at the cell surface, but their activation can be induced by either ligand binding or effects on their intracellular domain, indicating bi-directional signalling (Hynes, 2002). It has been shown that integrin signals are involved in broader functions in cell behaviour in addition to cytoskeleton anchorage, including cell survival, proliferation, cell cycle and differentiation. Detachment from the ECM results in cell death by anoikis via activation of pro-apoptotic proteins and inhibition of anti-apoptotic proteins by integrins. Additionally, it has been found that modulation of the activation of several CDKs involved in G<sub>1</sub>/S phase is integrin-

dependent (Miranti and Brugge, 2002).

Besides integrins, there are two critical components recruited to focal adhesions, FAK and integrin-linked kinase (ILK). FAK, a non-receptor tyrosine kinase, localises to focal adhesions and links integrins to intracellular signals. Like FAK, ILK also acts as a multifunctional adaptor in focal adhesions and is important for actin cytoskeleton assembly, cell adhesion and spreading (Schatzmann *et al.*, 2003).

Cadherins are a large family of transmembrane cell adhesion molecules which mediate  $Ca^{2+}$ -dependent intracellular adhesion, actin cytoskeleton anchoring and signalling. The cadherin family includes E, N and P-cadherin, which are linked to the actin cytoskeleton by cytoplasmic catenins ( $\alpha$ ,  $\beta$  and  $\gamma$ ). Cadherins, especially E-cadherin, are known to stabilise cell-cell interactions in epithelial cells via adherens junctions, where the actin cytoskeleton is closely linked to cadherin-mediated cell adhesion, similar to the association with integrins at focal adhesions, suggesting an inside-out signalling by cadherins occurring in an analogous way to that by integrins (Gumbiner, 2005).

Changes of cell behaviour involving epithelial-mesenchymal transition (EMT) in normal physiological and pathological events involve the loss of cell-cell contacts, accompanied by increased cell motility on ECM, indicating crosstalk between cadherins and integrins (Chen and Gumbiner, 2006). Three mechanisms for integrin-cadherin coordination have been reported. Firstly, growth factor-induced scattering of epithelial cells is associated with increased integrin-mediated adhesion and the loss of cadherins at the cell periphery, but with no effect on cadherin adhesion activity. Actomyosin contractility induced by integrin-ECM adhesion has been shown to be responsible for the disruption of cadherin-mediated adhesion (de Rooij *et al.*, 2005). Secondly, several transcription factors such as Twist, Snail and Slug induce EMT by inhibition of cell-cell adhesion protein expression and induction of genes mediating cell migration (Kang and Massague, 2004). Expression of SIP1 (Smad interacting protein-1) in human epithelial A431 cells results in EMT, which is accompanied by cadherin switching, resulting in repression of E-cadherin and induction of N-cadherin (Vandewalle *et al.*, 2005). Also, it has been shown that Slug (Bolos *et al.*, 2003) and Zeb-1 (Aigner *et al.*, 2007) downregulate E-cadherin expression and induce EMT. Snail has been known to be involved not only in E-cadherin downregulation but also in repression of tight junction

proteins, such as Claudin -1 and ZO-1 (Zonula occludens-1) (Ohkubo and Ozawa, 2004). Moreover, there is evidence that induction of N-cadherin results from integrin-dependent nuclear translocation of Twist (Alexander *et al.*, 2006), suggesting that integrin-induced changes in cell differentiation lead to effects on cadherins and cell-cell contacts. Thirdly, cadherins and cell-cell adhesion are also known to be regulated by integrin-mediated adhesion via a signalling pathway involving FAK and src. It has been shown that FAK decreases cell motility, leading to accumulation of N-cadherin at cell-cell contacts through integrin signalling (Yano *et al.*, 2004). In addition, Src induced adhesion to collagen I triggers the recruitment of FAK to E-cadherin complexes, resulting in the loss of E-cadherin expression and adhesion (Koenig *et al.*, 2006). Furthermore, many studies have shown that Src and FAK are critical in integrin-cadherin cross-regulation (Avizienyte and Frame, 2005).

In human normal bladder tissues, E-cadherin and various catenins show homogeneous membrane localisation (Syrigos *et al.*, 1998), and loss of E-cadherin has also been viewed as a dominant factor in bladder cancer progression (Imao *et al.*, 1999). Studies have shown an important role in tumourigenesis of  $\alpha 6\beta 4$  integrin, which is the most commonly expressed integrin located at the basal layer of normal urothelium (Grossman *et al.*, 2000). However in bladder cancer cells significant reduction of integrin  $\beta 4$  has been observed accompanied by overexpression of  $\alpha 6\beta 1$  integrin (Harabayashi *et al.*, 1999). Interestingly, inhibition of  $\beta 1$  integrin causes marked reduction of adhesion and migration in T24 bladder line (Heyder *et al.*, 2005).

Invasive bladder cancer, which can develop either from superficial papillary tumours or CIS, exhibits a significant metastatic potential, so identification of molecules that initiate metastasis in cancer cells may be useful in prevention therapy.

Currently, the existing therapies, whether they are surgical, radiological or drug based, generally have little success in many cases. Chemoprevention, using natural or synthetic chemicals to reverse the onset, suppress or prevent the development of carcinogenesis process (Gescher *et al.*, 1998) therefore constitutes a novel approach to cancer therapy.

## **1.7 Cancer chemoprevention**

In the last a few decades, the incident and cure rates of cancer have not improved, despite a much better understanding of the process of tumourigenesis (Reddy *et al.*, 2003). With some conventional treatments (such as surgery, radiotherapy or chemotherapy) seemingly approaching their limit, chemoprevention strategies are becoming increasingly seen as a promising approach to reducing the incidence of cancer.

Dietary habits and tobacco smoke are the two leading causes of cancer, and as such, a healthier lifestyle may contribute significantly to prevention of cancer. Epidemiological evidence has shown that a high intake of fruits and vegetables can decrease the risk of some common cancers and may also be associated with improved survival of patients (Reddy *et al.*, 2003; Tsugane and Sasazuki, 2007; Pierce *et al.*, 2007). Fruits and vegetables are rich sources of many bioactive compounds including vitamins, polyphenols, alkaloids and terpenes. Dietary phytochemicals, such as indole-3-carbinol (I3C), 3,3'-diindolylmethane (DIM), curcumin, (-)- epigallocatechin-3-gallate (EGCG), resveratrol and genistein, have shown protective effects, suggesting a role as chemopreventive agents in various stages of cancer as well as for other chronic diseases (Howells *et al.*, 2007).

Tumourigenesis is a multistep process, characterised by three stages:

1) Initiation is triggered by mutations in DNA which if not repaired, can eventually disrupt the normal balance between proliferation and cell death. Chemopreventive agents that can prevent or reduce DNA damage at this stage are called blocking agents. These dietary agents can act as antioxidant molecules, able to scavenge reactive oxygen species (ROS), as well as altering the metabolism of pro-carcinogenic molecules. The physiological homeostasis of ROS maintains important cellular processes in normal cells, while increased ROS production has been observed in cancer cells and is associated with DNA damage and multistep carcinogenesis. The rationale behind the protective effects of blocking agents includes: modifying phase I/II drug metabolising enzymes by which a pro-carcinogen is converted to an ultimate carcinogen, scavenging ROS and other oxidative species, and altering DNA repair rates (Manson, 2003; Russo, 2007). Initiation is the earliest stage of carcinogenesis in the absence of adequate DNA repair. If prevention at this stage does not succeed, carcinogenesis will progress with the accumulation of DNA damage.

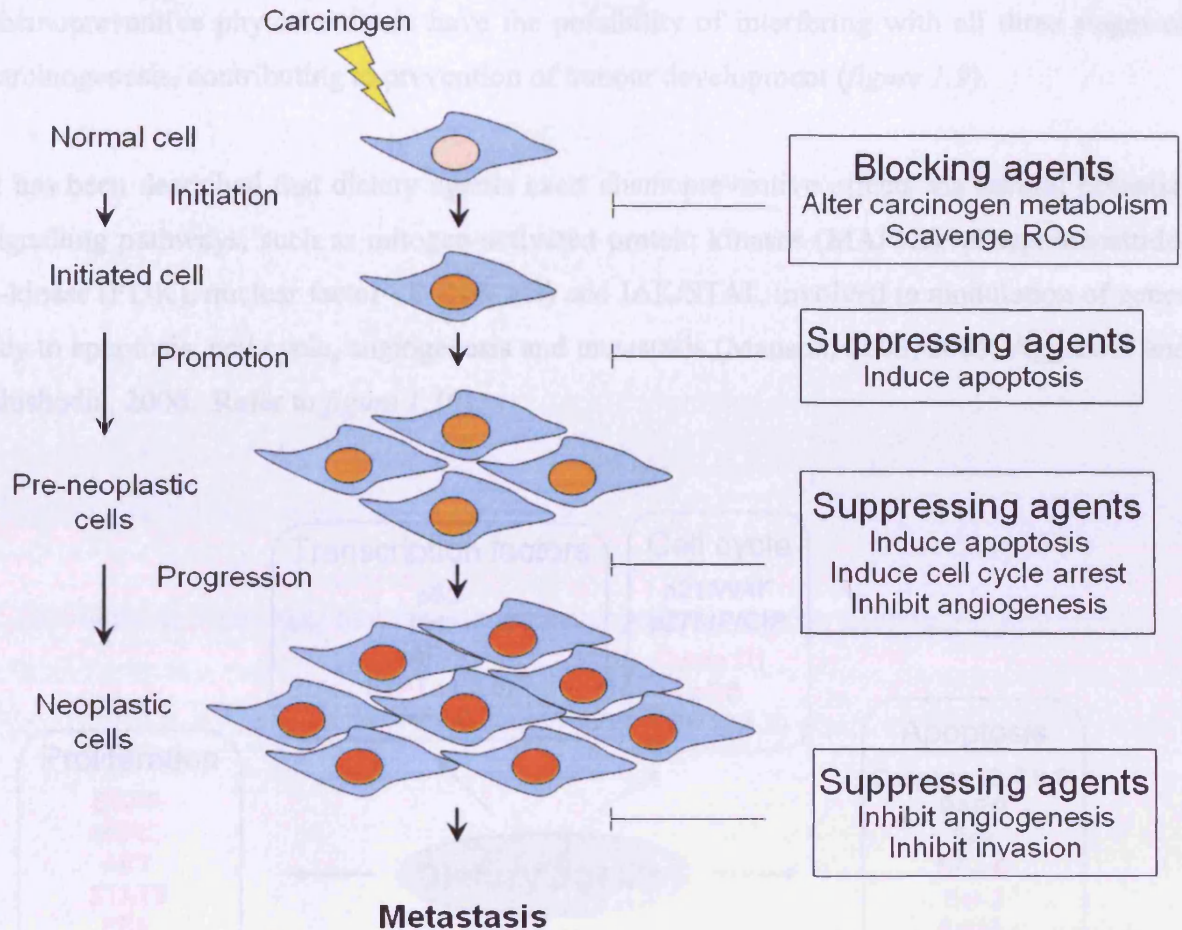


**Figure 1.9 Chemoprevention during carcinogenesis.** Possible stages in carcinogenesis targeted by blocking or suppressing agents and some molecular mechanisms involved (Surh, 2003).

2) Promotion is considered to be an ongoing and reversible process, in contrast to initiation. The accumulation of actively proliferating initiated cells offers a cellular population for further progression of tumourigenesis.

3) Progression, a further clonal expansion procedure, may subsequently result in the formation of tumour with invasive and metastatic potential. Chemopreventive agents which inhibit the malignant transformation of initiated cells in either promotion or progression stage are called suppressing agents. Suppressing agents can not only block or reverse the progression of initiated cells into pre-neoplastic ones, but also halt or slow down the development of malignant stages (promotion to progression). Suppressing mechanisms include alterations in key oncogenes and tumour suppressors, induction of apoptosis, cell cycle arrest and inhibition of angiogenesis and invasion (Manson *et al.*, 2000). Taken together,

chemopreventive phytochemicals have the possibility of interfering with all three stages of carcinogenesis, contributing to prevention of tumour development (*figure 1.9*).

It has been described that dietary agents exert chemopreventive effects via several potential signalling pathways, such as mitogen-activated protein kinases (MAPKs), phosphoinositide-3-kinase (PI3K), nuclear factor- $\kappa$ B (NF- $\kappa$ B) and JAK/STAT, involved in modulation of genes key to apoptosis, cell cycle, angiogenesis and metastasis (Manson, 2003, 2005; Aggarwal and Shishodia, 2006. Refer to *figure 1.10*).

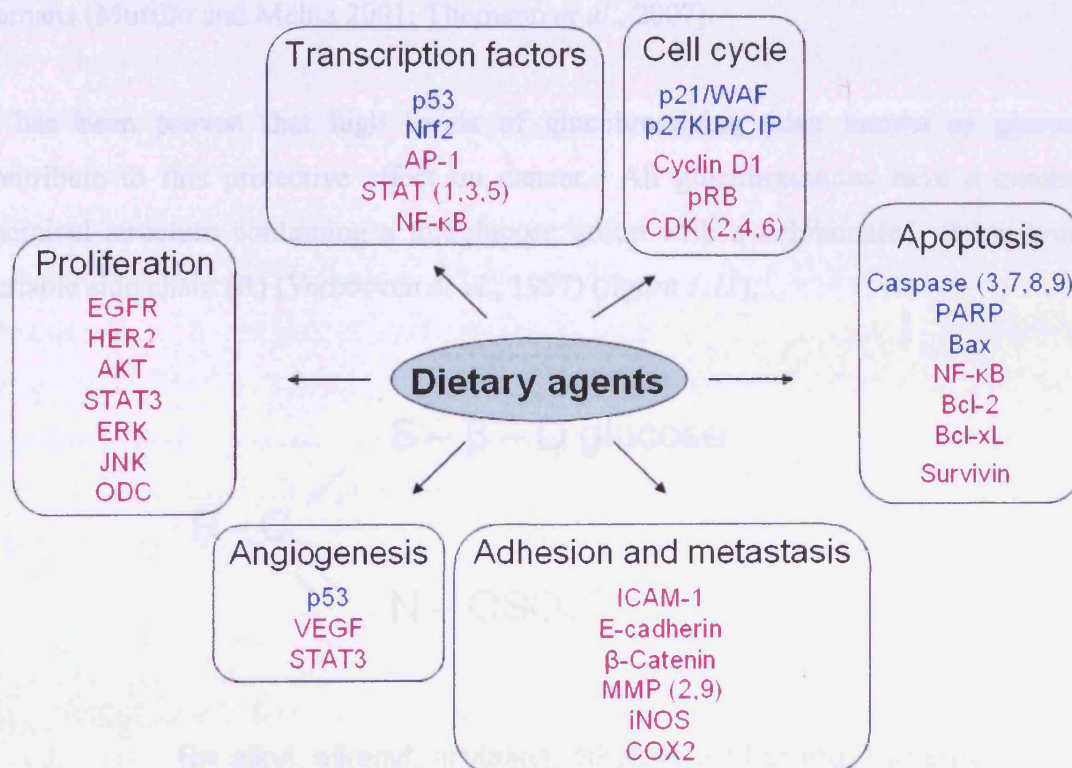


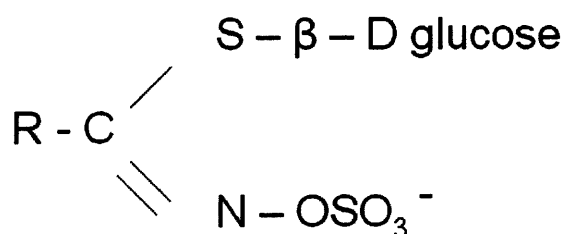
**Figure 1.10 Molecular targets of dietary agents.** The diagram illustrates some of the proteins modulated by dietary agents (but does not imply that these molecules are direct targets of dietary agents). Blue/Pink denotes an increase/decrease in the levels, phosphorylation status or activity of the various components.

Abbreviations: AP-1, activator protein-1; COX2, cyclooxygenase 2; ERK, extracellular regulated kinase; HER2, EGFR family member ERBB2; ICAM-1, intercellular adhesion molecule 1; iNOS, inducible nitric oxide synthase; JNK, c-jun N-terminal kinase; Nrf2, nuclear erythroid 2 p45-related factor 2; ODC, ornithine decarboxylase.

## 1.8 Indoles

Characteristics for good chemopreventive potential include: nontoxic, efficacious, inexpensive and available in ingestible form. The Cruciferae family is one group of vegetables which has been widely regarded as having potential anticarcinogenic activity. Cruciferous vegetables, particular those of the *Brassica* genus such as broccoli, cabbage, Brussels sprouts and cauliflower, have been found to possess chemopreventive properties. Increased consumption of cruciferous vegetables or active compounds present in these vegetables has shown a positive influence on carcinogenesis and against cancer recurrence in humans (Murillo and Mehta 2001; Thomson *et al.*, 2007).

It has been proven that high levels of glucobrassicins (also known as glucosinolates) contribute to this protective effect on cancer. All glucobrassicins have a common basic chemical structure containing a thioglucose group with a sulphonated oxime group and a variable side chain (R) (Verhoeven *et al.*, 1997) (*figure 1.11*).



R= alkyl, alkenyl, arylalkyl, alkylthioalkyl or indolylmethyl

*Figure 1.11 Chemical structure of glucobrassicins.*

### 1.8.1 Chemistry of I3C and DIM

Once cruciferous vegetables are physically damaged by cutting or chewing, the enzyme myrosinase is released to initiate the glucobrassicin hydrolysis. The products of hydrolysis mainly depend on the side chain of the glucobrassicin, and as such, glucobrassicins with an indole side chain, which are predominant in brassica vegetables, form indoles. At neutral pH glucobrassicin hydrolysis forms an unstable isothiocyanate, which degrades to a thiocyanate ion and indole-3-carbinol (I3C). I3C may then form condensation products at acid pH, such



Some *in vivo* studies have shown that effects of I3C may be attributed to its acid condensation products, such as DIM, and not to I3C itself (reviewed in Verhoeven *et al.*, 1997). Additionally, it has been demonstrated that DIM is a more potent inhibitory agent compared with I3C in C33A, human cervical cancer cells (Chen *et al.*, 2001) and DU145, human prostate cancer cells (Garikapaty *et al.*, 2006).

In mice, DIM, which is produced in the stomach after consumption of cruciferous vegetables, has an inhibitory effect on prostate cancer (Nachshon-Kedmi *et al.*, 2004a) and cervical cancer (Chen *et al.*, 2001). Many *in vitro* studies have shown anti-proliferative and pro-apoptotic effects of DIM in human breast cells (Rahman and Sarkar, 2005; Rahman *et al.*, 2006), prostate cancer cell lines (Nachshon-Kedmi *et al.*, 2004b; Li *et al.*, 2007), colon cancer cells (Kim *et al.*, 2007), pancreatic cancer cells (Abdelrahim *et al.*, 2006), hepatoma HepG2 cells (Gong *et al.*, 2006) and thyroid cancer cell lines (Tadi *et al.*, 2005). *Table 1.5* shows a summary of *in vivo* and *in vitro* studies undertaken with I3C and DIM acting as inhibitory agents, demonstrating that the role as tumour inhibitors is not cell-type specific.

During the past two or three decades, there has been a better understanding of how certain dietary agents can alter carcinogenesis. Using cDNA microarray, the effect of I3C and DIM on gene expression has been investigated in PC3 human prostate cancer cells (Li *et al.*, 2003). After 24 hours of DIM treatment, 738 genes show a greater than two-fold change, with downregulation of 677 genes and upregulation of 61 genes. Similarly, a total of 727 genes have a greater than two-fold change in expression after 24 hours of I3C treatment, among which 685 are downregulated and 42 are upregulated. More importantly, molecules found to be specifically modulated by I3C and DIM are critically involved in the regulation of proliferation, cell cycle, apoptosis, angiogenesis and metastasis.

I3C can significantly inhibit NF- $\kappa$ B DNA binding activity and induce apoptosis in human prostate cancer cells (Chinni *et al.*, 2001), and has also been found to suppress NF- $\kappa$ B activation, leading to the inhibition of NF- $\kappa$ B regulated gene expression (including cyclin D1, COX2, MMP9, survivin, IAP1, XIAP, Bcl-2) and the potentiation of apoptosis in myeloid and leukemia cells (Takada *et al.*, 2005). Similarly, DIM induces apoptosis of breast cancer cells by inactivation of NF- $\kappa$ B (Rahman and Sarkar, 2005), and represses NF- $\kappa$ B downstream target genes, MMP9 and urokinase-type plasminogen activator (uPA), which in turn inhibits invasion and angiogenesis (Kong *et al.*, 2007).

**Table 1.5 Summary of studies using I3C and DIM as cancer chemopreventive agents**

Agent	<i>In vivo/ in vitro</i>	Model	Cancer type	References
<b>I3C</b>				
	<i>in vivo</i>	Rodents	Breast	Stoner <i>et al.</i> , 2002
	<i>in vivo</i>	Rat	Breast	Grubbs <i>et al.</i> , 1995
	<i>in vivo</i>	Mouse	Bone marrow	Agrawal <i>et al.</i> , 1999
	<i>in vivo</i>	Rat	Colon	Wargovich <i>et al.</i> , 1996; Xu <i>et al.</i> , 1996
	<i>in vivo</i>	Rat	Lung	Arif <i>et al.</i> , 2000
	<i>in vivo</i>	Mouse	Skin	Srivastava and Shukla, 1998
	<i>in vivo</i>	Rat	Liver	Manson <i>et al.</i> , 1998; Kassie <i>et al.</i> , 2003
	<i>in vivo</i>	Mouse	Liver	Oganesian <i>et al.</i> , 1997;
	<i>in vitro</i>	Human	Breast	Howells <i>et al.</i> , 2002; Rahman <i>et al.</i> , 2004
	<i>in vitro</i>	Human	Pancreas	Lian <i>et al.</i> , 2004
	<i>in vitro</i>	Human	Prostate	Chinni and Sarkar, 2002
	<i>in vitro</i>	Human	Melanoma	Kim <i>et al.</i> , 2006
	<i>in vitro</i>	Human	Myeloid	Takada <i>et al.</i> , 2005
	<i>in vitro</i>	Human	Leukemia	Takada <i>et al.</i> , 2005
<b>DIM</b>				
	<i>in vivo</i>	Mouse	Prostate	Nachshon-Kedmi <i>et al.</i> , 2004a
	<i>in vivo</i>	Mouse	Cervix	Chen <i>et al.</i> , 2001
	<i>in vitro</i>	Human	Breast	Rahman and Sarkar, 2005; Rahman <i>et al.</i> , 2006
	<i>in vitro</i>	Human	Colon	Kim <i>et al.</i> , 2007
	<i>in vitro</i>	Human	Prostate	Nachshon-Kedmi <i>et al.</i> , 2004b; Li <i>et al.</i> , 2007
	<i>in vitro</i>	Human	Cervix	Chen <i>et al.</i> , 2001
	<i>in vitro</i>	Human	Pancreas	Abdelrahim <i>et al.</i> , 2006
	<i>in vitro</i>	Human	Thyroid	Tadi <i>et al.</i> , 2005
	<i>in vitro</i>	Human	Liver	Gong <i>et al.</i> , 2006

Akt has also been shown to be an important target for I3C and DIM, with a decrease in phosphorylated Akt in I3C-treated prostate cancer cells, (Li *et al.*, 2003). In breast cancer cells, inactivation of Akt and induction of apoptosis are induced by DIM (Rahman and Sarkar, 2005). Additionally, I3C and DIM exert an inhibitory effect on MAPK pathway in prostate cancer cells (Li *et al.*, 2003).

In addition to inactivation of NF- $\kappa$ B, Akt and MAPK, upregulation of caspase 3, 7, 8, 9, cleavage of PARP, inhibition of Bcl-2 and repression of survivin have been shown to be involved in apoptosis induced by I3C or DIM in many different human cancer cells (Kim *et al.*, 2006; Kim *et al.*, 2007; Nachshon-Kedmi *et al.*, 2004b; Rahman *et al.*, 2006).

In human LNCaP prostate cancer cells, I3C selectively inhibits both the transcripts and protein levels of CDK6, markedly reduces CDK2 enzymatic activity and strongly increases the expression of p16 CDK inhibitor (Zhang *et al.*, 2003), and similar observations were also made in MCF7 human breast cancer cells (Cover *et al.*, 1998). It also induces p21 CDK inhibitor and G<sub>1</sub> cell cycle arrest which require p53 activation (Hsu *et al.*, 2006). Similarly, I3C treatment causes p53-dependent G<sub>1</sub> arrest and upregulation of p21 in human breast cancer cells (Brew *et al.*, 2006). However, DIM treated breast cancer cells show a G<sub>1</sub> arrest and activation of p21 (WAF1/CIP1) expression independently of p53 (Hong *et al.*, 2002). The expression of cell cycle-related proteins, such as cyclin E, p27 (KIP1), and CDK2 are modulated by I3C in breast cancer cell lines (Garcia *et al.*, 2005). EGFR and src are shown to be involved in I3C-induced cell death and cell cycle in human breast cancer cells (Moiseeva *et al.*, 2007). Firestone and Bjeldanes (2003) have shown that DIM accumulates in the nucleus of I3C- treated cells, suggesting a role in the transcriptional activities of I3C. It induces a G<sub>1</sub> cell cycle arrest, accompanied by inhibition of CDK6 and stimulation of p21 (WAF1/CIP1) gene expression.

The androgen receptor (AR) which is expressed in nearly all human prostate cancers plays an important role in mediation of proliferation and differentiation in prostate. I3C treatment inhibits AR expression and responsiveness (Hsu *et al.*, 2005). Moreover, it has also been found that DIM has an inhibitory effect on AR phosphorylation, expression and nuclear translocation, suggesting that it is also an androgen antagonist (Bhuiyan *et al.*, 2006).

**Table 1.6 Summary of cell signalling components modulated by I3C and DIM**

Agent	Cancer type	Altered molecules	References
<b>I3C</b>			
	Prostate	NF- $\kappa$ B ↓	Chinni <i>et al.</i> , 2001
	Myeloid	NF- $\kappa$ B ↓	Takada <i>et al.</i> , 2005
	Leukemia	NF- $\kappa$ B ↓	Takada <i>et al.</i> , 2005
	Prostate	Akt ↓ MAPK ↓	Li <i>et al.</i> , 2003
	Prostate	p53 ↑ p21 ↑	Hsu <i>et al.</i> , 2006
	Prostate	CDK2,6 ↓ p16 ↑	Zhang <i>et al.</i> , 2003
	Breast	p53 ↑ p21 ↑	Brew <i>et al.</i> , 2006
	Breast	Cyclin E ↑ p21 ↑ p27 ↑	Moiseeva <i>et al.</i> , 2007
	Breast	CDK2 ↓	Garcia <i>et al.</i> , 2005
	Prostate	AR ↓	Hsu <i>et al.</i> , 2005
	Breast	ER ↓	Meng <i>et al.</i> , 2000; Fan <i>et al.</i> , 2006
	Pancreas	STAT3 ↓	Lian <i>et al.</i> , 2004
	Melanoma	Bcl-2 ↓	Kim <i>et al.</i> , 2006
<b>DIM</b>			
	Breast	NF- $\kappa$ B ↓ Akt ↓	Rahman and Sarkar, 2005
	Breast	Survivin ↓ Bcl-2 ↓ cdc25a ↓ p21 ↑	Rahman <i>et al.</i> , 2006
	Breast	p21 ↑	Hong <i>et al.</i> , 2002
	Prostate	Akt ↓	Garikapaty <i>et al.</i> , 2006
	Prostate	MAPK ↓	Li <i>et al.</i> , 2003
	Prostate	MMP9 ↓ uPA ↓	Kong <i>et al.</i> , 2007
	Prostate	Caspase (3,6,9) ↑ PARP cleavage ↑	Nachshon-Kedmi <i>et al.</i> , 2004a
	Prostate	AR ↓	Bhuiyan <i>et al.</i> , 2006
	Colon	Caspase (3,7,8,9) ↑ Fas ↑ tBid ↑	Kim <i>et al.</i> , 2007

I3C is known as a negative regulator of estrogen due to its repression of estrogen receptor (ER) transcription activity and estrogen-responsive gene expression (Meng *et al.*, 2000; Fan *et al.*, 2006). On the other hand, I3C can induce G<sub>1</sub> cell cycle arrest independently of ER signalling in human breast cancer cells (Cover *et al.*, 1998).

STAT3 is also target molecule of I3C (Lian *et al.*, 2004). However, since very few published papers indicate that members of the STAT family are downregulated by chemopreventive compounds, more in depth studies are needed to fully elucidate the mechanisms of actions. *Table 1.6* shows a summary of modulation by I3C and DIM of cell signalling components taken from recent studies.

Besides anticarcinogenic properties, indoles have also shown some adverse effects. In rats, I3C treatment (10 days with 50mg/kg body weight) caused hepatotoxicity via upregulating plasma alanine aminotransferase and ornithine transcarbamylase activities and produced neurological impairment (Shertzer and Sainsbury, 1991). Also excessive glucobrassicin intake resulted in thyroid gland hypertrophy and inhibiting uptake I3C by the thyroid in animals, but this was not observed in humans (Heaney and Fenwick, 1995). There are also a few *in vivo* studies indicating I3C as a tumour promoter when given after a carcinogen (*table 1.7*).

***Table 1.7 Summary of studies indicating I3C as a tumour promoter***

Agent	Cancer type	Animal	Reference
I3C	Colon	Rat	Pence <i>et al.</i> , 1986
	Thyroid	Rat	Kim <i>et al.</i> , 1997
	Pancreas	Hamster	Birt <i>et al.</i> , 1987
	Liver	Trout	Dashwood <i>et al.</i> , 1991
	Liver	Rat	Kim <i>et al.</i> , 1997
	Liver	Rat	Ito <i>et al.</i> , 1989

However, data from Manson *et al.*, (1998) has shown that I3C exhibits an inhibitory effect on aflatoxin B<sub>1</sub>-induced hepatocarcinogenesis in rats whether administrated before or after the carcinogen. Although glutathione *S*-transferase (GST-P)-positive liver cell foci were

significantly increased after 13 weeks I3C treatment in this study which is in agreement with the results of Kim *et al.*, (1997), after 43 weeks all animals were protected from liver tumour formation by I3C, suggesting that some surrogate endpoint markers sometimes may not truly assess the chemopreventive effect of I3C. Long-term exposure (up to 12 months) to DIM (daily dose up to 20mg/kg) in rats produced no observed toxicity (Leibelt *et al.*, 2003).

### **1.8.3 Dietary agents and bladder cancer**

The latent period of most cancers, which is normally around 10-20 years, provides ample time for preventive measures. Although papillary TCCs account for approximately 70-80% of bladder cancers with relatively low progression frequency, the recurrence rates are 60% within 3 years after resection (Lutzeyer *et al.*, 1982). Carcinogens that can be concentrated in urine, thus prolonging exposure to bladder lining, may be responsible for the high risk of recurrence. However, there is also the possibility for chemopreventive agents to be concentrated and held in bladder for longer times. Kamat and Lamm (1999) have reviewed several dietary components as chemopreventive agents in bladder cancer. The antioxidant Vitamin C, also known as ascorbic acid, acts as a free radical scavenger, and is abundant in citrus fruits, blackcurrants, tomatoes and potatoes. There is evidence to demonstrate that it is protective against bladder carcinogenesis in rats. The reduced formation *in vivo* of carcinogenic N-nitroso compounds, which may act as potential causative agents in bladder cancer, has been attributed to the cancer preventive ability of vitamin C. Similarly, vitamin E is also an antioxidant and free radical scavenger, rich in wheat germ, cereals, nuts and spinach. Vitamin E is also indicated as a potential chemopreventive agent in bladder cancer due to its inhibition of N-nitroso compound formation. In addition, vitamin A, vitamin B6, soy protein and garlic extract have been reported to suppress bladder tumours.

A recent study has shown that curcumin, an active compound in turmeric, acts as an apoptosis-inducer in human bladder cancer cells (Tong *et al.*, 2006). EGCG, major phytochemical in green tea, inhibits cell growth and suppresses migration of bladder cancer cells via downregulation of N-cadherin and inactivation of Akt. In mice, reduction of bladder tumour volume has been observed following EGCG continuous administration with no detectable toxicity (Rieger-Christ *et al.*, 2007). Shan *et al.*, (2006) have investigated the chemopreventive effect of sulforaphane (an isothiocyanate from cruciferous vegetables) in human bladder cancer cells, showing inhibition of proliferation, G<sub>0</sub>/G<sub>1</sub> cell cycle arrest and induction of apoptosis. So far, no studies on the effectiveness of I3C or DIM in the

chemoprevention of bladder cancer have been published and this is another major focus within this thesis.

#### ***1.8.4 Bioavailability of Indoles***

A wide range of dietary constituents exhibit a preferential inhibitory effect on tumour cell lines compared with cells from non-tumour tissue (reviewed in Aggarwal and Shishodia, 2006). Besides their chemopreventive properties, the safety of these dietary phytochemicals has to be defined. Considering the recipients in chemopreventive trials are probably in good health, dietary compounds can only be administered at doses which are free of any unwanted side effects (Russo, 2007).

Using an HPLC method, I3C and its derivatives have been identified and quantified in mice following I3C oral administration of a dose of 250mg/kg (Anderton *et al.*, 2004a). The maximal level in plasma of I3C was 28 $\mu$ M observed at 15 minutes and no longer detectable by 1 hour. I3C was also distributed in liver, kidney, lung, heart and brain, as was DIM, but at a lower concentration and more persistent. In another study (Anderton *et al.*, 2004b), mice were orally administered with DIM at 250mg/kg. The maximum level of DIM in plasma was around 24 $\mu$ M during 0.5 to 1 hour and the tissue distribution was similar to that following I3C administration. Due to lack of data for the achievable levels of I3C or DIM in humans, the physiological relevant concentrations of I3C and DIM have to be extrapolated from animals studies. The maximum concentrations of I3C achieved in animals are 28 $\mu$ M (plasma) and 170 $\mu$ M (liver), whereas maximum plasma and tissue concentrations of DIM achieved in mice are 24 $\mu$ M and 200 $\mu$ M following DIM administration.

A very recent review (Howells *et al.*, 2007) summarises outcomes of many *in vitro* studies using low doses of I3C or DIM, showing significant effects on many signalling molecules key to cell growth, cell cycle and apoptosis. It is therefore important to use achievable doses of dietary agents, thus helping to determine which of the many reported mechanisms of action are clinically relevant.

## ***AIMS***

The aims of this study were to investigate the role of STATs in human bladder cancer and the potential chemopreventive mechanisms of action of indoles. In order to achieve this, the following areas were addressed:

- **Determination of STATs status in a panel of human bladder tumours**
- **Determination of STATs expression and localisation in a panel of human bladder cancer cells**
- **Investigation of the upstream activators by which STATs are phosphorylated**
- **Investigation of the effects of STATs on cell proliferation**
- **Investigation of the effects of STATs on cell adhesion and migration**
- **Investigation of the effects of indoles on cell proliferation of a panel of human bladder cancer cells**
- **Investigation of the effects of indoles on cell adhesion of a panel of human bladder cancer cells**
- **Investigation into the mechanisms by which indoles elicits their effect on adhesion**

## **CHAPTER 2**

### **MATERIALS AND METHODS**

## **2.1 Materials**

### **2.1.1 Chemicals**

Unless otherwise stated, all chemicals were purchased from Sigma-Aldrich Company Limited, Poole, Dorset, U.K., and solvents from Fisher Scientific, Loughborough, Leicestershire, U.K.

Acrylamide (30% acrylamide: bis acrylamide)	Anachem
Agarose	Gibco BRL
Annexin V kit	Bender MedSystems
Apo-ONE homogeneous Caspase 3/7 kit	Promega
One Shot® Top10 competent cells	Invitrogen
DAPI	Invitrogen
DNA molecular weight marker	Gibco BRL
ECL detection kit	Amersham
ECL-hyperfilm	Amersham
Epidermal growth factor	Gibco BRL/Peptotech UK
Fetal calf serum (FCS)	Gibco BRL/Hyclone Perbio
Haematoxylin QS	Vector
Hema gurr rapid staining set	BDH/VWR
Hoechst 33258	Gift from Dr. XM Sun
Human Fibronectin	BD Biosciences
Hybond nitrocellulose	Amersham
Luciferase assay system	Promega
Marvel (dried milk powder)	Premier brands
Nucleofection kit	Ambion/Amara
Phalloidin	Molecular Probes
Piceatannol	Calbiochem
Plasmid purification kit	Qiagen
Polyvinylidene difluoride (PVDF) membranes	Millipore
PP2	Calbiochem
Protein molecular weight markers	Bio-Rad/Invitrogen
Rat tail Collagen type I	BD Biosciences
SOC medium	Invitrogen
Tissue staining kit	Dako

Trypsin/EDTA	Gibco BRL
Tyrphostin AG490	Upstate Biotechnology
Versene	Gibco BRL
Western transfer buffer (for nitrocellulose membrane)	Geneflow

### 2.1.2 Antibodies

$\beta$ - Actin	Abcam
Phospho - Akt (serine 473)	Biosource
Total Akt	Cell Signaling Technology
Alexa Fluor 488 goat anti-mouse/rabbit IgG	Molecular probes
Alexa Fluor 594 goat anti-mouse/rabbit IgG	Molecular probes
Caspase 3	Gift from Dr. M. MacFarlane, MRC Toxicology Unit
Cyclin D1	Cell Signaling Technology
E - cadherin	BD Biosciences
N - cadherin	BD Biosciences
P - cadherin	BD Biosciences
$\beta$ - catenin	BD Biosciences
Phospho - EGFR (Tyr1110)	Santa Cruz Biotechnology
Total EGFR (1005)	Santa Cruz Biotechnology
ERK 1/2	Cell Signaling Technology
Phospho - ERK 1/2	Cell Signaling Technology
Fra-1	Santa Cruz Biotechnology
Lamin A/C	Santa Cruz Biotechnology
PARP	Cell Signaling Technology
Rat anti-human fibronectin antibody mAb 16G3	Gift from Dr. Katherine Clark, Department of Biochemistry (Ref. Nagai <i>et al</i> , 1991)
Rat anti-human integrin- $\beta_1$ antibody mAb13	Gift from Dr. Katherine Clark (Ref. Akiyama <i>et al.</i> , 1989)
Phospho - STAT1 (Tyr701)	Cell Signaling Technology
Total STAT1	Cell Signaling Technology
Phospho - STAT3 (Tyr705)	Cell Signaling Technology/Calbiochem
Total STAT3	Cell Signaling Technology
Total STAT3 (F-2)	Santa Cruz Biotechnology

Phospho - STAT5 (Tyr694)	Cell Signaling Technology/Calbiochem
Total STAT5a (L-20)	Santa Cruz Biotechnology
Total STAT5b (G-2)	Santa Cruz Biotechnology
Survivin	Novus Biologicals

### ***2.1.3 Plasmids and oligos***

pβgal control Vector	Clontech (BD Biosciences)
pSG5 Vector	Gift from Dr. Christopher Dawson, University of Birmingham (Originally made by Dr. R Jove's group, Stratagene)
pGRR5-Luc	Gift from Dr. Christopher Dawson (Originally made as a CAT-based reporter vector by Dr. DA Cantrell's group, Ref. Beadling <i>et al.</i> , 1996)
pRc/CMV Stat3-C Flag	Gift from Dr. Christopher Dawson (Originally made by Dr. JE Darnell's group, Ref. Bromberg <i>et al.</i> , 1999)
Scrambled siRNA	Ambion
siRNAs to STAT1 (#42860)	Ambion
siRNAs to STAT3 (#42861)	Ambion
siRNAs to STAT5a (#138786,107004)	Ambion
siRNAs to STAT5b (#108362)	Ambion

### ***2.1.4 Suppliers addresses***

Abcam plc, Cambridge, UK  
Ambion, Texas, USA  
Amersham Pharmacia Biotech, Buckinghamshire, UK  
Anachem, Bedfordshire, UK  
Bender Medsystems, Vienna, Austria  
BD Biosciences, Cowley, Oxford, UK  
BDH, Darmstadt, Germany  
Bio-Rad, Hertfordshire, UK  
Biosource, California, USA  
Calbiochem, Darmstadt, Germany  
Cell Signaling Technology, Hertfordshire, UK  
Dako, Glostrup, Denmark  
Geneflow, Staffordshire, UK

Gibco-BRL (Invitrogen Life Technologies), Paisley, UK

Invitrogen, California, USA

Millipore, Massachusetts, USA

Molecular Probes, Leiden, Holland

Novus Biologicals, Colorado, USA

Promega, Mannheim, Germany

Qiagen, West Sussex, UK

Santa Cruz Biotechnology, California, USA

Upstate Biotechnology, Milton Keynes, UK

Vector Laboratories, California, USA

## **2.2 Buffers**

### ***Adhesion assay buffer***

#### ***1) 1% Heat-denatured BSA***

1g BSA was dissolved in 100ml medium without serum, filtered (0.22 $\mu$ m) and heat-denatured in 85°C water bath for 10-12 minutes. The 10x stock was stored at -20°C and used at a final concentration of 1x diluted with serum-free medium.

#### ***2) 0.2% Crystal violet solution***

0.2% (w/v) crystal violet was dissolved in 10% ethanol and filtered through a 0.22 $\mu$ m filtration paper. The stock was stored at room temperature.

#### ***3) Solubilisation buffer***

250ml 0.2M NaH<sub>2</sub>PO<sub>4</sub> (pH4.5) and 125ml ethanol made up to 500ml in distilled water. The stock was filtrated through a 0.22  $\mu$ m filter and stored at room temperature.

### ***Annexin Buffer***

The Annexin buffer was supplied as a 4x stock and diluted to 1x in distilled water prior to use. The stock was consisted of 10mM HEPES (pH 7.4), 150mM NaCl and 2.5mM CaCl<sub>2</sub> and stored at 4°C.

### ***Cell lysis buffer***

The lysis buffer consisted of 50mM Tris-HCl (pH 6.8), 2% SDS, 10% glycerol, prepared in distilled water. The stock was stored at room temperature.

### ***Nonidet P40 buffer***

150mM NaCl, 1% NP-40, 50mM Tris-HCl (pH8.0), and protease inhibitors (1mM DTT, 10mM  $\beta$ -glycerophosphate, 5mM NaF, 0.1mM  $\text{Na}_3\text{VO}_4$ , 10ug/ml leupeptin, 2ug/ml aprotinin, 0.1mM PMSF) added immediately prior to use. The stock was made up to 100ml in distilled water and stored at 4°C.

### ***Nuclear protein buffer A***

10mM HEPES (pH7.9), 10mM KCl, 10mM EDTA, 0.1mM EGTA, 1mM DTT and 0.1% protease inhibitor cocktail added immediately prior to use. The stock was made up to 200ml in distilled water and stored at 4°C.

### ***Nuclear protein buffer B***

10% v/v Nonidet P40 made up to 100ml in distilled water and stored at 4°C.

### ***Nuclear protein buffer C***

20mM HEPES (pH7.9), 0.4M NaCl, 1mM EDTA, 1mM EGTA, 1mM DTT and 0.1% protease inhibitor cocktail added immediately prior to use. The stock was made up to 100ml in distilled water and stored at 4°C.

### ***Polyacrylamide stacking gel***

A 10ml polyacrylamide stacking gel consisted of 6.8ml water, 1.7ml 30% acrylamide, 1.25ml 1M Tris-HCl (pH 6.8), 100 $\mu$ l 10% SDS. Polymerisation was initiated upon addition of 100 $\mu$ l ammonium persulphate and 10 $\mu$ l TEMED.

### ***Polyacrylamide resolving gel***

Volumes of water and acrylamide varied according to the percentage gel cast. A 10ml polyacrylamide resolving gel consisted of:

2.5ml 1.5M Tris-HCl (pH 8.8), 100 $\mu$ l 10% SDS and acrylamide solution (acrylamide and NN-Methylenebisacrylamide 29:1) as follows

6% - 5.3ml water, 2ml 30% acrylamide mix

8% - 4.6ml water, 2.7ml 30% acrylamide mix

10% - 4ml water, 3.3ml 30% acrylamide mix

12% - 3.3ml water, 4ml 30% acrylamide mix

15% - 2.3ml water, 5ml 30% acrylamide mix

Polymerisation was initiated upon addition of 100 $\mu$ l ammonium persulphate and 10 $\mu$ l TEMED.

### ***Protein loading buffer***

Bromophenol blue (0.4%) and 50% v/v  $\beta$ -mercaptoethanol were made up to an appropriate volume and stored at room temperature.

### ***Protein running buffer (5x)***

The 5x stock consisted of 125mM Tris, 2.5M glycine and 0.5% SDS and diluted to 1x with distilled water prior to use. The stock was stored at room temperature.

### ***Reporter gene assay buffer (luciferase and $\beta$ -galactosidase)***

#### ***1) Mg<sup>2+</sup> buffer***

0.1M MgCl<sub>2</sub>, 4.5M  $\beta$ -mercaptoethanol, made up to an appropriate volume in distilled water and stored at -20°C.

#### ***2) Sodium phosphate buffer***

The sodium phosphate (0.1M, pH7.5) buffer consisted of 41ml 0.2M Na<sub>2</sub>HPO<sub>4</sub>, 9ml 0.2M NaH<sub>2</sub>PO<sub>4</sub>, made up to 100ml in distilled water and stored at room temperature.

#### ***3) Ortho-nitrophenyl- $\beta$ -galactoside (ONPG)***

4mg/ml ONPG made up to an appropriate volume in 0.1M sodium phosphate (pH 7.5) buffer and stored at -20°C.

### ***TAE buffer (50x stock)***

The stock consisted of 242g Tris base, 57.1ml glacial acetic acid, and 100ml 0.5M EDTA (pH 8.0), made up to 1L in distilled water and stored at room temperature. TAE buffer was diluted to a 1x working solution prior to use.

### ***TBST***

The TBST buffer consisted of 20mM Tris-HCl (pH 8.0), 150mM sodium chloride and 0.1% Tween-20, made up to the appropriate volume in distilled water. It was stored at room temperature.

### ***Western stripping buffer***

The stock consisted of 62.5mM Tris (pH 6.8) and 2% SDS in distilled water. Immediately prior to use, 0.7% v/v  $\beta$ -mercaptoethanol was added. It was stored at room temperature.

### ***Western transfer buffer (For PVDF membrane)***

The buffer consisted of 47mM Tris, 37mM glycine, 20% methanol and 1% SDS, made up to the appropriate volume in distilled water and stored at room temperature.

### ***2.3 Cell lines***

Six human bladder cell lines RT4, RT112, HT1376, T24, J82, UMUC3 and human epidermoid carcinoma A431 cells were obtained from the American Type Culture Collection and the European Collection of Cell Culture.

***Table 2.1 Information on bladder cell lines***

	Origin	Histological Grade	Phenotype
RT4	Human, urinary bladder, transitional papillary tumour	G1	epithelial
RT112	Human, urinary bladder, transitional carcinoma	G2	
HT1376		G3	
T24			
UMUC3			mesenchymal
J82			

All cell culture was undertaken in a class II laminar flow cabinet. Cell lines tested negative for mycoplasma infection.

### ***2.3.1 Maintenance of cell lines***

Unless otherwise stated, all cell lines were routinely cultured in Dulbecco's modified Eagle's medium (DMEM), supplemented with 10% FCS and 1% non-essential amino acids. All cell lines were maintained at 37°C, 5% CO<sub>2</sub> and 100% humidity.

#### ***2.3.1.1 Passaging of cells***

Cells were routinely passaged at approximately 80% confluence and following resurrection from storage, bladder cells were not subcultured more than twenty times, and other cell lines no more than thirty times. Cells were gently washed twice in PBS to remove all medium, then 1-5ml of 1x T/E added (depending on the size of flasks or dishes). The cells were incubated at 37°C until all the cells had just lifted off, whereupon the T/E was neutralised with the addition of 5-20ml of medium containing 10% FCS. Cells were pelleted at 200xg for 3 minutes, resuspended in 10ml medium containing 10% FCS, and 2ml of cell suspension was then added to a fresh T150 flask containing 25ml of medium. Cells were not re-passaged within 2 days of subculturing.

### ***2.3.2 Treatment of cells***

Cells were seeded at the required density and allowed to adhere overnight prior to treatment.

#### ***2.3.2.1 Treatment of cells with serum starvation or EGF/serum stimulation***

Cells were seeded in T25 flasks and gently washed three times in PBS to remove all medium containing FCS. Then serum-free medium was added overnight followed by replacement with fresh medium, with or without serum for a further 1 hour, or serum-free medium containing EGF (100ng/ml) for a further 5 minutes.

#### ***2.3.2.2 Treatment of cells with indoles or inhibitors***

Cells were seeded on 6-well plates overnight, and treated with appropriate concentrations of I3C or DIM in fresh medium for appropriate time.

Cells were gently washed three times in PBS to remove all medium containing FCS, then treated with serum-free medium containing appropriate concentrations of AG490 (50µM), PP2 (10µM) or Piceatannol (50µM) for appropriate time.

An untreated control and an equivalent percentage DMSO control were included. In no experiment did the level of DMSO exceed 0.1%.

#### ***2.4 Preparation of cell fractions***

Cells were seeded at concentrations between  $2 \times 10^4$  cells and  $2 \times 10^5$  cells per well in 6-well plates depending upon the duration of treatment, and allowed to adhere overnight before commencing treatment.

##### ***2.4.1 Whole cell lysates***

Plates or flasks were placed on ice, the medium was removed and cells were washed twice with ice-cold PBS. Cell lysis buffer (100-150 $\mu$ l) was added, and all cells were scraped into eppendorf tubes. The cell lysates were cleared by centrifugation at 13000xg for 5 minutes and stored at -20°C.

##### ***2.4.2 Nuclear protein***

Cells were washed twice by ice-cold PBS and pelleted at 1500xg for 5 minutes at 4°C, then resuspended and lysed in buffer A (400 $\mu$ l for a large flask) by gentle pipetting in a yellow tip. Cells are incubated on ice for 15 minutes, after which buffer B (25 $\mu$ l) was added and vortexed vigorously for 10 seconds. The supernatant containing cytoplasm was collected after centrifugation at 13000rpm in microfuge for 30 seconds. The nuclear pellet was resuspended in buffer C (50 $\mu$ l) and mixed on a shaking platform for 15 minutes at 4°C. The nuclear extract was centrifuged for 5 minutes at 13000rpm in microfuge at 4°C and the supernatant stored in aliquots at -70°C.

##### ***2.4.3 BCA protein assay***

Prior to use, protein concentration of cell lysates was determined in order that equal protein loading on gels could be achieved within each set of experiments.

The working reagent was prepared freshly by mixing 50 parts of BCA<sup>TM</sup> reagent A with 1 part of BCA<sup>TM</sup> reagent B. Each standard or unknown sample (25 $\mu$ l) (diluted in cell lysis buffer if necessary) was added into 96-well plate, and was mixed with 200 $\mu$ l of working reagent. The microplate was placed on a plate shaker for 5 minutes, and then was incubated

at 37°C for 30 minutes. After cooling down to room temperature, the absorbance at 550nm was determined using a Tecan GENios microplate reader and Magellan software.

Protein concentrations of samples were determined from a standard curve prepared for each experiment, using known concentrations of bovine serum albumin (BSA) prepared in the same diluent.

### ***2.5 Western blotting***

Samples of known protein concentration were added to protein loading buffer (unless stated otherwise), and were then boiled for 5 minutes prior to loading onto a polyacrylamide gel. Using the Bio-Rad Mini-PROTEAN Tetra electrophoresis vertical system, the samples were electrophoresed in 1x protein running buffer at 120V for 1-2 hours, depending upon the percentage of resolving gel, before being transferred.

The proteins were transferred in western transfer buffer, onto hybond-N nitrocellulose using a Bio-Rad wet blotting system or onto Immobilon-P membrane (polyvinylidene difluoride membrane) using Sigma semi-dry blotting system at 0.2A 100V for 2 hours. Once transferred, the membrane was either dried (Im-P) or washed in TBST and blocked, gently rocking in 5% non fat milk for 1 hour at room temperature. The membrane was then washed twice in TBST and incubated with primary antibody for 1 hour at room temperature or overnight at 4°C. Following 3 x 10 minute washes in TBST, the appropriate secondary antibody was added for 1 hour at room temperature, and the membrane was then washed for 5 x 5 minutes in TBST.

The membrane was then developed in ECL reagent for 1 minute, and placed protein side up into an autoradiographic cassette. It was exposed to ECL-hyperfilm and the blot was developed in the dark using an X-ograph automated developer.

To re-probe the blot with an antibody against a constantly expressed protein as a loading control, the membrane was first placed in 50ml stripping buffer at 60°C for 60 minutes, then washed three times in TBST prior to re-blocking and addition of an appropriate primary antibody.

### 2.5.1 Antibody binding

Unless otherwise stated, whole cell lysates (40 $\mu$ g) were loaded and all membranes were blocked in 5% milk in TBST, with primary antibodies diluted to 1:1000 in 5% milk/ TBST, and secondary antibodies diluted to 1:5000 in 5% milk/TBST.

**Table 2.2 Antibodies: conditions for use**

Primary and Secondary antibody	Dilution of antibody	Antigen molecular weight	% running gel
p-Akt (Ser473) anti-rabbit IgG		60KDa	8%
Total Akt anti-rabbit IgG		60KDa	8%
Caspase3 anti-rabbit IgG	Primary antibody 1:2000 in TBST and secondary antibody 1:5000 in TBST	Proform 32KDa Cleaved 18KDa	15%
Cyclin D1 anti-rabbit IgG		36KDa	12%
E-Cadherin anti-mouse IgG	Primary antibody 1:2000 in 5% milk	120KDa	8%
N-Cadherin anti-mouse IgG	Primary antibody 1:200 in 5% milk	120KDa	8%
P-Cadherin anti-mouse IgG	Primary antibody 1:250 in 5% milk	120KDa	8%
$\beta$ -Catenin anti-mouse IgG	Primary antibody 1:2000 in 5% milk	92KDa	8%
p-EGFR (Tyr1110) anti-goat IgG	Secondary antibody 1:1000 in 5% milk	170KDa	6%
EGFR anti-rabbit IgG	Primary antibody 1:4000 in 5% milk	170KDa	6%
p-ERK1/2 (Thr202/Tyr204) anti-rabbit IgG		44/42KDa	10%

Total ERK 1/2 anti-rabbit IgG		44/42KDa	10%
Fra-1 anti-rabbit IgG	Primary antibody 1:500 in 5% milk	46KDa	10%
Lamin A/C anti-mouse IgG	Primary antibody 1:1000 in 2% BSA	A: 69KDa C: 62KDa	8%
PARP anti-rabbit IgG	Primary antibody 1:800 in 5% milk and secondary antibody 1:2000 in 5% milk	Proform 116KDa Cleaved 89/24KDa	8%
p-STAT1 (Tyr701) anti-rabbit IgG		$\alpha$ : 91KDa $\beta$ : 84KDa	8%
STAT1 anti-mouse IgG	Primary antibody 1:100 for immunoprecipitation	$\alpha$ : 91KDa $\beta$ : 84KDa	8%
p-STAT3 (Tyr705) anti-rabbit IgG ( Cell signaling)		$\alpha$ : 86KDa $\beta$ : 79KDa	8%
p-STAT3 (Tyr705) anti-mouse IgG ( Calbiochem)	Primary antibody 1:500 in 5% milk	$\alpha$ : 86KDa $\beta$ : 79KDa	8%
STAT3 anti-rabbit IgG	Primary antibody 1:100 for immunoprecipitation	$\alpha$ : 86KDa $\beta$ : 79KDa	8%
p-STAT5 (Tyr694) anti-rabbit IgG ( Cell signaling)		90KDa	8%
p-STAT5 (Tyr694) anti-rabbit IgG ( Calbiochem)	Primary antibody 1:1000 in 5% BSA and secondary antibody 1:2000 in 1% milk	90KDa	8%
STAT5a (L-20) anti-rabbit IgG	Primary antibody 1:500 in 5% milk	92KDa	8%
STAT5b (G-2) anti-mouse IgG	Primary antibody 1:500 in 5% milk	94KDa	8%
Survivin anti-rabbit IgG	Secondary antibody 1:2000 in 5% milk	16KDa	15%

### ***2.5.2 Immunoprecipitation of STAT proteins***

Cells were washed with ice-cold PBS and lysed in NP-40 buffer with protease inhibitors on ice. The extract was then transferred to prechilled eppendorf tubes and centrifuged at 2000xg for 10mins at 4°C. The supernatant was incubated for 1-2 hours at 4°C with indicated amount of primary antibody and then protein G sepharose added overnight at 4°C. After centrifugation at 300xg for 1 minute, supernatant was removed and the pellet was washed three times in NP-40 buffer. Samples were then resuspended in protein loading buffer, boiled for 5 minutes before loading on to a polyacrylamide gel and processed as for standard western blotting.

## ***2.6 Assessment of cell proliferation and cell death***

### ***2.6.1 Cell cycle analysis***

Flow cytometry of propidium iodide (PI) stained cells is able to identify the percentage of cells in different phases of cell cycle. In principle, PI intercalates with DNA, and the fluorescent staining of cells is therefore directly proportional to the total amount of DNA present, which will double during S phase.

Cells were seeded at concentrations between  $2 \times 10^4$  and  $8 \times 10^4$  cells per well in 6-well plates depending upon the duration of treatment, left to adhere overnight and then treated with appropriate concentrations of DIM up to 96 hours. Adherent cells were trypsinised and washed in PBS, then resuspended in 200 $\mu$ l PBS. Cells were fixed by the addition of 2ml ice cold 70% ethanol, then vortexed vigorously and incubated at 4°C for a minimum of 2 hours. This step permeabilises the membrane to allow staining by PI in the next step. The fixed cells were pelleted by centrifugation at 600xg for 10 minutes and resuspended in 800 $\mu$ l PBS, whereupon RNase and PI were added to give a final concentration of 0.1mg/ml and 5 $\mu$ g/ml respectively. The cells were incubated at 4°C overnight before analysis of DNA content. This was carried out using the Becton Dickinson FACscan apparatus and Cell Quest software, with subsequent data analysis performed using Modfit LT software.

### **2.6.2 Annexin V staining for apoptosis**

(Based on the method described by Vermes *et al.*, 1995)

Labelling with PI and a fluorescein isothiocyanate (FITC) labelled annexin V staining allows the determination of live, apoptotic and necrotic populations of cells. When cells undergo apoptosis, the perturbation of membranes results in phosphatidylserine (PS) of the inner leaflet becoming exposed on the outer leaflet of cells.

Annexin V has a high affinity for PS which allows apoptotic and necrotic cells to be distinguished from live cells. Live cells that have not been committed to the apoptotic process take up neither annexin V nor PI. Necrotic cells are distinguished from apoptotic cells via PI uptake into the nucleus.

Cells were plated at  $4 \times 10^4$  cells per well in 6-well plates, and treated with the appropriate concentrations of I3C or DIM. Floating cells in medium were reserved, whilst adherent cells were washed in PBS, trypsinised, then combined with the floating cells. After centrifugation for 5 minutes at 350xg at 4°C, cells were resuspended in 10ml fresh medium containing 10% FCS and incubated at 37°C for 30 minutes. Cell suspensions were pelleted at 200xg for 5 minutes and resuspended in 1ml of annexin buffer and 1  $\mu$ l of annexin V FITC conjugate, then incubated at room temperature for 8 minutes. After the addition of PI to a final concentration of 1.5  $\mu$ g/ml and 1 minute incubation at room temperature, the cells were placed on ice and the apoptotic status of the cells determined on a FACScan, using the Cell Quest software.

### **2.6.3 Hoechst 33258 staining for apoptosis**

Hoechst stain is used to fluorescently label DNA for microscopy. It is also commonly used to visualise nuclei and mitochondria. The dye is excited by ultraviolet light and emits blue/cyan fluorescent light.

Cells were seeded at  $4 \times 10^4$  cells per well in 6-well plates, and treated with the appropriate concentrations of DIM for 48 hours. After the addition of 5  $\mu$ l Hoechst 33258 solution (50  $\mu$ g/ml) and 40 minutes incubation at 37°C, the apoptotic status of the cells was analysed by viewing the morphology of the stained nuclei under a fluorescence microscope.

#### 2.6.4 Caspase3/7 assay

Cells were seeded at  $1-2 \times 10^4$  per well on 96-well plates and allowed to adhere overnight before treatment with DIM for 16, 24 and 48 hours. Samples consisted of a blank control (cell culture medium without cells, which was used as a measure of background fluorescence associated with the culture system), DMSO control (DMSO treated cells, used to determine the basal caspase activity of the cell culture system, because DIM was solubilised in DMSO), in the presence of 10, 50 and  $80 \mu\text{M}$  DIM. The cells were maintained in medium with appropriate treatment and at the end of the incubation period  $100 \mu\text{l}$  of Apo-ONE Caspase 3/7 reagent (with substrate diluted 1:100 in buffer provided in this kit) was added per well. Contents of wells were gently mixed using a plate shaker at 300-500rpm for 1 hour at room temperature. The fluorescence of each well was measured at an excitation wavelength of 485nm and an emission wavelength of 535nm.

In brief, the principle of this assay is as follows (based on technical bulletin of Apo-ONE™ Homogeneous Caspase-3/7 assay kit provided by Promega). The Apo-ONE® Homogeneous Caspase-3/7 Buffer can permeabilise cultured mammalian cells rapidly and efficiently, and the caspase-3/7 substrate Z-DEVD-R110 (rhodamine 110, bis-N-CBZL-aspartyl-L-glutamyl-L-valyl-L-aspartic acid amide), exists as a profluorescent substrate prior to the assay. When the buffer and substrate are mixed and added to the sample, the DEVD peptide is cleaved by cellular caspase-3/7 activity, then the rhodamine 110 leaving group becomes intensely fluorescent (*figure 2.1*).

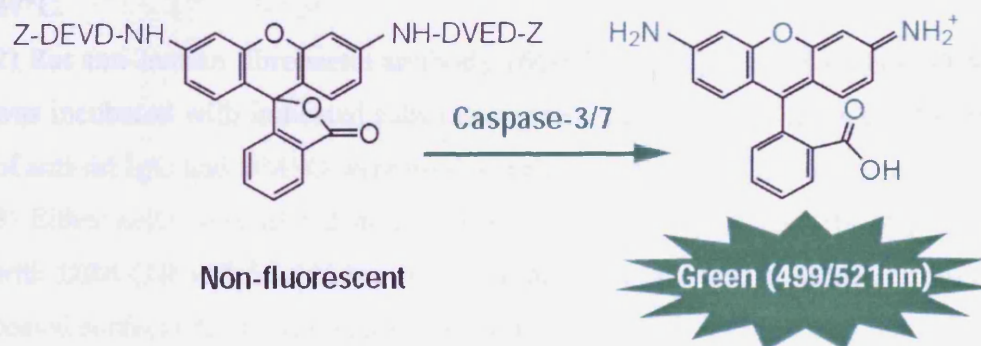


**Figure 2.1** Cleavage of the non-fluorescent caspase substrate Z-DEVD-R110 by caspase-3/7 to create the fluorescent rhodamine 110 (Taken from [www.Promega.com](http://www.Promega.com), instructions for use of Apo-ONE™ Homogeneous Caspase-3/7 Assay kit).

## **2.7 Assessment of cell motility**

### **2.7.1 Adhesion assay**

The extracellular matrix components, fibronectin and collagen I were used as substrates for this assay. Working solutions of fibronectin were prepared in 0.1M NaHCO<sub>3</sub> to final concentrations of 10µg/ml and 50µg/ml, respectively, whilst collagen I was diluted in 0.02N acetic acid to a final concentration of 50µg/ml.

96 well-plates were coated with 80µl of substrates solutions for 1 hour at 37°C or overnight at 4°C followed by washing three times with PBS and blocking with 200µl of 0.1% BSA in serum-free medium for 1 hour at 37°C. Cells were washed twice, collected with versene (0.48mM EDTA) and resuspended with 0.1% BSA in serum-free medium. The cells were then seeded at density of 3x10<sup>4</sup> cells per well for indicated times prior to the assay. Cells were subsequently washed three times in serum-free medium and fixed and stained in crystal violet dye for 5 minutes. Then wells were washed thoroughly with serum-free medium three times, and the dye was extracted from stained cells in solubilisation buffer for 15 minutes at room temperature with shaking. The absorbance at 550nm was determined using a Tecan GENios microplate reader and Magellan software.

### **2.7.2 Treatment of cells for adhesion assay**

Three different approaches were used.

- 1) Cells were allowed to attach to indicated substrate-coated surfaces in the presence of rat anti-human integrin-β1 antibody mAb13 (10µg/ml) or anti-rat IgG (10µg/ml) for 1 hour at 37°C.
- 2) Rat anti-human fibronectin antibody 16G3 (20µg/ml) with or without DIM (10 and 50µM) was incubated with indicated substrates-coated surfaces for 1 hour at 37°C (the same amount of anti-rat IgG and DMSO were used as vehicles), then washed off before cells were seeded.
- 3) Either cells were plated in the presence of DIM (1, 10 and 50µM), or cells were treated with DIM (10 and 50µM) for 16 hours, and then allowed to attach to indicated substrates-coated surfaces for indicated times at 37°C.

### **2.7.3 Transwell migration assay**

Transwell inserts were placed into a 12-well plate. The lower and upper chambers were supplemented with 2ml and 500µl DMEM medium with 10% FCS, respectively. After incubation at 37°C overnight, indicated cells were seeded at a density of 6x10<sup>4</sup> per well. The

migration assay was run for 24 hours at 37°C, the inserts were removed, and the cells were stained with Hema Gurr rapid staining set, and the non-migrating cells were wiped out with a cotton swab. The number of migrating cells was counted in ten randomly chosen fields using a microscope with a ×40 lens.

## ***2.8 Immunohistochemistry***

### ***2.8.1 Ethical approval***

This study involved samples from a human bladder tumour collection selected for immunohistochemical staining which was approved by the local Research Ethics Committee (REC). For superficial tumours, the REC number is 06/Q2501/22 and University Hospitals of Leicester (UHL) R&D number is 09999 from 2006, and for muscle-invasive tumours, the REC number is 6433 and UHL R&D number is 7330, amendment No.1 from 21 September 2004.

### ***2.8.2 Tissue preparation and staining***

Archival blocks of human superficial and muscle invasive tumour tissues used in this study were collected from UHL. Tumour tissues were placed in formalin and processed into paraffin blocks by UHL.

Subsequently, all processing of embedded tissues was performed by Mrs Jenny Edwards, MRC Toxicology Unit, Leicester, UK. The sections (5µm) were cut onto SuperFrost® plus microscope slides which electrostatically attract tissue section binding, through placing a permanent positive charge on standard microscope slides. The first section from each block was stained with haematoxylin and eosin in order to examine the tumour status. Subsequent sections were cut on to numbered slides so that serial sections from each block could be examined in order.

Sections of paraffin-embedded normal and bladder tumour specimens were deparaffinised in two changes of xylene for two minutes each and rehydrated through two washes of 100% ethanol and one wash of 95% ethanol for two minutes each. After washing in distilled water for 5 minutes, slides were submerged into heated Tris-EDTA buffer (pH9.0) or citric acid buffer (pH6.0) and microwaved for 10 minutes at full power, followed by 20 minutes at half power in a 900W microwave. Slides were left to cool in buffer for 20 minutes and rinsed in PBS, before being incubated with the peroxidase blocking solution for 10 minutes in a

humidified chamber. After rinsing and washing in PBS for 5 minutes, slides were incubated for 40 minutes at room temperature with the indicated primary antibody diluted in 0.05M Tris-HCl buffer, to which 1% BSA was added before use. The concentration for each antibody was as follows:

***Table 2.3 Antibodies: dilution for use***

<b>Antibody</b>	<b>Dilution</b>
p-STAT1 (Tyr701), anti-rabbit	1: 100
STAT1, anti-mouse	1: 100
p-STAT3 (Tyr705), anti-rabbit	1: 100
STAT3 (F-2), anti-rabbit	1: 50
p-STAT5 (Tyr694), anti-rabbit	1: 50
STAT5a (L-20), anti-rabbit	1: 100
STAT5b (G-2), anti-mouse	1: 100

A negative control was also included, which was incubated in blocking solution without any primary antibody.

Slides were then washed in PBS and incubated with peroxidase-conjugated anti-mouse or anti-rabbit IgG for 30 minutes at room temperature. Following 5 minutes wash in PBS, the substrate-chromogen was added for 10 minutes at room temperature. After washing in distilled water, the slides were rinsed in tap-water, counterstained with haematoxylin for 5 seconds and rinsed again in tap water. The slides were put back through distilled water, graded alcohol solutions, and xylene. Once air dried, the slides were mounted with DPX mountant, and analysed using Axio Vision 4.5 imaging system.

## 2.9 Immunocytochemistry

Cells were plated at  $1 \times 10^5$  per well on a 6mm, Teflon 10-well microscope slide, or seeded on cover slips placed in a 6-well plate and allowed to adhere overnight at 37°C. Cells were treated with appropriate agent for the appropriate amount of time. After treatment, medium was removed and cells were washed twice in PBS and fixed in 4% paraformaldehyde for 20 minutes at room temperature. Cells were washed in PBS before being permeabilised with 0.5% Triton X100 for 10 minutes. This was followed by three washes in PBS for 5 minutes each. Cells were then blocked with 3% BSA and incubated in a dark, humid chamber for 60 minutes. Primary antibody diluted in 3% BSA was added in an appropriate concentration and the slides were incubated in a dark, humid chamber for 60 minutes.

**Table 2.4 Antibodies/binding protein: dilution for use**

<b>Antibody/binding protein</b>	<b>Dilution</b>
Actin (phalloidin)	1:200
E-cadherin, anti-mouse	1:400
N-cadherin, anti-mouse	1:100
P-cadherin, anti-mouse	1:100
$\beta$ -catenin, anti-mouse	1:400
STAT1, anti-mouse	1:150
p-STAT3 (Tyr705), anti-rabbit	1:100
STAT3, anti-rabbit	1:150
STAT5a, anti-rabbit	1:150
STAT5b, anti-mouse	1:150
pSTAT5 (Tyr694), anti-rabbit	1:100
$\alpha$ -tubulin, anti-mouse	1:2000

After three washes in PBS for 5 minutes each, cells were incubated with secondary antibodies conjugated with Alexa Fluor 488/594 dye diluted 1:1000 in medium with 10% FCS for 60

minutes in a dark, humid chamber. Three more 10 minute washes in PBS followed, before slides were incubated with DAPI (4', 6-diamidino-2-phenyl-indole, dihydrochloride) diluted 1:20000 in PBS for nuclear staining. Each slide/cover slip was mounted by Fluoromount G and analysed using a fluorescence microscope.

## **2.10 Preparation and transfection of plasmid DNA and siRNAs**

### **2.10.1 Plasmids and siRNAs**

p $\beta$ gal-control is a vector which expresses  $\beta$ -galactosidase reporter gene in mammalian cells and can be used to normalise transfection efficiencies. pSG5 is an empty vector used as a negative control in transfection experiments.

pGRR5-Luc reporter is a modified version of pGRR5-CAT (Beadling *et al.*, 1996) where CAT was replaced by the firefly luciferase gene. An oligonucleotide comprising a consensus TTCNNGAA motif was initially identified as a  $\gamma$ -interferon-activated sequence (GAS) present upstream of interferon-inducible genes. A pentamer of the IFN- $\gamma$  response region (GRR) 20mer oligonucleotide (GTATTTCCCAGAAAAGGAAC) upstream of a thymidine kinase minimal promoter was introduced in pBLCAT2 (Luckow and Schutz, 1987).

Stat3-C flagged pRc/CMV construct activates STAT transcription constitutively. Murine Stat3 was cloned into pRcCMV-Neo tagged the 3' end with a FLAG epitope (Wen *et al.*, 1995; Bromberg 1998). The Stat3-C construct was made by site-directed mutagenesis of wild-type Stat3 using primer pairs 5'-GCTATAAGATCATGGATTGTACCTGCATCCTG GTGTCTCC. Within the C-terminal loop in the SH2 domain of the Stat3 molecule, substituting cysteine residues for A662 and N664 allows for dimerisation to form without a phosphate on Y705 (Bromberg *et al.*, 1999). Maps of all plasmids described in this section are shown in *figure 2.2*.

Scrambled siRNA and specific siRNAs to STAT (1/3/5) were diluted to 100 $\mu$ M in nuclease-free ddH<sub>2</sub>O, and 2 $\mu$ l of indicated siRNA was used for each transfection experiment.

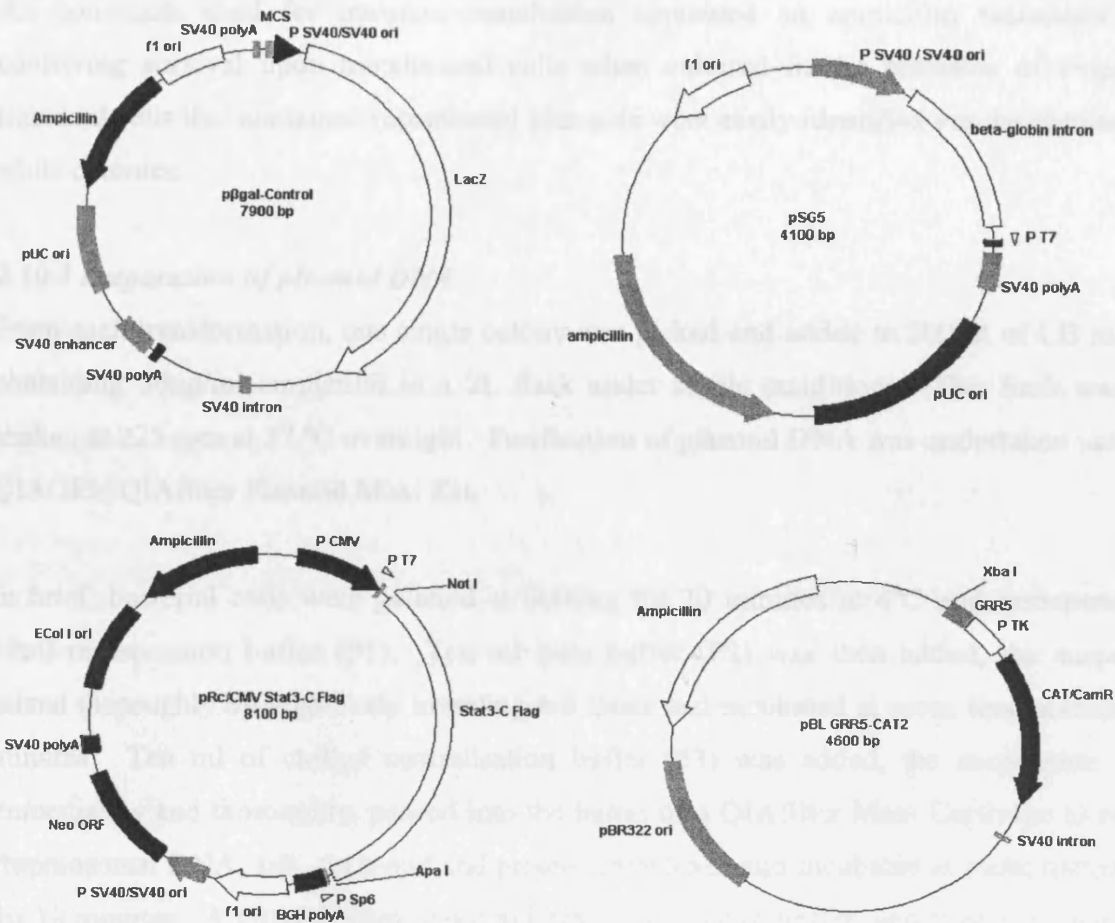


**Figure 2.2 Plasmid maps.** It shows the maps of pβgal vector, pSG5 empty vector, pRc/CMV Stat3-C flag construct and pBL GRR5-CAT2 reporter.

### 2.10.2 Transformation of competent bacteria

(Based on methods described in Molecular Cloning, Edition 3 Sambrook and Russell, 2001)  
 A 10μl aliquot of One Shot® Top10 competent cells was thawed on ice, 0.5μg of plasmid DNA was added, gently mixed by tapping and incubated on ice for 30 minutes. The cells were then heat-shocked for 30 seconds in a 42°C water bath and then placed on ice. Pre-warmed SOC medium (50μl) was added, and the bacteria were incubated at 225 rpm for 1 hour at 37 °C and plated on an ampicillin LB agar plate and further incubated at 37 °C overnight.

Agar plates for bacterial cell transformation were prepared by the addition of 50μg/ml ampicillin to liquid L-agar, and approximately 10ml applied to sterile petri dishes. Once set, the dishes were inverted and allowed to dry at room temperature for 1 hour.

All constructs used for transient transfection contained an ampicillin resistance gene, conferring survival upon transformed cells when cultured in the presence of ampicillin. Bacterial cells that contained recombinated plasmids were easily identified via the formation of white colonies.

### ***2.10.3 Preparation of plasmid DNA***

From each transformation, one single colony was picked and added to 200ml of LB medium containing 50 $\mu$ g/ml ampicillin in a 2L flask under sterile conditions. The flask was then shaken at 225 rpm at 37 °C overnight. Purification of plasmid DNA was undertaken using the QIAGEN QIAfilter Plasmid Maxi Kit.

In brief, bacterial cells were pelleted at 6000xg for 20 minutes at 4°C and resuspended in 10ml resuspension buffer (P1). Ten ml lysis buffer (P2) was then added, the suspension mixed thoroughly by vigorously inverting 4-6 times and incubated at room temperature for 5 minutes. Ten ml of chilled neutralisation buffer (P3) was added, the suspension mixed immediately and thoroughly, poured into the barrel of a QIAfilter Maxi Cartridge to remove chromosomal DNA, salt, detergent and protein complexes and incubated at room temperature for 10 minutes. A QIAGEN-tip was equilibrated with QBT buffer, and then the clear lysate produced in the cartridge was applied to the tip and allowed to enter the resin by gravity flow. The tip was washed twice with wash buffer (QC buffer), the DNA eluted with 15ml high salt buffer (QF buffer) and precipitated with 10.5ml isopropanol at room temperature. The precipitated DNA was centrifuged at 15000xg for 30 minutes at 4°C and the supernatant was carefully decanted. Pelleted DNA was washed with 5ml 70% ethanol and centrifuged at 15000xg for 10 minutes at 4°C and allowed to air dry before resuspension in a suitable volume of distilled water.

DNA concentration was measured by both UV spectrophotometry at 260/280 nm and quantitative analysis on an agarose gel. For pure DNA,  $A_{260/280}$  ratio should lie between 1.8 and 2.0. Following quantitative analysis, 1 $\mu$ l DNA loading buffer was added, and 0.5 $\mu$ g of each plasmid DNA run on a 1% agarose gel (containing 0.01 $\mu$ l/ml of 10mg/ml ethidium bromide) at 80V for 45 minutes. DNA bands were then visualised and photographed using an Uvp bioDoc-It transilluminator and camera system.

#### ***2.10.4 Transient transfection of plasmid DNA and siRNAs into cells***

Plasmids containing the reporter genes for luciferase and  $\beta$ -galactosidase and indicated siRNAs were transiently transfected into cells using electroporation/ nucleofection.

##### ***2.10.4.1 Electroporation of J82 cells***

Cells were seeded into a T150 flask and allowed 48 hours to reach approximately 70% confluence. Following 2-3 hours incubation with fresh medium containing 10% FCS at 37°C, cells were gently washed in PBS and harvested by 1x T/E. Cells were pelleted at 200xg for 3 minutes and resuspended in PBS. The required amount of cells in suspension ( $2 \times 10^6$  cells for each sample) was mixed with indicated plasmids and siRNAs, transferred to cuvettes and incubated on ice for 20 minutes. Electroporation was carried out with a Bio-Rad Gene Pulser set at 250V, 250 $\mu$ F. After the addition of 500 $\mu$ l pre-warmed medium, the cell suspension was titrated at least 20 times to mix thoroughly and was then transferred into a 6-well plate containing pre-warmed medium.

##### ***2.10.4.2 Nucleofection of RT112 cells***

Cells (~70% confluent) were gently washed in PBS and harvested in 1x T/E before being pelleted by centrifugation and resuspended in PBS. The required amount of cells ( $2 \times 10^6$  cells for each sample) was pelleted and resuspended in pre-warmed nucleofection solution. Cell suspensions were mixed with indicated plasmids and siRNAs, and transferred to Amaxa certificated cuvettes. Nucleofection was carried out with an Amaxa nucleofector device using the A23 progame. After the addition of 500 $\mu$ l pre-warmed medium, each cell suspension was titrated at least 20 times to mix thoroughly with plastic pipettes provided in Amaxa kits and transferred into a 6-well plate containing pre-warmed medium.

#### ***2.10.5 Reporter gene assays***

Cells were co-transfected with both luciferase and  $\beta$ -galactosidase plasmids to correct for differences in transfection efficiency. Transfected cells were washed twice in PBS, harvested by scraping and pelleted by centrifugation before the addition of 60 $\mu$ l 1x reporter lysis buffer.

##### ***2.10.5.1 Measurement of $\beta$ -galactosidase activity***

Transfected cells from the 6-well plates were harvested as above, and lysed in 60 $\mu$ l 1x reporter lysis buffer by three cycles of freezing (liquid nitrogen) and thawing (37°C water bath). Following 10 minutes incubation on ice, cellular debris was pelleted by centrifugation

at 10000xg for 1 minute, and 20 $\mu$ l cell lysate mixed with 180 $\mu$ l assay buffer containing the substrate ortho-nitrophenyl- $\beta$ -galactosidase (ONPG) in a 96-well plate. In the presence of  $\beta$ -galactosidase, ONPG is converted to galactose and ortho-nitrophenyl (ONP). ONPG is colourless. ONP is also colourless at neutral or acid pH, but in an alkaline solution it is bright yellow. The amount of yellow colour can be measured in a spectrophotometer indicating the amount of ONP formed in a given time. The reaction was incubated at 37°C, and the absorbance at 405nm was determined using a Tecan GENios microplate reader and Magellan software.

#### *2.10.5.2 Measurement of luciferase activity*

Six  $\mu$ l of the final lysate (made as above) mixed with Luc-substrate and the luciferase activity was measured using a SIRIUS Berthold detection system luminometer. Luciferase values were then corrected for transfection efficiency by normalising against  $\beta$ -galactosidase values.

### **2.11 Statistical analysis**

All statistical analysis was undertaken using SPSS 12.0.2. Data were assessed for statistical significance using oneway ANOVA as appropriate, followed by Scheffe's significant difference post hoc test and Student's t-test. Results were deemed significant if a p value of  $\leq 0.05$  was reached.

## **CHAPTER 3**

### **EXPRESSION OF STAS AND CADHERINS IN HUMAN BLADDER TISSUES**

## **INTRODUCTION**

The STAT family, mainly STAT3, STAT5 and to a lesser extent STAT1, has been observed to be overactive in a variety of human tumours, such as breast (Cotarla *et al.*, 2004), brain (Schaefer *et al.*, 2002), colon (Ma *et al.*, 2004), ovarian (Chen *et al.*, 2004) and prostate (Ni *et al.*, 2002). However, the status of STATs in human bladder tumours is not known.

The classic cadherins, including E-, N- and P-cadherin, represent a family of transmembrane glycoproteins involved in calcium-dependent cell-cell adhesion, cell motility and invasion. Bringuier *et al.*, first reported in 1993 that decreased E-cadherin in bladder tumours is associated with poor survival in patients. In contrast to E-cadherin, aberrant expression of N-cadherin is correlated with the invasive phenotype of bladder cancer cell lines (Girolodi *et al.*, 1999) and the promotion of invasive potential in bladder tumours (Lascombe *et al.*, 2006). P-cadherin has been reported to be localised to the basal cell compartment of normal bladder mucosa (Shimoyama *et al.*, 1989), but, any potential role in bladder tumorigenesis has not been investigated.

Bladder tumours consist of two main groups, superficial (Ta, T1) and muscle-invasive (T2-T4). Additionally, superficial tumours can be further divided into low- (G1) or high-risk (G2, G3, CIS). Histologically, superficial tumours are better differentiated than more invasive tumours.

The aim of work described in this chapter is to determine STATs expression in human bladder tumours, including high grade superficial and muscle invasive lesions, and any possible association with tumour progression, grade and stage. In six human bladder cell lines which have been examined (discussed in chapter 4), three epithelial lines are E-cadherin<sup>+ve</sup> which only express pSTAT5, whereas three mesenchymal cell lines are E-cadherin<sup>-ve</sup> and have phosphorylated STAT3. So, three cadherins (E, N and P) have been investigated in a series of superficial and muscle invasive tumours, in order to find out

whether the STAT expression profile is linked to cadherins, providing a further insight of the possible role of STAT as potential prognosis marker.

## **RESULTS**

### **3.1 Human bladder specimens**

A total of 29 paraffin embedded transitional cell carcinoma samples, containing 9 superficial and 20 muscle invasive bladder tumours, representing different grades and stages, were obtained from an archival tissue bank (UHL, UK). Sections of human normal bladder epithelial tissue were provided by Mr Richard Edwards, MRC Toxicology Unit, Leicester, LE1 9HN, UK.

Tumours were evaluated in the Pathology Department, Leicester General Hospital, UHL, UK, staging according to the 2002 tumour-node-metastasis staging system and grading according to the 1973 WHO classification. Grades and stages of all human bladder tumour tissues used in this study are shown in *table 3.1*. Grades and stages for three muscle invasive blocks 18, 19 and 20 are lacking.

Only representative stainings are included in this chapter. There are more staining for STATs and cadherins in both superficial and muscle-invasive bladder tumours shown in appendices.

### **3.2 Determination of STATs status in normal bladder epithelium**

In order to determine the pattern of STATs expression within the bladder, several sections of human normal bladder epithelium were investigated using immunohistochemistry. As shown in the representative sections in *figure 3.1*, staining for STAT1, STAT3 and STAT5 was observed in normal epithelium. However, expression of phosphorylated proteins was essentially absent.

**Table 3.1 Grade and stage of human bladder tumour tissues (n=26)**

Block number	Grade	Pathological stages
1	G3	pT1
2	G3	pT1
3	G3	pT1
4	G3	pT1
<b>Superficial</b>	G3	pT1
6	G3	pT1
7	G3	pT1
8	G3	pT1
9	G3	pT1
1	G2	pT2*
2	G2	pT2
3	G2	pT2
4	G3	pT2
5	G3	pT2
6	G3	pT2
7	G3	pT2
8	G3	pT2
<b>Muscle invasive</b>	G3	pT2
10	G3	pT2
11	G3	pT2
12	G3	pT2
13	G3	pT2
14	G3	pT2
15	G3	pT2
16	G3	pT2
17	G3	pT3

*\* Muscle-invasive tumours are reported at least T2 by pathologists*

3.1.1 Immunohistochemistry of STAT proteins  
 The expression profile of STAT proteins in normal bladder epithelium was investigated in this study, with immunohistochemistry (IHC) using anti-STAT1, STAT3 and STAT5 antibodies. The results are shown in Figure 3.1.

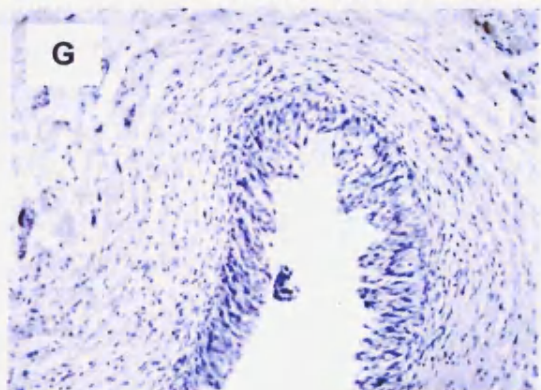
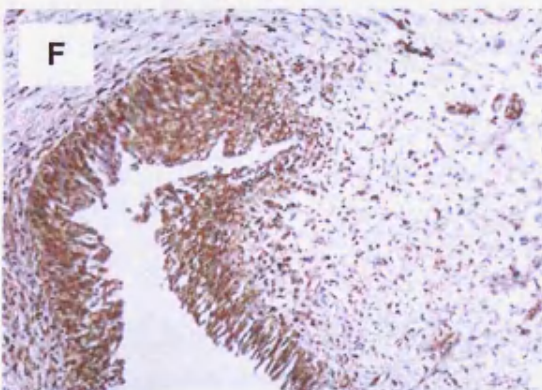
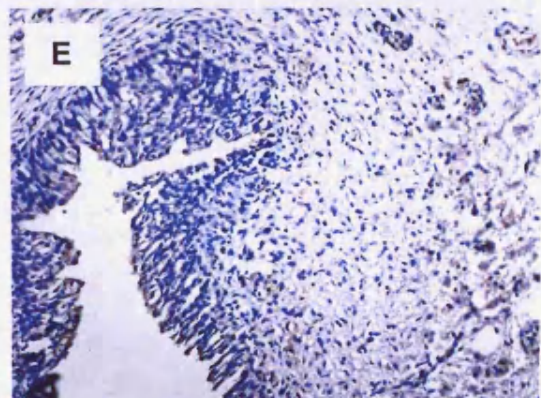
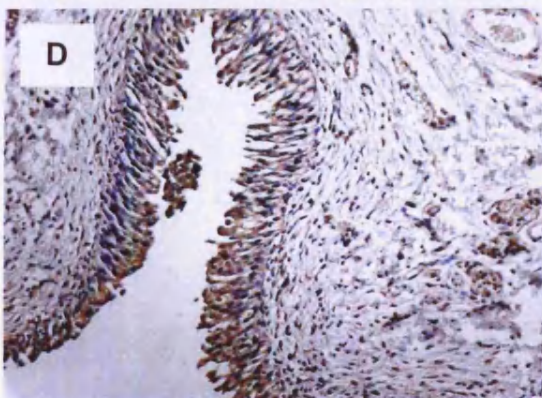
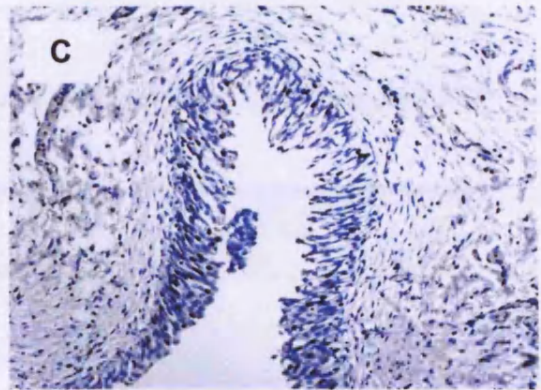
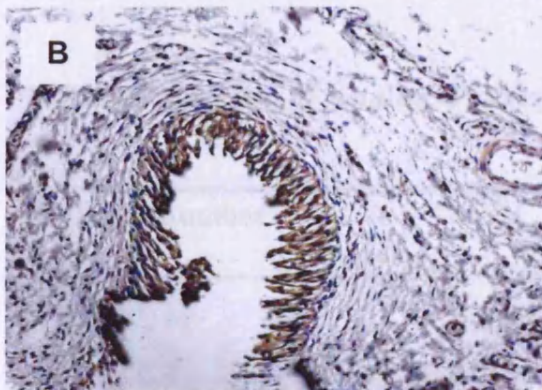
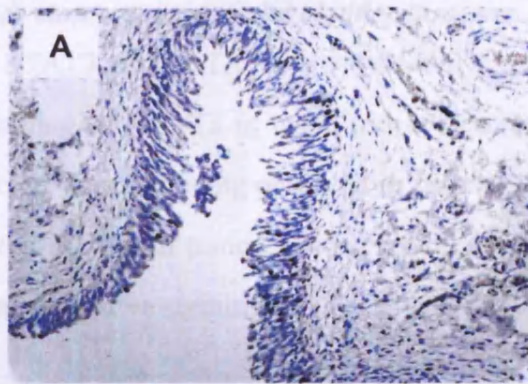


**Figure 3.1** Expression of STAT (1, 3, 5) in normal bladder epithelium. One set of semi-serial tissue sections was prepared to stain for different members of STAT family. A. Negative control, B. STAT1, C. pSTAT1, D. STAT3, E. pSTAT3, F. STAT5b, G. pSTAT5. (photographed by  $\times 20$  lens)

### 3.3 Determination of STATs status in superficial bladder tumours

The expression profile of STAT3 and pSTAT3 in superficial bladder tumours is shown in *table 3.2*. Widespread staining of STAT3 in cytoplasm was observed in all nine samples used in this study, with nuclear staining being observed in four tumours. Some cytoplasmic staining of pSTAT3 was seen in 33% of tumours, however no nuclear staining was observed in any of the tumours. Representative staining of STAT3 and pSTAT3 in superficial bladder tumours is shown in *figure 3.2*.

**Table 3.2 Pattern of staining in superficial tumours for STAT3 and pSTAT3**

Block number	STAT3		pSTAT3	
	Cytoplasm	Nuclear	Cytoplasm	Nuclear
1	++	-	-	-
2	++	++	-	-
3	++	-	-	-
4	T, +	O, +	-	-
5	++	-	-	-
6	++	-	-	-
7	T, +	O, ++	O, +	-
8	++	++	O, +	-
9	++	-	O, +	-

*-*, no staining detected; *+*, weak staining; *++*, strong staining; *O*, occasional staining; *T*, staining throughout tissue

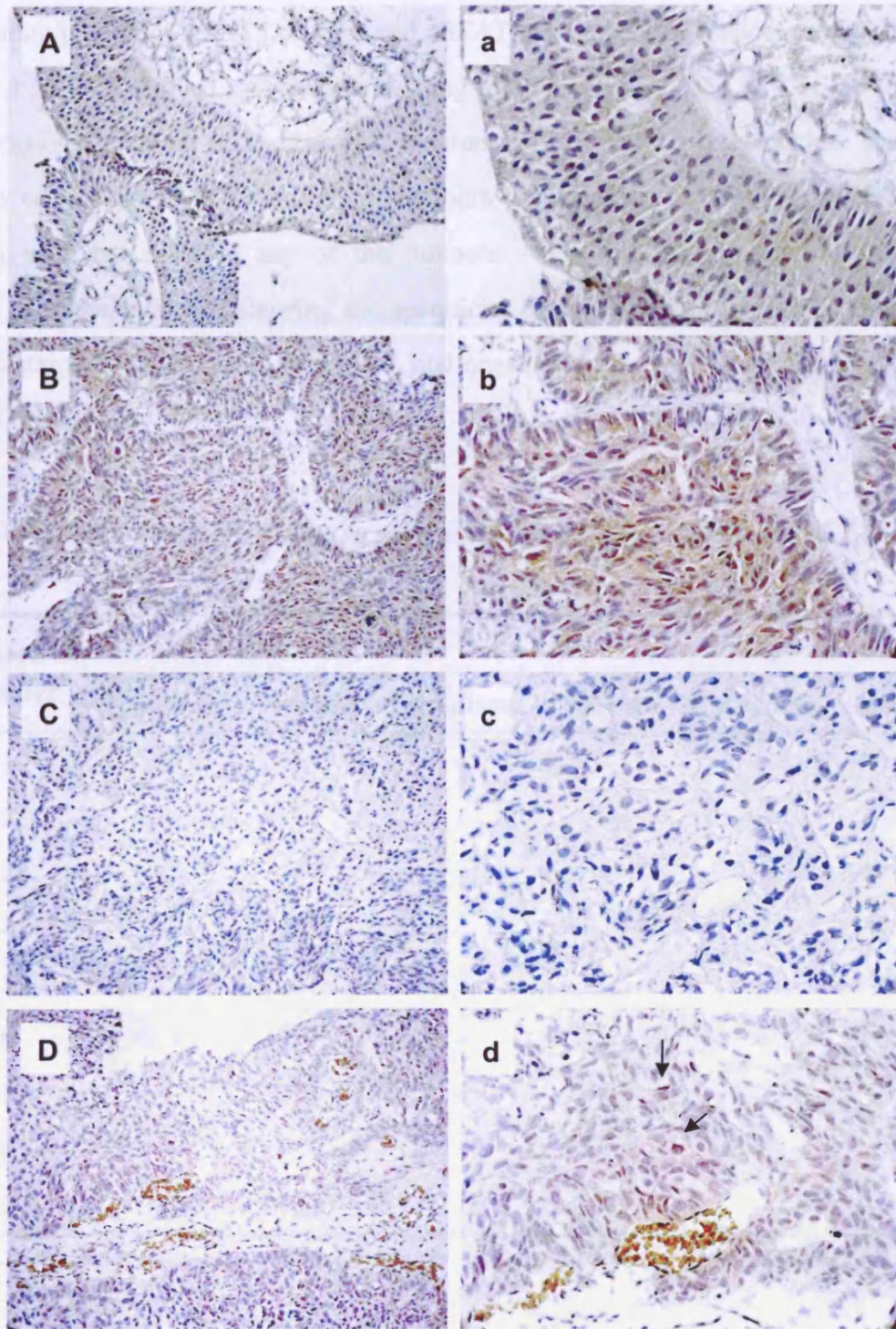


**Figure 3.2 Expression of STAT3 and pSTAT3 in superficial bladder tumours.** (A) Weak cytoplasmic staining of STAT3 (Block 7); (B) Widespread STAT3 staining in cytoplasm and nuclei (Block 8); (C) Absence of pSTAT3 (Block 4); (D) Weak cytoplasmic staining of pSTAT3 with very few nuclear staining (see arrows) (Block 7) (photographed by  $\times 20$  lens). a, b, c and d (photographed by  $\times 40$  lens) represent enlarged areas from A, B, C and D, respectively.

The staining pattern of STAT5 (a & b) and pSTAT5 in superficial bladder tumours is shown in *table 3.3*. Widespread cytoplasmic staining of STAT5b was seen in 4 of the 9 samples, with occasional staining in another two tumours. Universally strong nuclear staining for STAT5b was observed in 89% (8/9) of tumours. In contrast to STAT5b, no STAT5a or pSTAT5 was detectable in any of the tumours. (Positive staining in muscle invasive tumours provides evidence showing the specificity of these two antibodies). Examples of STAT5b staining are shown in *figure 3.3*, and negative staining of STAT5a and pSTAT5 is depicted in *figure 3.4*.

**Table 3.3 Pattern of staining in superficial tumours for STAT5 and pSTAT5**

Block number	STAT5b		STAT5a		pSTAT5	
	Cytoplasm	Nuclear	Cytoplasm	Nuclear	Cytoplasm	Nuclear
1	++	++	-	-	-	-
2	++	++	-	-	-	-
3	+	++	-	-	-	-
4	-	++	-	-	-	-
5	-	++	-	-	-	-
6	O, +	T, ++	-	-	-	-
7	T, ++	T, ++	-	-	-	-
8	-	-	-	-	-	-
9	O, +	T, ++	-	-	-	-

-, no staining detected; +, weak staining; ++, strong staining; O, occasional staining; T, staining throughout tissue

The pattern of STAT1 and pSTAT1 staining observed in superficial bladder tumours is shown in *table 3.4*, with representative staining depicted in *figure 3.5*.

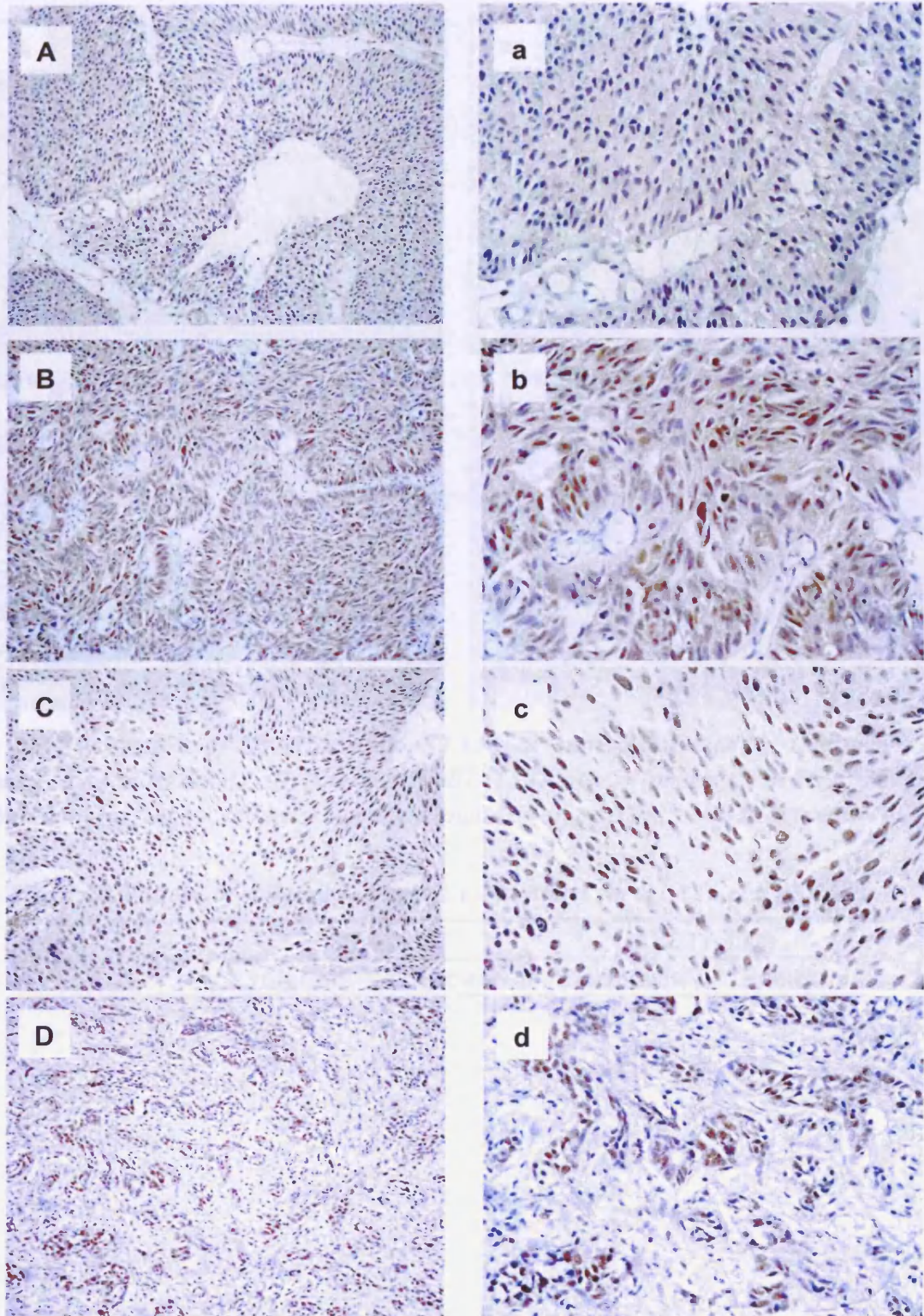


**Figure 3.3** Expression of STAT5b in superficial bladder tumours. (A) Absence throughout the lesion (Block 8); (B) Widespread staining in cytoplasm and nuclei (Block 7); (C) Widespread nuclear staining (Block 9); (D) Scattered tumour cells with nuclear staining (Block 3) (photographed by  $\times 20$  lens). a, b, c and d (photographed by  $\times 40$  lens) represent enlarged areas from A, B, C and D, respectively.

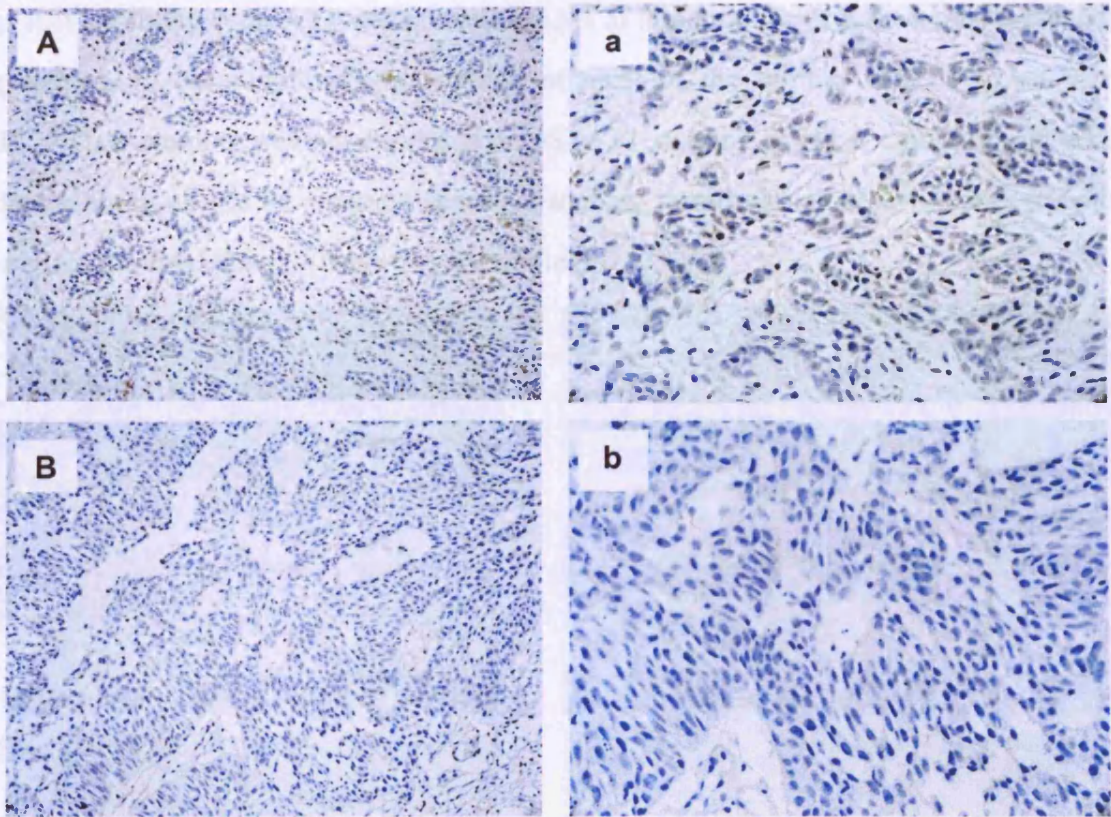


**Figure 3.4** Expression of STAT5a and pSTAT5 in superficial bladder tumours. (A) Absence of STAT5a (Block 3); (B) Absence of pSTAT5 (Block 5) (photographed by  $\times 20$  lens). a and b (photographed by  $\times 40$  lens) represent enlarged areas from A and B, respectively.

**Table 3.4** Pattern of staining in superficial tumours for STAT1 and pSTAT1

Block number	STAT1		pSTAT1	
	Cytoplasm	Nuclear	Cytoplasm	Nuclear
1	-	-	-	-
2	O, ++	-	-	-
3	O, +	-	-	-
4	+	-	-	-
5	-	-	-	-
6	++	-	-	-
7	-	-	-	-
8	-	-	-	-
9	+	-	-	-

- , no staining detected; + , weak staining; ++ , strong staining; O , occasional staining

Cytoplasmic staining of STAT1 was present in 55% of tumours, varying from only a few cells being stained, to cases with strong staining of most of the tumour cells. However, no STAT1 nuclear staining was observed and no pSTAT1 staining in either cytoplasm or nuclei was detectable in any of the tumours (positive staining in muscle invasive tumours provides evidence for the specificity of these two antibodies).

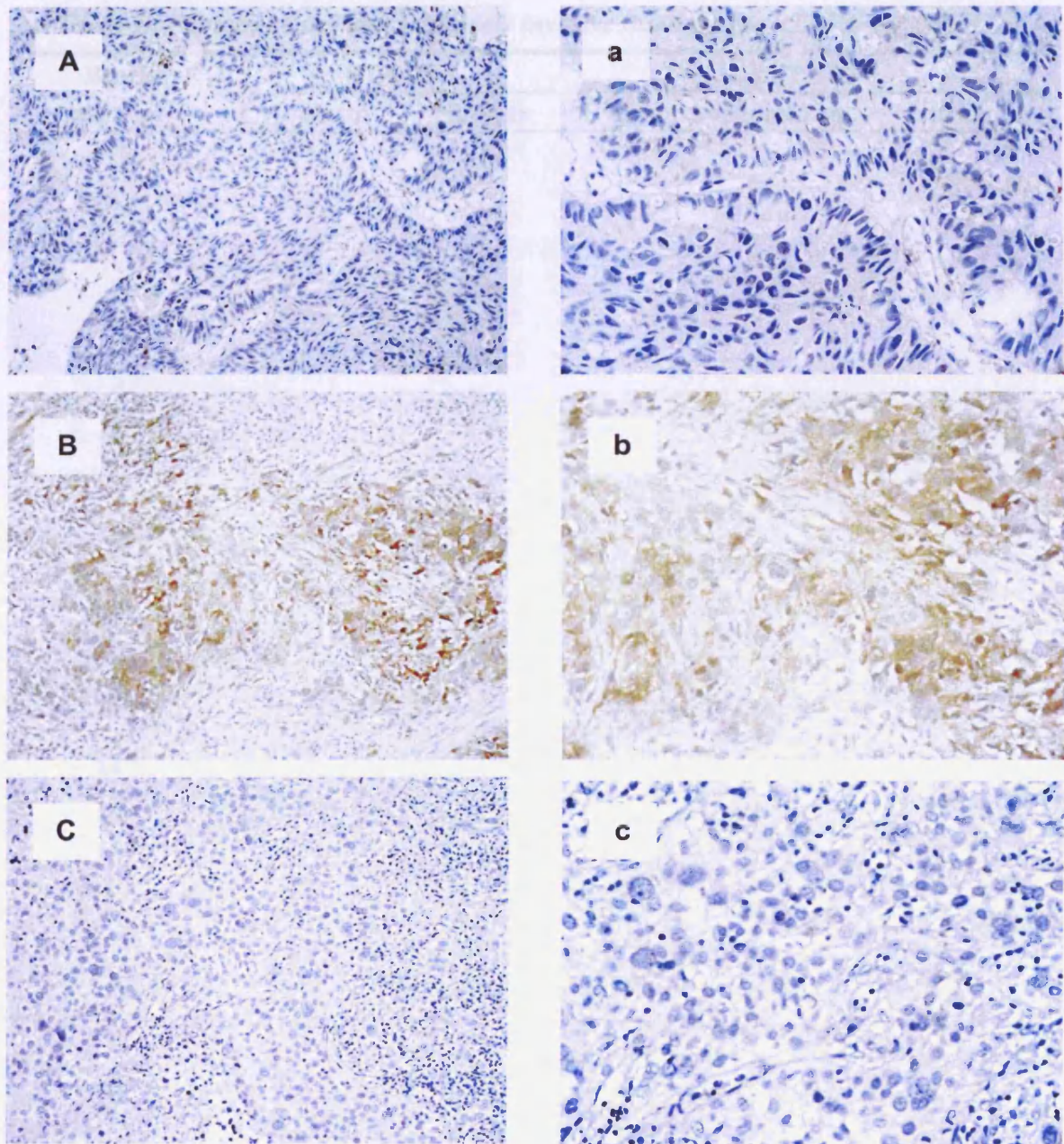


**Figure 3.5** *Expression of STAT1 and pSTAT1 in superficial bladder tumours.* (A) Absence of STAT1 throughout the superficial bladder lesion (Block 7); (B) Widespread staining of STAT1 in cytoplasm (Block 6); (C) Absence of pSTAT1 throughout the lesion (Block 6) (photographed by  $\times 20$  lens). a, b and c (photographed by  $\times 40$  lens) represent enlarged areas from A, B and C, respectively.

### 3.4 Determination of STATs status in muscle invasive bladder tumours

Immunohistochemistry was performed on 20 human muscle invasive bladder tumours to identify the expression profile of STAT family members, and staining of nine blocks (\*) was done by Dr MK Cheng. The staining pattern of STAT3 and pSTAT3 is shown in *table 3.5*.

**Table 3.5 Pattern of staining in muscle invasive tumours for STAT3 and pSTAT3**

Block number	STAT3		pSTAT3	
	Cytoplasm	Nuclear	Cytoplasm/Membrane	Nuclear
1*	++	-	-	-
2*	T, ++	-	-	+++
3	T, +++	++	-	+++
4*	T, ++	T, +++	-	-
5	++	-	C, M, ++	-
6	++	-	C, ++	+++
7	T, +++	T, +++	-	-
8*	T, ++	T, ++	-	-
9	-	-	-	++
10*	++	++	-	++
11*	T, ++	O, +++	-	T, ++
12*	++	+++	-	-
13*	T, +++	++	C, ++	++
14	+++	-	-	O, ++
15	T, +++	++	C, T, +++	T, +++
16	T, +++	-	-	++
17	++	-	C, M, ++	++
18*	T, ++	T, ++	-	-
19	T, ++	T, +++	-	++
20	T, ++	O, ++	C, ++	++

-, no staining detected; ++, strong staining; +++, very strong staining; C, cytoplasmic staining; M, membranous staining; O, occasional staining; T, staining throughout tissue

Nineteen out of 20 samples showed widespread and strong cytoplasmic staining of STAT3, and nuclear staining was seen in 60% of cases. Examples of negative, cytoplasmic and nuclear staining are shown in *figure 3.6*.

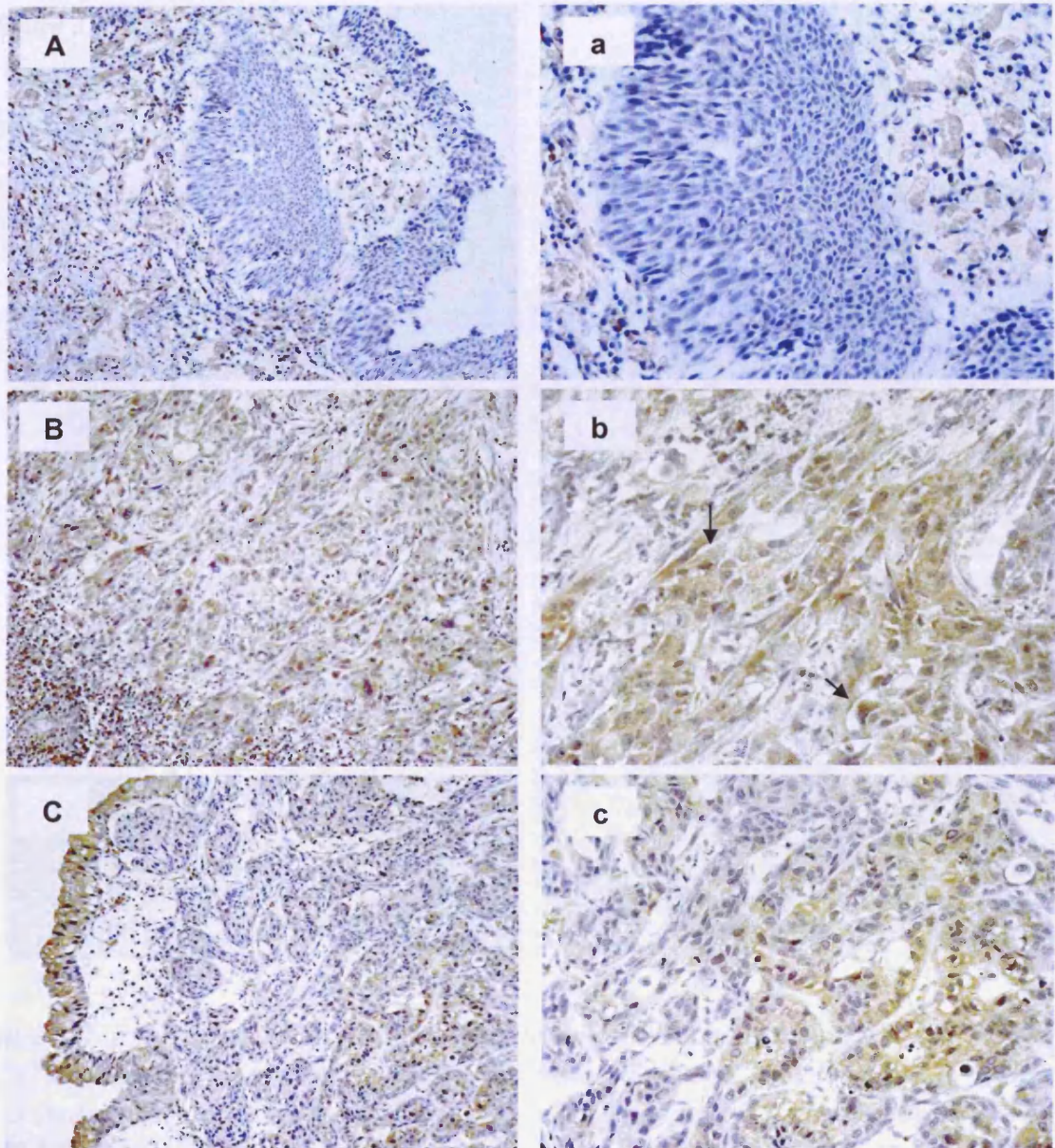


**Figure 3.6** *Expression of STAT3 in muscle invasive bladder tumours. (A) Absence of STAT3 (Block 14); (B) Widespread cytoplasmic staining throughout the lesion, with some positive nuclei (see arrows) (Block 15); (C) Scattered nuclear staining and focal cytoplasmic staining (Block 20) (photographed by  $\times 20$  lens). a, b and c (photographed by  $\times 40$  lens) represent enlarged areas from A, B and C, respectively.*

Some positive staining was seen in the cytoplasm in a third of muscle invasive samples, among which two tumours also showed membranous staining of pSTAT3. Nuclear staining of pSTAT3 was present in 65% of tumours, varying from small patches of stained cells, to samples with widespread and marked nuclear staining of most of the tumour cells, as shown in figure 3.7.

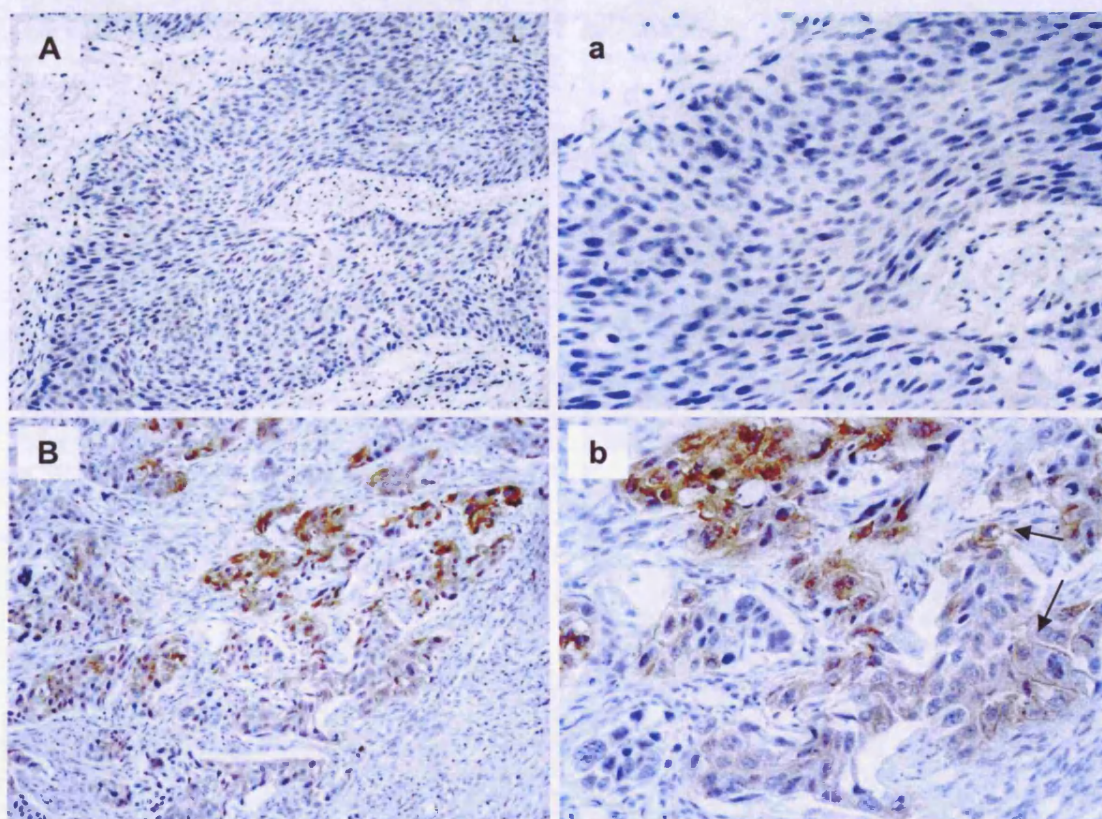


**Figure 3.7** Expression of pSTAT3 in muscle invasive bladder tumours. (A) Absence of pSTAT3 throughout the lesion (Block 3); (B) Membranous pSTAT3 localised in some focal areas (see arrows) and strong cytoplasmic staining (Block 5) (photographed by  $\times 20$  lens). a and b (photographed by  $\times 40$  lens) represent enlarged areas from A and B, respectively.

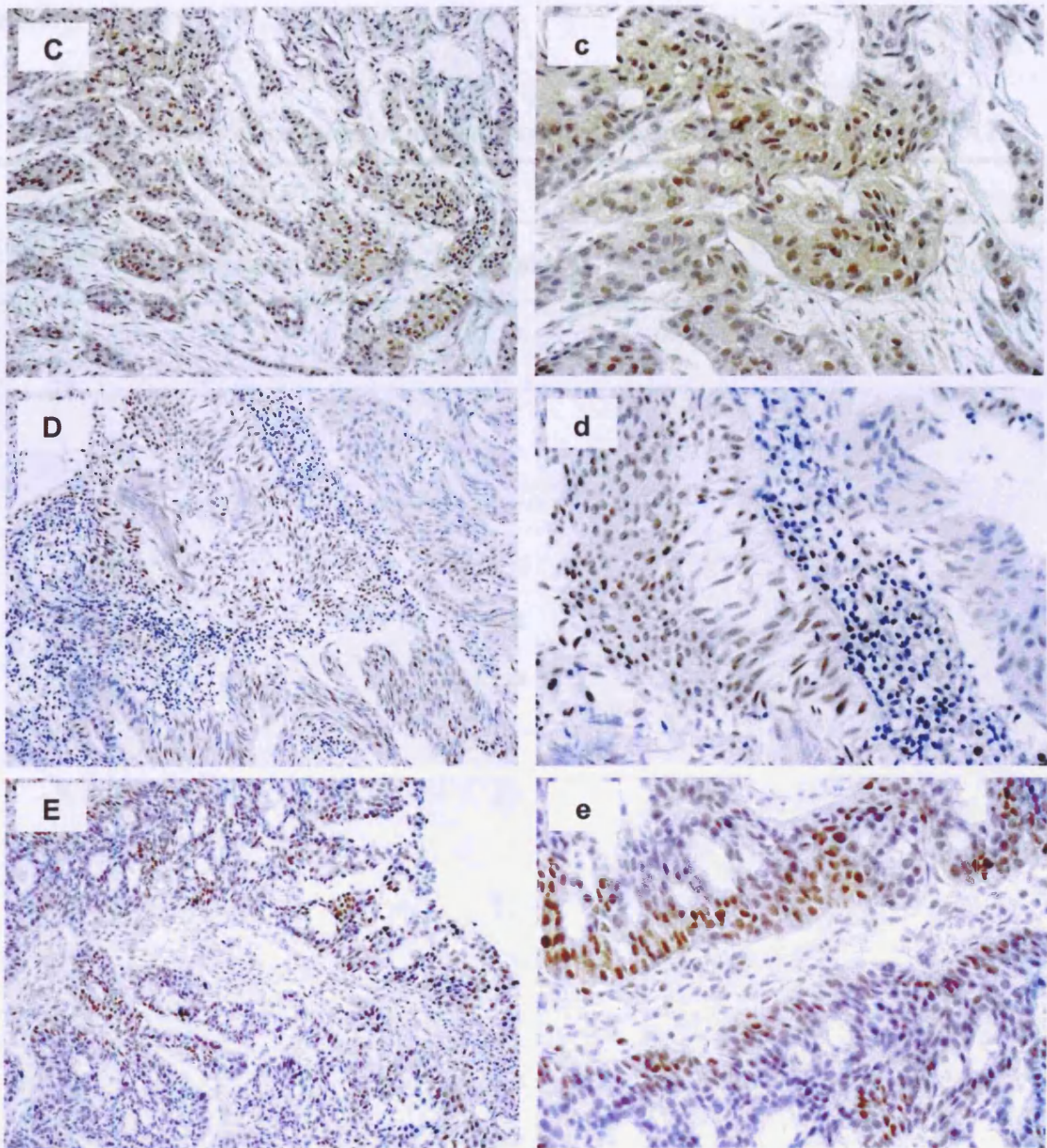


**Figure 3.7(continued) Expression of pSTAT3 in muscle invasive bladder tumours.** (C) Widespread staining of cytoplasm and nuclei (Block 20); (D) Widespread nuclear staining throughout the lesion (Block 11); (E) Nuclear staining in patches (Block 14) (photographed by  $\times 20$  lens). c, d and e (photographed by  $\times 40$  lens) represent enlarged areas from C, D and E, respectively.

The pattern of STAT5 and pSTAT5 staining observed in muscle invasive tumours is shown in table 3.6.

STAT5b was detected in 5 of the 9 (78%) tumours, with nuclear staining being observed in all

**Table 3.6 Pattern of staining in muscle invasive tumours for STAT5 and pSTAT5**

Block number	STAT5b		STAT5a		pSTAT5	
	Cytoplasm	Nuclear	Cytoplasm	Nuclear	Cytoplasm /Membrane	Nuclear
1*	x	x	x	x	-	-
2*	T, ++	+++	T, ++	+++	M, +	-
3	+++	+++	-	T, +++	M, +	-
4*	+++	T, ++	++	T, +++	M, +	O, ++
5	T, ++	T, ++	x	x	C, ++	-
6	+++	+++	x	x	-	-
7	x	x	x	x	-	-
8*	++	T, +++	T, ++	++	-	++
9	++	+++	x	x	-	-
10*	T, ++	T, +++	-	T, ++	M, ++	-
11*	T, +++	T, +++	T, ++	T, +++	M, O, +	O, ++
12*	T, ++	++	T, +++	T, +++	M, O, ++	-
13*	+	++	+	T, ++	M, ++	O, ++
14	++	++	x	x	-	-
15	T, ++	T, +++	x	x	M, ++	-
16	++	++	x	x	-	-
17	++	++	x	x	-	-
18*	T, +	T, ++	T, ++	T, +++	-	-
19	x	x	x	x	-	-
20	T, ++	++	x	x	C, +	O, ++

-, no staining detected; x, no available data; +, weak staining; ++, strong staining; +++, very strong staining; C, cytoplasmic staining; M, membranous staining; O, occasional staining; T, staining throughout tissue

Of the seventeen samples stained for STAT5b, all were positive in both the cytoplasm and nucleus, with staining widespread and strong in most cases. Cytoplasmic staining of STAT5a was detected in 7 of the 9 (78%) tumours, with nuclear staining being observed in all cases. Examples of STAT5 (a & b) staining are shown in *figure 3.8*.

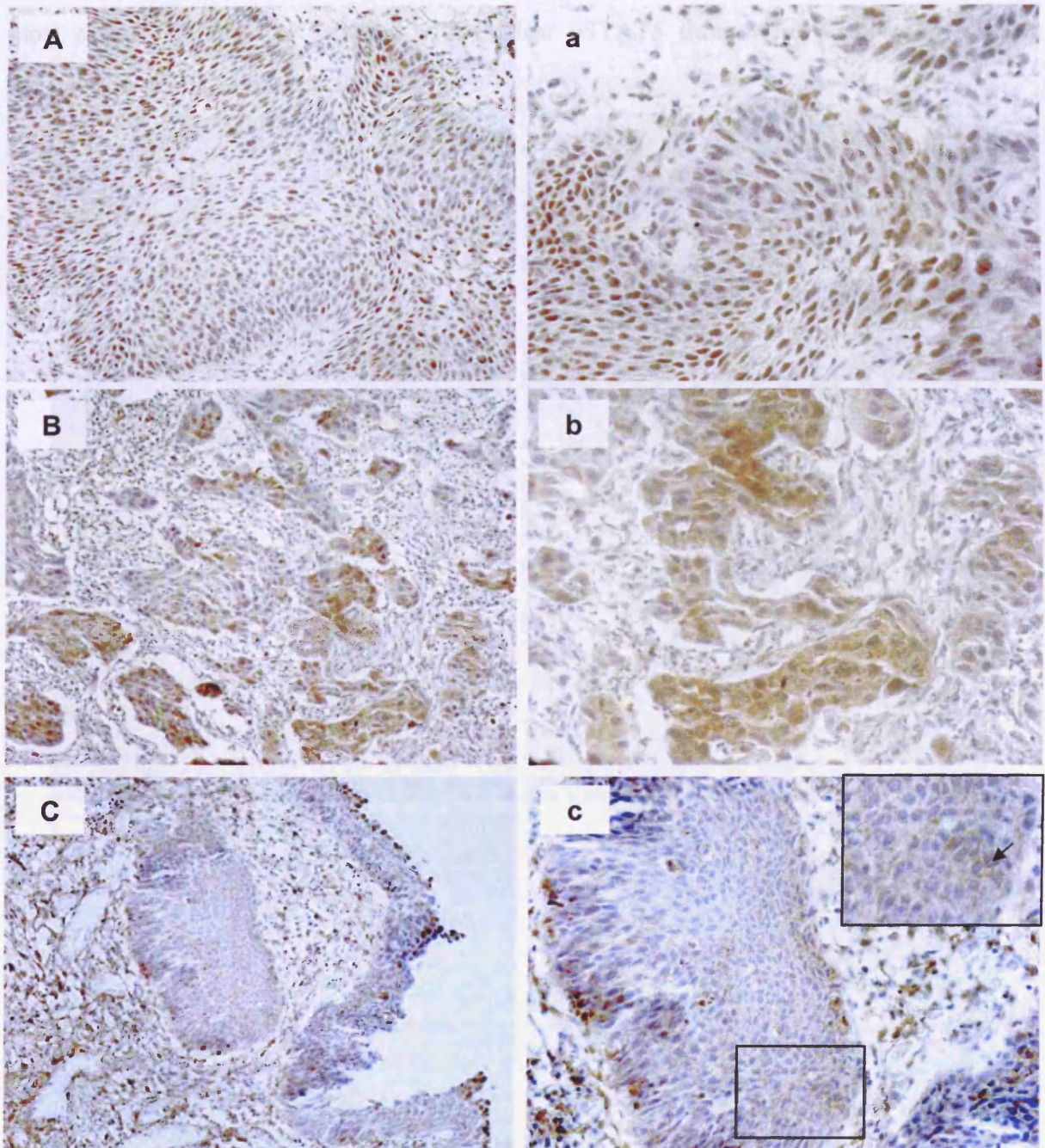


**Figure 3.8** Expression of STAT5 in muscle invasive bladder tumours. (A) Widespread nuclear staining of STAT5a (Block 3); (B) Widespread staining for STAT5b in cytoplasm and nuclei throughout the lesion (Block 5); (C) Occasional membranous staining of STAT5b in focal areas (see arrows) (Block 14) (photographed by  $\times 20$  lens). a, b and c (photographed by  $\times 40$  lens) represent enlarged areas from A, B and C, respectively.

Cytoplasmic staining of pSTAT5 was only observed in 2 of the 20 (10%) samples, but 40% of tumours showed membranous staining which varied from occasional staining in patches of cells to widespread staining in most tumour cells (*figure 3.9*). Some positive nuclear staining was observed in 20% (5/20) of samples, but with only a few positive small patches in most cases. Of the five samples with nuclear pSTAT5 three were positive and 2 was negative for pSTAT3 nuclear staining.

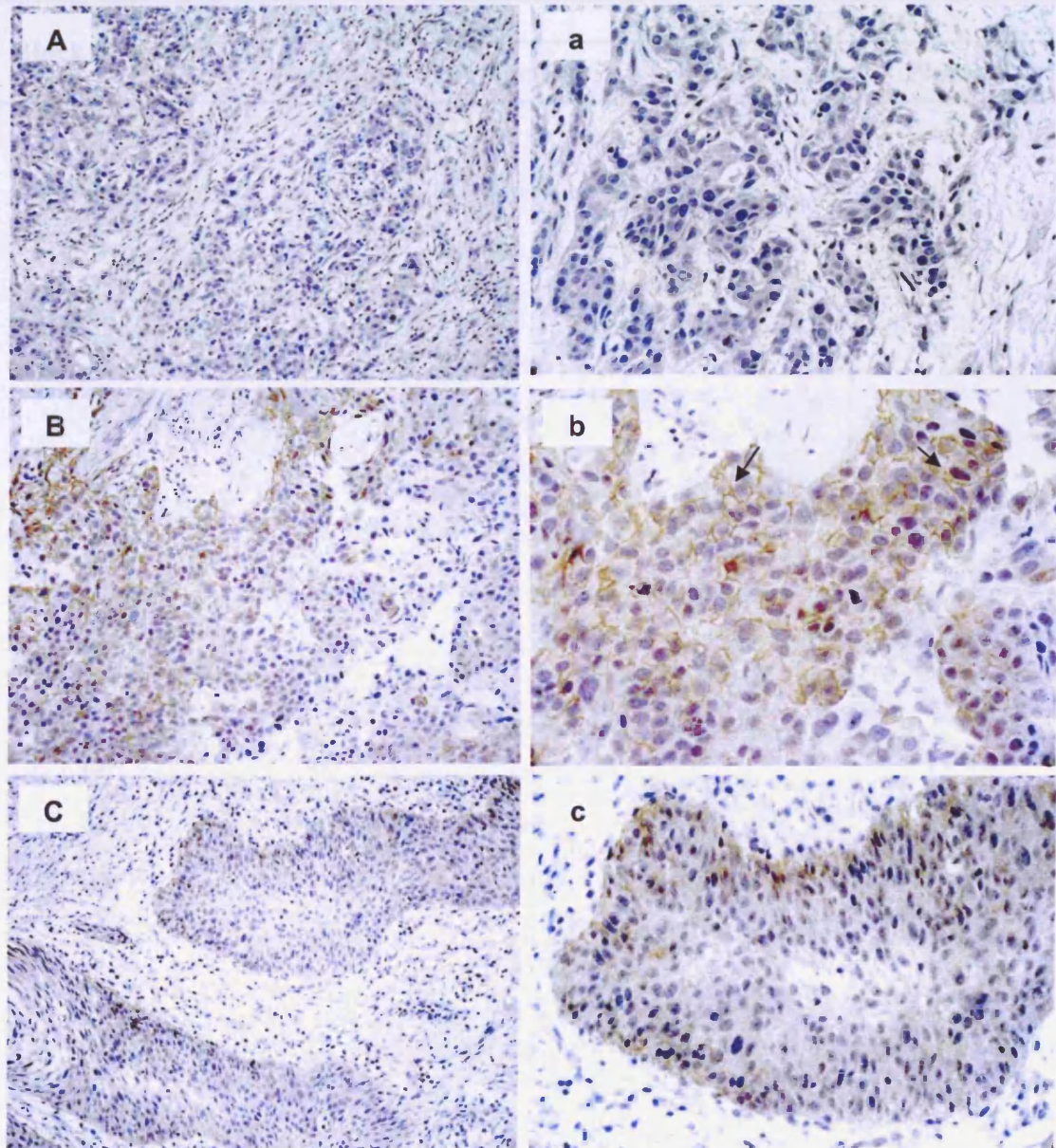


**Figure 3.9** Expression of pSTAT5 in muscle invasive bladder tumours. (A) Absence of pSTAT5 throughout the lesion (Block 17); (B) Widespread membranous staining (Block 10); (C) Weak cytoplasmic and some nuclear staining (Block 3) (photographed by  $\times 20$  lens). a, b and c (photographed by  $\times 40$  lens) represent enlarged areas from A, B and C, respectively.

The expression of STAT1 and pSTAT1 in muscle invasive tumours is shown in *table 3.7*. Fourteen of the 15 tumours (93%) stained positively for STAT1 in cytoplasm, and nuclear staining was frequently observed, being present in 53% of specimens. Examples of STAT1 staining are shown in *figure 3.10*

**Table 3.7 Pattern of staining in muscle invasive tumours for STAT1 and pSTAT1**

Block number	STAT1		pSTAT1	
	Cytoplasm	Nuclear	Cytoplasm	Nuclear
1*	-	-	-	-
2*	++	++	-	++
3	O, +++	O, ++	-	O, ++
4*	++	O, ++	-	O, ++
5	x	x	x	x
6	x	x	x	x
7	+	-	-	-
8*	++	++	-	T, ++
9	T, ++	+++	O, +	-
10*	+	++	-	-
11*	O, +++	O, ++	+	O, ++
12*	++	-	-	O, ++
13*	+ / +++	++	-	O, ++
14	T, +++	-	-	++
15	x	x	x	x
16	T, +++	-	-	+++
17	x	x	x	x
18*	++	-	-	-
19	+++	-	-	-
20	x	x	x	x

-, no staining detected; x, no available data; +, weak staining; ++, strong staining; +++, very strong staining; O, occasional staining; T, staining throughout tissue

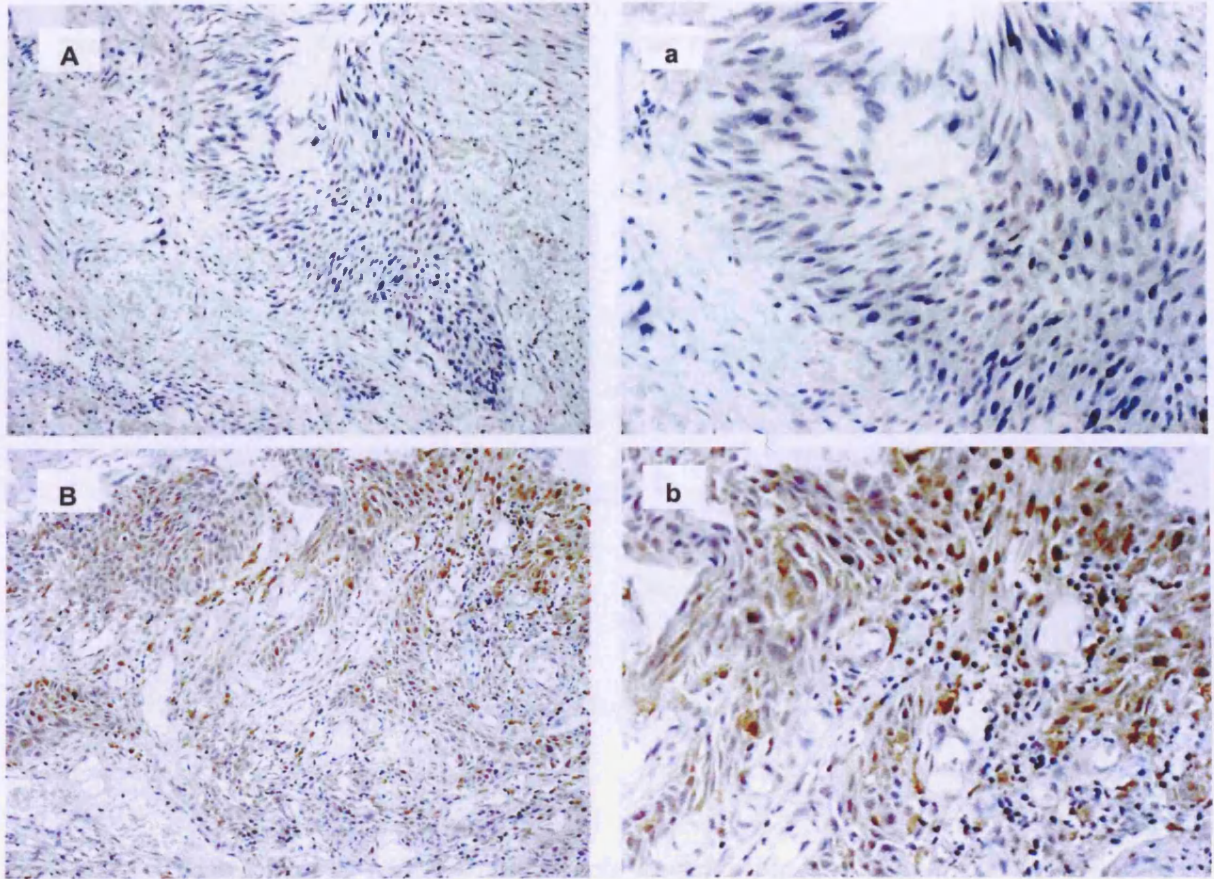


**Figure 3.10** Expression of STAT1 in muscle invasive bladder tumours. (A) Absence of staining for STAT1 (Block 3); (B) Widespread cytoplasmic and nuclear staining in the same lesion (Block 3) (photographed by  $\times 20$  lens). a and b (photographed by  $\times 40$  lens represent enlarged areas from A and B, respectively).

Nuclear staining of pSTAT1 was present in 9 of 15 (60%) tumour samples, varying from scattered patches of positive nuclei to widespread strong nuclear staining in large areas. In contrast to the frequent location in nuclei, only 13% (2 of 15) of tumours showed cytoplasmic staining, which was very faint and present in a few focal areas. Representative staining of pSTAT1 is shown in *figure 3.11*.

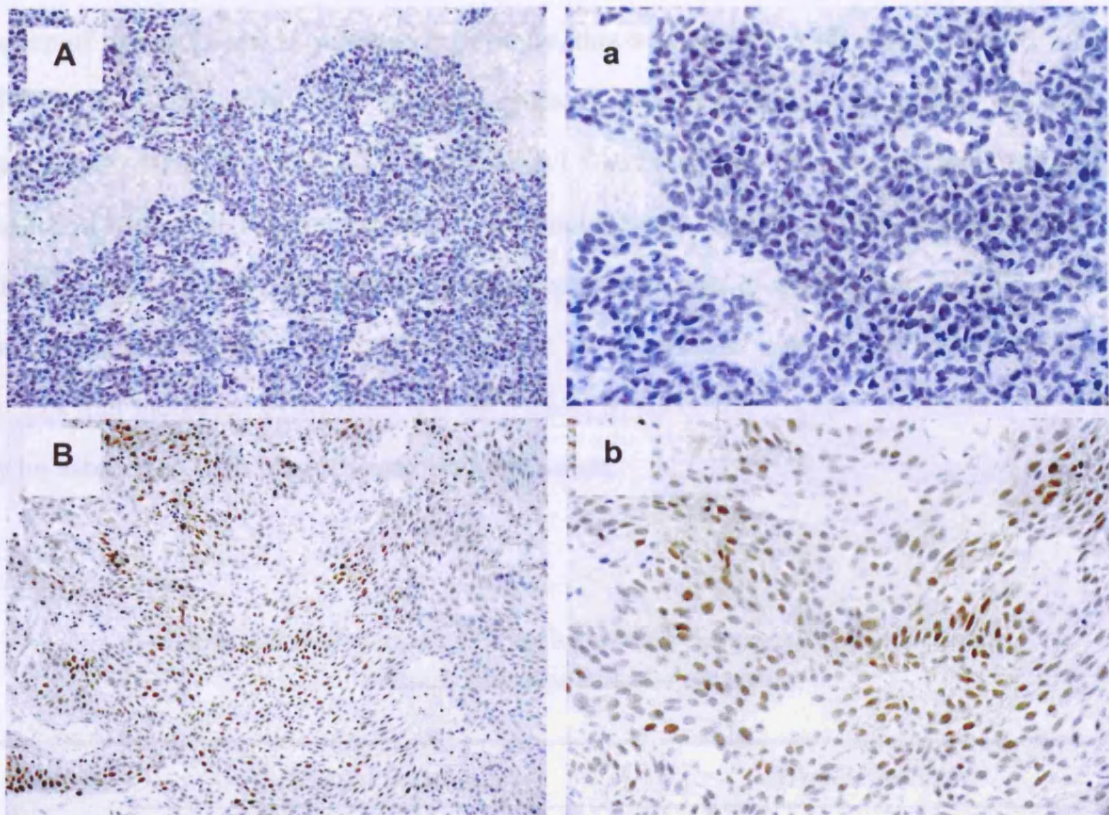


**Figure 3.11 Expression of pSTAT1 in muscle invasive bladder tumours.** (A) Absence of pSTAT1 (Block 12); (B) Widespread nuclear staining (Block 3) (photographed by  $\times 20$  lens). a and b (photographed by  $\times 40$  lens) represent enlarged areas from A and B, respectively.

### 3.5 Relationship between STAT expression and stage of bladder tumours

In superficial bladder tumours, cytoplasmic staining of STAT3 was observed in all nine samples, some of which also showed nuclear staining (*table 3.2*). STAT5b was frequently detected in both cytoplasm and nucleus, but no staining of STAT5a was detectable (*table 3.3*). The STAT1 staining observed in half the specimens was entirely cytoplasmic, with no nuclear staining observed in any of the tumours (*table 3.4*). Interestingly, pSTAT3 was the only phosphorylated STAT observed in superficial tumours (33%), but was confined to the cytoplasm (*table 3.2*).

In muscle invasive bladder tumours, staining of STAT3 (60%), STAT5a (78%), STAT5b (100%) and STAT1 (53%) occurred in both the cytoplasm and nucleus. In contrast to the absence of nuclear stain in superficial tumours, this was observed for pSTAT1, pSTAT3 and pSTAT5 in 60%, 65% and 25% of muscle invasive tumour samples, respectively. Cytoplasmic stain for pSTAT1 and pSTAT5 was absent in superficial tumours but significantly increased in muscle invasive tumours. As shown in *table 3.8*, in spite of the limited amount of analysed samples, percentage expression of each of the STATs in muscle invasive bladder tumours is higher than that in superficial tumours in most cases. That indicates that increased expression and activation, in particular nuclear localisation of, STATs may be associated with bladder tumour progression.

**Table 3.8 Difference of STATs staining between superficial and muscle invasive bladder tumours**

Stained markers	Superficial		Muscle invasive	
	Cytoplasm	Nuclear	Cytoplasm / Membrane	Nuclear
<b>STAT3</b>	100% (9/9)	45% (4/9)	95% (19/20)	60% (12/20)
<b>pSTAT3</b>	33% (3/9)	ND	30% (6/20)	65% (13/20)
<b>STAT5b</b>	67% (6/9)	89% (8/9)	100% (17/17)	100% (17/17)
<b>STAT5a</b>	ND	ND	78% (7/9)	100% (9/9)
<b>pSTAT5</b>	ND	ND	50% (10/20)	25% (5/20)
<b>STAT1</b>	55% (5/9)	ND	93% (14/15)	53% (8/15)
<b>pSTAT1</b>	ND	ND	13% (2/15)	60% (9/15)

*The percentage of positive staining was calculated from tumour numbers in brackets. Compared with staining in superficial tumours, the increased percentages of positive stained muscle invasive tumours are shown in red. ND = no detected stain.*

### 3.6 Determination of cadherin status in superficial bladder tumours

A total of 9 human superficial bladder tumours were stained by Dr MK Cheng for E, N or P-cadherin using immunohistochemistry. Table 3.9 summarises the staining patterns in superficial bladder cancers. The staining observed for E-cadherin was either cytoplasmic or membranous in location. Positive stain in cytoplasm was seen in 6 of 9 (67%) tumour samples, with membranous E-cadherin being observed in all 9 samples. The membranous stain of E-cadherin was widespread in most cases, and examples are shown in figure 3.12.

**Table 3.9 Pattern of staining in superficial tumours for cadherins**

Block number	E-cadherin		N-cadherin		P-cadherin	
	Cytoplasm	Membrane	Cytoplasm /Membrane	Nuclear	Cytoplasm	Membrane
1	+	+/+++	-	-	O, ++	O, ++
2	++	++	-	++	-	++
3	++	++	M, ++	-	-	++
4	++	O, ++	C, ++	-	O, ++	++
5	-	T, ++	M, O, ++	-	-	++
6	+	+	-	++	+	++
7	-	+/+++	-	+	-	-
8	O, ++	T, +++	-	-	-	++
9	-	++	-	+	++	++

*-*, no staining detected; *+*, weak staining; *++*, strong staining; *C*, cytoplasmic staining; *M*, membranous staining; *O*, occasional staining; *T*, staining throughout tissue

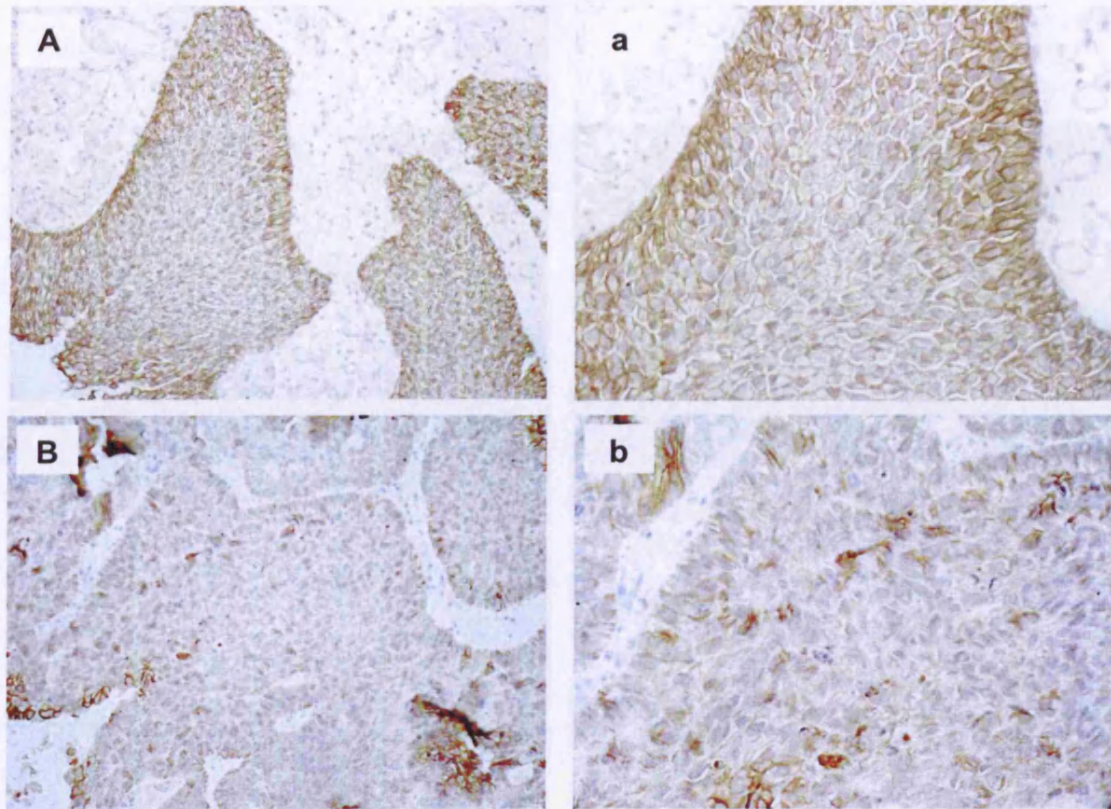


**Figure 3.12 Expression of E-cadherin in superficial bladder tumours.** (A) Widespread and strong membrane staining throughout the lesion (Block 8); (B) Heterogeneous staining (Block 7) (photographed by  $\times 20$  lens). a and b (photographed by  $\times 40$  lens) represent enlarged areas from A and B, respectively.

On the other hand, only 2 tumours showed membranous N-cadherin and 1 of 9 samples was observed to have cytoplasmic stain. Nuclear N-cadherin was seen in just under half (4 of 9) of the specimens (*figure 3.13*). No cytoplasmic P-cadherin was detectable in 55% of cases. But membranous stain was present in 8 of 9 (89%) specimens. This was, however, present in restricted areas showing association with the border of the tumour (*figure 3.14*).

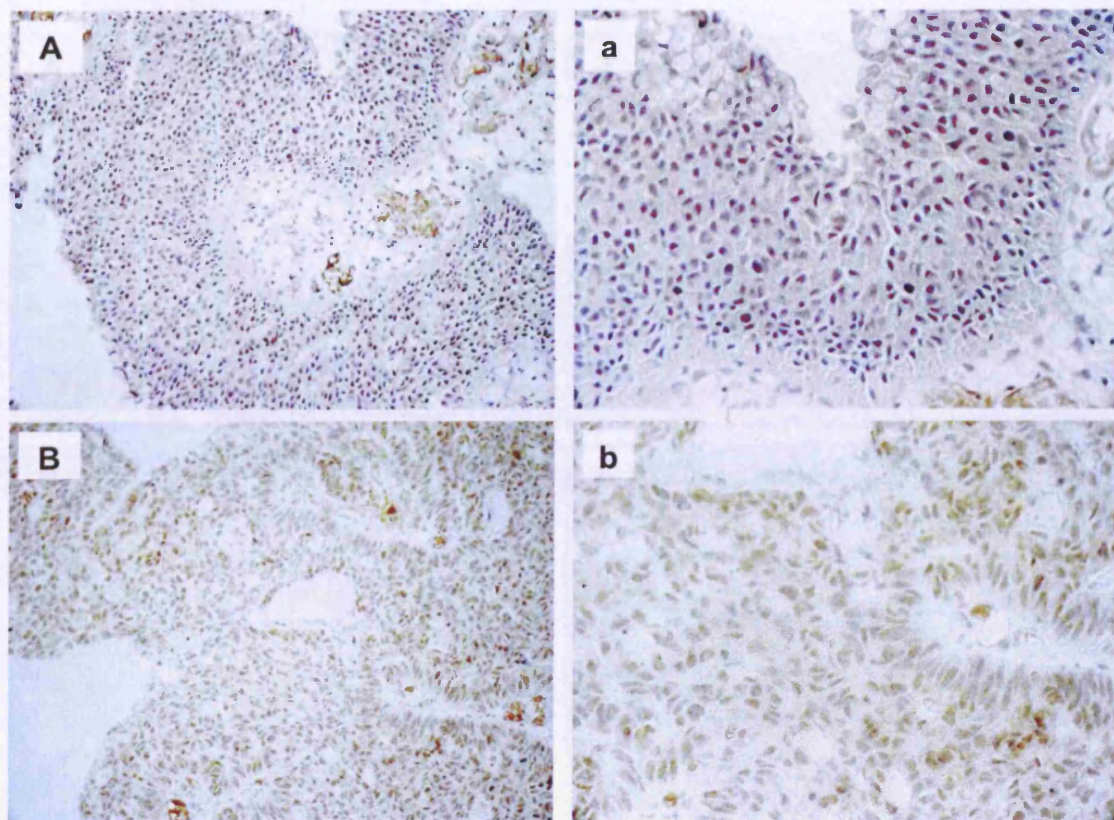


**Figure 3.13** Expression of N-cadherin in superficial bladder tumours. (A) Absence of N-cadherin throughout the lesion (Block 8); (B) Widespread but faint nuclear staining (Block 7) (photographed by  $\times 20$  lens). a and b (photographed by  $\times 40$  lens) represent enlarged areas from A and B, respectively.

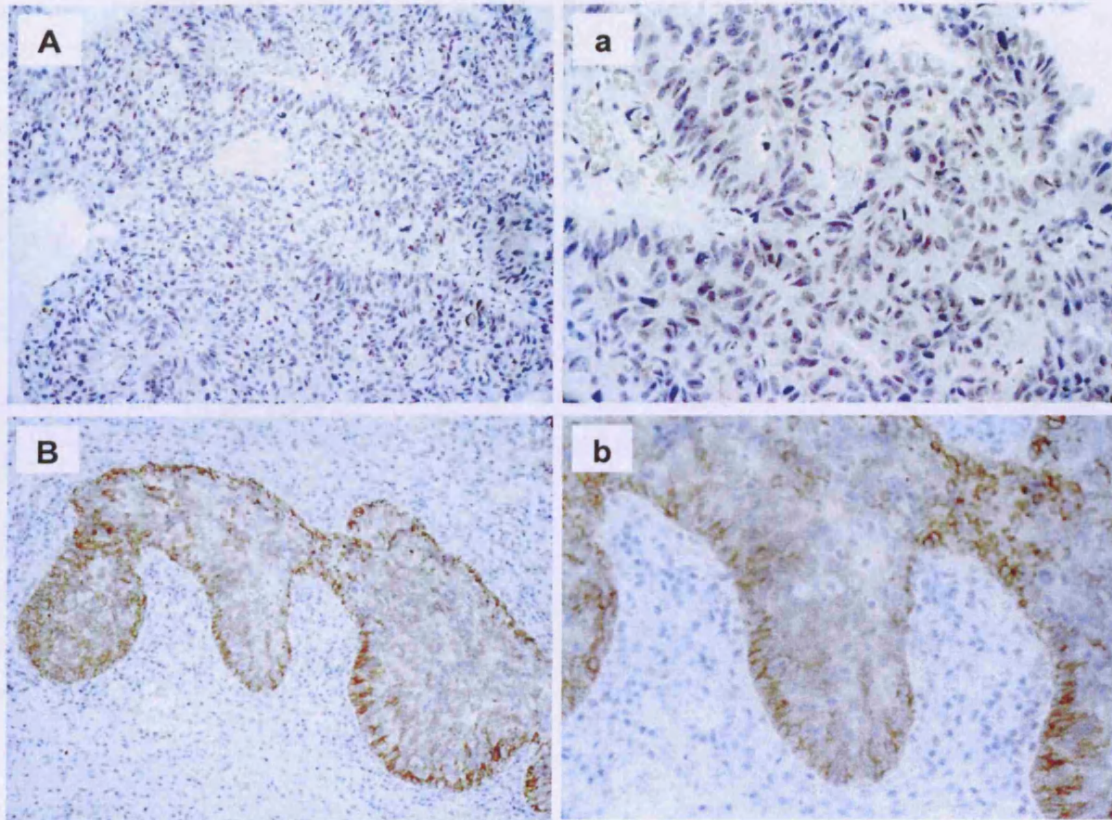


**Figure 3.14** *Expression of P-cadherin in superficial bladder tumours. (A) Absence of P-cadherin throughout the lesion (Block 7); (B) Restricted and strong membranous staining (Block 3) (photographed by  $\times 20$  lens). a and b (photographed by  $\times 40$  lens) represent enlarged areas from A and B, respectively.*

### 3.7 Determination of cadherin status in muscle invasive bladder tumours

Nine human muscle invasive bladder tumours were stained with E, N and P-cadherins using immunohistochemistry again by Dr MK Cheng.

The staining pattern of each cadherin is shown in *table 3.10*. Similar to the staining obtained in superficial specimens, all nine muscle invasive tumours showed some membranous E-cadherin. As shown in *figure 3.15*, the amount of membrane staining observed varied from strong stain in a few tumour cells, to more widespread stain in large focal areas. Cytoplasmic stain of E-cadherin was present in 6 of 9 (67%) samples.

*Table 3.10 Pattern of staining in muscle invasive tumours for cadherins*

Block number	E-cadherin		N-cadherin		P-cadherin	
	Cytoplasm	Membrane	Cytoplasm	Membrane	Cytoplasm	Membrane
2	++	+	-	-	O, ++	O, ++
3	++	+ / ++	-	-	++	++
4	-	+ / ++	-	-	++	++
8	++	+ / ++	x	x	++	++
10	-	+ / ++	-	-	-	+++
11	++	+ / ++	++	-	+++	+++
12	-	+	-	O, +	++	-
13	-	++	-	-	++	++
18	+ / ++	+	x	x	++	++

*-*, no staining detected; *x*, no available data; *+*, weak staining; *++*, strong staining; *+++*, very strong staining; *O*, occasional staining

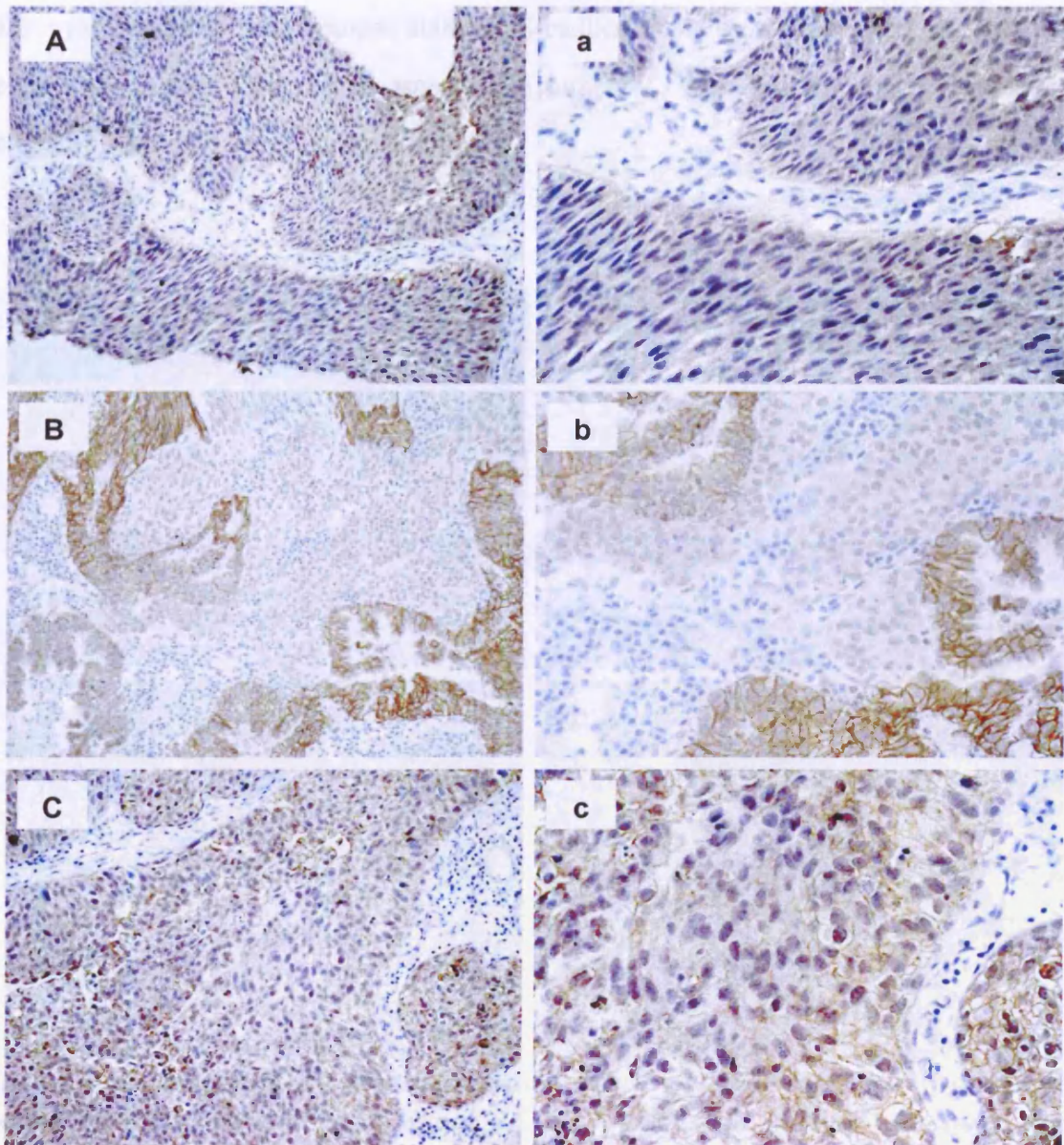


**Figure 3.15** *Expression of E-cadherin in muscle invasive bladder tumours. (A) Weak cytoplasm staining (Block 3); (B) Restricted, strong membrane staining (Block 11); (C) More widespread but faint membrane staining (Block 2) (photographed by ×20 lens). a, b and c (photographed by ×40 lens) represent enlarged areas from A, B and C, respectively.*

Either cytoplasmic or membranous stain of N-cadherin was seen only in 2 tumours, with no nuclear stain being observed in any of the tumours. *Figure 3.16* shows representative N-cadherin stain in muscle invasive tumours.

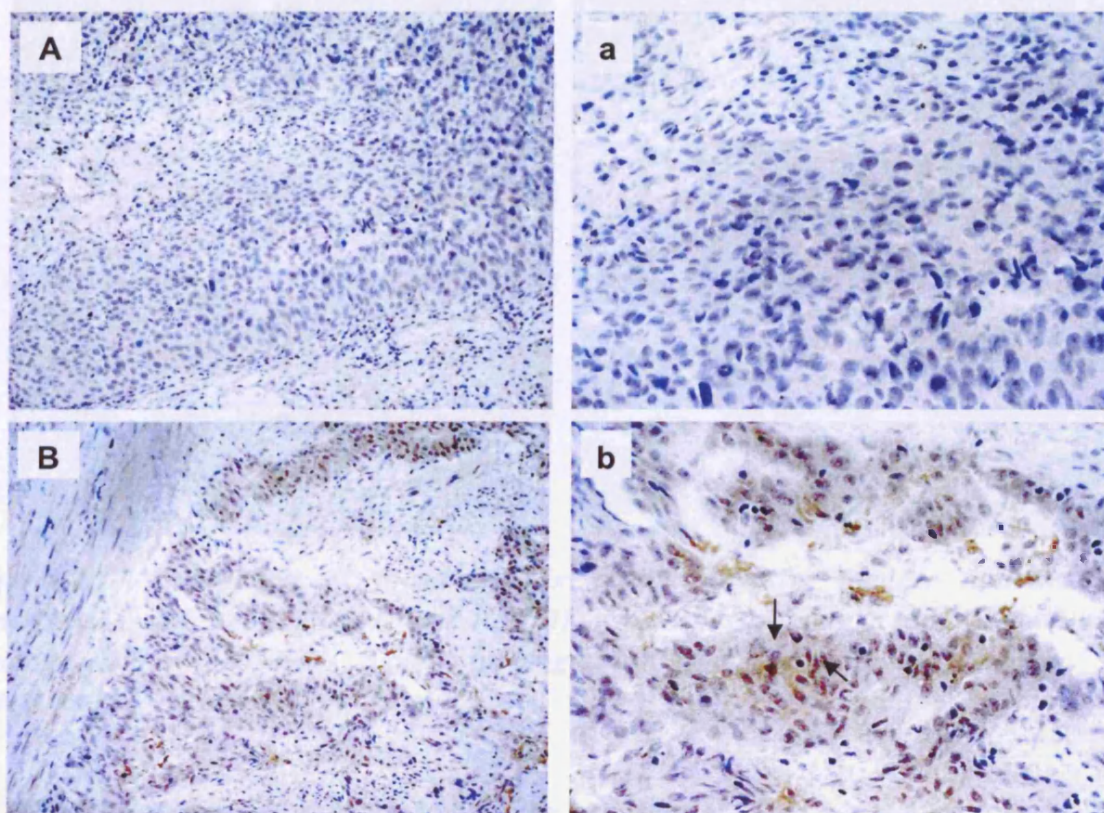


**Figure 3.16** *Expression of N-cadherin in muscle invasive bladder tumours.* (A) Absence of N-cadherin throughout the lesion (Block 2); (B) Cytoplasmic staining with some nuclear staining (see arrows) (Block 11) (photographed by  $\times 20$  lens). a and b (photographed by  $\times 40$  lens) represent enlarged areas from A and B, respectively.

Either cytoplasmic or membrane-localised P-cadherin was observed in 8 of 9 (89%) tumours, with expression at both sites in 7 samples. Staining was widespread in most cases, with examples shown in *figure 3.17*. Membranous P-cadherin staining in both superficial and muscle invasive tissues was strongest at the outer edge of tumour areas.

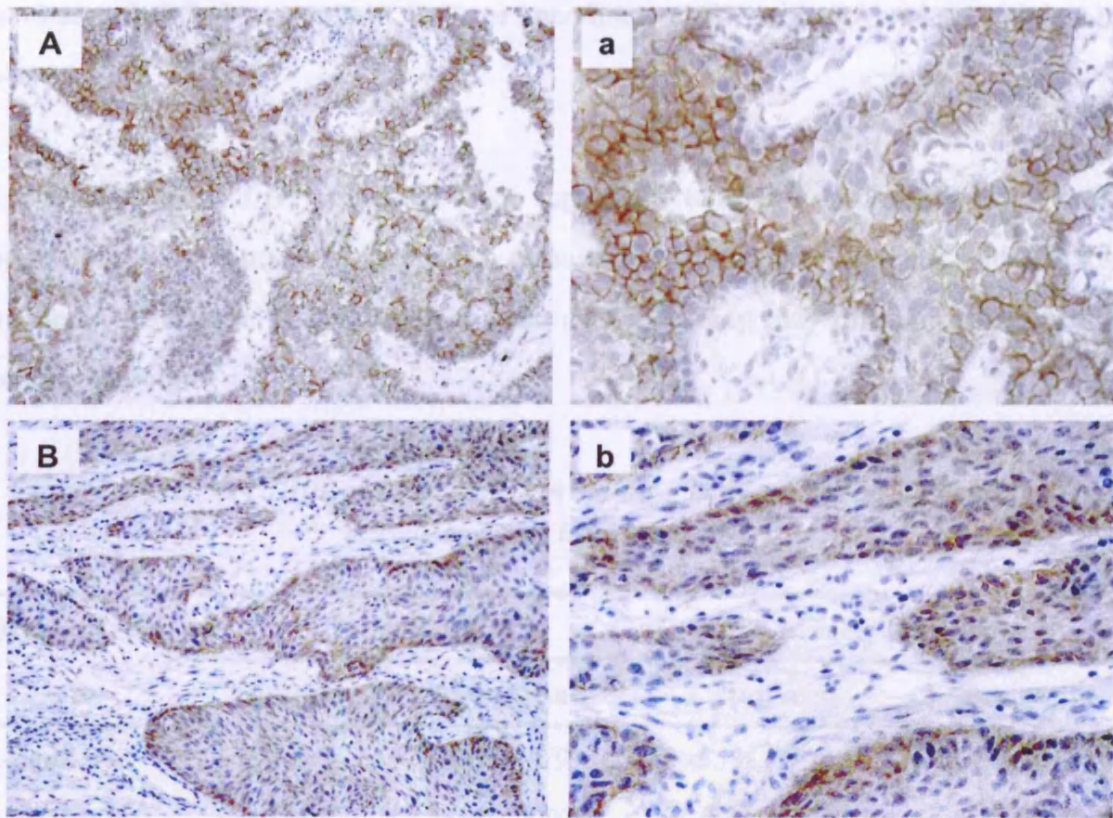


**Figure 3.17** *Expression of P-cadherin in muscle invasive bladder tumours.* (A) Widespread membrane staining (Block 10); (B) Cytoplasmic staining in focal areas (Block 3) (photographed by  $\times 20$  lens). a and b (photographed by  $\times 40$  lens) represent enlarged areas from A and B, respectively.

### **3.8 Relationship between cadherin expression and stage of bladder tumours**

In superficial tumours, the percentage of E-cadherin expression in cytoplasm was 67% (6/9) which was similar in muscle-invasive samples (55%). Membrane E-cadherin was detected in all specimens, either superficial or muscle-invasive. The P-cadherin staining in membrane was observed in 89% of superficial samples, with cytoplasmic staining being observed in 45% of tumours. Similarly, membrane P-cadherin occurred in 8 of 9 (89%) muscle-invasive tumours. Interestingly, P-cadherin was much more frequently expressed in the cytoplasm of muscle-invasive specimens (89%).

Apparent nuclear staining of N-cadherin was only observed in 4 of 9 (45%) superficial tumours. Additionally, N-cadherin was expressed in either cytoplasm or membrane in 33% (3/9) of superficial specimens. However, in muscle-invasive bladder tumours, N-cadherin

was observed only in cytoplasm (1/7) or membrane (1/7), with no nuclear staining being observed.

As shown in *table 3.11*, compared with superficial tumours, an increase of P-cadherin expression in cytoplasm was observed in muscle-invasive bladder tumours, with the loss of N-cadherin in nuclei. It suggests that three cadherins may play different roles in bladder cancer progression.

**Table 3.11 Difference in cadherin staining between superficial and muscle invasive bladder tumours**

Biomarkers	Superficial		Muscle invasive	
	Cytoplasm	Membrane	Cytoplasm	Membrane
<b>E-cadherin</b>	67% (6/9)	100% (9/9)	55% (5/9)	100% (9/9)
<b>P-cadherin</b>	45% (4/9)	89% (8/9)	89% (8/9)	89% (8/9)
	Cytoplasm	Nuclear		
	/Membrane			
<b>N-cadherin</b>	33% (3/9)	45% (4/9)	15% (1/7)	15% (1/7)

*The percentage of positive staining was calculated from tumour numbers in brackets. Compared with staining in superficial tumours, the increased percentages in muscle invasive tumours are shown in red.*

### **3.9 Relationship between STATs and cadherins expression in bladder tumours**

Six human bladder cell lines examined in this study (discussed in Chapter 4) have shown that three epithelial lines which are E-cadherin<sup>+ve</sup> only express phosphorylated STAT5, while three mesenchymal cells which are E-cadherin<sup>-ve</sup> have activated STAT3. In superficial bladder tumours, E-cadherin staining was observed in all 9 samples, however, no staining of pSTAT5 was detectable in any of the tumours. As shown in *table 3.12*, positive staining of both pSTAT3 and cadherins (E, N or P) were presented in 33% (3/9), 29% (2/7) and 25% (2/8) of superficial tumours, respectively.

**Table 3.12 Coexpression of phosphorylated STATs and cadherins in superficial and muscle invasive bladder tumours**

<b>Superficial</b>			
<b>Positive marker</b>	<b>E-cadherin (9/9)</b>	<b>N-cadherin (7/9)</b>	<b>P-cadherin (8/9)</b>
<b>pSTAT3 (3/9)</b>	33% (3/9)	29% (2/7)	25% (2/8)
<b>Muscle invasive</b>			
<b>Positive marker</b>	<b>E-cadherin (9/9)</b>	<b>N-cadherin (2/7)</b>	<b>P-cadherin (9/9)</b>
<b>pSTAT3 (14/20)</b>	55% (5/9)	50% (1/2)	55% (5/9)
<b>pSTAT5 (11/20)</b>	89% (8/9)	100% (2/2)	89% (8/9)

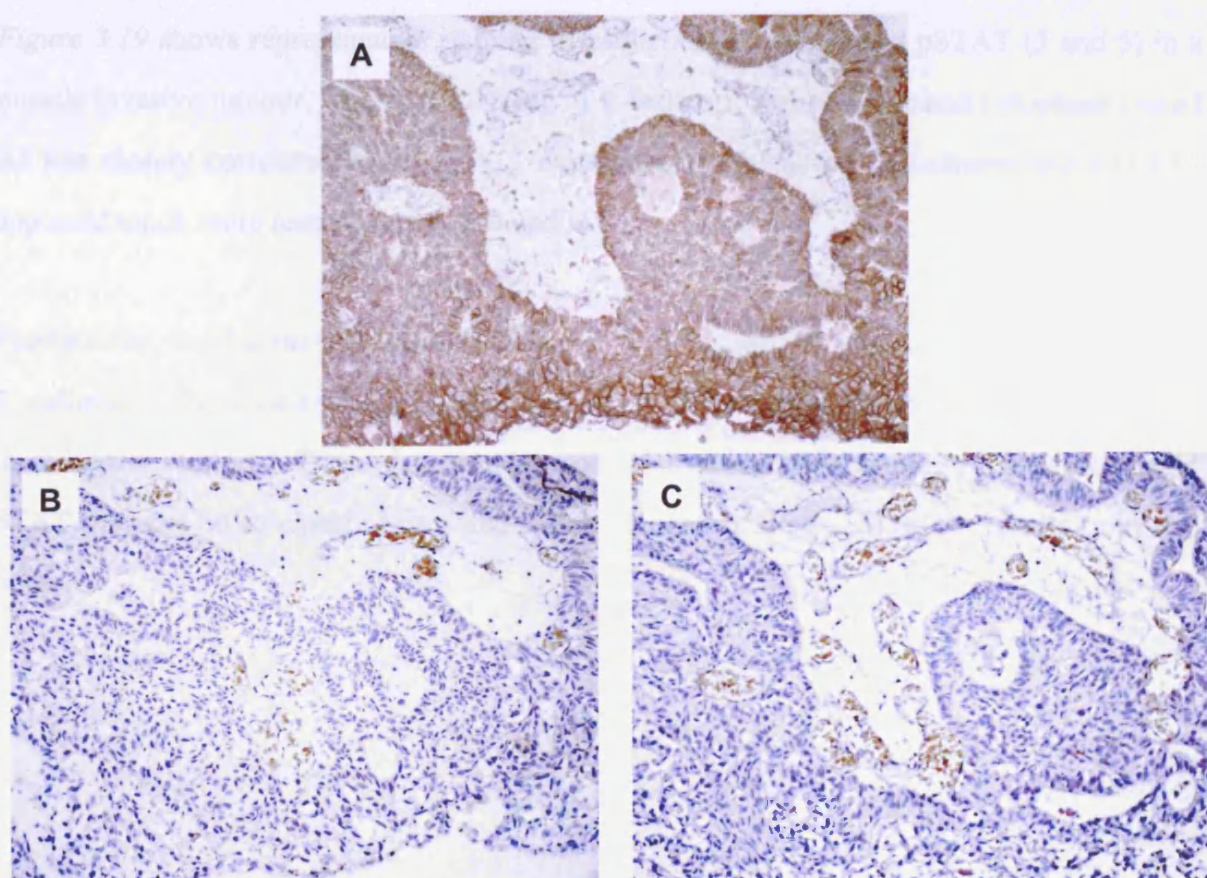


**Figure 3.18 Expression of E-cadherin and pSTAT (3 and 5) in superficial bladder tumours. (A) Strong membrane staining of E-cadherin; (B) Negative staining of pSTAT3; (C) Negative staining of pSTAT5 (Same areas of sections from Block 7 were photographed by  $\times 20$  lens).**

In semi serial sections, staining was positive for E-cadherin and negative for pSTAT (3 and 5) in the same area of superficial block 7, suggesting no link between E-cadherin and phosphorylated STAT (3 and 5) (*figure 3.18*).

Unlike the situation with STATs, no significant alteration in percentages of cadherin staining was observed in muscle invasive tumours, compared with superficial ones (*table 3.11*). In muscle invasive tumours, co-expression of pSTAT3 and cadherins was presented in half of tumours (E-cadherin 55% (5/9), N-cadherin 50% (1/2) and P-cadherin 55% (5/9)). pSTAT5 staining was observed in 89% (8/9) of E- or P-cadherin positive samples and 2 tumours (100%) in which N-cadherin staining was seen (*table 3.12*).

*Figure 3.19* shows representative staining of cadherins (E and N) and pSTAT (3 and 5) in a muscle invasive tumour. Positive staining of E-cadherin in membrane and cytoplasm (panel A) was closely correlated with pSTAT3 expression (panel C) but N-cadherin and pSTAT5 appeared much more restricted (panel B and D).

Furthermore, focal areas with either E-cadherin<sup>+ve</sup>, N-cadherin<sup>-ve</sup>, pSTAT3<sup>-ve</sup> or pSTAT5<sup>+ve</sup> or E-cadherin<sup>+ve</sup>, N-cadherin<sup>-ve</sup>, pSTAT3<sup>+ve</sup> and pSTAT5<sup>-ve</sup> staining (*figure 3.20*) were observed in the same section. These data provide some indication that staining of phosphorylated STAT may not be so closely associated with cadherins as suggested by the results from cell lines.

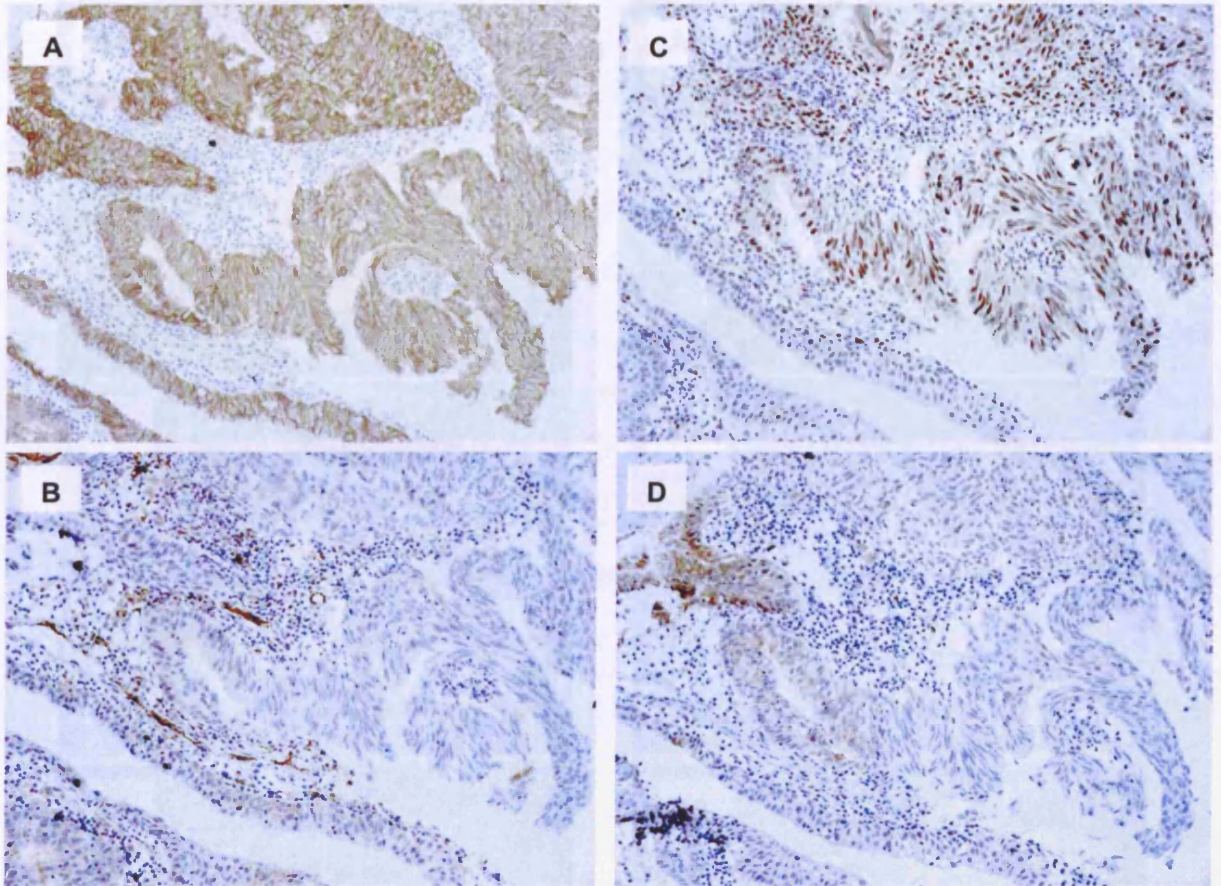


**Figure 3.19** Expression of E and N-cadherin and pSTAT (3 and 5) in muscle invasive bladder tumours. (A) Strong membrane and some cytoplasmic staining of E-cadherin; (B) Occasional staining of N-cadherin in cytoplasm; (C) Widespread nuclear staining of pSTAT3; (D) Occasional nuclear and membrane staining of pSTAT5 (Same areas of sections from Block 11 were photographed by  $\times 20$  lens).

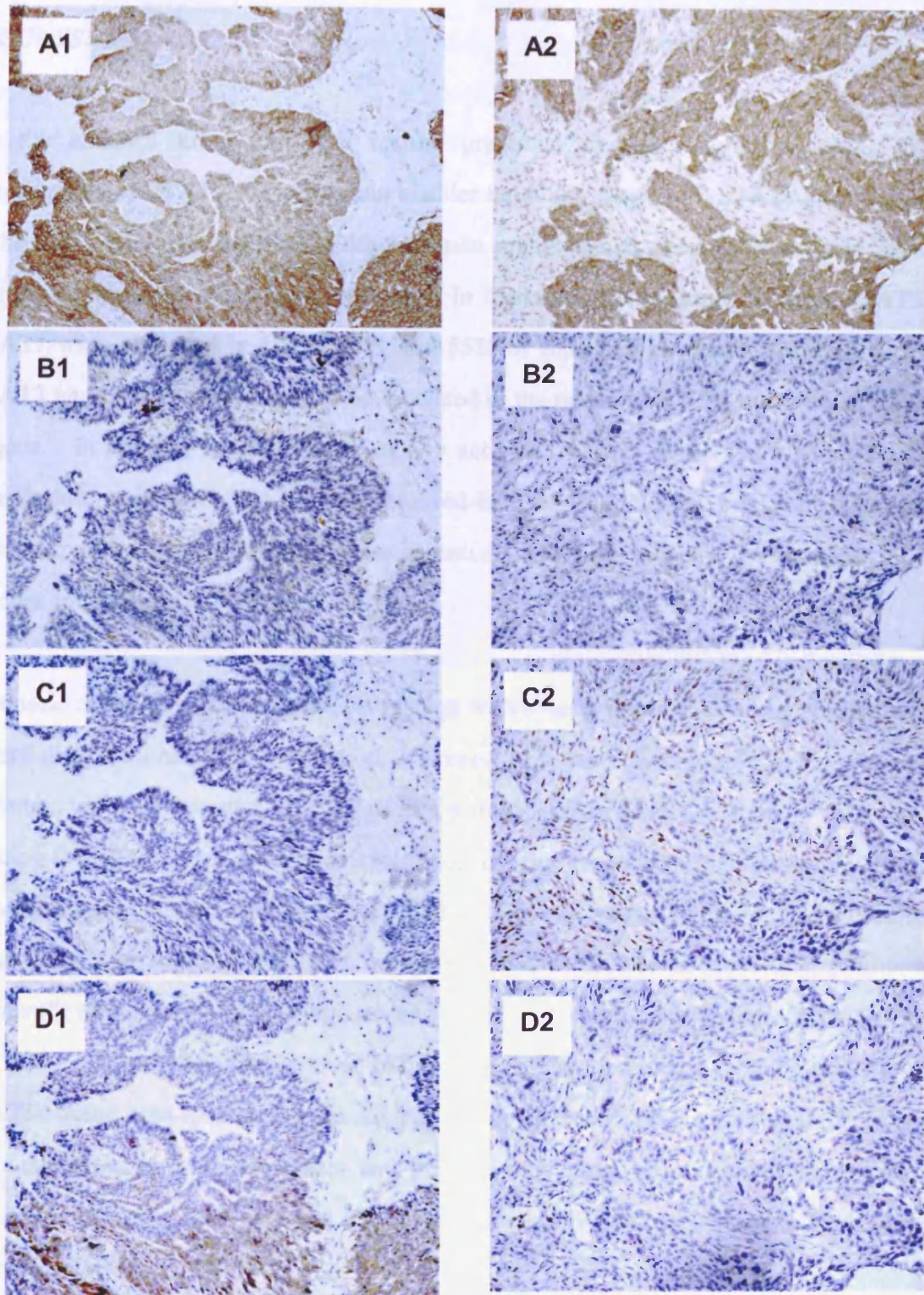


**Figure 3.20** Expression of E and N-cadherin and pSTAT (3 and 5) in muscle invasive bladder tumours. (A1&A2) Strong membrane staining of E-cadherin; (B1&B2) Negative staining of N-cadherin; (C1) Negative staining of pSTAT3; (C2) Nuclear staining of pSTAT3; (D1) Occasional nuclear and membrane staining of pSTAT5; (D2) Negative staining of pSTAT5 (A1-D1 and A2-D2 were two representative areas of sections from Block 13, photographed by  $\times 20$  lens).

## ***DISCUSSION***

To the author's knowledge, the results presented in this chapter represent the first investigation of STAT status in human bladder tumours. Although STATs have been shown to be overactive in a number of other human malignancies, their potential role in bladder cancer has not previously been reported. In this study cytoplasmic STAT3, STAT5b and STAT1 were observed in 100%, 67% and 55% of superficial tumours, respectively. Only STAT3 and STAT5b were seen to be localised to the nucleus, in 45% and 89% of superficial lesions. In contrast to the absence of any activated STATs in normal bladder epithelium, cytoplasmic stain for pSTAT3 was observed in 3 of 9 (33%) superficial bladder tumours. However, pSTAT5 and pSTAT1 were essentially absent, similar to the situation in normal bladder epithelium.

In muscle invasive specimens, the percentage with cytoplasmic STAT3 was similar to that in superficial tumours. The expression, however, was more widespread in muscle invasive tumours, with 13 samples (65%) having staining throughout the tissue. Also, nuclear staining for STAT3 was stronger and localised in larger areas in 60% of tumours. Similarly, cytoplasmic and nuclear staining of STAT5b and STAT1 was more intense and widespread in most cases. In addition, STAT5a, which was not detectable in superficial tumours, was frequently observed in both cytoplasm and nuclei. Overall, cytoplasmic STAT3, STAT5b and STAT1 were observed in over half of superficial specimens, with only STAT3 and STAT5b being seen localised to the nucleus. However, four STAT members (1, 3, 5a and 5b) were expressed in both cytoplasm and nucleus in a large proportion of muscle invasive tumours, suggesting that increased STAT expression may be associated with bladder tumour progression.

Interestingly, in muscle invasive lesions, all three phosphorylated STATs (1, 3 and 5) were observed, which were essentially absent in normal bladder epithelium. Cytoplasmic stain for pSTAT3 was present in 6 of 20 (30%) samples, whereas two tumours exhibited membranous pSTAT3. Although there was no increase in the percentage of samples with pSTAT3

staining in cytoplasm and membrane in muscle invasive bladder tumours, compared with superficial samples, the staining was much more widespread and stronger. In contrast to the absence of nuclear activated STAT3 in superficial tumours, this was present in 13 of 20 (65%) of muscle invasive tumours, suggesting that the presence of nuclear pSTAT3 may be linked to bladder tumour invasion. Results in this study are consistent with those in several other tissues. Kusaba *et al.*, (2005) found that in human colorectal adenocarcinomas, pSTAT3 expression is more intense in the most invasive areas, indicating a correlation between pSTAT3 and the depth of tumour invasion. Recently, a study by Yakata *et al.*, (2007) has shown that expression of pSTAT3 correlates with the degree of tumour invasion in human gastric carcinomas, with pSTAT3 showing significantly greater expression in more aggressive tumours. Importantly, Niu *et al.*, (2005) have reported that activated STAT3 inhibits p53 via binding to p53 promoter both *in vivo* and *in vitro*. Moreover, blocking of STAT3 results in upregulation of p53, thus leading to p53-mediated apoptosis and growth arrest in tumour cells. Alterations in p53 are frequently found in invasive and high grade superficial bladder carcinomas (Bakkar *et al.*, 2003) and are associated with a greater risk of recurrence (Orlow *et al.*, 1999).

In human head and neck carcinomas, Masuda *et al.*, (2002) reported that activation of STAT3 is significantly correlated with tumour stage. Patients with pSTAT3<sup>-ve</sup> colorectal tumours exhibited higher survival probability than patients with pSTAT3<sup>+ve</sup> tumours (Kusaba *et al.*, 2006). Recently, activation of STAT3 has also been associated with poor prognosis in human ovarian (Rosen *et al.*, 2006) and gastric carcinomas (Yakata *et al.*, 2007).

So far, the role of pSTAT5 and pSTAT1 in human malignancies is poorly understood. In bladder cancer, as results in this chapter show, neither cytoplasmic nor nuclear staining of pSTAT5 and pSTAT1 was seen in neither normal bladder epithelium nor in any of the superficial tumours. In muscle invasive specimens, either cytoplasmic or membranous stain of pSTAT5 and pSTAT1 was present in 50% and 13% of samples, respectively, while nuclear pSTAT5 and pSTAT1 was seen in 25% and 60% of tumours. This suggests that there may

also be a link between the presence of active STAT5 and STAT1 and invasive bladder tumours.

In this study, due to incomplete information on clinical outcome, it remains unclear whether activation of STATs can be linked to poor survival in patients. Also, only a small number of bladder tumours has been examined, insufficient to provide a comprehensive understanding of the role of STATs in human bladder cancer.

In normal bladder epithelial, E-cadherin was localised to cell-cell borders and the staining was more intense than in bladder tumours (Popov *et al.*, 2000; Bornman *et al.*, 2001). In contrast, N-cadherin expression was absent in normal urothelium, appeared in stage pT<sub>1</sub>, and increased in pT<sub>2</sub>-pT<sub>3</sub> tumors, and in most cases, increased N-cadherin expression in invasive tumors was associated with loss of E-cadherin expression (Lascombe *et al.*, 2006). In other studies on the role of E-cadherin (Sun and Herrera, 2004) and N-cadherin (Lascombe *et al.*, 2006) in human bladder cancer, expression of these proteins was correlated with the suppression or promotion of invasive potential, respectively. In breast carcinomas, P-cadherin, but not E or N-cadherin expression has been strongly correlated with several clinicopathological features, including high grade (poor differentiation), lack of oestrogen receptors and presence of EGFR (Kovacs *et al.*, 2003). Rieger-Christ *et al.*, (2001) have shown that membranous P-cadherin is observed in the basal cells of normal bladder mucosa, and becomes extensive in bladder tumours. However, the role of P-cadherin in bladder tumourigenesis is not well understood.

A number of bladder tumours, including 9 superficial and 9 muscle invasive lesions were also stained for three cadherins (E, N and P). In this study, membranous E-cadherin was observed in 100% (9/9) of G3pT1 superficial tumours, with 6 samples also exhibiting cytoplasmic E-cadherin. Similarly, P-cadherin was localised to cytoplasm in 45% of superficial tumours, and membrane in 8 of 9 (89%) superficial samples. N-cadherin was present in 33% of superficial specimens with either cytoplasmic or membranous stain, and 45% of tumours showed nuclear stain. Notably, co-expression of E-, N- and P-cadherin was recorded in some superficial lesions, consistent with a previous study by Rieger-Christ *et al.*,

(2001). Their *in vitro* observations have also shown that some bladder cancer cell lines coexpress E-, N- and P-cadherin, indicating that the expression of these cadherins is not mutually exclusive in bladder cancer. A study in colon tumours has shown that P-cadherin is co-expressed with E-cadherin on the membrane, but is independent of E-cadherin expression (Hardy *et al.*, 2002). So far, cadherins are reported to be localised in membrane or cytoplasm in most studies. It was rather unexpected that nuclear N-cadherin was present in half of the superficial bladder tumours. In a recent study, aberrant nuclear staining of E-cadherin has been observed in solid pseudopapillary tumors of the pancreas, due to a close correlation between E-cadherin and  $\beta$ -catenin which was localised to the nucleus (Serra *et al.*, 2007). Several studies have demonstrated a complex between N-cadherin and  $\beta$ -catenin (Lee *et al.*, 2003; Wahl 3rd *et al.*, 2003). This suggests that nuclear localisation of N-cadherin in bladder tumours could be attributed to a cadherin/catenin complex.

E-cadherin was also localised to cytoplasm and membrane in the majority of muscle invasive lesions. Also, cytoplasmic P-cadherin was present in a greater proportion of invasive tumours than superficial tumours. However, there was limited expression of N-cadherin, localised to focal islands of cells within the tumour, being observed in cytoplasm and membrane, with no nuclear stain in any of muscle invasive tumours. Unlike E- and P-cadherin (Shimoyama *et al.*, 1989), expression of N-cadherin has not been observed in normal bladder mucosa. Lascombe *et al.*, (2006) have shown that N-cadherin acts in an invasive mode in bladder cancer. In this study, a small proportion of superficial and invasive bladder lesions display N-cadherin expression, suggesting aberrant cadherin expression in bladder carcinoma.

Compared with superficial tumours, membranous staining of E-cadherin was overall diffused and weaker in muscle invasive tumours, although no decrease in the percentage samples positive for E-cadherin was observed. This possibly suggests that reduction of E-cadherin expression is associated with more aggressive bladder tumours. A few studies have investigated whether the decreased E-cadherin expression has a prognostic role in bladder carcinoma. Sun and Herrera (2004) and other earlier reports have found that the loss or

reduced expression in E-cadherin was linked to poor tumour differentiation and more invasive potential. However, two more recent studies (Szekely *et al.*, 2006; Koksai *et al.*, 2006) have shown no significant correlation between E-cadherin expression and bladder tumour grade, stage or overall survival. Interestingly, Bindels *et al.*, (2000) have demonstrated a dual paradoxical role of E-cadherin in bladder tumorigenesis. Compared to RT112 cells (E-cadherin<sup>+ve</sup> bladder line), J82 and T24 (E-cadherin<sup>-ve</sup> bladder lines) cells display a higher invasive capacity. In their study, T24 (E-cadherin<sup>-ve</sup> bladder cell line) cells were transfected with full-length mouse *E-cadherin* cDNA, resulting in an enhanced intraepithelial expansion without any effect on cell proliferative and invasive capacity, indicating that E-cadherin can promote the intraepithelial expansion whereas the loss of E-cadherin is associated with more invasive potential.

In present study, only a small number of human bladder tumours have been examined, so it is not clear whether any of these three cadherins can be potential prognostic markers, or whether there is any link between STAT and cadherin expression in bladder carcinoma.

Patients having higher risk bladder tumours could be followed more frequently, or treated more radically, if the more aggressive behaviour of tumours could be predicted accurately. To address this question, a larger number of bladder tumours of different stage and grade need to be studied in future work.

## **CHAPTER 4**

### **STATS SIGNALLING IN BLADDER CANCER CELLS**

## **INTRODUCTION**

STATs 1, 3 and 5 are activated by a series of ligands and are involved in various biological processes, such as embryogenesis, apoptosis and development (Bromberg, 2002). Either growth factor receptors, such as EGF, HGF and PDGF receptors, which possess intrinsic tyrosine kinase activity, or cytokine receptors, which have no intrinsic enzymatic activity, can activate STAT proteins directly or indirectly, by means of JAK proteins. Non-receptor tyrosine kinases, such as src, can also activate STAT proteins independently of receptor engagement. Tyrosine phosphorylation is required for STAT transcriptional activity, and phosphorylation of a conserved C-terminal serine residue is necessary for maximal STAT transcriptional activity (Decker and Kovarik, 2000). In cancer, STATs become constitutively activated as a result of one or more persistently activated upstream tyrosine kinases (Buettner *et al.*, 2002).

The role of STATs in oncogenesis is mediated through the expression of genes involved in blocking apoptosis, such as Mcl-1 (Epling-Burnette *et al.*, 2001), Bcl-x<sub>L</sub> (Zushi *et al.*, 1998) and survivin (Aoki *et al.*, 2003); proliferation, such as c-myc (Bowman *et al.*, 2001) and cyclin D1 (Masuda *et al.*, 2002); invasion, such as matrix metalloproteinase-9 (MMP-9) (Dechow *et al.*, 2004) and angiogenesis, such as VEGF (Niu *et al.*, 2002).

As noted previously, STAT3, STAT5 and STAT1 have been observed to be overactive in a range of human cancer cell lines, such as breast (Garcia *et al.*, 1997, Sartor *et al.*, 1997), head and neck (Grandis *et al.*, 1998), leukemia (Gouilleux-Gruart *et al.*, 1996, Shuai *et al.*, 1996, Liu *et al.*, 1999), lung (Liby *et al.*, 2006), lymphoma (Weber-Nordt *et al.*, 1996, Yu *et al.*, 1997, Lund *et al.*, 1999), prostate (Mora *et al.*, 2002) and multiple myeloma (Catlett-Falcone *et al.*, 1999<sup>2</sup>, Hodge *et al.*, 2004, Liby *et al.*, 2006). However, the status of STATs in human bladder cancer cells has not been well documented.

So far, only a few papers have found STAT activation in response to EGF in bladder cell lines. Kawamata *et al.*, (1999) have shown that EGF activates STAT1 and STAT3 in T24 cells, accompanied by the enhanced expression of p21<sup>waf1</sup> mRNA. However, EGF had no effect in RT4 cells. A more recent study has reported that only STAT3, but not STAT1 or STAT5 becomes phosphorylated following EGF treatment in T24 cells (Itoh *et al.*, 2006). Also, these

authors have shown that STAT3 is required for EGF-induced cell migration, invasion and tumour formation in nude mice.

The aim of work described in this chapter was to determine the expression profile of STATs in human bladder cancer cells, and identify upstream tyrosine kinases which specifically phosphorylate STATs in these lines. STAT was then knocked out in order to investigate the potential role of STATs in cell cycle, apoptosis and cell motility.

## **RESULTS**

### **4.1 Determination of STATs status in a panel of human bladder cell lines**

A panel of six human bladder cancer cell lines has been screened for STAT expression in serum-containing, serum-free or EGF-containing medium, consisting of epithelial (RT4, RT112 and HT1376) and mesenchymal (J82, T24 and UMUC3) phenotypes (*Chapter 2, table 2.1*). Masters *et al.*, (1986) reported that these cell lines are originally from invasive bladder cancers, with clinical staging T2 or above.

#### **4.1.1 Basal levels of total STAT1 and STAT3 under normal growth condition**

It was initially important to determine basal levels of total STAT1 and STAT3 within the six human bladder cancer cells when grown under normal condition, in order to see whether levels were significantly different among cell lines.

*Figure 4.1* depicts basal levels of total STAT1 and STAT3 under normal growth condition in the RT4, RT112, HT1376, T24, J82 and UMUC3 bladder cell lines. Overall, levels of STAT1 and STAT3 were similar among the six lines.

#### **4.1.2 Effect of serum starvation on STAT1 and STAT3 protein levels**

The effect of serum starvation and re-stimulation upon STAT1 and STAT3 levels was determined in all 6 bladder cell lines (*figure 4.1*). A431, a human epidermoid carcinoma cell line, in which STATs are clearly expressed, was used as positive control.

Serum-starvation and re-stimulation elicited no significant effect on levels of total STAT1 or STAT3 in any cell lines, suggesting that the constitutive expression of STATs is independent of autocrine growth factors in medium.

\* Antibodies against phospho-STAT1, 3 and 5 used here only detect tyrosine phosphorylation of STAT1, 3 and 5 on sites 701, 705 and 694, respectively.

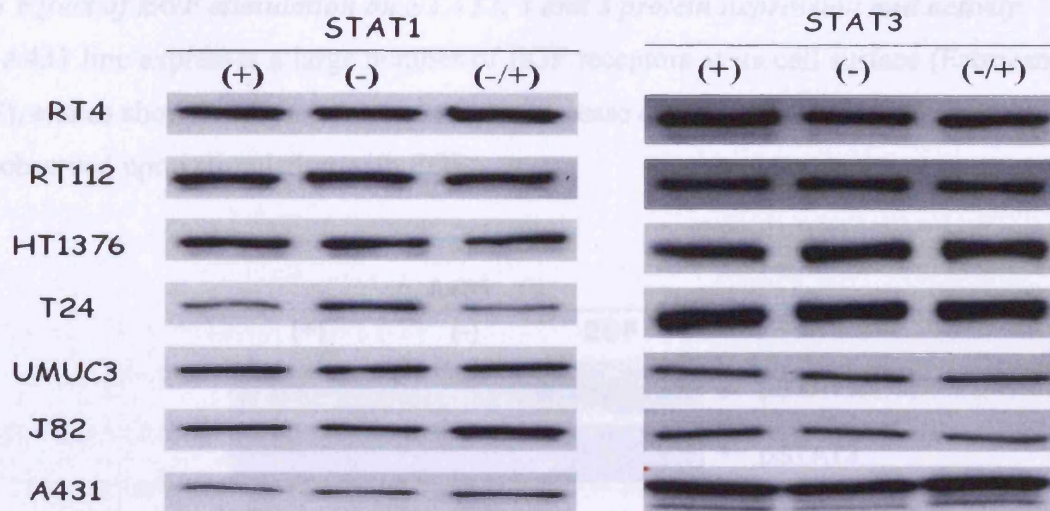


Figure 4.2 Effect of EGF stimulation on STAT1 and STAT3 phosphorylation status in A431 cells. Cells were grown in the presence of serum (+), or in serum-free (-) medium for 24 hours. The serum-starved cells were then incubated in serum-free or EGF-containing medium for a further 30 minutes. Blots were performed on 3 separate occasions.

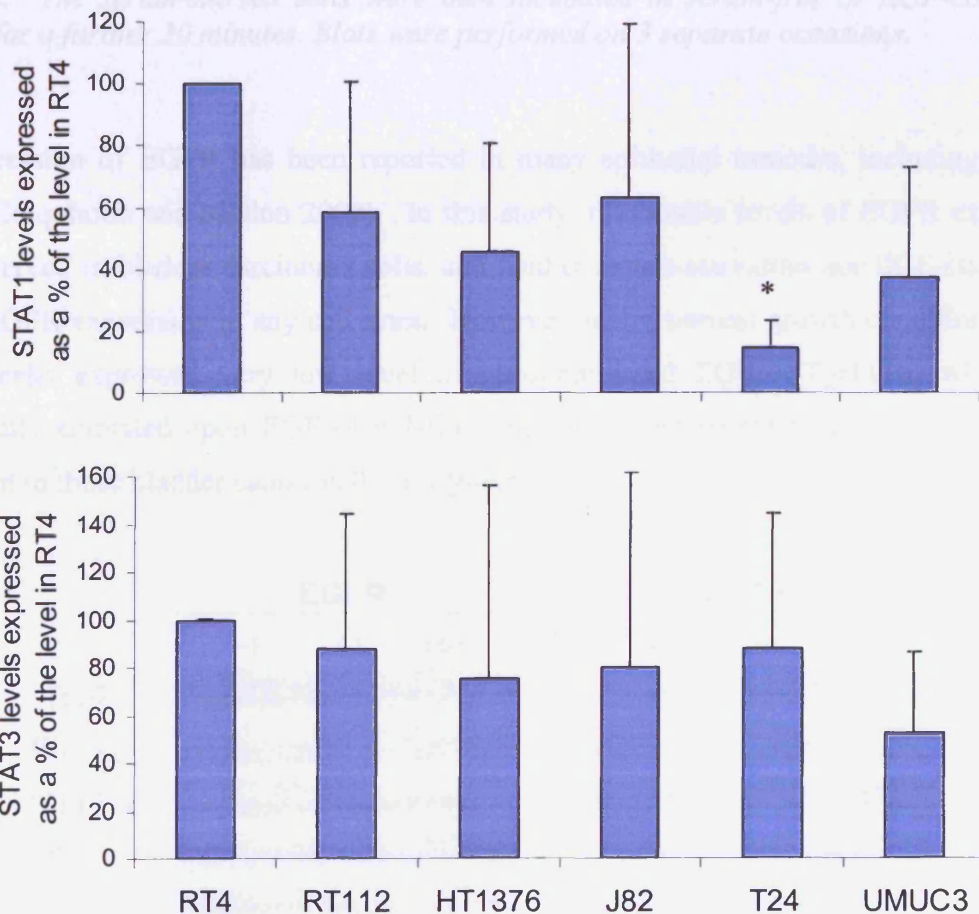
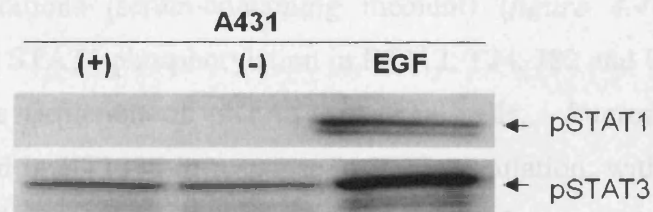


Figure 4.1 Effect of serum starvation and re-stimulation on total STAT1 and STAT3 expression levels in 6 bladder cell lines. Cells were grown in the presence of serum (+), or in serum-free (-) medium for 24 hours. The serum-starved cells were then incubated in serum-free or serum-containing (-/+) medium for a further 1 hour. The charts show relative levels normalised to tubulin, compared to those in RT4 cells as determined via densitometric analysis of blots. \* denotes a significant difference from total STAT1 levels in the RT4 cells ( $p < 0.05$ ,  $n = 3$ ,  $\pm$ SD) using oneway ANOVA followed by Student's *t*-test.

#### 4.1.3 Effect of EGF stimulation on STAT1, 3 and 5 protein expression and activity

The A431 line expresses a large number of EGF receptors at its cell surface (Fabricant *et al.*, 1977), and as shown in *figure 4.2*, a dramatic increase of STAT1 and STAT3 phosphorylation was observed upon stimulation with EGF.



**Figure 4.2** Effect of EGF stimulation on STAT1 and STAT3 phosphorylation status in A431 cells. Cells were grown in the presence of serum (+), or in serum-free (-) medium for 24 hours. The serum-starved cells were then incubated in serum-free or EGF-containing medium for a further 30 minutes. Blots were performed on 3 separate occasions.

Overexpression of EGFR has been reported in many epithelial tumours, including bladder cancer (Colquhoun and Mellon 2002). In this study, reasonable levels of EGFR expression were observed in bladder carcinoma cells, and neither serum-starvation nor EGF-stimulation altered EGFR expression in any cell lines. However, under normal growth condition all five bladder cells expressed very low level of phosphorylated EGFR (Tyr1110) which was significantly activated upon EGF stimulation, indicating that receptor activation was EGF-dependent in these bladder cancer cell lines (*figure 4.3*).

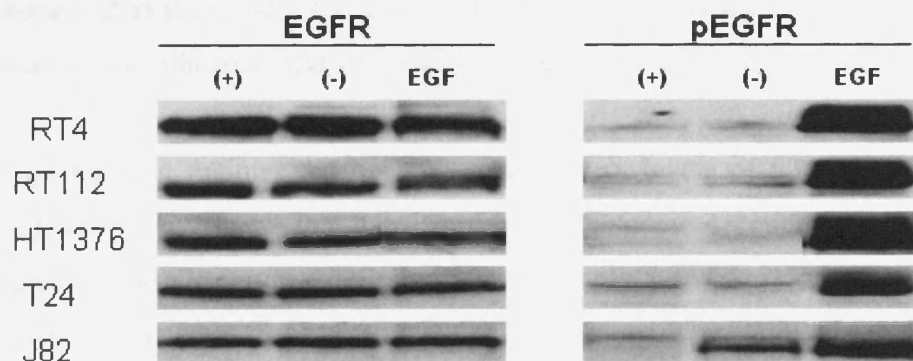


**Figure 4.3** Effect of EGF stimulation on EGFR expression and phosphorylation in bladder cancer cells. Cells were grown in the presence of serum (+), or in serum-free (-) medium for 24 hours. The serum-starved cells were then incubated in serum-free or EGF-containing medium for a further 5 minutes. Blots were performed only once.

As with serum starvation, EGF stimulation did not affect STAT1 protein levels in any cell line (*figure 4.4*). Although there appeared to be some decrease in T24 cells following EGF stimulation on the blot shown, this did not turn out to be statistically significant.

Only the RT4 bladder line expressed significant levels of phosphoSTAT1 (Tyr701) under normal growth conditions (serum-containing medium) (*figure 4.4*). However, serum withdrawal increased STAT1 phosphorylation in RT112, T24, J82 and UMUC3 cells, while it resulted in complete depletion of pSTAT1 in RT4 cells. Interestingly, pSTAT1 was significantly activated in HT1376 in response to EGF stimulation, with a further increase in STAT1 phosphorylation also observed in UMUC3 cells. In contrast, there was no further activation of pSTAT1 in RT4, RT112, J82 and T24 cell lines following EGF stimulation (*figure 4.4*). This indicated that STAT1 activation following serum withdrawal or EGF stimulation was cell-type specific.

As shown in *figure 4.5*, neither serum starvation nor EGF stimulation altered total STAT3 levels in any of the six cell lines. Under normal growth condition, phosphorylated STAT3 (Tyr705) was detected in the mesenchymal T24, J82 and UMUC3 cells but not the epithelial RT4, RT112 and HT1376 cells. In RT4 cells, STAT3 could not be phosphorylated by either serum starvation or EGF stimulation. Also, there was no further increase of pSTAT3 observed in T24, J82 and UMUC3 cells in response to serum starvation or EGF stimulation, indicating that these three cell lines express constitutive phosphorylation of STAT3. Although there was still no STAT3 phosphorylation detected in RT112 and HT1376 cells following serum starvation, STAT3 was significantly activated by EGF stimulation. This suggested that STAT3 phosphorylation was EGF-dependent in RT112 and HT1376 cell lines.

The differing treatment regimes did not affect the protein levels of STAT5a or STAT5b in any cell line (*figure 4.6*), except that there appeared to be some decrease in STAT5b level in RT112 cells in response to serum withdrawal. Interestingly, phosphorylated STAT5 (Tyr694) was only observed in RT4, RT112 and HT1376 cells, with no further increase detected following serum starvation or EGF stimulation. In J82 and T24 cell lines, STAT5 was activated in response to EGF stimulation, although under normal growth condition or following serum starvation, no pSTAT5 was detected (*figure 4.6*).

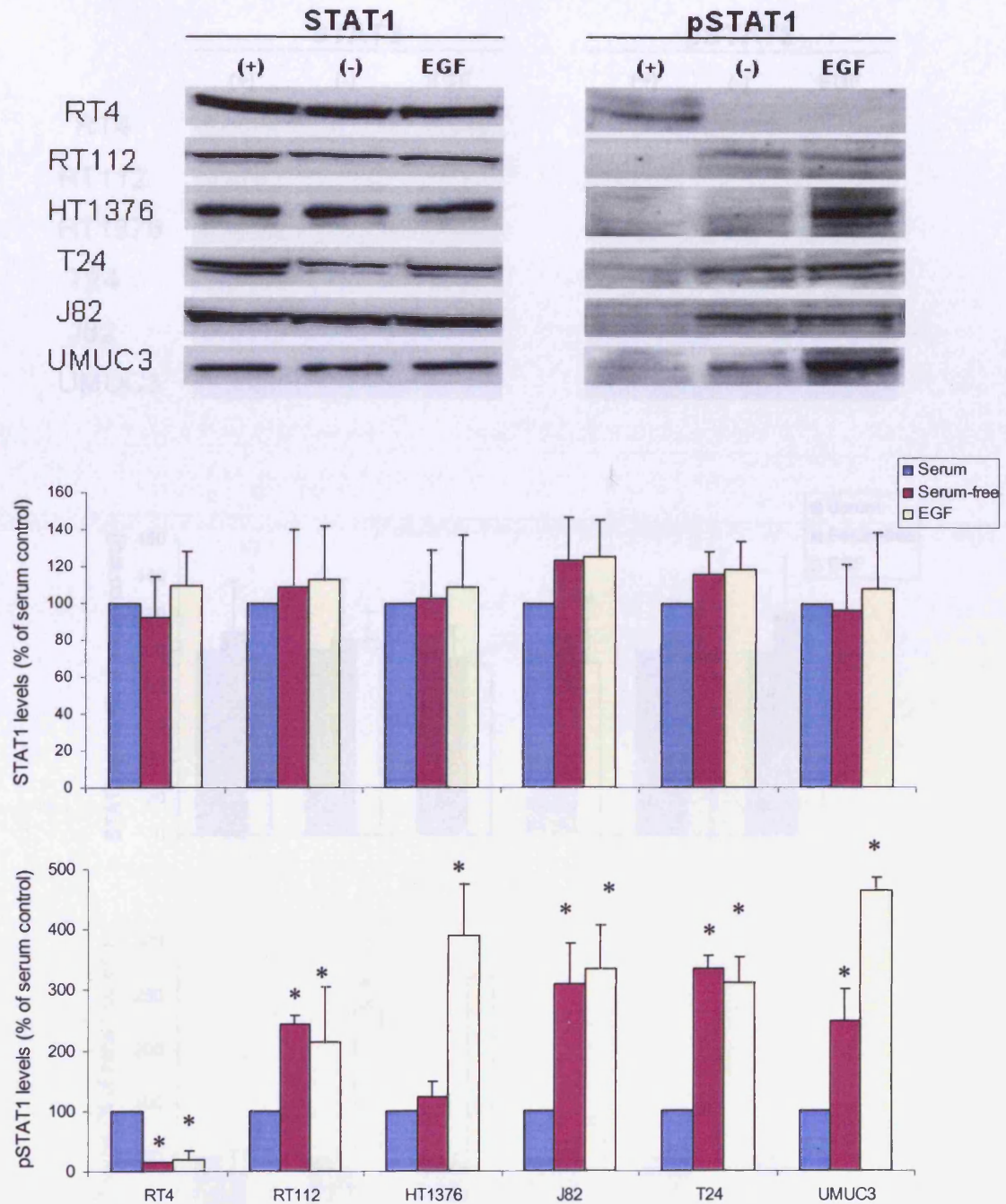


**Figure 4.4 Effect of serum starvation or EGF stimulation on total and phosphorylated STAT1 in bladder cell lines.** Cells were grown in the presence of serum (+), or in serum-free (-) medium for 24 hours. The serum-starved cells were then incubated in serum-free or EGF-containing medium for a further 5 minutes. The top panel shows representative western blots of total and phosphorylated STAT1 in each bladder cell line following treatment. The charts show relative levels normalised against tubulin, as determined via densitometric analysis of blots. \* denotes a significant difference from serum control ( $p < 0.05$ ,  $n = 3$ ,  $\pm SD$ ) using oneway ANOVA followed by Student's *t*-test.

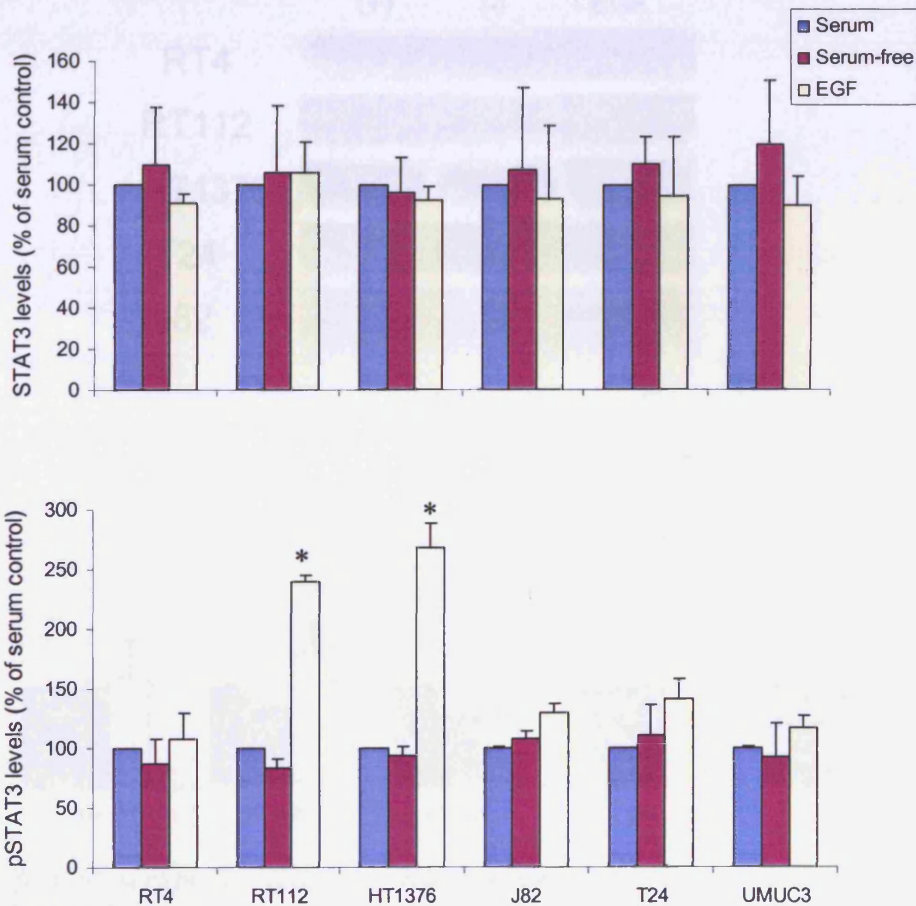
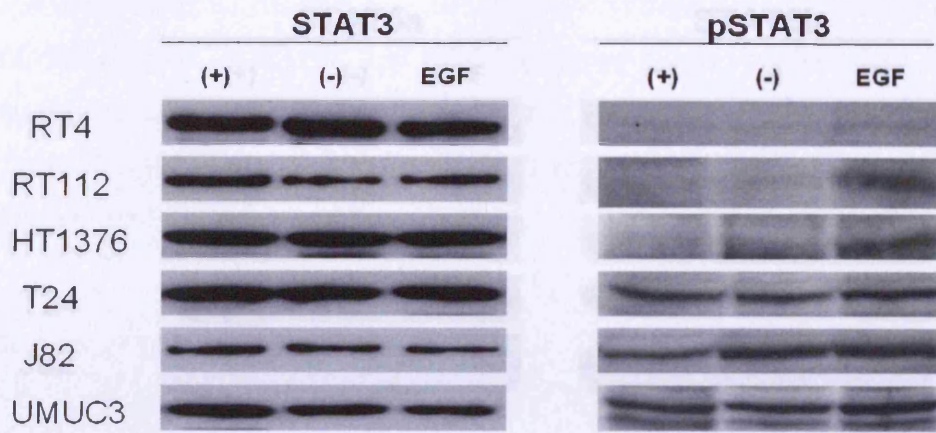


**Figure 4.5** Effect of serum starvation or EGF stimulation on total and phosphorylated STAT3 in bladder cell lines. Cells were grown in the presence of serum (+), or in serum-free (-) medium for 24 hours. The serum-starved cells were then incubated in serum-free or EGF-containing medium for a further 5 minutes. The top panel shows representative western blots of total and phosphorylated STAT3 in each bladder cell line following treatment. The charts show relative levels normalised against tubulin, as determined via densitometric analysis of blots. \* denotes a significant difference from serum control ( $p < 0.05$ ,  $n = 3$ ,  $\pm SD$ ) using one-way ANOVA followed by Student's *t*-test.

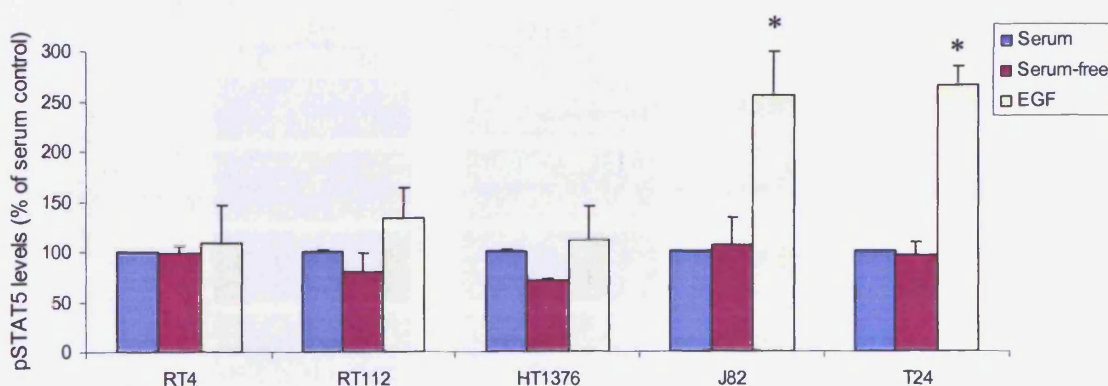


**Figure 4.6** Effect of serum starvation or EGF stimulation on total and phosphorylated STAT5 in bladder cell lines. Cells were grown in the presence of serum (+), or in serum-free (-) medium for 24 hours. The serum-starved cells were then incubated in serum-free or EGF-containing medium for a further 5 minutes. Blots were performed on 3 separate occasions (with the exception of STAT5a and b blots,  $n=2$ ). The chart shows relative levels normalised against tubulin, as determined via densitometric analysis of blots. \* denotes a significant difference from serum control ( $p<0.05$ ,  $n=3$ ,  $\pm SD$ ) using an oneway ANOVA followed by Student's *t*-test.

Data so far have shown an interesting STAT phosphorylation profile in bladder cell lines. Three epithelial lines, RT4, RT112 and HT1376 express phosphorylated STAT5, whereas three mesenchymal lines, T24, J82 and UMUC3 have phosphorylated STAT3. Thus, RT112 and J82 were chosen as representative lines of epithelial and mesenchymal groups in following experiments.

#### 4.2 Localisation of STATs in bladder cancer cells

Results so far have demonstrated the expression profile of total and phosphorylated STATs in a panel of bladder cancer cell lines. Next, the localisation of STATs in RT112 and J82 cell lines was investigated. Cytosolic and nuclear protein extracts were prepared as described in section 2.4.2.

In J82 cells, total STAT1, STAT3 and STAT5 (a and b) were observed to be localised in both cytoplasm and nuclei. Similarly, cytoplasmic and nuclear STAT1, STAT3 and STAT5a were seen in RT112 cells. However, STAT5b was only expressed in cytoplasm in RT112 cells (*figure 4.7*). Unfortunately, due to unresolved problems, complementary blots stained for phosphorylated STATs in both cell lines were unsuccessful on 2 separate occasions.

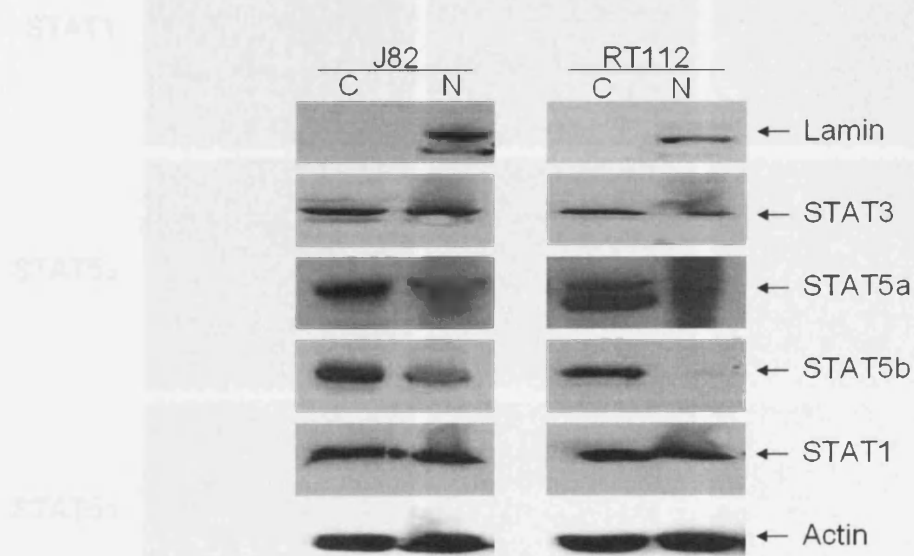


**Figure 4.7** Western blots showing STATs localisation in J82 and RT112 cell lines. Cells were grown in normal growth condition, and cytosolic (C) and nuclear (N) protein extracts from J82 and RT112 cells were probed for total STAT1, 3 and 5 (a and b) levels. Lamin was used as positive control for nuclear extracts. Blots were performed on 2 separate occasions.

Consistent with western blot data, immunocytochemistry staining showed STAT1, STAT3 and STAT5 (a and b) localised in both cytoplasm and nuclei in both cell lines, except STAT5b which was present only in cytoplasm of RT112 cells. Interestingly, pSTAT3 in J82 cells and pSTAT5 in RT112 cells were mainly localised in nuclei, with some cytoplasmic staining observed (*figures 4.8 and 4.9*).

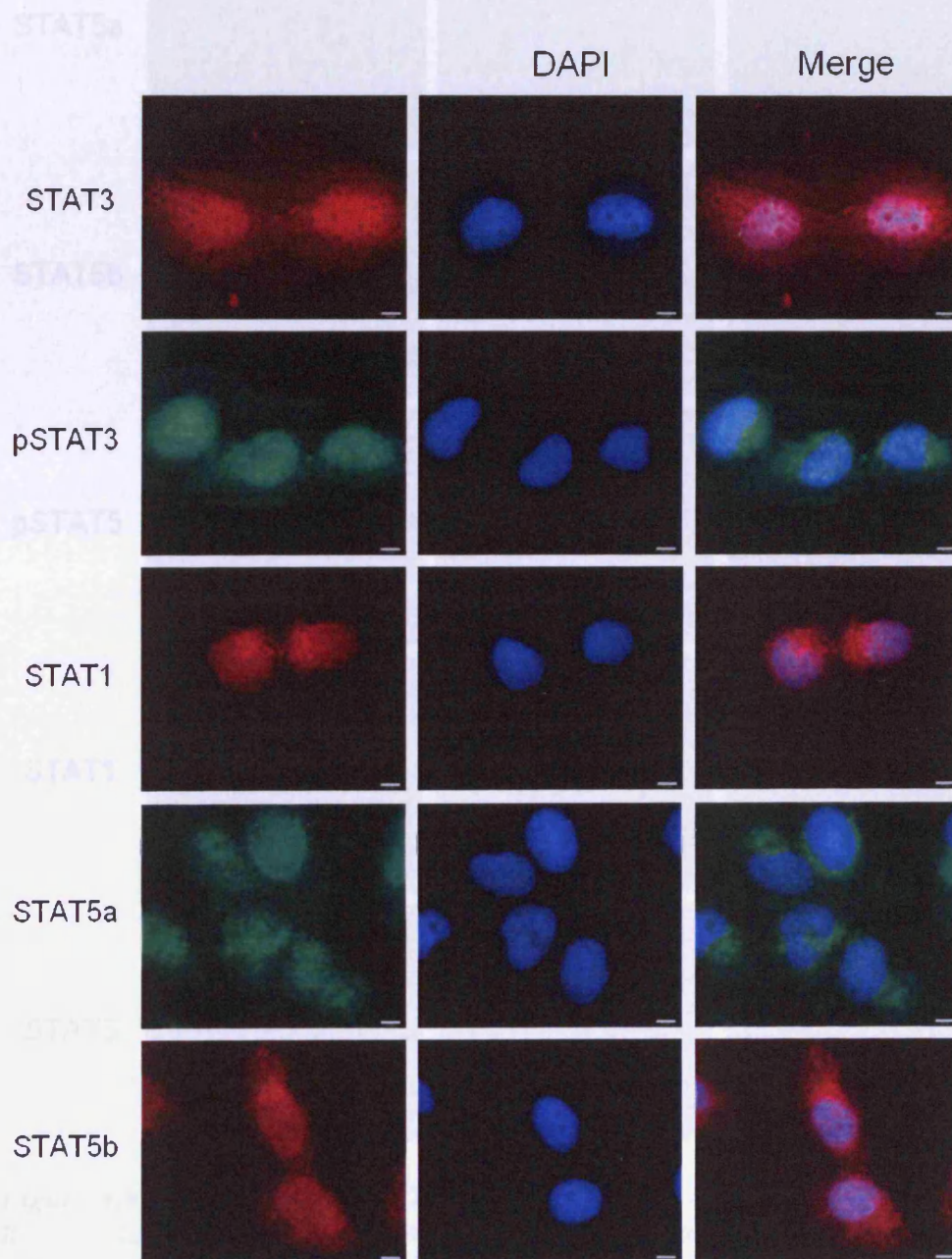


**Figure 4.8 Determination of STATs localisation in J82 cells by immunofluorescence.** J82 cells were seeded on cover slips and allowed to adhere overnight. At 60% confluent, cells were fixed and stained with antibodies against STAT3, pSTAT3, STAT1 and STAT5 (a and b), counterstained with DAPI and examined by fluorescence microscope (Scale bars equal to 6 $\mu$ m).

### 4.3 Transcriptional activity of STATs

In order to measure endogenous STAT transcriptional activity in bladder cancer cells, a pGRR5-Lac reporter, containing a promoter of the IFN- $\gamma$  response region (ORR) which is a STAT consensus binding site (section 2.7.6) was employed.

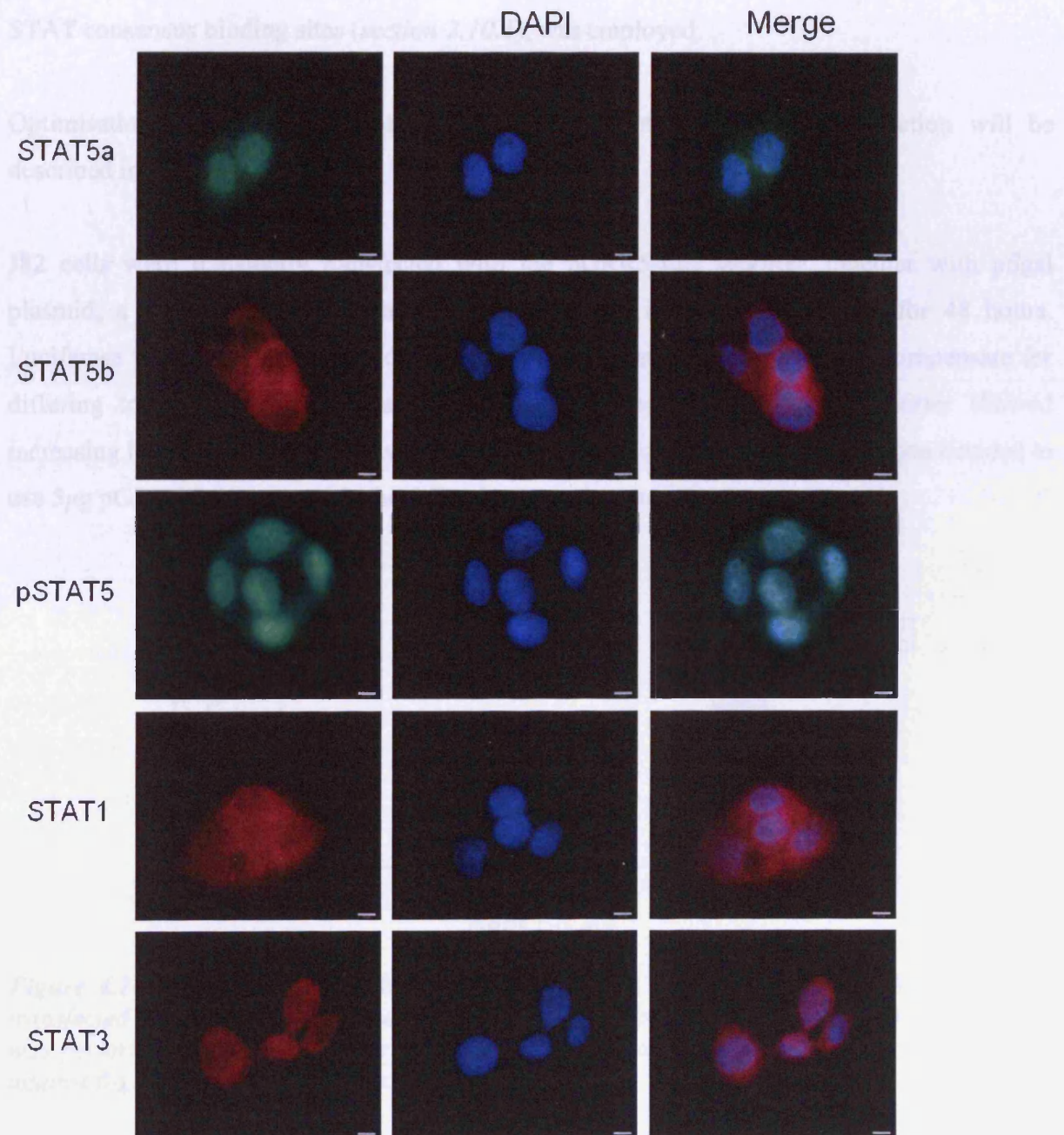


**Figure 4.9 Determination of STATs localisation in RT112 cells by immunofluorescence.** RT112 cells were seeded on cover slips and allowed to adhere overnight. At 60% confluent, cells were fixed and stained with antibodies against STAT5 (a and b), pSTAT5, STAT1 and STAT3, counterstained with DAPI and examined by fluorescence microscope (Scale bars equal to 6 $\mu$ m).

### 4.3 Transcriptional activity of STATs

In order to measure endogenous STAT transcriptional activity in bladder cancer cells, a pGRR5-Luc reporter, containing a pentamer of the IFN- $\gamma$  response region (GRR) which is STAT consensus binding sites (*section 2.10.1*), was employed.

Optimisation of J82 electroporation and establishment of RT112 nucleofection will be described in *section 4.5 and 4.6*.

J82 cells were transiently transfected with the pGRR5-Luc reporter, together with p $\beta$ gal plasmid, a reporter vector expressing  $\beta$ -galactosidase in mammalian cells, for 48 hours. Luciferase values were normalised against  $\beta$ -galactosidase values in order to compensate for differing transfection efficiencies. Increasing amounts of pGRR5-Luc reporter showed increasing levels of luciferase activity (*figure 4.10*). From these results, it was then decided to use 5 $\mu$ g pGRR5-Luc reporter in the following experiments.

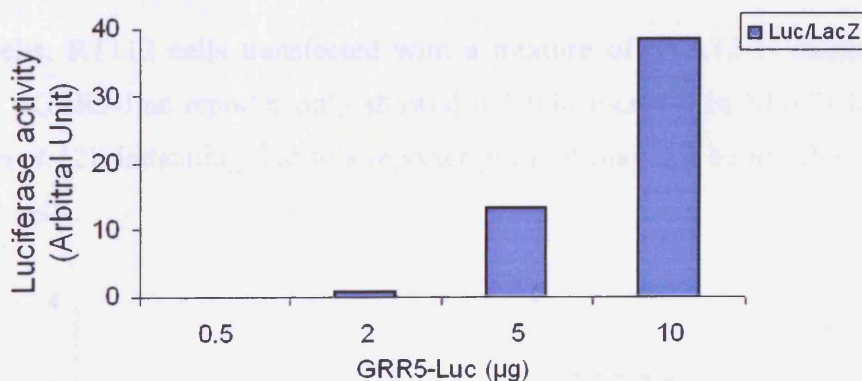


**Figure 4.10 Correlation of pGRR5-Luc reporter with luciferase activity.** J82 cells were transfected with increasing amounts of pGRR5-Luc reporter and p $\beta$ gal plasmid. Analysis was performed at 48 hours. The relative luciferase activity was calculated by normalising against  $\beta$ -galactosidase activity ( $n=1$ ).

The STAT3-C flagged pRc/CMV construct which activates STAT transcription constitutively was applied as a positive control in this luciferase assay. J82 cells were transiently transfected with this construct, together with pGRR5-Luc reporter for 48 hours. As shown in *figure 4.11*, without any induced tyrosine phosphorylation, STATs transcriptional activity induced by STAT3C was significantly increased, more than 10-fold, above background.

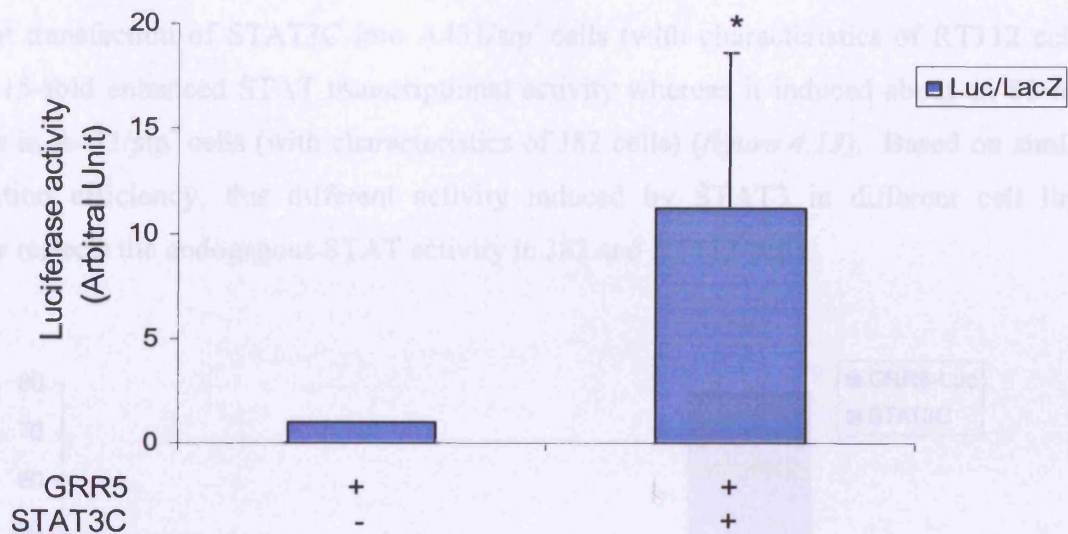


**Figure 4.11 Effect of STAT3C on STAT transactivation in J82 cells.** J82 cells were transiently transfected with the STAT3C construct, together with the pGRR5-Luc reporter. Analysis was performed at 48 hours. The relative luciferase activity was calculated by normalising against  $\beta$ -galactosidase activity and expressed as fold increase over control. \* denotes a significant difference from control ( $p < 0.05$ ,  $n = 8$ ,  $\pm SD$ ).

Unlike J82 cells, RT112 cells transfected with a mixture of STAT3-C flagged pRc/CMV construct and pGRR5-Luc reporter only showed a 3-fold increase in STATs transcriptional activity (figure 4.12), indicating that this reporter plasmid may not be as effective in RT112 cells as in J82 cells.

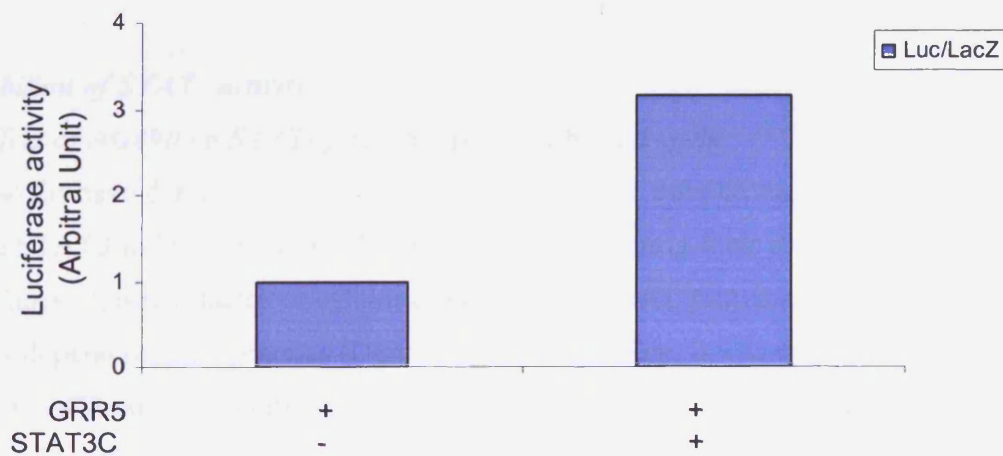


**Figure 4.12 Effect of STAT3C on STAT transactivation in RT112 cells.** RT112 cells were transiently transfected with the STAT3C construct, together with the pGRR5-Luc reporter. Analysis was performed at 72 hours. The relative luciferase activity was calculated by normalising against  $\beta$ -galactosidase activity and expressed as fold increase over control ( $n = 1$ ).

In support of these data, in an A431/sip model (*discussed in more details in section 4.7*), transient transfection of STAT3C into A431/sip<sup>-</sup> cells (with characteristics of RT112 cells) caused 15-fold enhanced STAT transcriptional activity whereas it induced about an 80-fold increase in A431/sip<sup>+</sup> cells (with characteristics of J82 cells) (*figure 4.13*). Based on similar transfection efficiency, this different activity induced by STAT3 in different cell lines possibly reflects the endogenous STAT activity in J82 and RT112 cells.

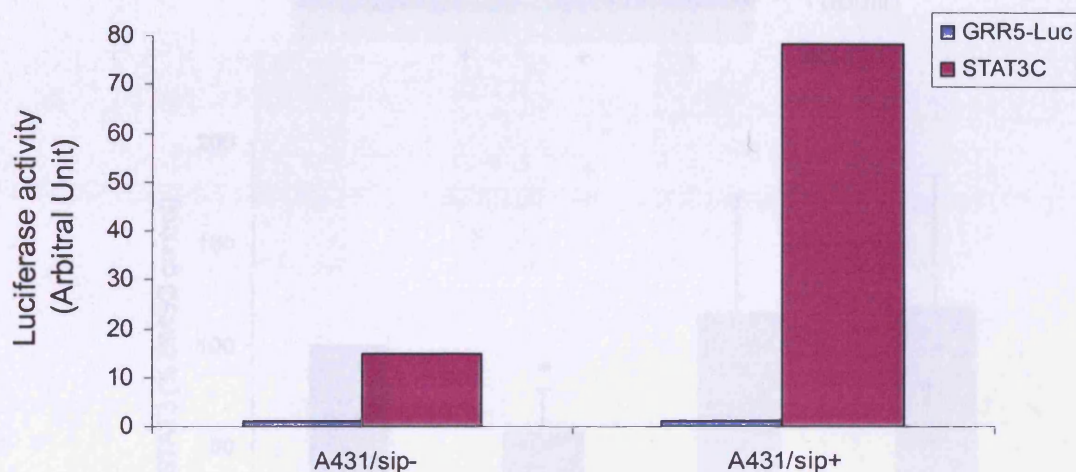


**Figure 4.13 Effect of STAT3C on STAT transactivation in A431/sip cells.** A431/sip cells were transiently transfected with the STAT3C construct, together with the pGRR5-Luc reporter. Analysis was performed at 48 hours. The relative luciferase activity was calculated by normalising against  $\beta$ -galactosidase activity and expressed as fold increase over control ( $n=1$ ) (Experiment performed by Mr Jakob Mejlvang).

#### 4.4 Inhibition of STATs activity

##### 4.4.1 Effect of AG490 on STATs phosphorylation and cell cycle

Results so far have demonstrated that under normal growth conditions, only STAT5 in RT112 cells and STAT3 in J82 cells were phosphorylated, suggesting their predominant role in these two cell lines. Growth factor or cytokine activation of STAT proteins is known to directly or indirectly depend on JAK proteins (Darnell 1997). Therefore, it was decided to use tyrphostin AG490, a JAK2-specific inhibitor, to determine the effect on STAT phosphorylation in both cell lines. AG490 was known to block STAT3 phosphorylation at a concentration of 50 $\mu$ M in several cell lines (Niwa *et al.*, 2005, Kim *et al.*, 2006). *Figure 4.14* showed inhibition of activated STAT3 by AG490 in J82 cells, represented by a small but significant decrease in

phosphorylation following a 50 $\mu$ M treatment for 1 hour. However, this inhibitory effect was reversed at 6 hours.

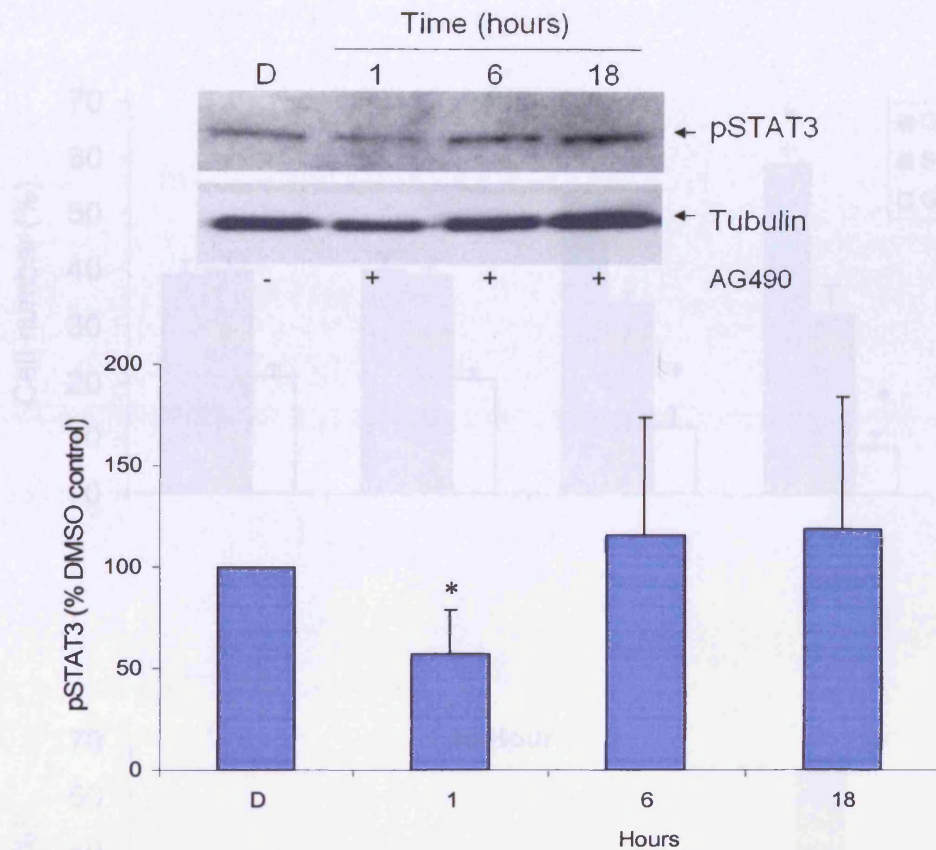
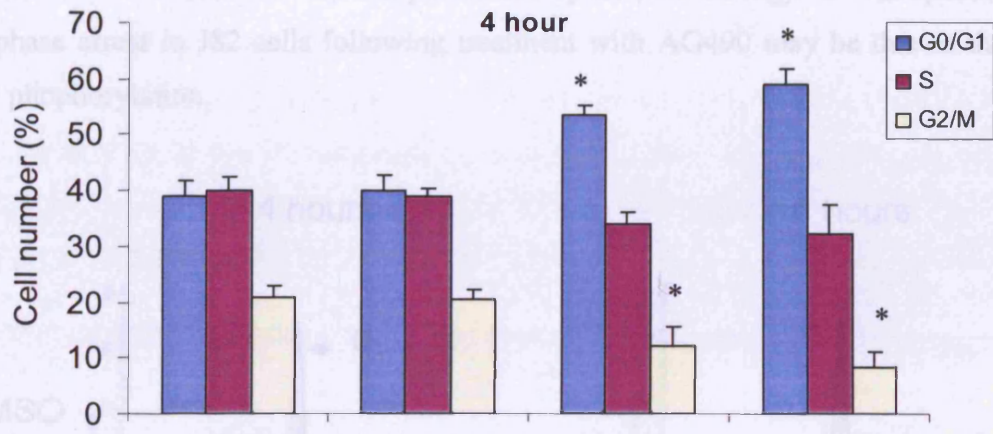


**Figure 4.14 Effect of AG490 on phosphorylated STAT3 levels in J82 cells.** Cells were treated with 50 $\mu$ M AG490 in serum-free medium for appropriate times. The vehicle for AG490 was DMSO which was present in all treatments to the same concentration. Blots were performed on 3 separate occasions. The chart shows relative levels normalised against tubulin, and expressed as a percentage of the DMSO control, as determined via densitometric analysis of blots. \* denotes a significant difference from DMSO control ( $p < 0.05$ ,  $n = 3$ ,  $\pm$ SD) using oneway ANOVA followed by Student's  $t$ -test. D=DMSO

Next, flow cytometric analysis was used to determine any change in cell cycle progression in J82 cells following a 50 $\mu$ M AG490 treatment. At 4 hours, there was a significant increase in the proportion of cells in G<sub>0</sub>/G<sub>1</sub> phase, accompanied by a significant decrease in cells in G<sub>2</sub>/M phase. Similar observations were made with 100 $\mu$ M AG490, and at 16 hours, a further increase of cells in G<sub>0</sub>/G<sub>1</sub> phase at the expense of a G<sub>2</sub>/M peak was observed, indicating at this dose the effect was time-dependent (figure 4.15a). However, at 16 hours the effect on cell cycle caused by 50 $\mu$ M AG490 was not maintained.

Consistent with western data shown in figure 4.14, it appeared that the inhibition of STAT3 phosphorylation and G<sub>0</sub>/G<sub>1</sub> phase arrest induced by 50µM AG490 were transient and reversible. Importantly, treating J82 cells with 100µM AG490 led to significant inhibition of

**A.** TAT3 from 1 hour, with almost complete depletion up to 8 hours, which was the longest time point examined (data not shown, performed by Dr MK Cheng). It was speculated that G<sub>0</sub>/G<sub>1</sub> phase arrest in J82 cells following treatment with AG490 may be due to loss of



**B.**

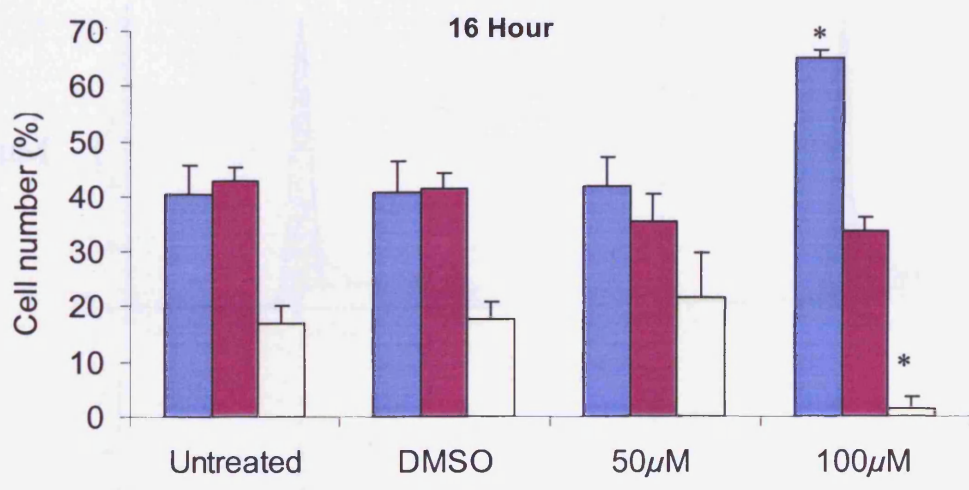


**Figure 4.15a Effect of AG490 upon cell cycle in J82 cells.** The charts show the percentage of cells in each phase of the cell cycle in the J82 cell line following AG490 treatment up to 16 hour. The experiment was performed on 3 separate occasions and data analysed using Modfit L. T. software. \* denotes a significant difference from DMSO control ( $p < 0.05$ ) (Data provided by Dr. MK Cheng).

Consistent with western data shown in *figure 4.14*, it appeared that the inhibition of STAT3 phosphorylation and G<sub>0</sub>/G<sub>1</sub> phase arrest induced by 50μM AG490 were transient and reversible. Importantly, treating J82 cells with 100μM AG490 led to significant inhibition of pSTAT3 from 1 hour, with almost complete depletion up to 8 hours, which was the longest time point examined (data not shown, performed by Dr MK Cheng). It was speculated that G<sub>0</sub>/G<sub>1</sub> phase arrest in J82 cells following treatment with AG490 may be due to the loss of STAT3 phosphorylation.

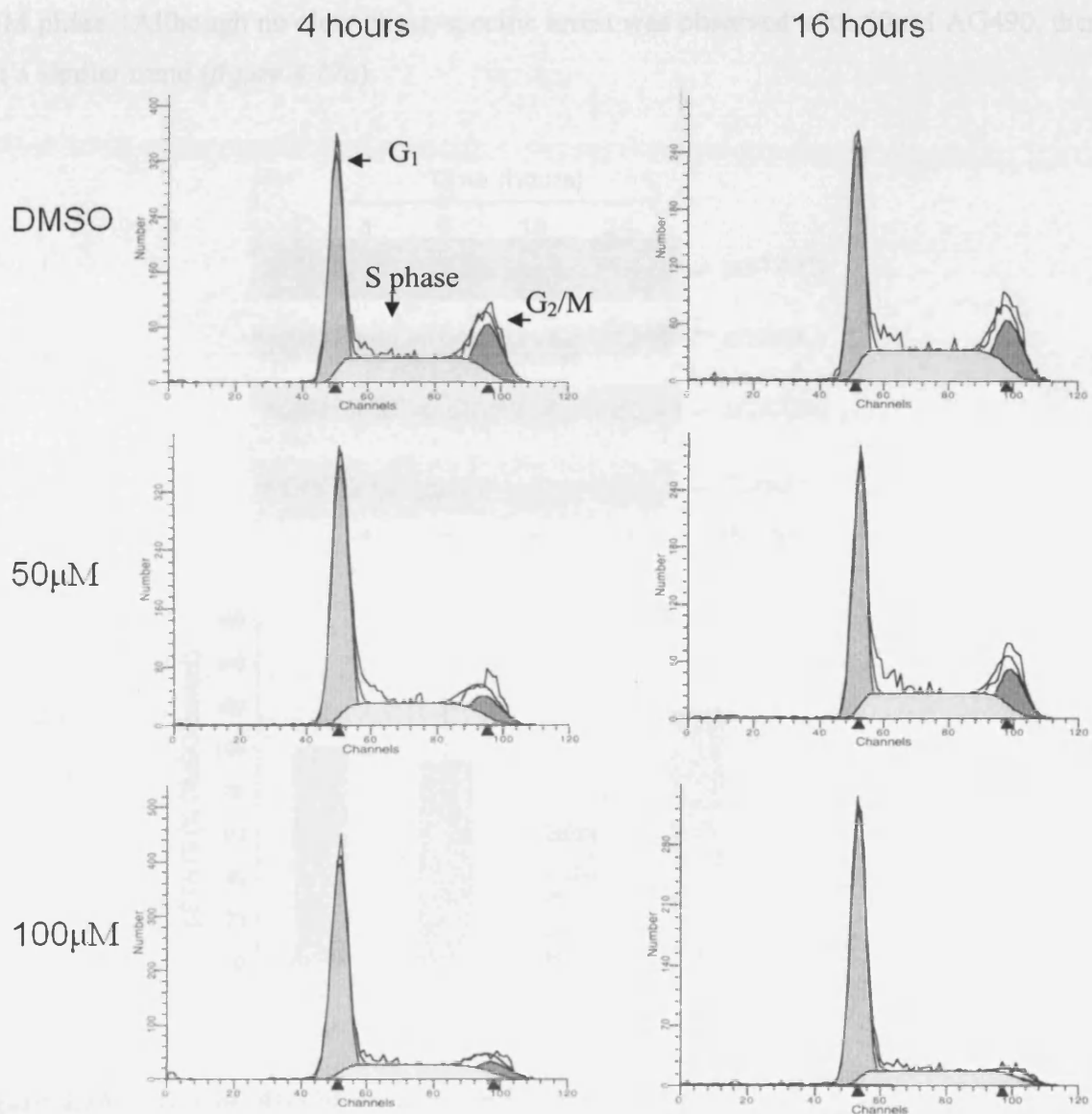


**Figure 4.15b** Flow cytometric analysis of J82 cells following AG490 treatment. J82 cells were stained by prodium iodide following an AG490 treatment up to 16 hours. The experiment was performed upon 3 separate occasions and data analysed using Modfit L.T. software.

In RT112 cells, STAT5 phosphorylation was significantly inhibited at 6 hours, reversed to basal level at 18 hours and almost completely depleted at 24 hours following a 50 $\mu$ M AG490 treatment. AG490 did not affect total STAT5a and STAT5b levels at any time point in RT112 cells (figure 4.16).

Flow cytometric analysis was carried out in order to determine the effect of AG490 upon cell cycle in RT112 cells. At 4 hours, RT112 cells treated with 100 $\mu$ M AG490 showed a significant increase in the proportion of cells in G<sub>0</sub>/G<sub>1</sub> phase and a significant decrease in G<sub>2</sub>/M phase. Although no clear phase-specific arrest was observed with 50 $\mu$ M AG490, there was a similar trend (figure 4.17a).

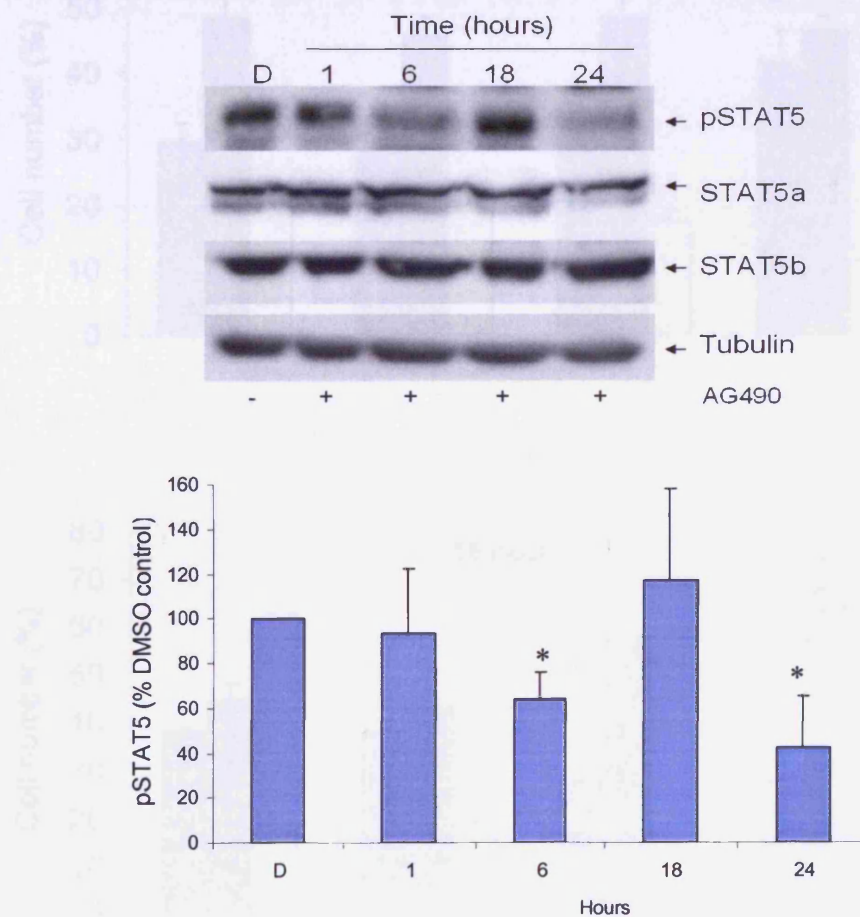
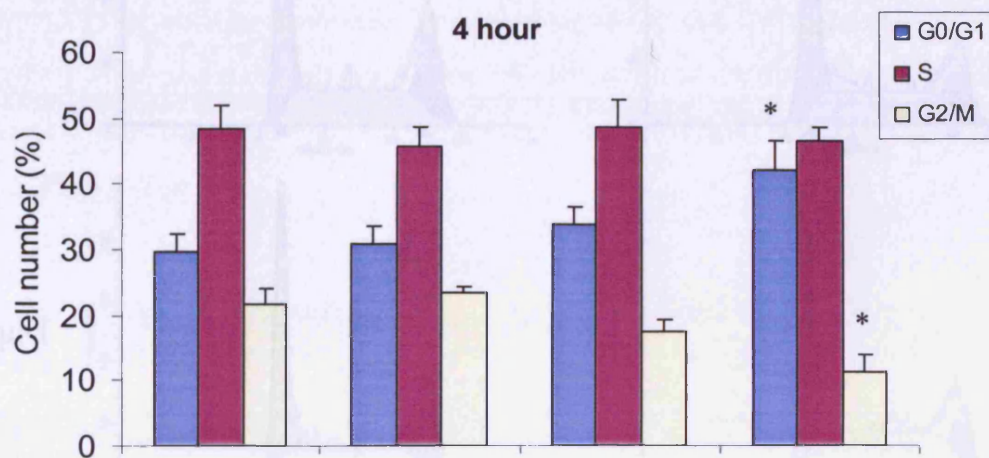


**Figure 4.16** Effect of AG490 on total and phosphorylated STAT5 levels in RT112 cells. Cells were treated with 50 $\mu$ M AG490 in serum-free medium for appropriate times. The vehicle for AG490 was DMSO which was present in all treatments to the same concentration. The chart shows relative pSTAT5 levels normalised against tubulin, and expressed as a percentage of the DMSO control, as determined via densitometric analysis of blots. \* denotes a significant difference from DMSO control ( $p < 0.05$ ,  $n = 4$ ,  $\pm$ SD) using oneway ANOVA followed by Student's *t*-test. D=DMSO

However, at 16 hours, the number of cells in G<sub>0</sub>/G<sub>1</sub> phase was significantly decreased in response to either 50 μM or 100 μM AG490 treatment, which was accompanied by a significant accumulation of cells in S phase following both treatments. As at 4 hours at the higher dose, a decrease in G<sub>2</sub>/M phase was observed at 16 hours, which was statistically significant (figure 4.17a). These data demonstrate that AG490 can cause G<sub>0</sub>/G<sub>1</sub> arrest in the first instance, followed eventually by S phase arrest in RT112 cells.

A.



B.

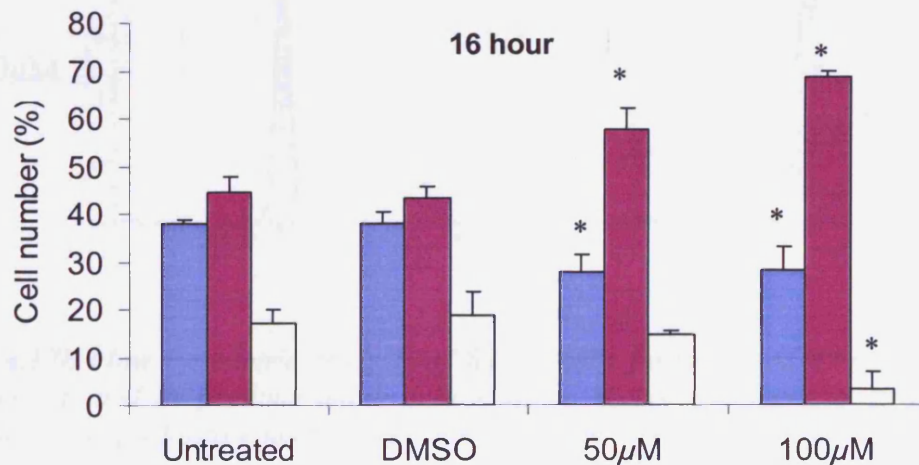


**Figure 4.17a Effect of AG490 upon cell cycle in RT112 cells.** The charts show the percentage of cells in each phase of the cell cycle in the RT112 cell line following AG490 treatment for up to 16 hour. The experiment was performed upon 3 separate occasions and data analysed using Modfit L. T. software. \* denotes a significant difference from DMSO control ( $p < 0.05$ ) (Data provided by Dr. MK Cheng).

Representative cell cycle plot based on DNA contents (as analysed by Modfit) for RT112 cells following an AG490 treatment up to 16 hours are shown in figure 4.17b.

(1997). Piceumaiol, a JAK1-specific inhibitor, was also employed to examine the effect on STAT3 phosphorylation in J82 and RT112 cells. Unfortunately, due to unresolvable problems, comparison plots stained for DNA contents were not possible on 2 separate occasions.

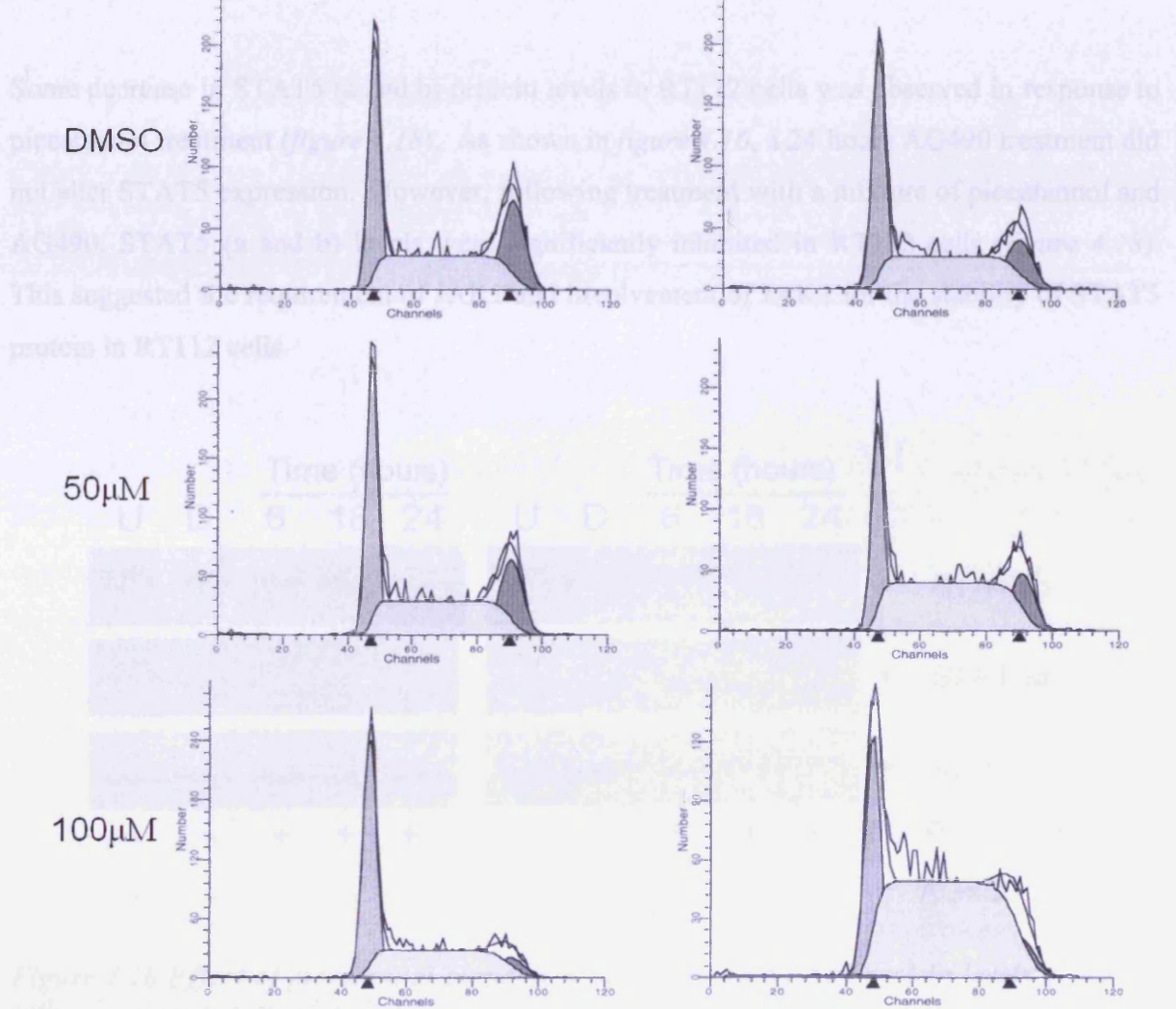


**Figure 4.17b** Flow cytometric analysis of RT112 cells following AG490 treatment. RT112 cells were stained by prodium iodide following an AG490 treatment up to 16 hours. The experiment was performed upon 3 separate occasions and data analysed using Modfit L.T. software.

#### 4.4.2 Effect of piceatannol on STAT and cadherin expression

Besides JAK2, JAK1 was also known to be involved in STAT activation (Shimoda *et al.*, 1997). Piceatannol, a JAK1-specific inhibitor, was also employed to examine the effect on STATs phosphorylation in J82 and RT112 cells. Unfortunately, due to unresolved problems, companion blots stained for phosphorylated STATs in both cell lines were unsuccessful on 2 separate occasions.

Some decrease in STAT5 (a and b) protein levels in RT112 cells was observed in response to piceatannol treatment (*figure 4.18*). As shown in *figure 4.16*, a 24 hours AG490 treatment did not alter STAT5 expression. However, following treatment with a mixture of piceatannol and AG490, STAT5 (a and b) levels were significantly inhibited in RT112 cells (*figure 4.18*). This suggested the requirement of JAK1 and involvement of JAK2 for the stability of STAT5 protein in RT112 cells.

#### 4.4.3 Effect of PP2 on STAT5 phosphorylation

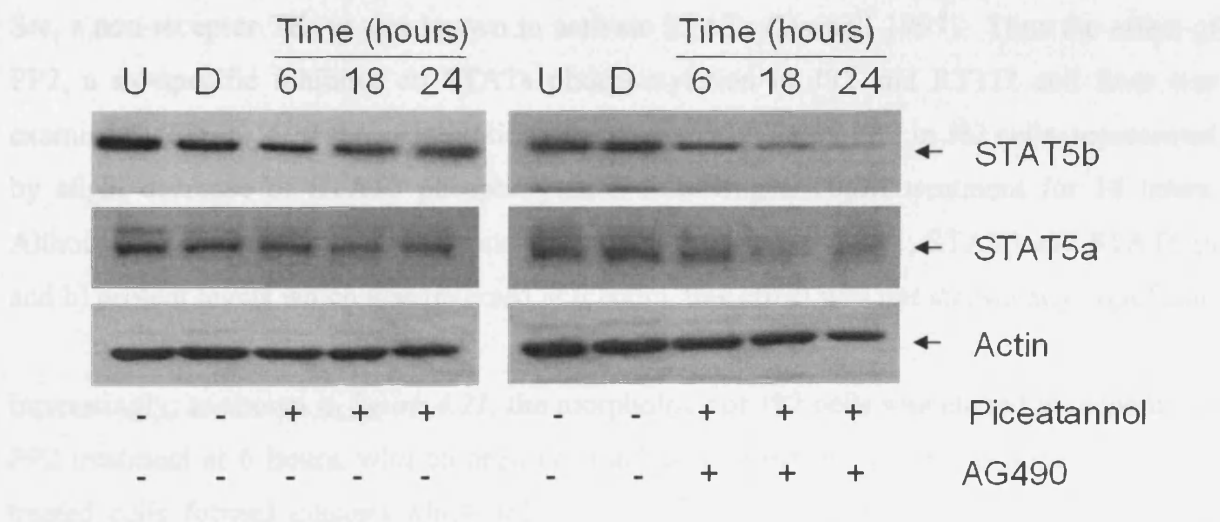


**Figure 4.18** Effect of piceatannol alone or with AG490 on STAT5 protein levels in RT112 cells. Cells were treated with 50 $\mu$ M piceatannol without or with 50 $\mu$ M AG490 in serum-free medium for appropriate times. The vehicle was DMSO which was present in all treatments to the same concentration. Blots were performed on 2 separate occasions. U=untreated, D=DMSO.

In J82 cells, either piceatannol (50 $\mu$ M) alone or combined with AG490 (50 $\mu$ M) showed an obvious inhibitory effect on STAT3 protein levels (Blots not shown due to poor quality, performed on 2 separate occasions), accompanied by altered N-cadherin expression (*figure 4.19*). The decrease of N-cadherin levels was dose-dependent, and interestingly, N-cadherin

appeared to be truncated or degraded following a 25 $\mu$ M piceatannol treatment, indicating a connection between JAK activity and cell adhesion molecules.

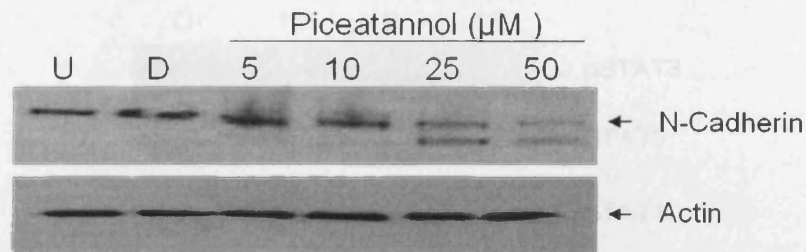


**Figure 4.19** Effect of piceatannol on N-cadherin expression in J82 cells. Cells were treated with increased doses of piceatannol in serum-free medium for 24 hours. The vehicle was DMSO which was present in all treatments to the same concentration. Blots were performed on 2 separate occasions. U=untreated, D=DMSO.

#### 4.4.3 Effect of PP2 on STATs phosphorylation

Src, a non-receptor TK, is also known to activate STATs (Darnell 1997). Thus the effect of PP2, a src-specific inhibitor on STATs phosphorylation in J82 and RT112 cell lines was examined. Figure 4.20 shows inhibition of activated STAT3 by PP2 in J82 cells, represented by slight decrease of STAT3 phosphorylation following a 10 $\mu$ M treatment for 18 hours. Although PP2 treatment at 1 hour caused a small decrease in STAT1, STAT3 and STAT5 (a and b) protein levels which was reversed at 6 hours, this effect was not statistically significant.

Interestingly, as shown in figure 4.21, the morphology of J82 cells was altered in response to PP2 treatment at 6 hours, with an apparent inhibitory effect on cell-matrix adhesion. PP2-treated cells formed clusters which might protect them from anoikis, suggesting that src activity may be associated with some cell-cell adhesion proteins in J82 cells.

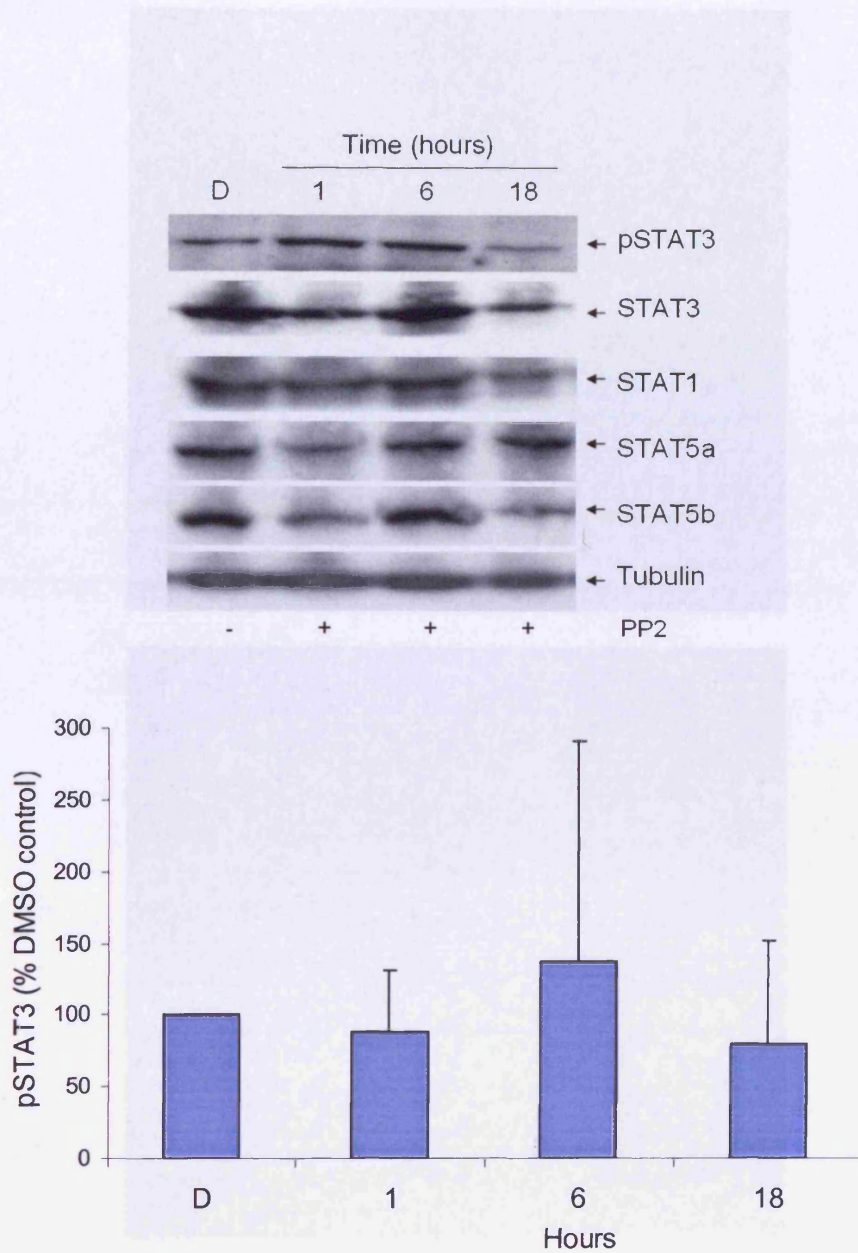


**Figure 4.20 Effect of PP2 on STATs levels in J82 cells.** Cells were treated with 10 $\mu$ M PP2 in serum-free medium for appropriate times. The vehicle for PP2 was DMSO which was present in all treatments to the same concentration. Blots were performed on 2 separate occasions. The chart shows relative pSTAT3 levels normalised against tubulin, then expressed as a percentage of the DMSO control, as determined via densitometric analysis of blots. D=DMSO

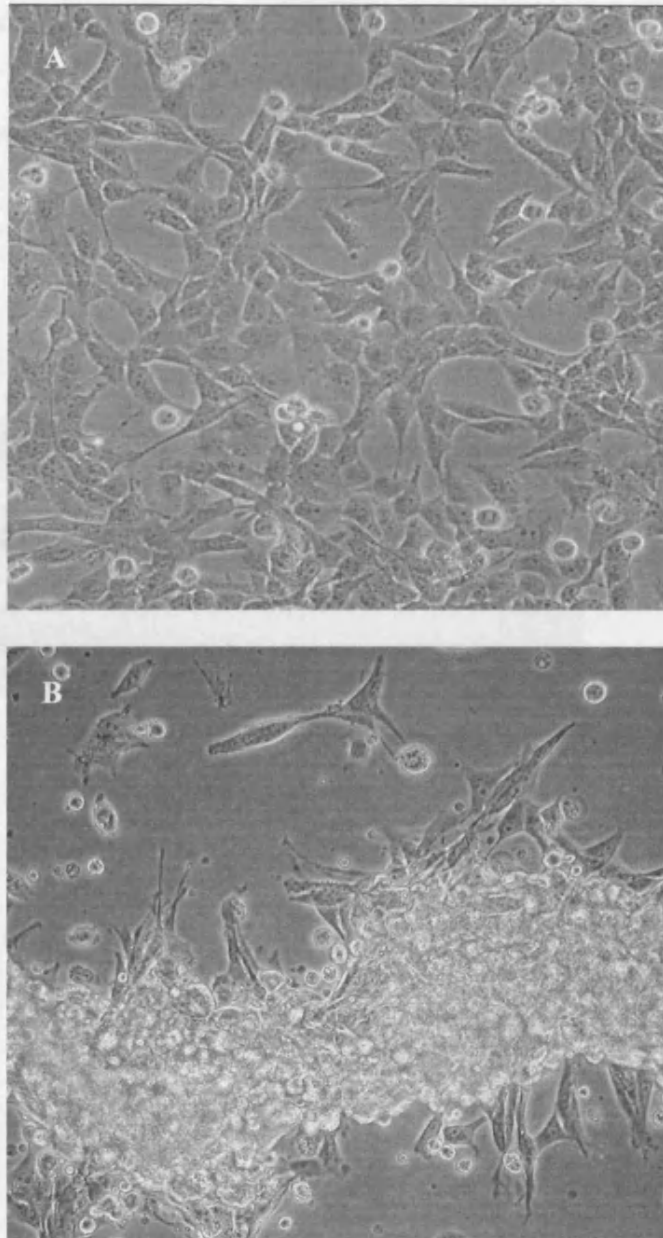


**Figure 4.21** *Effect of PP2 on cell aggregation and morphological appearance in J82 cells. Panel A features control J82 cells, treated for 6 hours with DMSO. Panel B represents J82 cells treated for 6 hours with 10 $\mu$ M PP2. Live images of cells were visualised by microscope (Phase-contrast,  $\times 20$  lens) (n=2).*

In RT112 cells, the effect of PP2 on STAT5 phosphorylation was inconsistent, as shown in *figure 4.22*. Following a 10 $\mu$ M PP2 treatment, no statistically significant alteration in STAT5 phosphorylation level was observed, although in the blot shown there appeared to be some increase from 6 hours, which may be associated with increased STAT5b protein levels.

Treatment with PP2 showed no effect on cell cycle in either J82 or RT112 cells (data not shown, performed by Dr MK Cheng), suggesting that src may be not involved in cell cycle process in bladder cancer cells.

and suggested some involvement of JAK2 and STAT5 in STAT5 expression and cell cycle arrest. In order to investigate the function of STAT5 in chosen bladder cells, siRNA/siRNA-specific STAT5s were employed.

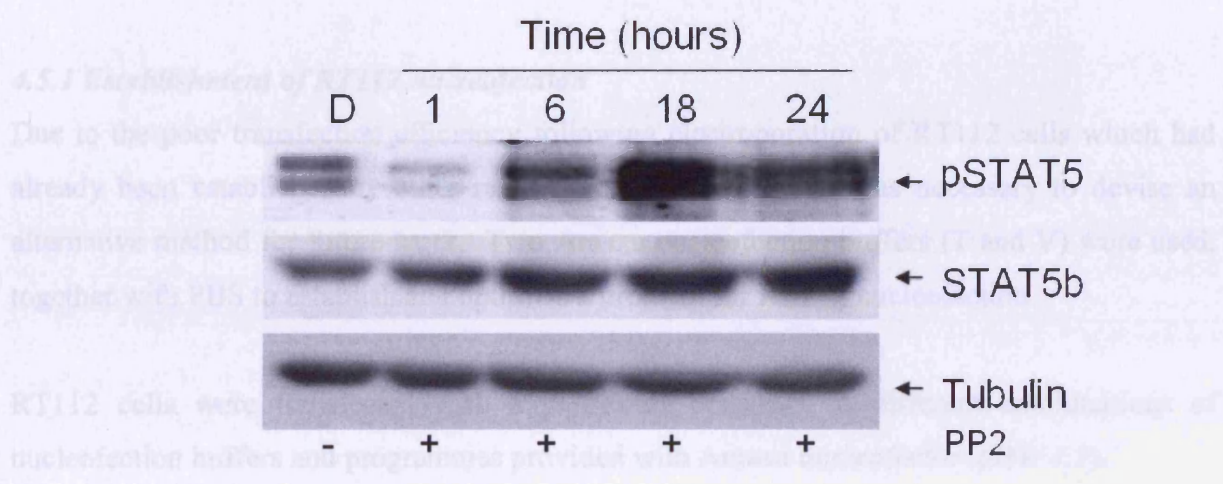
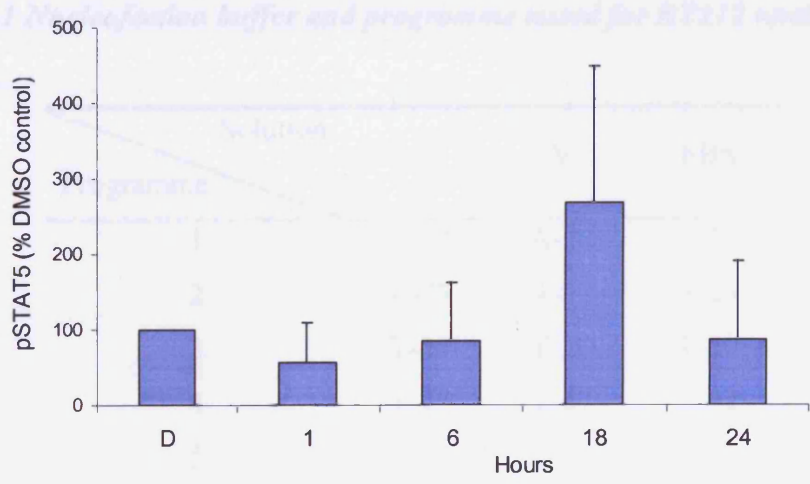


Table 4.1 Media, infection buffer and programme used for RT112 transfection



**Figure 4.22 Effect of PP2 on total and phosphorylated STAT5 levels in RT112 cells.** Cells were treated with 10 $\mu$ M PP2 in serum-free medium for appropriate times. The vehicle for PP2 was DMSO which was present in all treatments to the same concentration. Blots were performed on 3 separate occasions. The chart shows relative pSTAT5 levels normalised to tubulin, and expressed as a percentage of the DMSO control, as determined via densitometric analysis of blots. D=DMSO

#### 4.5 Inhibition of STAT expression in RT112 and J82 cells using siRNAs to STATs

Data so far have established the expression profile of total and phosphorylated STATs in a panel of bladder cancer cells and suggested some involvement of JAK1 and JAK2 in STAT expression and cell cycle arrest. In order to investigate the function of STATs in chosen bladder cells, siRNAs to specific STATs were employed.

##### 4.5.1 Establishment of RT112 nucleofection

Due to the poor transfection efficiency following electroporation of RT112 cells which had already been established by other researchers in the group, it was necessary to devise an alternative method for future work. Two Amaxa nucleofection buffers (T and V) were used, together with PBS to establish and optimise a protocol for RT112 nucleofection.

RT112 cells were transfected with a pGFPmax construct in different combinations of nucleofection buffers and programmes provided with Amaxa nucleofector (table 4.1).

**Table 4.1 Nucleofection buffer and programme tested for RT112 nucleofection**

Programme	Solution		
	T	V	PBS
1	A-23	A-23	A-23
2	A-27	A-27	A-27
3	T-20	T-20	T-20
4	T-27	T-27	T-27
5	T-16	T-16	T-16
6	T-01	T-01	T-01
7	G-16	G-16	G-16
8	O-17	O-17	O-17

The efficiency of transfection was determined by the percentage of cells containing GFP after 24 hours under a fluorescence microscope. Among the various samples, application of buffer T and programme A23 showed both high transfection efficiency (in a range of 58% - 86%) and cell viability (figure 4.23). For each sample, five areas were randomly chosen and the transfection efficiency was presented as the percentage of cells with GFP.

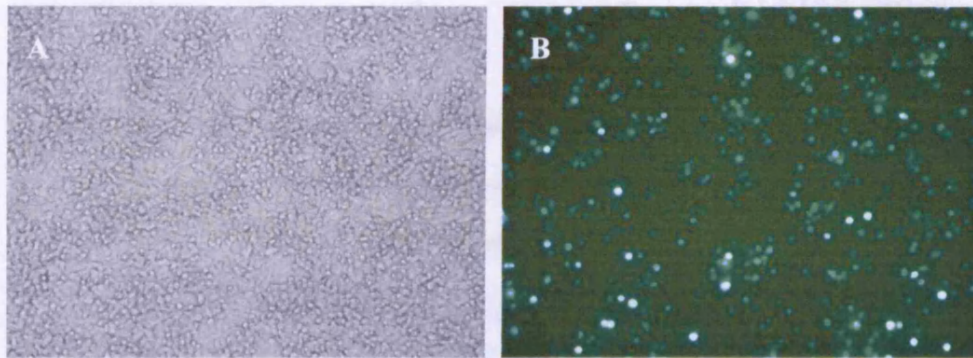


**Figure 4.23 GFP fluorescence showing efficiency of RT112 nucleofection.** RT112 cells were transiently transfected with pmaxGFP using buffer T and programme A23. Panel A shows transfected cells in a random area visualised with a light microscope (Phase-contrast), and panel B represents the cells transfected with GFP in the same area under a fluorescence microscope ( $\times 10$  lens).

RT112 cells were then transiently transfected with siRNA to STAT3, and the resulting knockdown examined after 48, 72 and 96 hours. As shown in figure 4.24, 72 hours after transfection was the optimum time point for highest efficiency of STAT3 knockdown.

#### 4.3.2 Establishment of STAT transfection in RT112

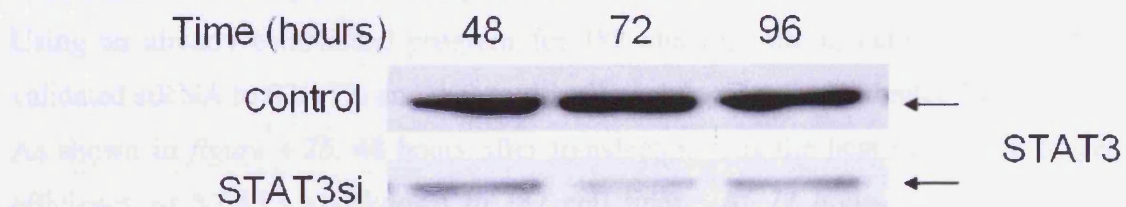


**Figure 4.24 Efficiency of STAT3 knockdown in RT112 cells.** RT112 cells were transfected with  $2\mu\text{l}$  STAT3 siRNA for 48, 72 and 96 hours. Control samples were transfected with  $2\mu\text{l}$  scrambled siRNA. Blots were performed on 2 separate occasions.

Also, siRNAs to STAT5a and STAT5b were transiently transfected into RT112 cells. As shown in figure 4.25, it appeared that similar transfection efficiency was achieved at all three time points. Interestingly, blocking STAT5a upregulated STAT5b protein levels at all time points, and vice versa.

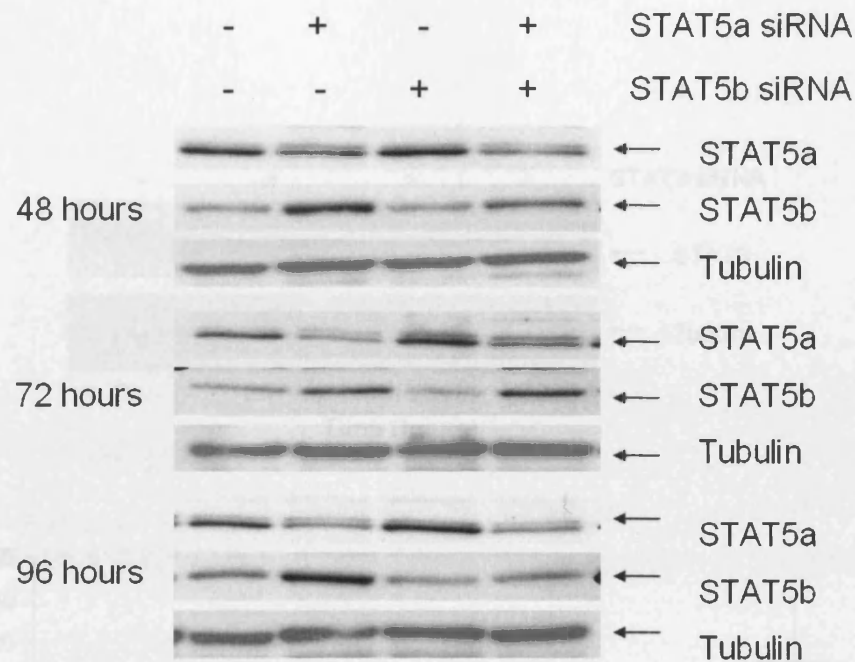


**Figure 4.25 Efficiency of STAT5 knockdown in RT112 cells.** RT112 cells were transfected with 2 $\mu$ l STAT5a or STAT5b siRNA alone or in combination for 48, 72 and 96 hours. Control samples were transfected with 2 $\mu$ l scrambled siRNA. Blots were performed on 2 separate occasions.

#### 4.5.2 Establishment of STAT transfection in J82 cells

Using an already established program for J82 electroporation, cells were transfected with validated siRNA to STAT3, and the resulting knockdown examined after 24, 48 and 72 hours. As shown in *figure 4.26*, 48 hours after transfection was the best time point to get highest efficiency of STAT3 knockdown in J82 cell lines. At 72 hours, STAT3 expression was reversed to basal level, possibly due to the degradation of siRNA in cells.

#### 4.5.3 Effect of individual STATs knockdown on other STATs protein levels and phosphorylation status in J82 cells

So far, the amount of siRNAs and the time point to achieve best transfection efficiency in J82 cells have been identified. In order to investigate the function of individual STATs, siRNAs to STAT1, STAT3 and STAT5 (a and b) alone or in combination were transiently transfected into J82 cells.

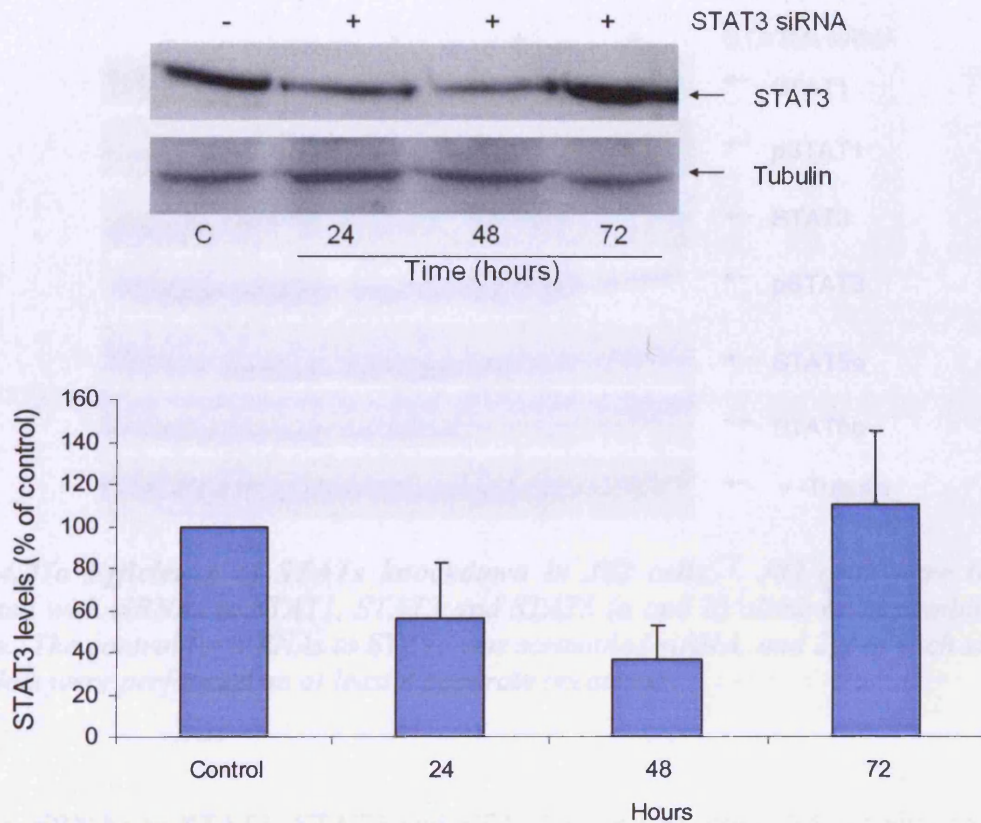


**Figure 4.26 Efficiency of knockdown STAT3 in J82 cells.** J82 cells were transfected with 2 $\mu$ l STAT3 siRNA for 24, 48 and 72 hours. C=control, transfected with 2 $\mu$ l scrambled siRNA. Blots were performed on 2 separate occasions. The chart shows STAT3 levels normalised against tubulin, and expressed as a percentage of control sample, as determined via densitometric analysis of blots.

As shown in *figure 4.27a and 4.27b*, STAT1, STAT3 and STAT5b protein levels were efficiently blocked by specific siRNAs, with 78%, 51% and 54% knockdown, respectively. Interestingly, it showed that knockdown of individual STATs altered the levels and phosphorylation of other STAT proteins. For example: 1) blocking STAT3 significantly activated STAT1 (316%); 2) blocking STAT5 (a and b) upregulated STAT3 at both total (199%) and phosphorylated (268%) levels, and induced STAT1 phosphorylation (265%). Phosphorylated STAT5 was undetectable at all treatments in J82 cells (data not shown).

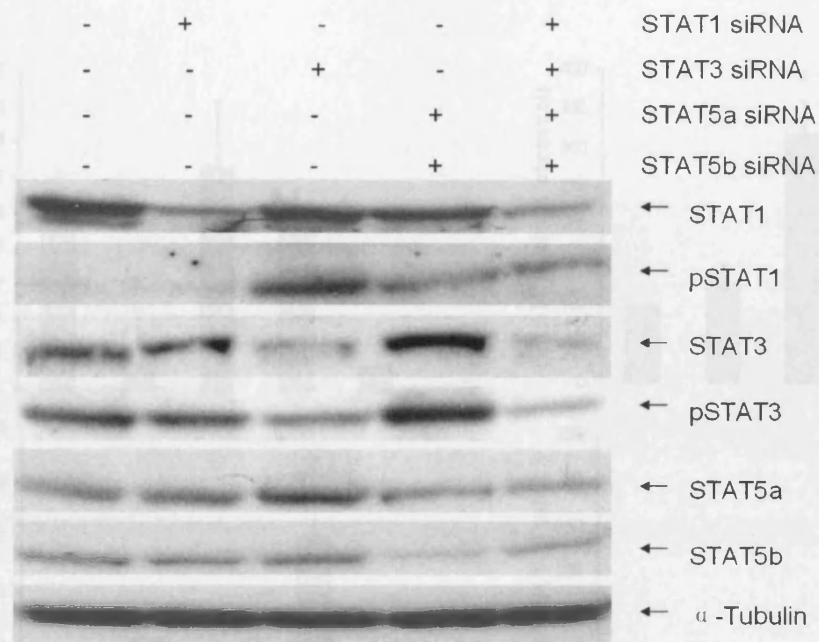


**Figure 4.27a Efficiency of STATs knockdown in J82 cells.** J82 cells were transiently transfected with siRNAs to STAT1, STAT3 and STAT5 (a and b) alone or in combination for 48 hours. The control for siRNAs to STATs was scrambled siRNA, and 2  $\mu$ l of each siRNA was used. Blots were performed on at least 4 separate occasions.

However, siRNAs to STAT1, STAT3 and STAT5 (a and b) alone did not alter the level of STATs transcriptional activity compared with control (*figure 4.28*), possibly due to their stimulatory effect on other STATs proteins as shown in western results in *figure 4.27a*. A significant decrease in STATs transcriptional activity was only observed when J82 cells were transiently transfected with siRNAs to STAT1, STAT3 and STAT5 in combination.

Thus knockdown of individual STATs leads to the upregulation and activation of other STATs, on either protein or phosphorylated levels. It was then important to determine one of the possibilities, whether there are hetero-dimers among different STAT members was then important to identify. Whole protein lysates from J82 cells were immunoprecipitated by addition of antibodies against STAT1, STAT3, STAT5 (a and b), respectively, then probed with  $\alpha$ -STAT1 or  $\alpha$ -STAT3. Western data stained with  $\alpha$ -STAT5a or  $\alpha$ -STAT5b were not shown due to the poor quality of blots in which there was no band detected in lanes of STAT1 and STAT3. As shown in *figure 4.29*, this indicated that there was no complex among STAT1, STAT3 and STAT5.

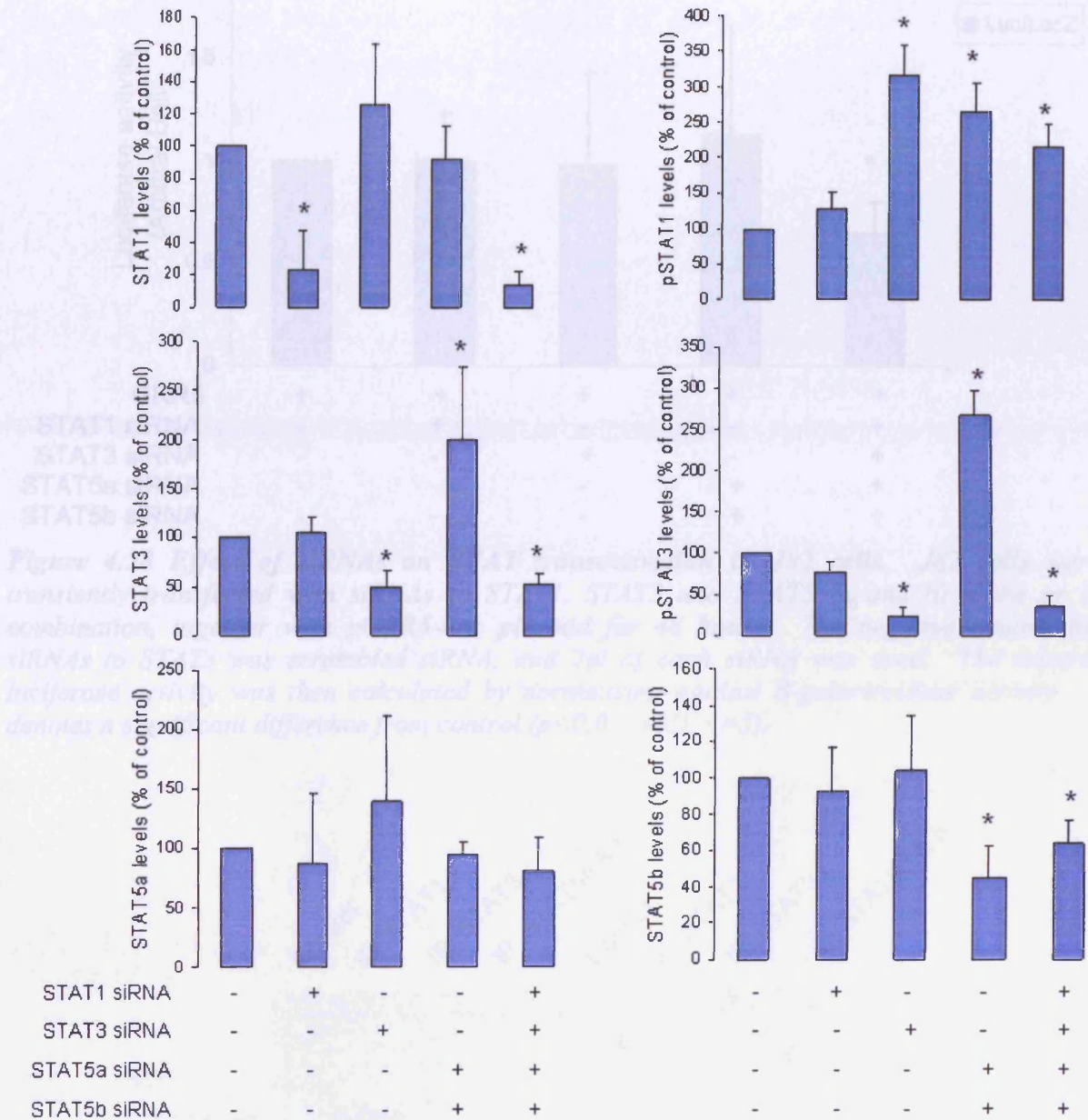


**Figure 4.27b Histograms showing efficiency of STATs knockdown in J82 cells.** The charts show relative levels of each STAT following knockdown normalised against tubulin, and expressed as a percentage of control sample, as determined via densitometric analysis of blots. \* denotes a significant difference from control ( $p < 0.05$ ,  $n = 4$ ,  $\pm SD$ ) using oneway ANOVA followed by Student's *t*-test.

Whether blocking STAT1, 3 or 5 alone or in combination by siRNAs would affect cell cycle or induce apoptosis, was examined by investigating cyclin D1, pro-caspase 3 and survivin expression on western blot. As shown in Figure 4.30, J82 cells transfected with siRNAs to STAT1, 3 or 5 did not show altered expression of cyclin D1 or pro-caspase 3. Knockdown of STAT1 under STAT1 had no effect on survivin expression.

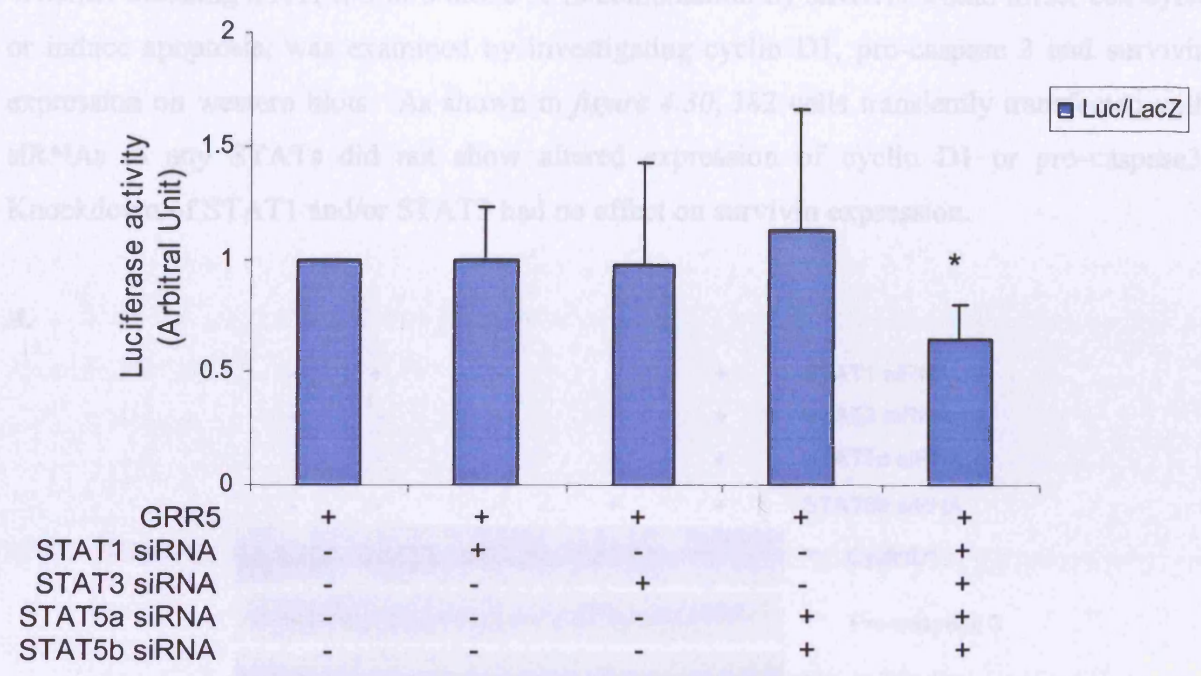


**Figure 4.28 Effect of siRNAs on STAT transactivation in J82 cells.** J82 cells were transiently transfected with siRNAs to STAT1, STAT3 and STAT5 (a and b) alone or in combination, together with pGRR5-Luc plasmid for 48 hours. The negative control for siRNAs to STATs was scrambled siRNA, and 2µl of each siRNA was used. The relative luciferase activity was then calculated by normalising against β-galactosidase activity. \* denotes a significant difference from control ( $p < 0.05$ ,  $\pm$ SD,  $n = 5$ ).

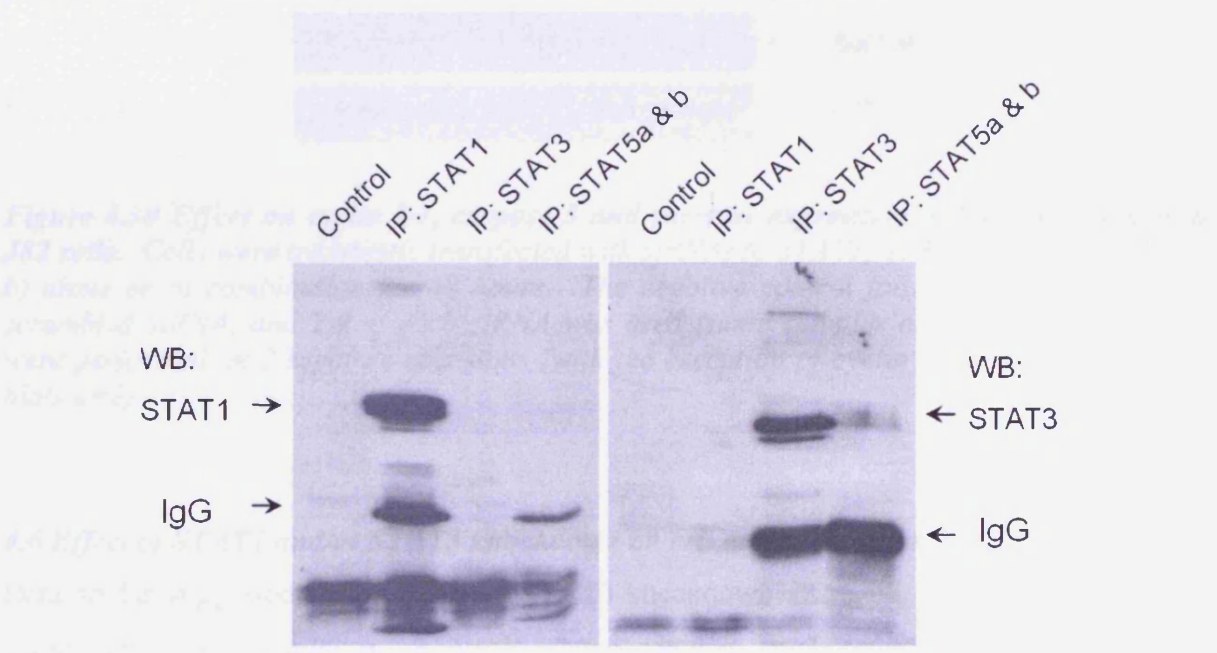
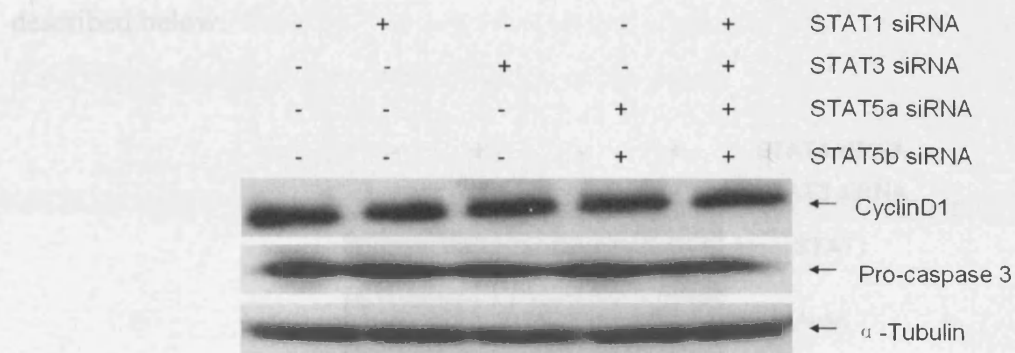


**Figure 4.29 Immunoprecipitation showing complex formation among STAT1, 3 and 5 in J82 cells.** Western blots of precipitates using STAT1, 3 or 5 (a and b) antibodies were prepared and incubated with anti-STAT1 or anti-STAT3 antibodies. In the control sample, no primary antibody was added ( $n = 1$ ).

Whether blocking STAT1, 3 or 5 alone or in combination by siRNAs would affect cell cycle or induce apoptosis, was examined by investigating cyclin D1, pro-caspase 3 and survivin expression on western blots. As shown in *figure 4.30*, J82 cells transiently transfected with siRNAs to any STATs did not show altered expression of cyclin D1 or pro-caspase3. Knockdown of STAT1 and/or STAT3 had no effect on survivin expression.

*Figure 4.30 showed the knockdown efficiency of STAT3 and/or STAT5 in J82 cells, and*

**A.** *show the effect of siRNAs to STATs on cyclin D1 and pro-caspase 3 expression as*



**B.**

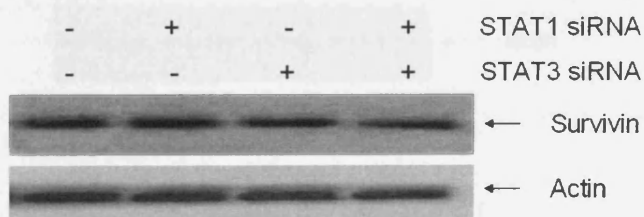


**Figure 4.30 Effect on cyclin D1, caspase 3 and survivin expression in STATs knockdown J82 cells.** Cells were transiently transfected with siRNAs to STAT1, STAT3 and STAT5 (a and b) alone or in combination for 48 hours. The negative control for siRNAs to STATs was scrambled siRNA, and 2 $\mu$ l of each siRNA was used (same samples as figure 4.27a). Blots were performed on 3 separate occasions (with the exception of cyclin D1 and pro-caspase 3 blots n=2).

#### 4.6 Effect of STAT1 and/or STAT3 knockdown on cell adhesion and migration in J82 cells

Data so far suggested that STAT1 or STAT3 knockdown J82 cells show no alteration to expression of cell cycle- or apoptosis-related proteins, such as cyclin D1, caspase3 or survivin. There is evidence in the literature to show that blocking of STAT3 signalling in endothelial cells results in inhibition of migration (Yahata *et al.*, 2003). Recently, it was reported that STAT3 deficient T24 bladder cells also show inhibition of cell migration and invasion (Itoh *et al.*, 2006).

As discussed previously, STAT3 is the only constitutively activated STAT in J82 cells (section 4.1.3), and blocking STAT3 results in the activation of STAT1 (figure 4.27a). Thus it was decided to transiently transfected siRNAs to STAT1 and STAT3 into J82 cells in order to block all potentially active STATs.

Figure 4.31 showed the knockdown efficiency of STAT1 and/or STAT3 in J82 cells, and cells from the same transfected pool were analysed for adhesion and migration assays as described below.

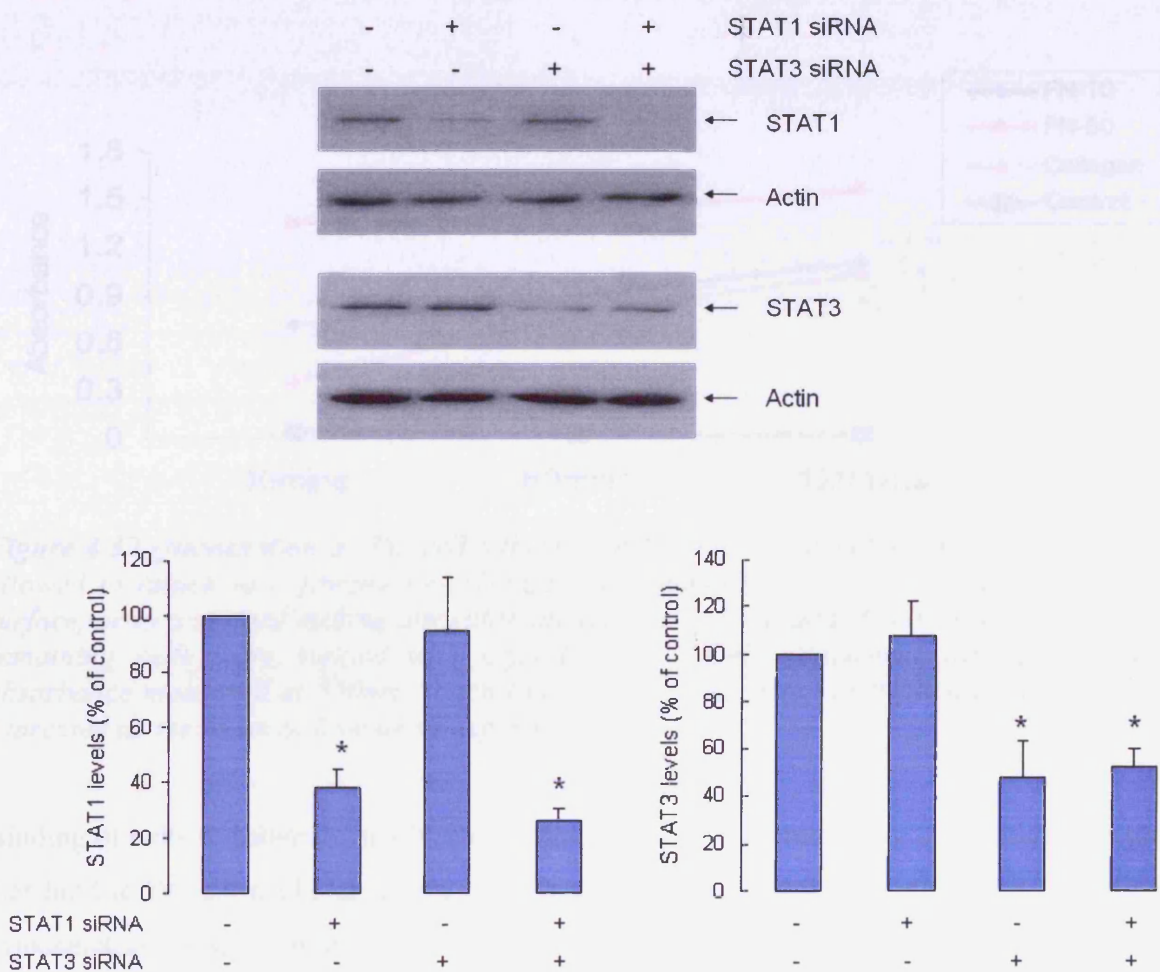


**Figure 4.31 Efficiency of STAT1 and/or STAT3 knockdown in J82 cells.** J82 cells were transfected with 2 $\mu$ l STAT1 and/or STAT3 siRNAs for 48 hours. Control samples were transfected with same amount of scrambled siRNA. Blots were performed on 4 separate occasions. The charts show relative levels normalised against tubulin, and expressed as a percentage of control sample, as determined via densitometric analysis of blots. \* denotes a significant difference from control ( $p < 0.05$ ,  $n = 4$ ,  $\pm$ SD) using oneway ANOVA followed by Student's t-test.

#### 4.6.1 Effect of STAT1 and/or STAT3 knockdown on cell adhesion in J82 cells

To determine the proper concentrations of substrates and time points, adhesion assays were performed as described in 2.7.1 over a period of 120 minutes with a panel of substrates. The absorbance values resulting from J82 cell adhesion to fibronectin (10 $\mu$ g/ml or 50 $\mu$ g/ml), collagen I (50 $\mu$ g/ml) or a non-specific adhesion to BSA alone are illustrated in figure 4.32.

At the higher concentration of fibronectin (50 $\mu$ g/ml), J82 cell adhesion was already saturated at 30 minutes. Therefore, fibronectin (10 $\mu$ g/ml) and collagen I (50 $\mu$ g/ml) showing a time-dependent increase, were used in all future experiments.

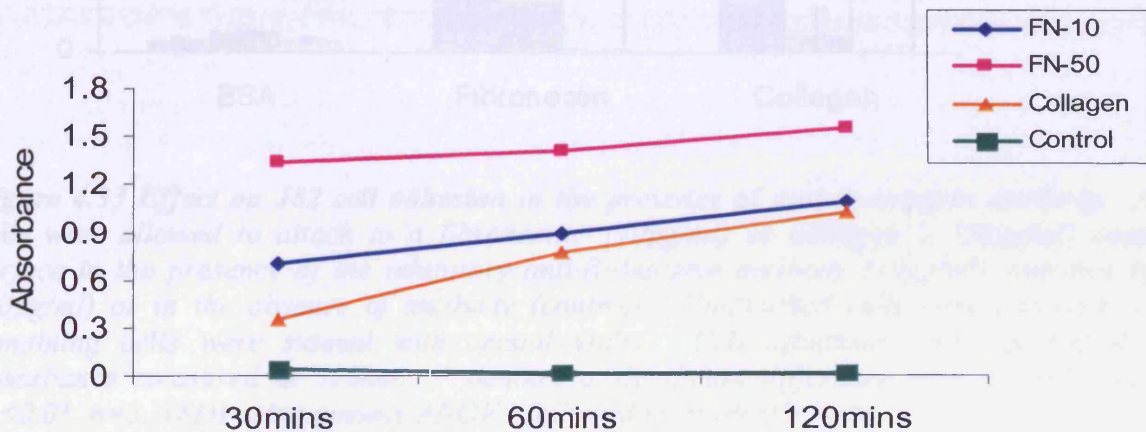


**Figure 4.32 Quantitation of J82 cell adhesion to fibronectin or collagen I.** J82 cells were allowed to attach to a fibronectin- (10 $\mu$ g/ml or 50 $\mu$ g/ml) or collagen I- (50 $\mu$ g/ml) coated surface, or to a surface lacking any substrate (control). Unattached cells were removed, and remaining cells were stained with crystal violet. Cell attachment was quantified by absorbance measured at 550nm. Each time point was assessed in triplicate and the results expressed as the mean of 2 separate experiments.

Binding of cells to substrate involves integrins, which are heterodimeric cell surface receptors that bind to the extracellular matrix (ECM), and provide a physical link to the intracellular cytoskeleton.  $\alpha$  and  $\beta$  integrin subunits form heterodimers with which extracellular ligands associate, and, as far as is known,  $\beta_1$  integrin locates in fibronectin and collagen adhesions. To identify the specificity of binding of J82 cells to fibronectin and collagen, rat anti-human integrin-  $\beta_1$  antibody (mAb13 inhibitory) was applied. To account for non-specific adhesion some wells were coated with BSA only. Attachment of J82 cells to fibronectin and collagen was significantly inhibited by mAb13 (figure 4.33).

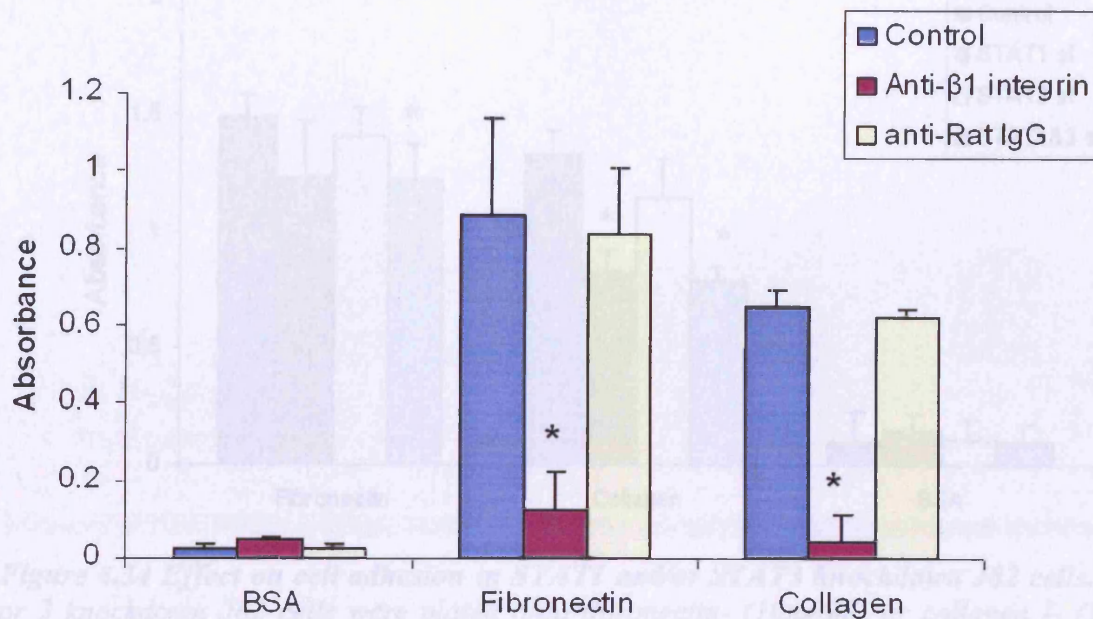


**Figure 4.33 Effect on J82 cell adhesion in the presence of anti-β<sub>1</sub>-integrin antibody.** J82 cells were allowed to attach to a fibronectin- (10μg/ml) or collagen I- (50μg/ml) coated surface in the presence of the inhibitory anti-β<sub>1</sub>-integrin antibody (10μg/ml), anti-Rat IgG (10μg/ml) or in the absence of antibody (control). Unattached cells were removed, and remaining cells were stained with crystal violet. Cell attachment was quantified by absorbance measured at 550nm. \* denotes a significant difference from DMSO control ( $p < 0.01$ ,  $n = 3$ ,  $\pm SD$ ) using oneway ANOVA followed by Student's *t*-test.

Following transfection with siRNAs, there was an obvious decrease in adhesion to collagen in STAT1 knockdown J82 cells, but not to fibronectin (figure 4.34). Knockdown of STAT1 and STAT3 led to a significant reduction in cell adhesion on both fibronectin and collagen. However, blocking STAT3 alone caused only a slight decrease in adhesion to either substrate, which was not statistically significant. These results suggested that STAT1 may play an important role in cell adhesion in J82 cells, and the fact that STAT3 knockdown elicited no effect on cell adhesion, may possibly be due to the induction of STAT1 phosphorylation (figure 4.27a).

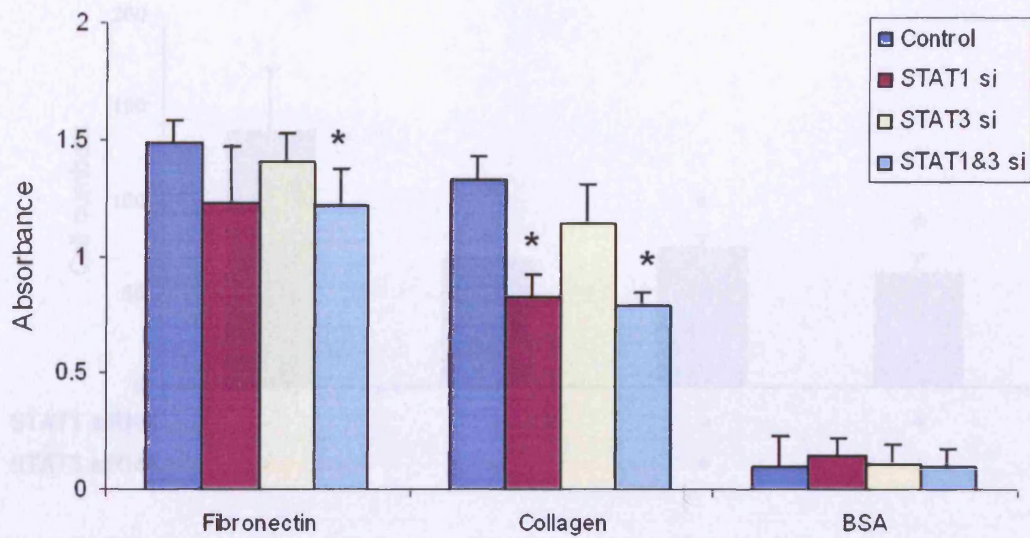


**Figure 4.34 Effect on cell adhesion in STAT1 and/or STAT3 knockdown J82 cells.** STAT1 or 3 knockdown J82 cells were plated onto fibronectin- (10 $\mu$ g/ml) or collagen I- (50 $\mu$ g/ml) coated surfaces or in the absence of any substrate (BSA) for 60 minutes at 37°C. Unattached cells were removed, and remaining cells were stained with crystal violet, and quantified by absorbance measured at 550nm. Each data point was done in triplicate. Control = J82 cells without transfection. \* denotes a significant difference from control ( $p < 0.05$ ,  $n = 4$ ,  $\pm$ SD) using oneway ANOVA followed by Student's *t*-test.

#### 4.6.2 Effect of STAT1 and/or STAT3 knockdown on migration

Effects of knocking down STAT1 and/or STAT3 on cell migration were investigated in order to further elucidate the function of these STATs in J82 cells. As shown in figure 4.35, knockdown of either STAT1 or STAT3 alone resulted in a significant decrease in cell migration. A similar effect was observed in J82 cells with double knockdown of STAT1 and STAT3, suggesting that both STAT1 and STAT3 may affect cell migration via the same pathway.

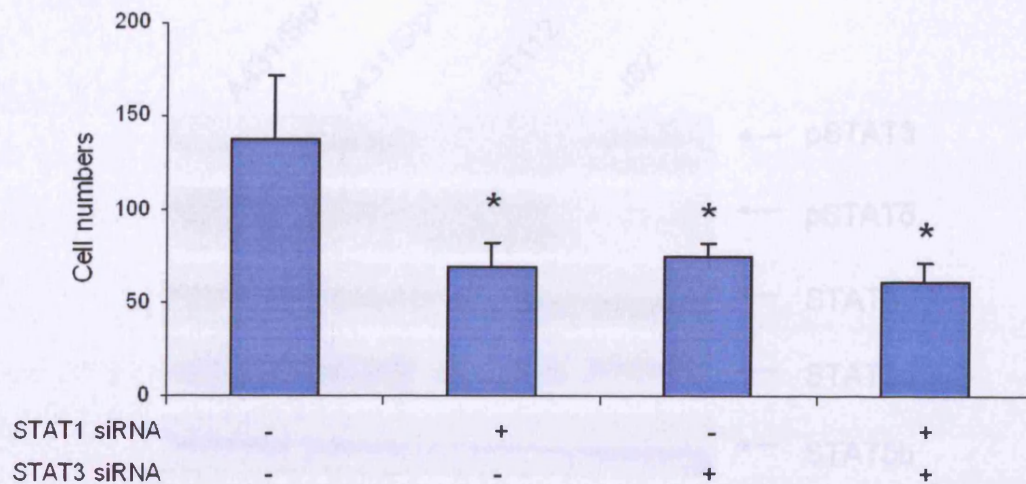


**Figure 4.35 Effect on cell migration in STAT1 and/or STAT3 knockdown J82 cells.** J82 cells were transfected with siRNAs to STAT1 and/or STAT3 and incubated for 48 hours. Control samples were transfected with scrambled siRNAs. \* denotes a significant difference from control ( $p < 0.05$ ,  $n = 4$ ,  $\pm SD$ ) using oneway ANOVA followed by Student's *t*-test.

#### 4.7 STATs phosphorylation status in A431/sip model of EMT

As noted in section 2.3 (table 2.1), the J82 cell line is originally from a higher grade bladder cancer, possessing a high *in vitro* invasive capacity compared to RT112 cells. J82 cells have phosphorylated STAT3 whereas RT112 cells express activated STAT5. It was therefore decided to investigate whether STAT3 activation is linked to cell invasion, using an A431/sip model developed for epithelial to mesenchymal transition (EMT) studies (Vandewalle *et al.*, 2005, Mejlvang *et al.*, 2007).

To generate the model system, A431 cells, which are E-cadherin<sup>+ve</sup>, were stably transfected with a construct containing Smad-interacting protein 1 (Sip1), a transcriptional repressor of E-cadherin. Ectopic expression of Sip1 induced by DOX leads to classical EMT, evident as increased invasiveness, downregulation of E-cadherin, Claudin 4 and upregulation of vimentin and N-cadherin (refer to Mejlvang *et al.*, 2007).

Interestingly, activation of STAT3 and downregulation of pSTAT5 was observed in A431/sip<sup>+</sup> cells (figure 4.36), suggesting that increased STAT3 phosphorylation may be associated with invasiveness in cancer cell lines.

## DISCUSSION

The role of the  
growth  
EGF stimulation  
total STAT3  
there was little  
The reported  
bladder cells  
markers, K19,  
bladder cancer  
type p53 (Casp  
(Cavaliari et al.

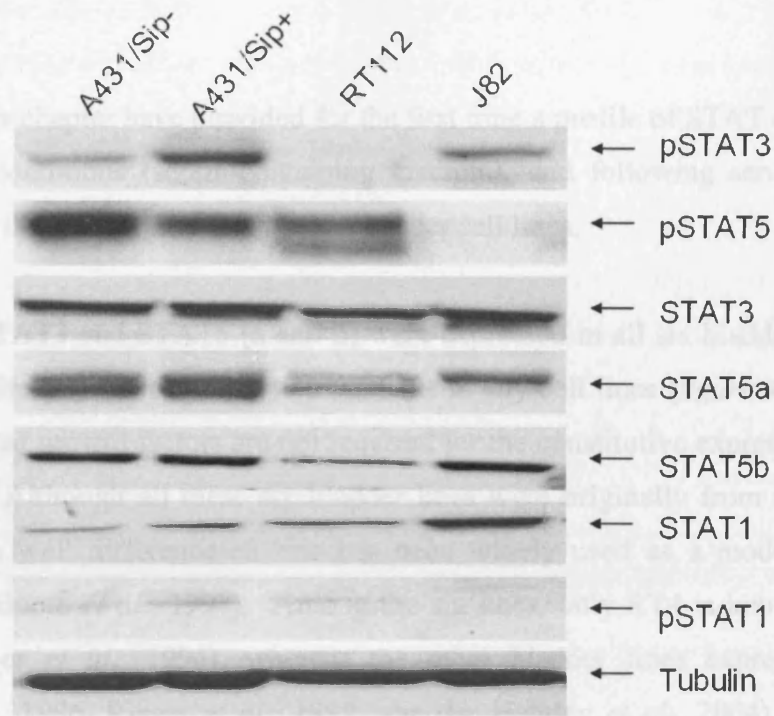


**Figure 4.36** *STATs phosphorylation status in A431/sip model of EMT. A431/sip<sup>-</sup> and A431/sip<sup>+</sup> samples were provided by Mr Jakob Mejlvang. Blots were performed on 2 separate occasions.*

STAT1 has been known to be involved in p53 function (Townsend et al., 2004). Consistent with this study, we observed that the highest mRNA levels of STAT1 were observed in bladder cancer cell lines, and in bladder cancer cell lines. In addition, in EMT cell lines, we observed that the expression of pSTAT1 expression and EGF was significantly higher in EMT cell lines compared to non-EMT cell lines. However, STAT1 expression was not significantly higher in EMT cell lines compared to non-EMT cell lines. EGF stimulation in all the cell lines resulted in a significant increase in pSTAT1 expression, which was consistent with the known role of EGF in STAT1 activation.

The role of STAT1 in bladder cancer is still unclear. It has been suggested that STAT1 may play a role in bladder cancer progression, and that it may be involved in the regulation of cell growth and survival. In this study, we observed that the expression of pSTAT1 was significantly higher in EMT cell lines compared to non-EMT cell lines, and that EGF stimulation resulted in a significant increase in pSTAT1 expression in all the cell lines. These findings suggest that STAT1 may play a role in bladder cancer progression, and that it may be involved in the regulation of cell growth and survival.

## ***DISCUSSION***

The results in this chapter have provided for the first time a profile of STAT expression under normal growth conditions (serum-containing medium), and following serum starvation or EGF stimulation in a panel of human bladder cancer cell lines.

Total STAT1, STAT3 and STAT5 (a and b) were expressed in all six bladder cell lines, and there was little alteration in response to treatments in any cell lines (*figure 4.4, 4.5 and 4.6*). This suggested that growth factors are not required for the constitutive expression of STAT in bladder cells. Although all these six bladder lines were originally from invasive bladder tumours, RT4, a well differentiated line has been widely used as a model of superficial bladder cancer (Booth *et al.*, 1997). Among the six lines, only RT4 is known to have wild type p53 (Cooper *et al.*, 1994), whereas the other bladder lines express mutated p53 (Kawasaki *et al.*, 1996, Rieger *et al.*, 1995, van der Heijden *et al.*, 2004). Under normal growth conditions, active STAT1 was only observed in RT4 cells (*figure 4.4*). In this case phosphorylated STAT1 may be associated with well differentiated and p53 wild type bladder cancer cells. STAT1 has been known to be associated with p53 directly (Townsend *et al.*, 2004). Consistent with this study, Arany *et al.*, (2003) have shown that the higher mRNA levels of STAT1 were observed in differentiated cells, compared with undifferentiated ones in head and neck cancers. In addition, in RT4 cells it appeared that serum was required for pSTAT1 expression, and EGF was not sufficient to re-activate STAT1 following serum starvation. However, STAT1 activation occurred in response to either serum starvation or EGF stimulation in all the other five bladder lines (*figure 4.4*), suggesting that STAT1 phosphorylation could be EGF-dependent or -independent.

The six bladder lines screened in this study can be divided into two groups, according to their phenotypes (*table 2.1*). Three epithelial lines RT4, RT112 and HT1376, are E-cadherin<sup>+ve</sup>, whereas three mesenchymal cell lines, T24, J82 and UMUC3 are E-cadherin<sup>-ve</sup>. In bladder cancers, decreased E-cadherin has been associated with invasive potential (Bringuier *et al.*, 1993), indicating that mesenchymal lines possess higher invasiveness than epithelial cells. Interestingly, the present study showed that constitutive phosphorylation of STAT5 was only observed in epithelial cell lines, while mesenchymal lines have phosphorylated STAT3 under normal growth conditions (*figure 4.5 and 4.6*), suggesting that active STAT3 could play an important role in bladder cancer cell invasive capacity. Also, the three mesenchymal cells,

plus HT1376, were known to be poorly differentiated cells (Booth *et al.*, 1997). It has been found that well-differentiated cells express lower levels of STAT3 than poorly differentiated cells in head and neck cancers (Arany *et al.*, 2003), which was consistent with the observation in bladder cancer cells.

RT112 and J82 are representatives of the epithelial and mesenchymal cell types in bladder cancer, and some characteristics of these two lines are summarised in *table 4.2*. The J82 cell line displays a higher *in vitro* invasive capacity than RT112 cells.

**Table 4.2 Some characteristics of bladder cells (J82 and RT112) and A431/sip cells**

	Epithelial	Mesenchymal	A431/Sip <sup>-</sup>	A431/Sip <sup>+</sup>
	RT112	J82		
pSTAT3	-	+	+	++
pSTAT5	+	-	++	+
E-cadherin	+	-	++	+
N-cadherin	-	+	-	+

A431/sip<sup>+</sup> (mesenchymal model) cells expressed less pSTAT5 and more pSTAT3, compared with A431/sip<sup>-</sup> (*figure 4.36*) similar to the J82 line. Induction of Sip1 expression in A431 cells led to a decrease in E-cadherin and caused EMT. In normal development, epithelial-mesenchymal transition (EMT) is recognised as a central feature with several critical developmental steps relying on this programme, including gastrulation, neural crest formation and heart morphogenesis. In the process of carcinogenesis, epithelial cells gain mesenchymal properties, inducing reduced intercellular adhesion and increased motility.

A hallmark of EMT is the inactivation of the E-cadherin adhesion complex, which contributes to cell differentiation, motility and wound healing. The E-cadherin/catenin system connects with the actin cytoskeleton, thus participating in the assembly of cell-cell adherens junctions. So far, multiple oncogenic pathways, involving Src, Ras, integrin, Wnt/ $\beta$ -catenin, Notch and PI3K/AKT have been implicated in the induction of EMT (Larue and Bellacosa, 2005).

Thus in these three cell types (*table 4.2*), there would appear to be a link between loss of E-cadherin, activation of pSTAT3 and EMT.

Neither serum starvation nor EGF stimulation altered the expression of pSTAT5 in epithelial lines or pSTAT3 in mesenchymal cells, suggesting that the observed STAT phosphorylation could be maintained independently of growth factors. On the other hand, activation of STAT3 in epithelial cells and of STAT5 in mesenchymal lines was EGF-inducible, except in RT4 cells (*figures 4.5 and 4.6*). A study (Arany *et al.*, 2003) in head and neck cancers has shown that STAT1 is expressed in well differentiated (low grade) tumors *in vivo* whereas the expression of STAT3 is high in poorly differentiated (high grade) tumors. Responses to growth factors are modified by differentiation-associated expression of STATs. In this study, RT4 (well differentiated cells), the only line expressing pSTAT1 under normal growth condition, did not show increased STAT3 activation in response to EGF, suggesting that there may have a differentiation-associated intracellular balance of STAT1/3 in bladder cancer cells.

Interestingly, PP2 treatment caused cell aggregation and altered morphology in J82 cells. Consistent with this observation, Nam *et al.*, (2002) found that PP2 significantly increased cell aggregation in a range of other cancer cells (including colon, liver and breast), and the treated cells were represented a tightening of cell adhesion. They also showed that E-cadherin/catenin expression can be enhanced by PP2, associated with the suppression of metastasis in cancer cells. However, in J82 cells which are E-cadherin<sup>-ve</sup>, this protein was not re-expressed in PP2-treated cells (data not shown), possibly due to the continued existence of E-cadherin suppressors or deletion/mutations of E-cadherin in these cells. Bornman *et al.*, (2001) have demonstrated that, the decreased expression of E-cadherin is attributed to the aberrant methylation of the CpG island flanking the 5' transcriptional start site of the *E-cadherin* gene, and methylation of this CpG island has been observed in bladder neoplasms ranging from low-grade papillary to advanced, invasive tumours. Chiang *et al.*, (2005) also have observed distinct morphology changes in several bladder cell lines, including J82, exposed to PP2, accompanied by upregulation in  $\gamma$ -catenin and a reduction in invasive capacity. Enhanced invasive capacity, induced by transfection of N-cadherin into E-cadherin-expressing bladder cells, was decreased by PP2 treatment (Rieger-Christ *et al.*, 2004).

PP2 treatment of J82 or RT112 cells had no effect on cell cycle (data not shown, performed by Dr MK Cheng). It should be pointed out that a second batch of PP2 which was purchased to carry out cell cycle analysis which did not cause any altered morphology in J82 cells.

In J82 and RT112 cells, there was some evidence to show that AG490 (JAK2 inhibitor) was able to downregulate STAT phosphorylation, but this effect was unsustainable, being reversible at some time points (*figures 4.14 and 4.15*). It was speculated that either the concentration of inhibitors used in this study may be not sufficient, or blockade of JAK2 may trigger other tyrosine kinases to activate STATs. Combined with piceatannol (JAK1 inhibitor) treatment, AG490 inhibited STAT3 expression (data not shown) in J82 cells and decreased STAT5 (a and b) protein levels in RT112 cells (*figure 4.18*), suggesting the involvement of JAKs in STATs expression in bladder cancer cells. In response to piceatannol treatment, a dose-dependent reduction in N-cadherin expression was observed, and N-cadherin appeared to be cleaved from 25 $\mu$ M (*figure 4.19*) accompanied by the formation of cell clusters (data not shown) in J82 cells, suggesting that JAK1 may be involved in cadherin-mediated cell-cell adhesion.

Cell cycle arrest in J82 and RT112 cells following AG490 treatment was observed (*figure 4.15 and 4.17*). J82 cells treated with 100 $\mu$ M AG490 underwent G<sub>0</sub>/G<sub>1</sub> phase arrest, accompanied by significant inhibition of pSTAT3 (data not shown, performed by Dr MK Cheng), an effect which appeared to be time-dependent. However, at 50 $\mu$ M AG490, any G<sub>0</sub>/G<sub>1</sub> phase arrest observed at 4 hours had disappeared at 16 hours, at which time reduction in STAT3 phosphorylation was reversed. This suggested that STAT3 activation might be important for cell cycle progression, in particular entry to S phase in J82 cells. However, in a recent study (Moran *et al.*, 2007), IL-6 activated JAK/STAT3 pathway are involved in regulation of CDK2/4 activity and p21 expression which result in G<sub>0</sub>/G<sub>1</sub> growth arrest in hepatocellular carcinoma.

In the RT112 line, a significant accumulation of cells in G<sub>0</sub>/G<sub>1</sub> phase and reduction in G<sub>2</sub>/M phase were observed at 4 hours with 100 $\mu$ M AG490 treatment. However, at 16 hours AG490 induced significant S phase arrest, with a decrease in the proportion of cells in G<sub>0</sub>/G<sub>1</sub> phase and disappearance of a G<sub>2</sub>/M peak. At 50 $\mu$ M, the pattern was similar but less significant. It was speculated that AG490 treatment caused a decrease in G<sub>2</sub>/M phase and accumulation in G<sub>0</sub>/G<sub>1</sub> phase at earlier time point, and resulted in S phase arrest eventually. Walz *et al.*, (2006) has found that activated JAK2 with a V617F point mutation promoted G<sub>1</sub>/S phase transition. Blocking JAK2V617F with siRNA led to inhibition of activated STAT5 which altered p27 and cyclin D2 expression. This suggested that AG490-induced cell cycle arrest may be a result of decrease in STAT5 phosphorylation in RT112 cells.

Studies have reported that activated STAT3 transcriptionally regulated cyclin D1 (Leslie *et al.*, 2006), and inhibition of constitutive STAT3 signalling induced cell cycle arrest and apoptosis in malignant cells (Turkson *et al.*, 2005). However, in this study, knockdown of STAT1, 3 or 5 (a and b) with siRNAs in J82 cells showed no alteration in cyclin D1, caspase 3 or survivin expression (*figure 4.30*). Interestingly, blocking either STAT3 or STAT5 (a and b) significantly activated STAT1 (*figure 4.27a*). In an *in vivo* study, Chapman *et al.*, (1999) have shown that in Stat3 null mammary glands, activation of Stat1 is observed and may act as a compensatory mechanism for the eventual initiation of involution. This led to hypothesis that STAT1 may be phosphorylated by same tyrosine kinases as STAT3/5, and once STAT3 and/or STAT5 blocked, STAT1 will be activated to compensate for the reduced level of active STATs in cells.

Furthermore, knockdown of STAT5 with siRNAs in J82 cells showed an obvious increase not only in STAT3 activation but also in STAT3 protein level, and vice versa (*figure 4.27a*). Immunoprecipitation results (*figure 4.29*) clearly showed that there was no complex formation among STAT1, 3 or 5 (a and b) in J82 cells. As noted previously, STAT3 and STAT5 (a and b) map to the distal region of human chromosome 17 (17q21.31, 17q11.2) (Copeland *et al.*, 1995). Data here suggested that STAT3 and STAT5 may transcriptionally regulate each other, and there may be a compensatory mechanism among all STAT family members to maintain levels of activated STATs in cells. Also, it was speculated that knockdown of individual STATs resulting in no effect on cell cycle and apoptosis involved proteins might be due to this compensatory mechanism.

In the current study, the most striking effect of knocking down STATs was upon cell adhesion and migration which were significantly inhibited (*figure 4.34 and 4.35*). Disruption of JAK/STAT signalling by SOCS3 negatively regulates cell motility (Niwa *et al.*, 2005), and Sliver *et al.*, (2004) have also shown that JAK/STAT pathway may contribute to ovarian cancer cell invasiveness, due to localisation of activated STAT3 to focal adhesions. In contrast, in human colorectal cancer cells, dominant-negative STAT3-Y705F causes a decrease in cell-cell homotypic adhesions, and increases cell motility and scattering (Rivat *et al.*, 2004). In this study, there was a significant reduction in adhesion on collagen and some decrease on fibronectin in STAT1 knockdown J82 cells, which suggested STAT1 might be involved in the regulation of cell adhesion in J82 cells. STAT3 deficiency did not significantly affect cell adhesion to either fibronectin or collagen. Thus knockdown of

STAT3 alone showed no effect on cell adhesion, possibly due to the activation of STAT1. Xie *et al.*, (2001) have found that during cell adhesion, STAT1 is activated and transiently and directly associated with FAK. Moreover, in FAK-deficient cells STAT1 activation is diminished, with decreased cell migration. Not only STAT1 but also STAT3 has been reported to be associated with cell migration. Delayed cell migration and the loss of collagen production have been observed in STAT3 deficient keloid fibroblasts (Lim *et al.*, 2006). In J82 cells, knockdown of either STAT1 or STAT3 alone resulted in a significant decrease in cell migration, but there was no further decrease in STAT1 and STAT3 combined knockout cells (*figure 4.35*). This indicated that STAT1 and STAT3 may affect cell migration via the same molecular mechanism involving proteins, such as FAK, with which both STAT1 and STAT3 are associated, as noted above. A study in the T24 bladder cell line has shown that activated STAT3 is required for maximal MMP-1 transcription, and expressing dominant-negative STAT3 in nude mice is capable of inhibiting EGF-induced cell migration and invasion (Itoh *et al.*, 2005).

In this chapter, the involvement of STATs and their potential role in bladder cancer cell lines has been described. The levels of STAT expression among the lines were similar overall, but STAT3/5 phosphorylation appeared to be cell phenotype-dependent, with activated STAT3 in mesenchymal lines which display higher invasive capability. The mechanism for constitutive STAT phosphorylation has yet to be determined, as to whether it is growth factor-dependent or -independent. Upstream tyrosine kinases in the STAT pathway have also been investigated. Disruption of JAK2/STAT signalling by AG490 caused cell cycle arrest, but few substantial effects of PP2 have been observed. There was some evidence of STAT1 and STAT3 being involved in cell adhesion and migration, providing further indication that increased STATs may be associated with cell invasion in bladder cancer.

## **CHAPTER 5**

### **EFFECTS OF INDOLES ON THE STAT SIGNALLING PATHWAY**

## **INTRODUCTION**

As previously discussed, overactive STATs play an important role in oncogenesis by mediating expression of genes involving in cell survival, proliferation and motility (*section 1.2.5*).

Constitutive activation of STAT3 could be inhibited by I3C in human pancreatic cancer cells (Lian *et al.*, 2004). Some other phytochemicals such as EGCG (Masuda *et al.*, 2001) and curcumin (Bharti *et al.*, 2003) have also been shown to suppress STAT activation in tumour cells, indicating that STAT signalling is targeted by various dietary agents.

I3C is also reported to induce G<sub>1</sub> cell cycle arrest, accompanied by inhibition of CDK6 and Rb and increases in p21 and p27 (reviewed in Aggarwal and Ichikawa, 2005). Similarly, DIM has been shown to cause cell cycle arrest and increase p21 expression in human breast cancer cells (Rahman *et al.*, 2006). Also, I3C and DIM appear to induce apoptosis in a wide variety of cells via the inhibition of Bcl-2 and induction of caspase (3, 6, 9) activation and PARP cleavage (refer to *table 1.6*). Kong *et al.*, (2007) have investigated the chemopreventive effect of DIM in human prostate cancer cells, showing inhibition of invasion which is correlated with reduction of MMP9 expression. These studies suggest that the STAT pathway with its links to cell cycle, apoptosis and invasion may provide a potential target for indoles.

In human bladder cancer cells, curcumin is an apoptosis-inducer (Tong *et al.*, 2006), and sulforaphane (an isothiocyanate from cruciferous vegetables) inhibits proliferation, causing G<sub>0</sub>/G<sub>1</sub> cell cycle arrest and induction of apoptosis (Shan *et al.*, 2006). Singh *et al.*, (2006) has shown that genistein causes G<sub>2</sub>/M arrest, downregulates NF- $\kappa$ B and induces apoptosis. In addition, EGCG inhibits cell growth and suppresses migration of bladder cancer cells via downregulation of N-cadherin and inactivation of Akt (Rieger-Christ *et al.*, 2007).

To date, there have been relatively few studies investigating the STAT pathway with respect to the mechanisms of action of indoles, and no studies on indoles as effective agents in the chemoprevention of bladder cancer have been published.

Studies described in this chapter examined the effect of indoles on the STAT pathway, cell cycle, apoptosis and invasion in human bladder cancer cells in order to provide further insight into their mechanisms of action.

## RESULTS

### 5.1 Effect of indoles on STATs protein levels and phosphorylation status

The basal levels of STATs protein and phosphorylation within six chosen bladder cancer cell lines when grown under normal conditions or serum starvation have already been determined (refer to Chapter 4, figures 4.4, 4.5 and 4.6). Besides J82 and RT112, T24 was also included to investigate the effect of indoles on STAT3 protein and phosphorylation levels.

#### 5.1.1 Effect of I3C on STAT3 protein levels and phosphorylation status

The effect of I3C upon STAT3 protein levels and phosphorylation status at concentrations up to 500 $\mu$ M was initially determined after 48 hours in three bladder cell lines, J82, T24 and RT112 (figures 5.1a and 5.1b). I3C does not influence STAT3 protein level in any of the three bladder cell lines. However, a significant reduction in STAT3 phosphorylation for T24 cells was observed for all treatments. The most striking effect was the almost complete inhibition of STAT3 phosphorylation in both T24 and J82 cells at 500 $\mu$ M. Consistent with the data shown in chapter 4 (figure 4.5), no STAT3 phosphorylation in RT112 cells was detectable.

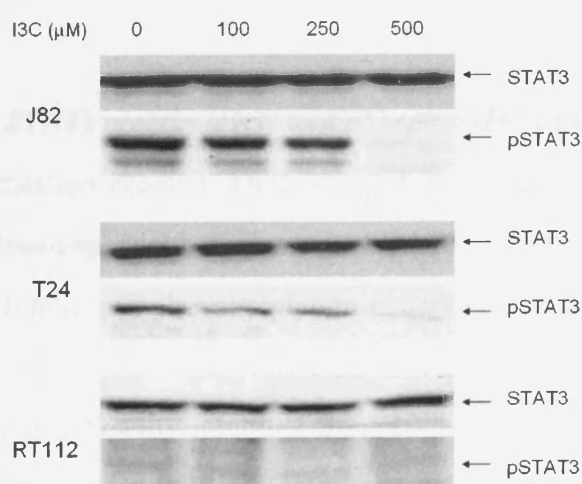


**Figure 5.1a** Effect of I3C on total and phosphorylated STAT3 levels in J82, T24 and RT112 cells. Cells were treated with 100, 250 or 500 $\mu$ M I3C for 48 hours. The vehicle for I3C was DMSO which was present in all samples to the same concentration. Each experiment was performed on at least 3 separate occasions (with the exception of RT112 blots  $n=2$ ), loading an equivalent amount of protein for each sample. Blots shown represent varying exposure times.

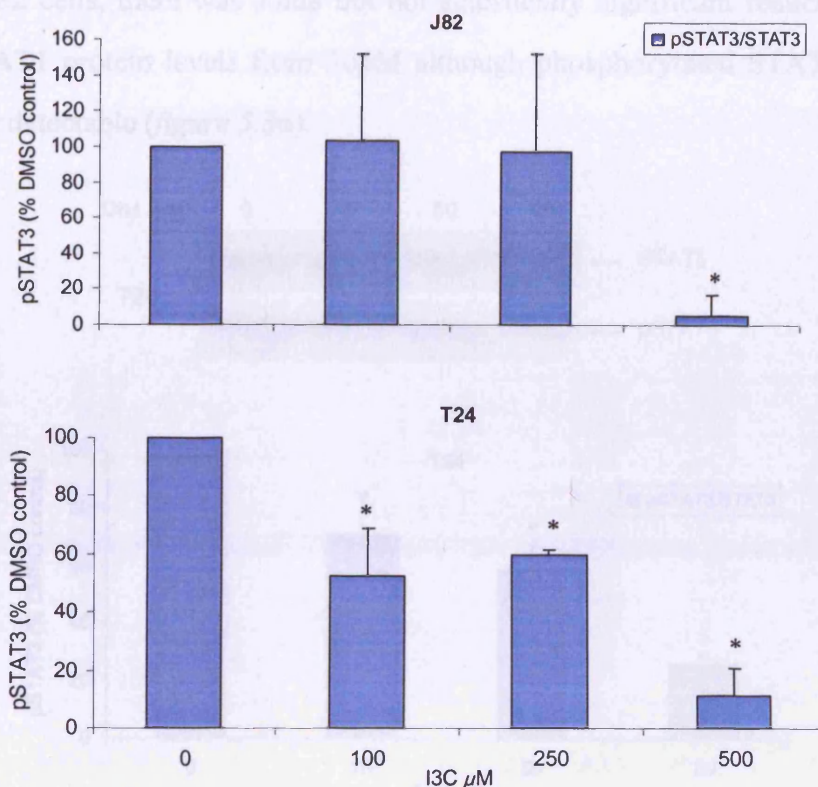


**Figure 5.1b** Histograms showing effect of I3C on phosphorylated STAT3 in J82 and T24 cells. Western blots were analysed by densitometry. pSTAT3 levels were normalised against total STAT3 levels, and expressed as a percentage of the DMSO control. \* denotes a significant difference from DMSO control ( $p < 0.05$ ,  $n = 3$ ,  $\pm SD$ ) using oneway ANOVA followed by Student's *t*-test.

### 5.1.2 Effect of DIM on STATs protein levels and phosphorylation status

Similarly, the I3C condensation product, DIM, elicited no effect on STAT3 protein level. However, it induced a dose-dependent decrease in STAT3 phosphorylation for T24 cells, demonstrating that the inhibition in phosphorylation observed was not due to a decrease in total protein level (figure 5.2). Cell lines varied in their response to DIM, in that STAT3 phosphorylation was only significantly inhibited from  $50\mu\text{M}$  in J82 cells, but again with no effect on total STAT3 level. I3C or DIM suppressed STAT3 phosphorylation in both T24 and J82 cells, suggesting that this effect was not cell type specific.

However, in J82 cells, there was some but not statistically significant reduction in STAT5 (a&b) and STAT1 protein levels from 50 $\mu$ M although phosphorylated STAT5 and STAT1 levels were not detectable (figure 5.3a).

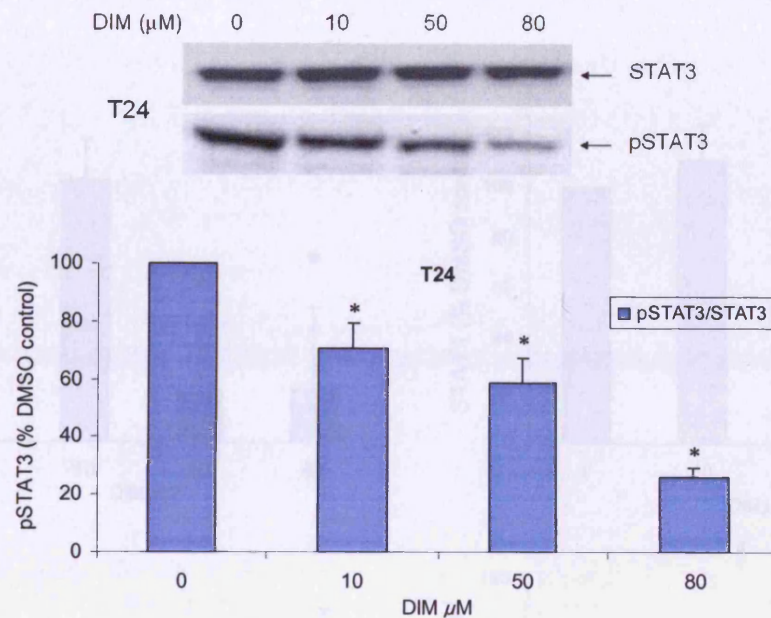


**Figure 5.2 Effect of DIM on total and phosphorylated STAT3 levels in T24 cells.** Cells were treated with 10, 50 or 80 $\mu$ M DIM for 48 hours. The vehicle for DIM was DMSO which was present in all samples to the same concentration. The chart shows pSTAT3 levels in T24 cells determined by densitometric analysis. \* denotes a significant difference from DMSO control ( $p < 0.05$ ,  $n = 3$ ,  $\pm$ SD) using oneway ANOVA followed by Student's *t*-test.

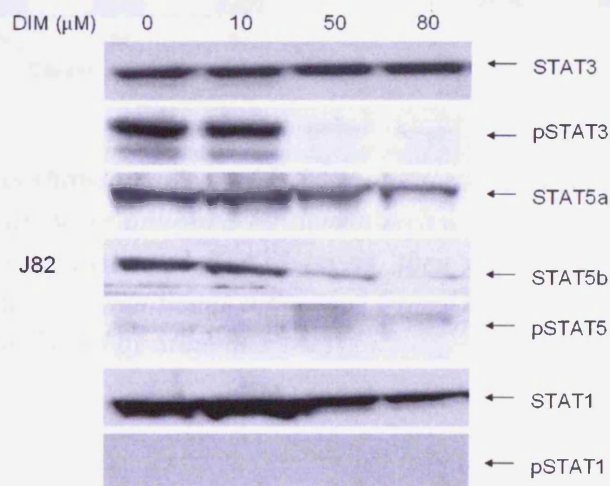


**Figure 5.3a Effect of DIM on total and phosphorylated STAT levels in J82 cells.** Cells were treated with 10, 50 or 80 $\mu$ M DIM for 48 hours. Each experiment was performed on at least 3 separate occasions (with the exception of STAT5a and b blots  $n = 2$ ), loading an equivalent amount of protein for each sample.

Since total STAT5 (a and b) and STAT1 levels were variable following DIM treatment, with some blots showing an increase, the DIM-induced changes in total STAT5 and STAT1 for the J82 cells were represented graphically in *figure 5.3b*, in order to show the SD for these blots.

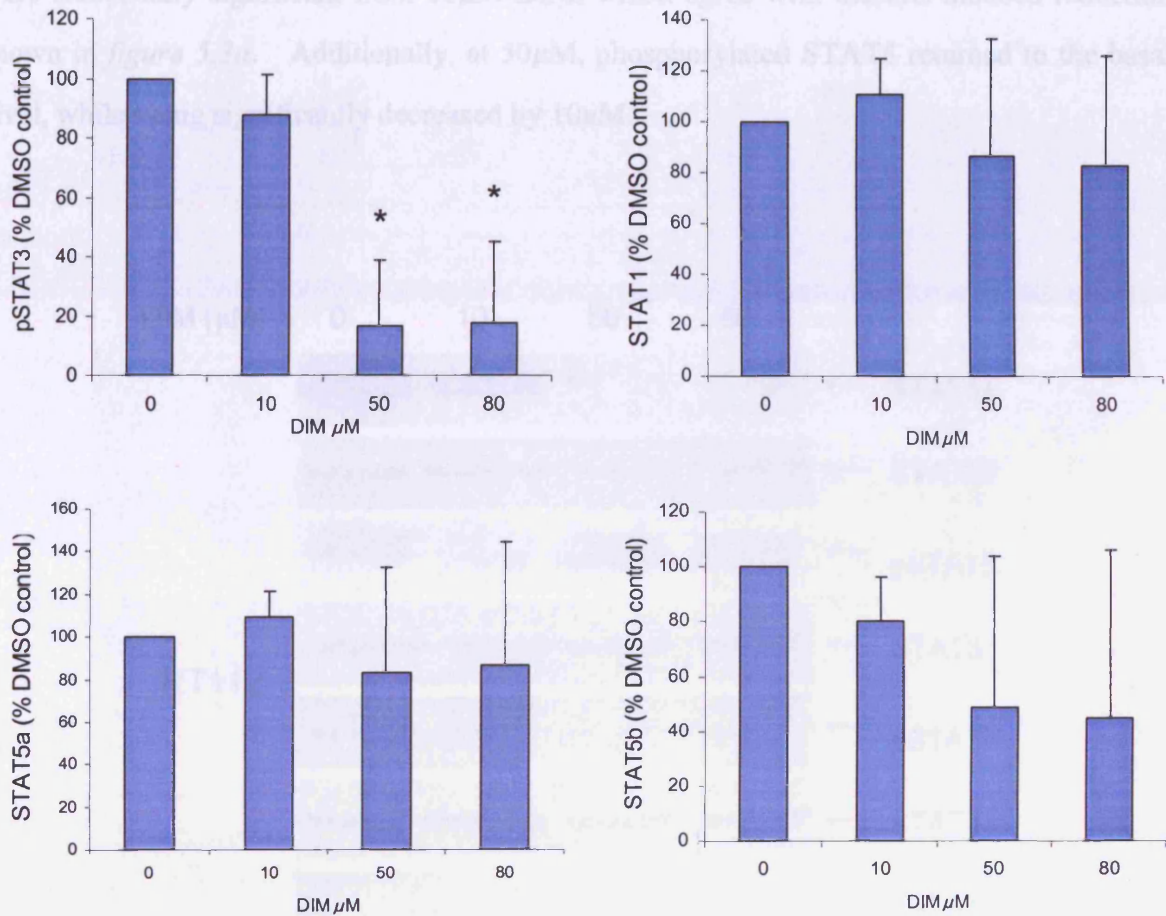


**Figure 5.3b** Histograms showing effect of DIM on total and phosphorylated STAT levels in J82 cells. Western blots were analysed by densitometry. pSTAT3 and total STAT1 and 5 levels were normalised against total STAT3 levels, then expressed as a percentage of the DMSO control. \* denotes a significant difference from DMSO control ( $p < 0.05$ ,  $n = 3$ ,  $\pm SD$ ) using oneway ANOVA followed by Student's *t*-test.

Figure 5.4a shows the total and phosphorylated STAT1, 3 and 5 levels in RT112 cells following a 48 hour DIM treatment. As with the mesenchymal cell lines, DIM has no effect on STAT3 protein level in epithelial RT112 cells. Also, STAT1 protein level was constant at all treatments. As shown in figure 5.4b, the decreases in STAT5a and b protein levels were statistically significant from 10 $\mu$ M DIM, which agree with the I3C-induced reduction shown in figure 5.3a. Additionally, at 50 $\mu$ M, phosphorylated STAT5 returned to the basal level, while being significantly decreased by 10 $\mu$ M.

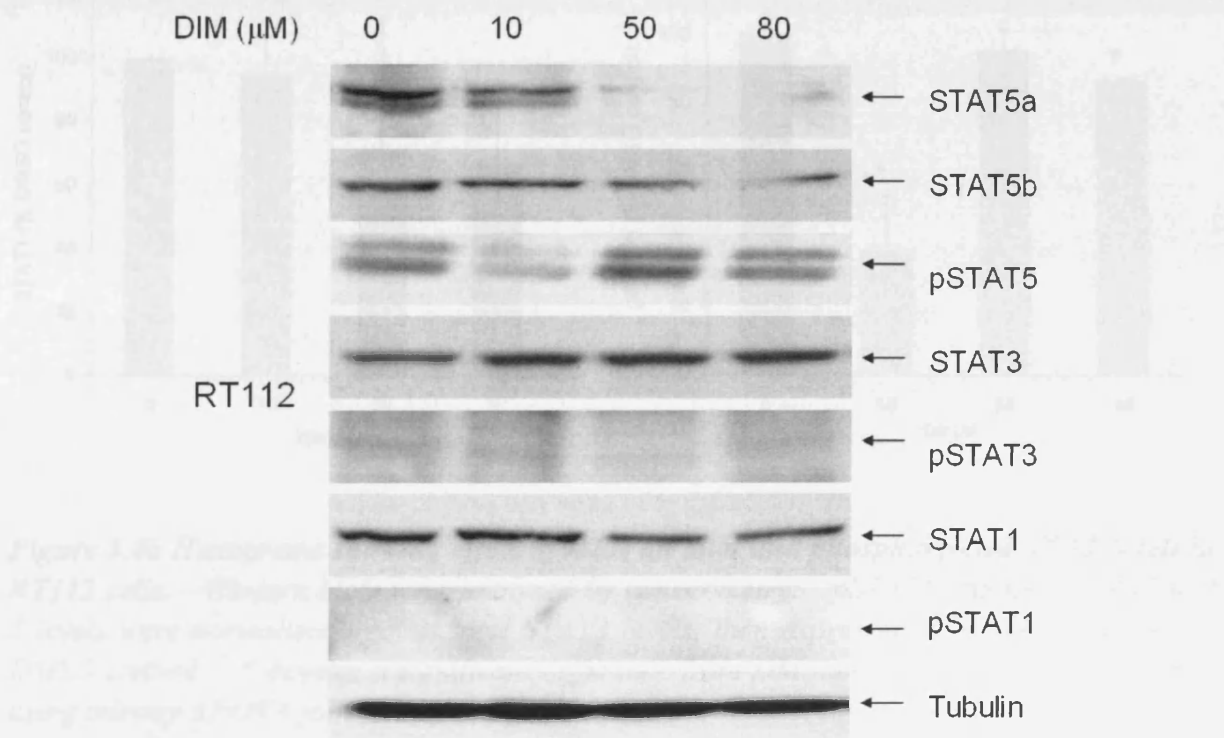


**Figure 5.4a** Effect of DIM on total and phosphorylated STAT levels in RT112 cells. Cells were treated with 10, 50 or 80 $\mu$ M DIM for 48 hours. Each experiment was performed on at least 3 separate occasions (with the exception of total STAT1 blot n=2), loading an equivalent amount of protein for each sample. Blots shown represent varying exposure times.

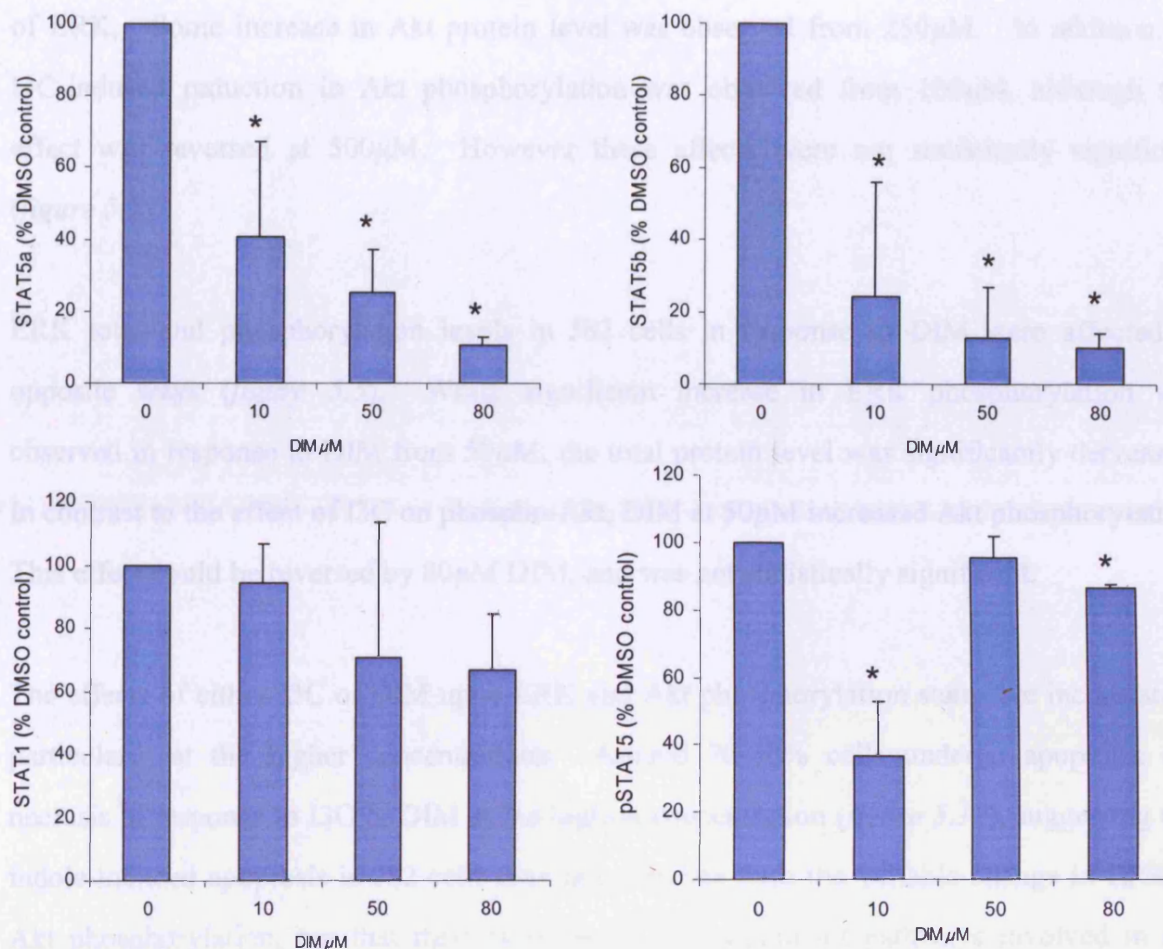


**Figure 5.4b** Histograms showing effect of DIM on total and phosphorylated STAT levels in RT112 cells. Western blots were analysed by densitometry. pSTAT5 and total STAT1 and 5 levels were normalised against total STAT3 levels, then expressed as a percentage of the DMSO control. \* denotes a significant difference from DMSO control ( $p < 0.05$ ,  $n = 3$ ,  $\pm SD$ ) using oneway ANOVA followed by Student's *t*-test.

### 5.2 Effect of indoles on ERK and Akt protein levels and phosphorylation status in J82 cells

Data so far have demonstrated that both I3C and DIM inhibited STAT3 phosphorylation without any change in STAT3 protein level, and also induced apoptosis (section 5.3.2) in J82 cells. It was therefore important to determine whether STAT3 phosphorylation status correlated with ERK or Akt phosphorylation levels which are important to cell survival.

Following a 48 hour I3C treatment, there was little effect on total and phosphorylated levels of ERK. Some increase in Akt protein level was observed from 250 $\mu$ M. In addition, an I3C-induced reduction in Akt phosphorylation was observed from 100 $\mu$ M, although this effect was reversed at 500 $\mu$ M. However these effects were not statistically significant (*figure 5.5*).

ERK total and phosphorylation levels in J82 cells in response to DIM were affected in opposite ways (*figure 5.5*). While significant increase in ERK phosphorylation was observed in response to DIM from 50 $\mu$ M, the total protein level was significantly decreased. In contrast to the effect of I3C on phospho-Akt, DIM at 50 $\mu$ M increased Akt phosphorylation. This effect could be reversed by 80 $\mu$ M DIM, and was not statistically significant.

The effects of either I3C or DIM upon ERK and Akt phosphorylation status are inconsistent, particularly at the higher concentrations. Around 70-80% cells undergo apoptosis and necrosis in response to I3C or DIM at the highest concentration (*figure 5.12*), suggesting that indole-induced apoptosis in J82 cells may not correlate with the variable change in ERK or Akt phosphorylation, but that there is some other predominant pathways involved in this process.

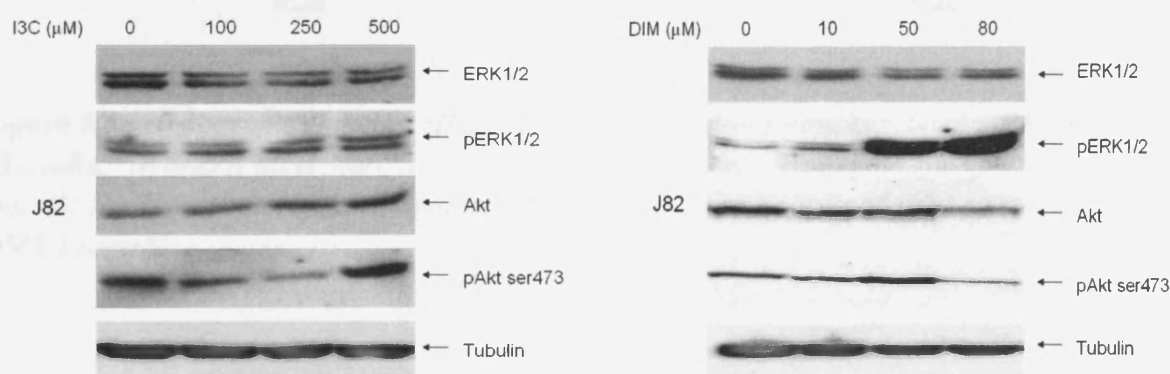


**Figure 5.5 Effect of I3C or DIM on total and phosphorylated ERK and Akt levels in J82 cells.** Cells were treated with either I3C (left, 100, 250 or 500 $\mu$ M) or DIM (right, 10, 50 or 80 $\mu$ M) for 48 hours. Each experiment was performed on at least 3 separate occasions, loading an equivalent amount of protein for each sample. Blots shown represent varying exposure times.

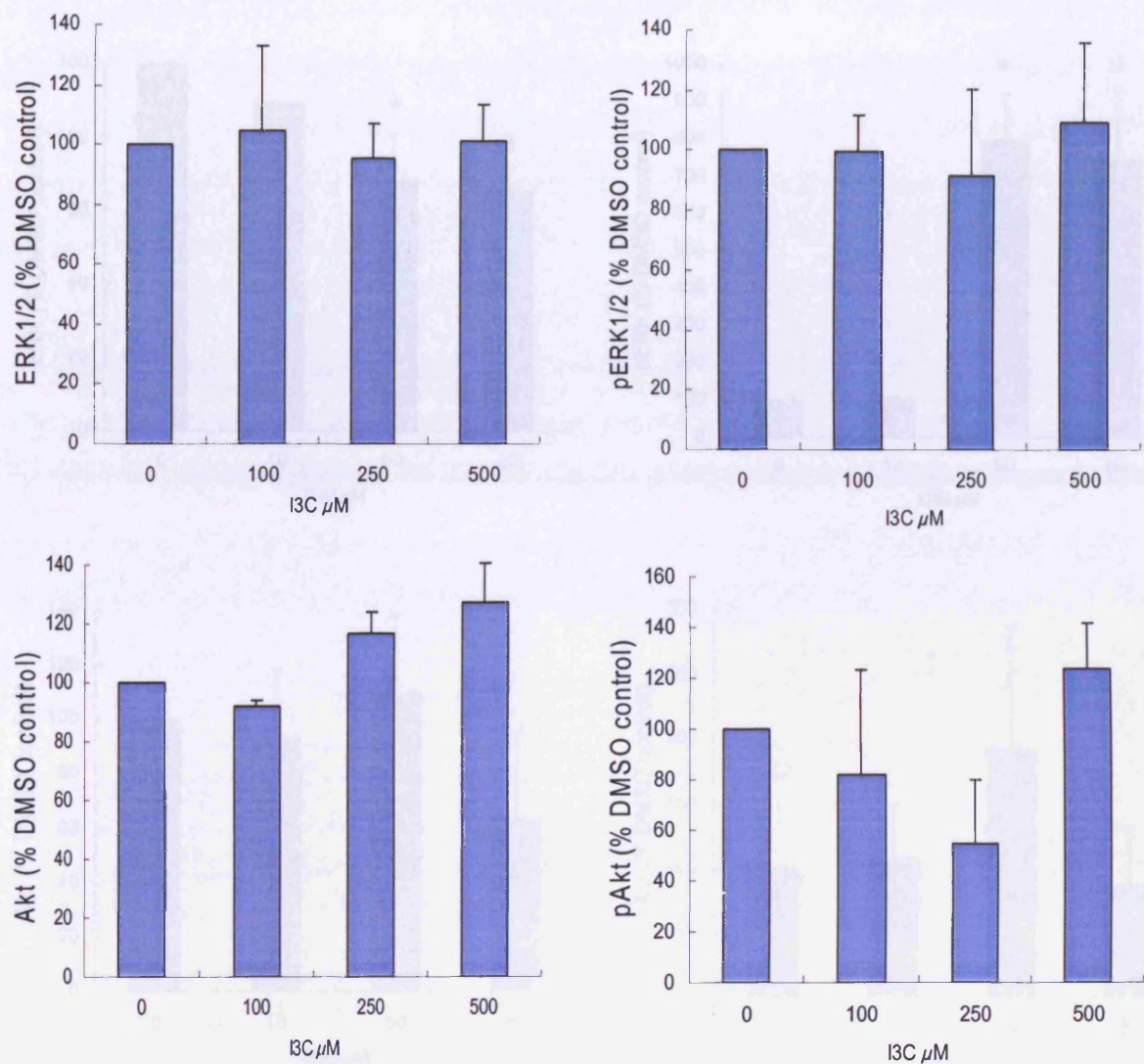


**Figure 5.6a** Histograms showing effect of I3C on total and phosphorylated ERK and Akt in J82 cells. Western blots were analysed by densitometry. Total and phosphorylated ERK and Akt levels were normalised against tubulin levels, then expressed as a percentage of the DMSO control.

5.3 Effect of indoles on cell proliferation and apoptosis

The finding that STAT phosphorylation was inhibited by TIC or DIM in M1 three week old

lines in these experiments to investigate the overall effect of DIM on whether the effect of

indoles on cell proliferation and induction of apoptosis. However, the effect of

indoles on cell proliferation and induction of apoptosis was not affected by DIM. DIM had

no effect on overall cell cycle time.

The effect of DIM on cell cycle time was investigated by measuring the time taken for

cells to reach the G1/S phase of the cell cycle. The mean values of the percentage of cells in each phase

of the cell cycle are shown in Figure 5.6a. The mean values of the percentage of cells in each phase

of the cell cycle are shown in Figure 5.6a. The mean values of the percentage of cells in each phase

of the cell cycle are shown in Figure 5.6a. The mean values of the percentage of cells in each phase

of the cell cycle are shown in Figure 5.6a. The mean values of the percentage of cells in each phase

of the cell cycle are shown in Figure 5.6a. The mean values of the percentage of cells in each phase

of the cell cycle are shown in Figure 5.6a. The mean values of the percentage of cells in each phase

of the cell cycle are shown in Figure 5.6a. The mean values of the percentage of cells in each phase

of the cell cycle are shown in Figure 5.6a. The mean values of the percentage of cells in each phase

of the cell cycle are shown in Figure 5.6a. The mean values of the percentage of cells in each phase

of the cell cycle are shown in Figure 5.6a. The mean values of the percentage of cells in each phase

of the cell cycle are shown in Figure 5.6a. The mean values of the percentage of cells in each phase

of the cell cycle are shown in Figure 5.6a. The mean values of the percentage of cells in each phase

of the cell cycle are shown in Figure 5.6a. The mean values of the percentage of cells in each phase

of the cell cycle are shown in Figure 5.6a. The mean values of the percentage of cells in each phase

of the cell cycle are shown in Figure 5.6a. The mean values of the percentage of cells in each phase

of the cell cycle are shown in Figure 5.6a. The mean values of the percentage of cells in each phase

of the cell cycle are shown in Figure 5.6a. The mean values of the percentage of cells in each phase

of the cell cycle are shown in Figure 5.6a. The mean values of the percentage of cells in each phase

of the cell cycle are shown in Figure 5.6a. The mean values of the percentage of cells in each phase

of the cell cycle are shown in Figure 5.6a. The mean values of the percentage of cells in each phase

of the cell cycle are shown in Figure 5.6a. The mean values of the percentage of cells in each phase

of the cell cycle are shown in Figure 5.6a. The mean values of the percentage of cells in each phase

of the cell cycle are shown in Figure 5.6a. The mean values of the percentage of cells in each phase

of the cell cycle are shown in Figure 5.6a. The mean values of the percentage of cells in each phase

of the cell cycle are shown in Figure 5.6a. The mean values of the percentage of cells in each phase

of the cell cycle are shown in Figure 5.6a. The mean values of the percentage of cells in each phase

of the cell cycle are shown in Figure 5.6a. The mean values of the percentage of cells in each phase

of the cell cycle are shown in Figure 5.6a. The mean values of the percentage of cells in each phase

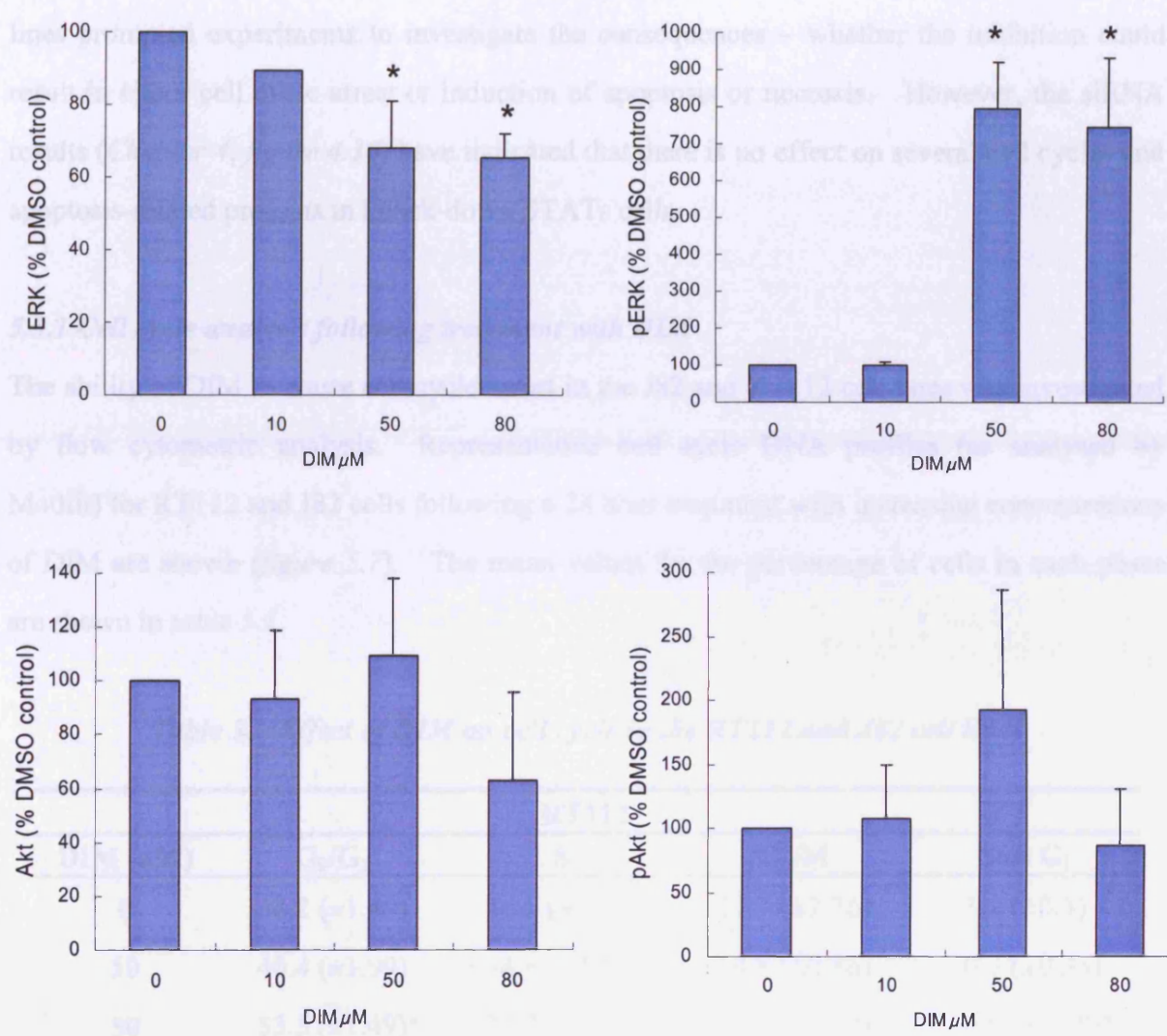


**Figure 5.6b** Histograms showing effect of DIM on total and phosphorylated ERK and Akt in J82 cells. Western blots were analysed by densitometry. Total and phosphorylated ERK and Akt levels were normalised against tubulin levels, then expressed as a percentage of the DMSO control. \* denotes a significant difference from DMSO control ( $p < 0.05$ ,  $n = 3$ ,  $\pm SD$ ) using oneway ANOVA followed by Student's  $t$ -test.

### 5.3 Effect of indoles on cell proliferation and apoptosis

The finding that STAT phosphorylation was inhibited by I3C or DIM in all three bladder cell lines prompted experiments to investigate the consequences – whether the inhibition could result in either cell cycle arrest or induction of apoptosis or necrosis. However, the siRNA results (*Chapter 4, figure 4.30*) have indicated that there is no effect on several cell cycle- and apoptosis-related proteins in knock-down STATs cells.

#### 5.3.1 Cell cycle analysis following treatment with DIM

The ability of DIM to cause cell cycle arrest in the J82 and RT112 cell lines was investigated by flow cytometric analysis. Representative cell cycle DNA profiles (as analysed by Modfit) for RT112 and J82 cells following a 24 hour treatment with increasing concentrations of DIM are shown (*figure 5.7*). The mean values for the percentage of cells in each phase are shown in *table 5.1*.

**Table 5.1 Effect of DIM on cell cycle in the RT112 and J82 cell lines**

RT112				
DIM ( $\mu$ M)	G <sub>0</sub> /G <sub>1</sub>	S	G <sub>2</sub> /M	Sub G <sub>1</sub>
0	38.2 ( $\pm$ 1.89)	44.1 ( $\pm$ 2.14)	17.7 ( $\pm$ 2.36)	1.2 ( $\pm$ 0.3)
10	40.4 ( $\pm$ 1.99)	44.8 ( $\pm$ 2.46)	14.8 ( $\pm$ 0.86)	0.7 ( $\pm$ 0.33)
50	53.5 ( $\pm$ 1.49)*	36.7 ( $\pm$ 4.16)	9.8 ( $\pm$ 2.77)*	6.8 ( $\pm$ 2.58)*
J82				
DIM ( $\mu$ M)	G <sub>0</sub> /G <sub>1</sub>	S	G <sub>2</sub> /M	Sub G <sub>1</sub>
0	41.1 ( $\pm$ 2.89)	39.2 ( $\pm$ 2.34)	19.7 ( $\pm$ 0.79)	1.1 ( $\pm$ 0.08)
10	41.8 ( $\pm$ 3.08)	37.9 ( $\pm$ 2.91)	20.4 ( $\pm$ 1.78)	1.6 ( $\pm$ 0.09)
50	45.7 ( $\pm$ 1.49)	22.4 ( $\pm$ 2.69)*	31.8 ( $\pm$ 2.97)*	7.4 ( $\pm$ 2.21)*

*It shows the percentage of cells in each phase of the cell cycle in the RT112 and J82 cell lines following a 24 hour DIM treatment. \* denotes a significant difference from DMSO control (n=3,  $\pm$ SD,  $p < 0.05$ ). (Data provided by Dr MK Cheng)*

Cell cycle arrest is characterised by an accumulation of cells within a specific phase of the cycle, which can be visualised by an alteration to the peak areas in DNA profiles. DIM

(50 $\mu$ M) induced a significant accumulation of cells in G<sub>0</sub>/G<sub>1</sub> phase in RT112 cells, while it showed a decrease in the G<sub>2</sub>/M peak profile. In contrast, G<sub>2</sub>/M arrest was observed in J82 cells following a 50 $\mu$ M DIM treatment, which could explain the decrease in S phase. In both lines, a significant increase of the percentages of cells in sub G<sub>1</sub> following 50 $\mu$ M DIM treatment may be indicative of the occurrence of apoptosis.

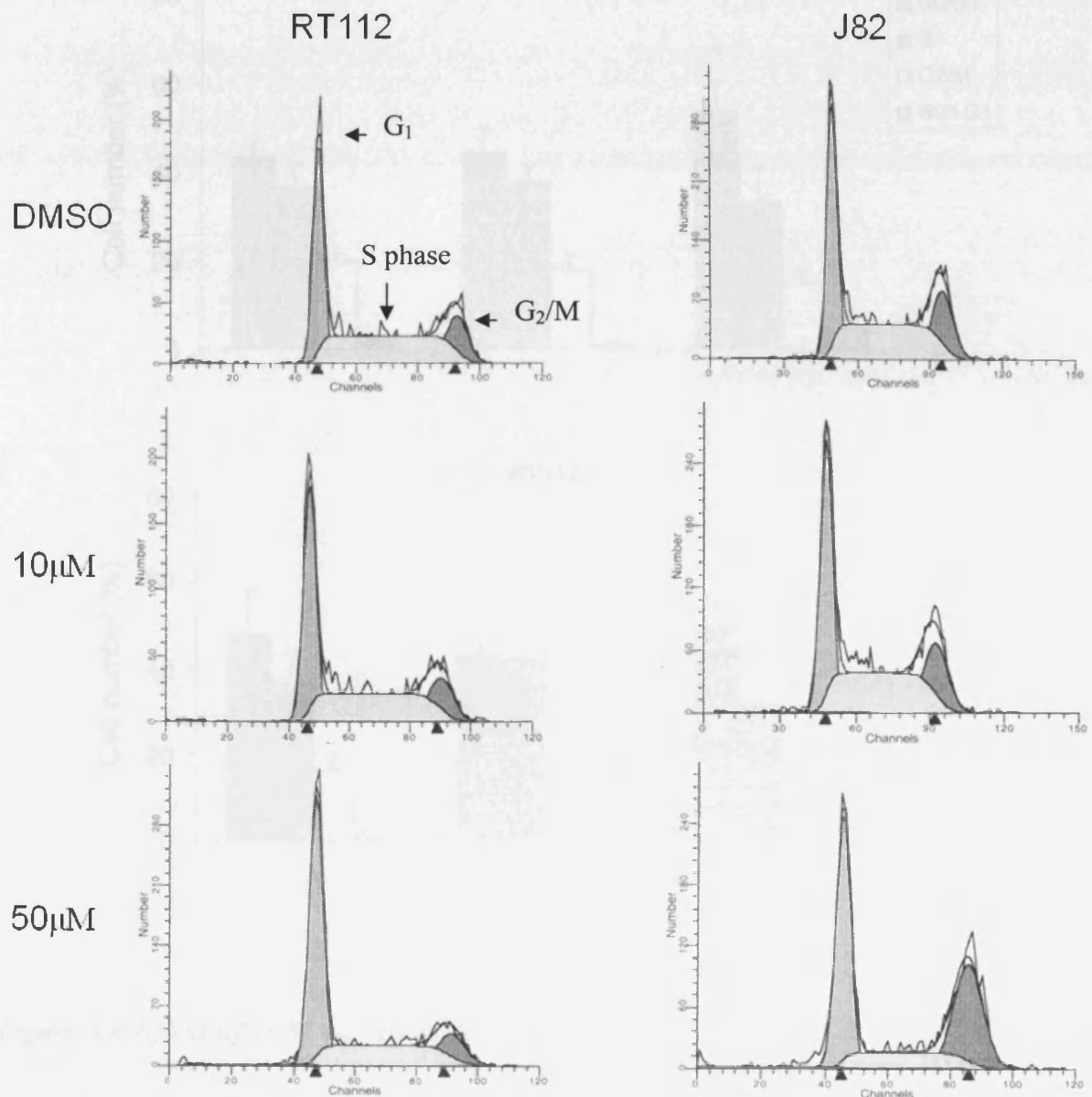


**Figure 5.7** Flow cytometric analysis of prodium iodide stained RT112 and J82 cells following DIM treatment. Cells were treated with DIM (10 or 50 $\mu$ M) for 24 hours. The experiment was performed upon 3 separate occasions and data analysed using Modfit L.T. software.

However, as shown in *figure 5.8*, at 48 hours there was an alteration of peak profile in J82 cells following a 50 $\mu$ M DIM treatment, switching from G<sub>2</sub>/M to G<sub>0</sub>/G<sub>1</sub> arrest. In RT112 cells, no clear phase-specific cell cycle arrest was observed following a 48 hour DIM treatment.

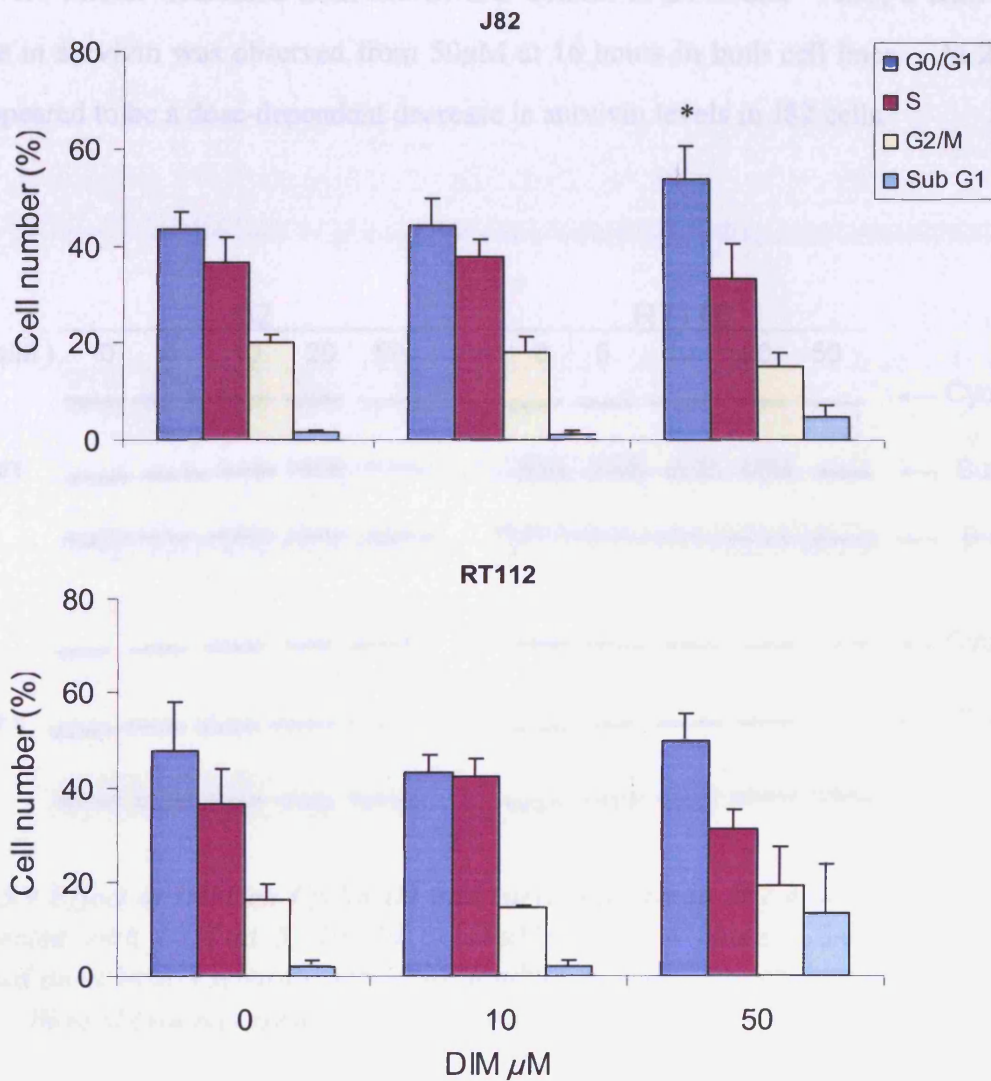


**Figure 5.8** Effect of DIM on cell cycle in J82 and RT112 cells. Cells were treated with DIM (10 or 50 $\mu$ M) for 48 hours. \* denotes a significant difference from DMSO control ( $p < 0.05$ ,  $n = 3$ ,  $\pm$ SD). (Data provided by Dr MK Cheng)

Either G<sub>0</sub>/G<sub>1</sub> or G<sub>2</sub>/M arrest suggests that DIM may be able to specifically affect components of the cell cycle process within these two cell lines. So, cyclin D1 and survivin levels were assessed following treatment with 5, 10, 20 or 50µM up to 24 hours (*figure 5.9*).

At 50µM, cyclin D1 levels appeared to decrease slightly at 16 hours in both cell lines, and levels were further decreased from the DMSO control at 24 hours. Also, a DIM-induced decrease in survivin was observed from 50µM at 16 hours in both cell lines. At 24 hours, there appeared to be a dose-dependent decrease in survivin levels in J82 cells.

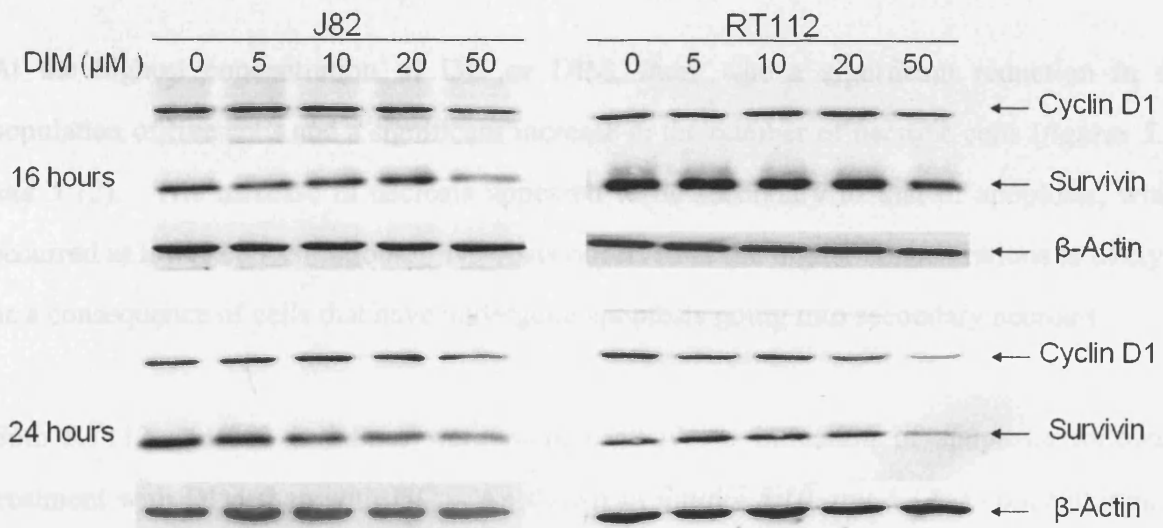


**Figure 5.9 Effect of DIM on Cyclin D1 and survivin levels in J82 and RT112 cells.** Cells were treated with DIM at 5, 10, 20 or 50µM up to 24 hours. Each experiment was performed on at least 3 separate occasions, loading an equivalent amount of protein for each sample. Blots shown represent varying exposure times (Data provided by Dr MK Cheng).

### ***5.3.2 Assessment of apoptosis in response to indoles***

#### ***5.3.2.1 Assessment of apoptosis by annexin V staining in response to indoles***

To determine the extent of apoptosis occurring in response to I3C and DIM, RT112 and J82 cells were stained with FITC-conjugated annexin V and PI as described in 2.6.2. I3C induced apoptosis with a concentration of 100 $\mu$ M in RT112 cells and 250 $\mu$ M in J82 cells (*figures 5.10 & 5.12*), and this effect was dose-dependent. At 500 $\mu$ M, there was a significant reduction in the population of live cells, and a significant increase in apoptotic and necrotic cells. Similarly, a dose-dependent increase in the percentage of apoptotic cells reached significance following treatment with DIM from 10 $\mu$ M and a significant increase in the population of necrotic cells was observed from 50 $\mu$ M DIM (*figures 5.10 & 5.12*).

At the highest concentration of I3C or DIM, there was a significant reduction in the population of live cells and a significant increase in the number of necrotic cells (*figures 5.10 and 5.12*). The increase in necrosis appeared to be secondary to that of apoptosis, which occurred at lower concentrations. Necrosis observed at the higher concentrations is likely to be a consequence of cells that have undergone apoptosis going into secondary necrosis.

Both RT112 and J82 cell lines were more sensitive to induction of apoptosis following treatment with DIM than with I3C. As shown in *figures 5.10 and 5.12*, a concentration of 50 $\mu$ M DIM induced a similar degree of apoptosis as did 250 $\mu$ M I3C at 48 hours treatment.

Following I3C or DIM treatment, a large number of cells rounded up, detached from the flasks and floated in medium following indole treatments of J82 and RT112 cells and apoptosis was confirmed by FACS. Another bladder cell line, RT4 was previously found to be the most radioresistant line among several human bladder cell lines, including J82 and RT112 (Moneef *et al.*, 2003). It was therefore important to assess the effect of indoles on induction of apoptosis in RT4 cells. In contrast, while RT4 cells behaved similar as J82 and RT112 cells, dual staining of annexin V and PI gave a very different profile (*figure 5.14*), which was unsuitable for assessment of apoptosis by FACS in these cells. The effect of apoptosis induced by indoles in RT4 cells was therefore assessed via other methods.

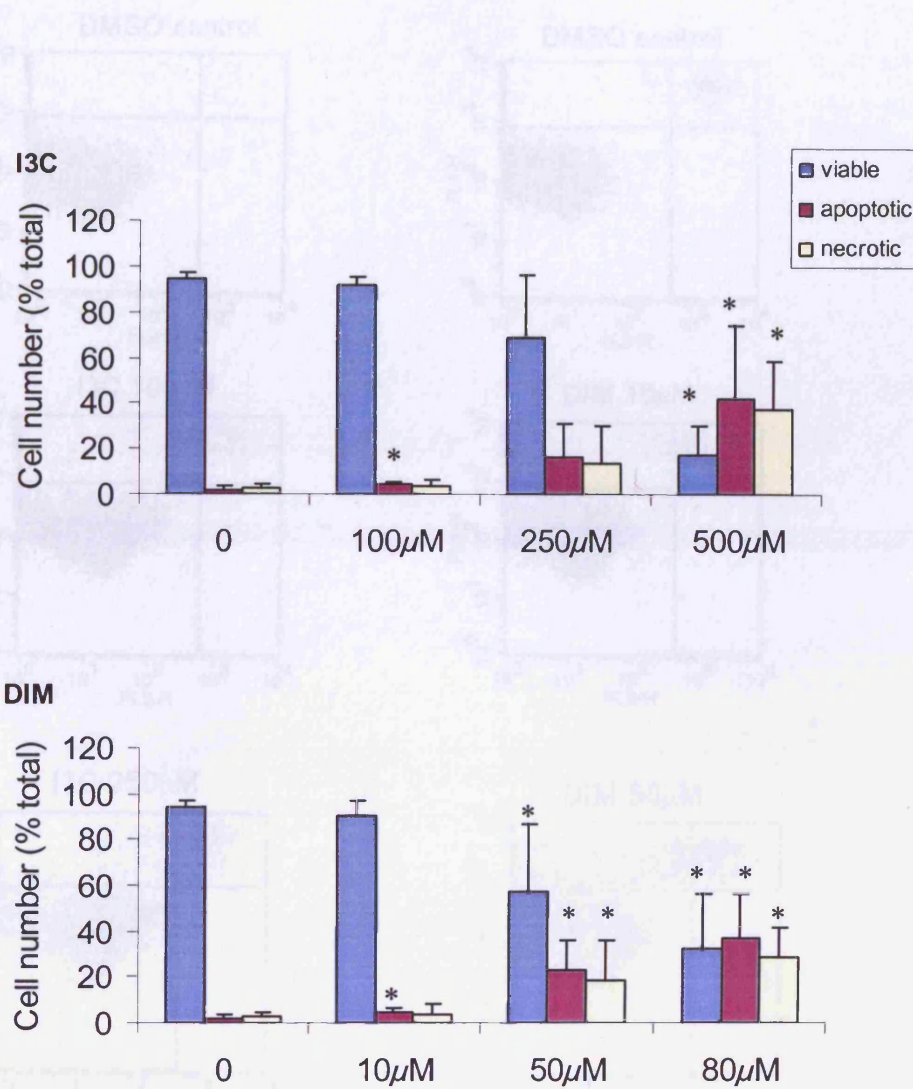


**Figure 5.10 Effect of I3C or DIM on apoptosis in RT112 cells.** Cells were treated with I3C (top) at 100, 250 or 500 $\mu$ M or DIM (lower) at 10, 50 or 80 $\mu$ M for 48 hours. Apoptosis and necrosis was assessed by annexin V and PI staining. \* denotes a significant difference from DMSO control ( $p < 0.05$ ,  $n = 5$ ,  $\pm$ SD) using oneway ANOVA followed by Scheffe's significant difference post hoc test and Student's t-test.

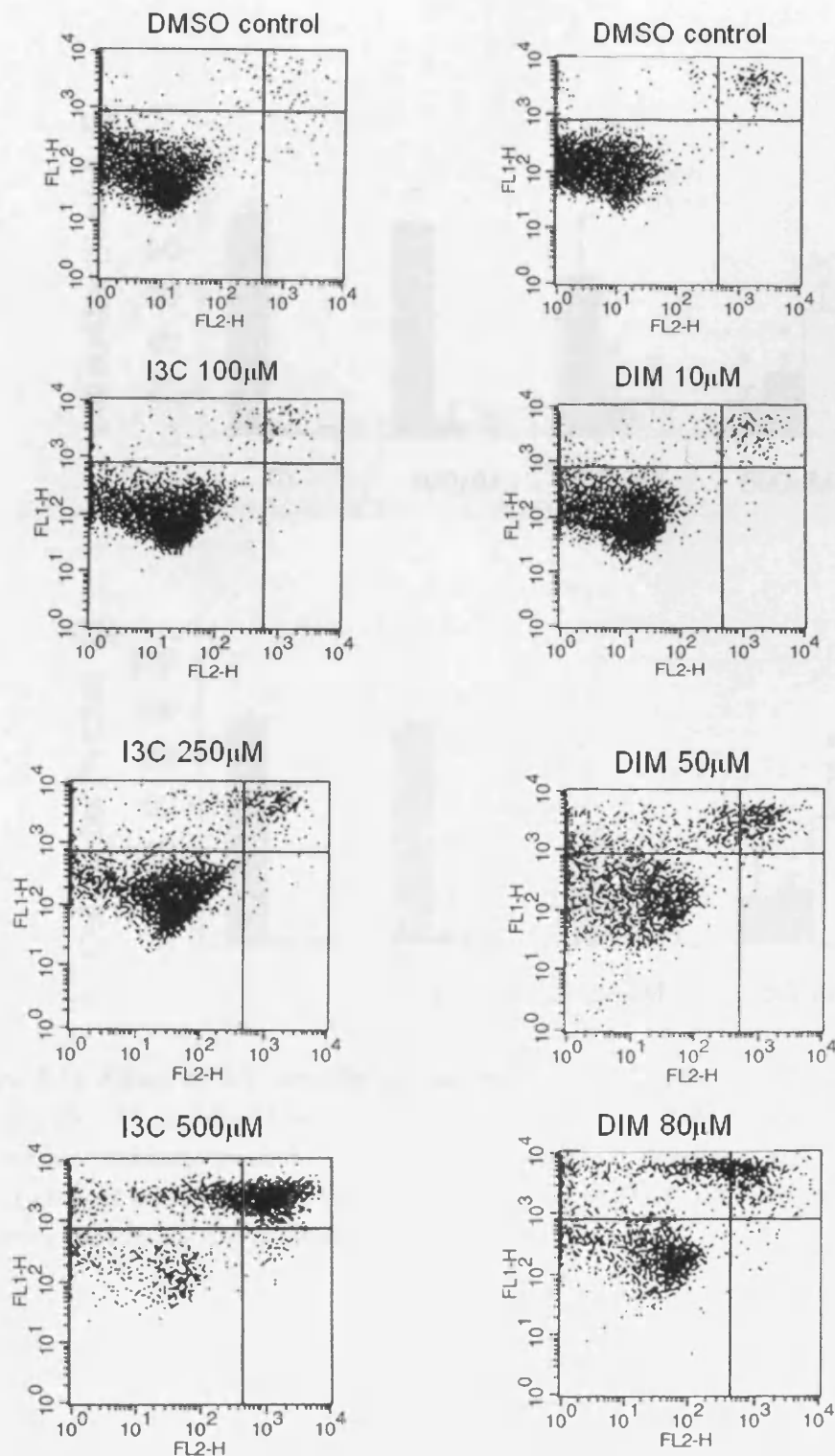


**Figure 5.11** Plots showing effect of I3C or DIM on apoptosis in RT112 cells. Representative dot plots for figure 5.10, showing annexin V and PI staining in the RT112 cells following a 48 hour I3C (left) or DIM (right) treatment. Y axis (FL1-H) represents annexin V staining, and X axis (FL2-H) represents PI staining. Live cells are present in the bottom left corner, apoptotic cells in the top left corner, and necrotic cells in the top right corner.

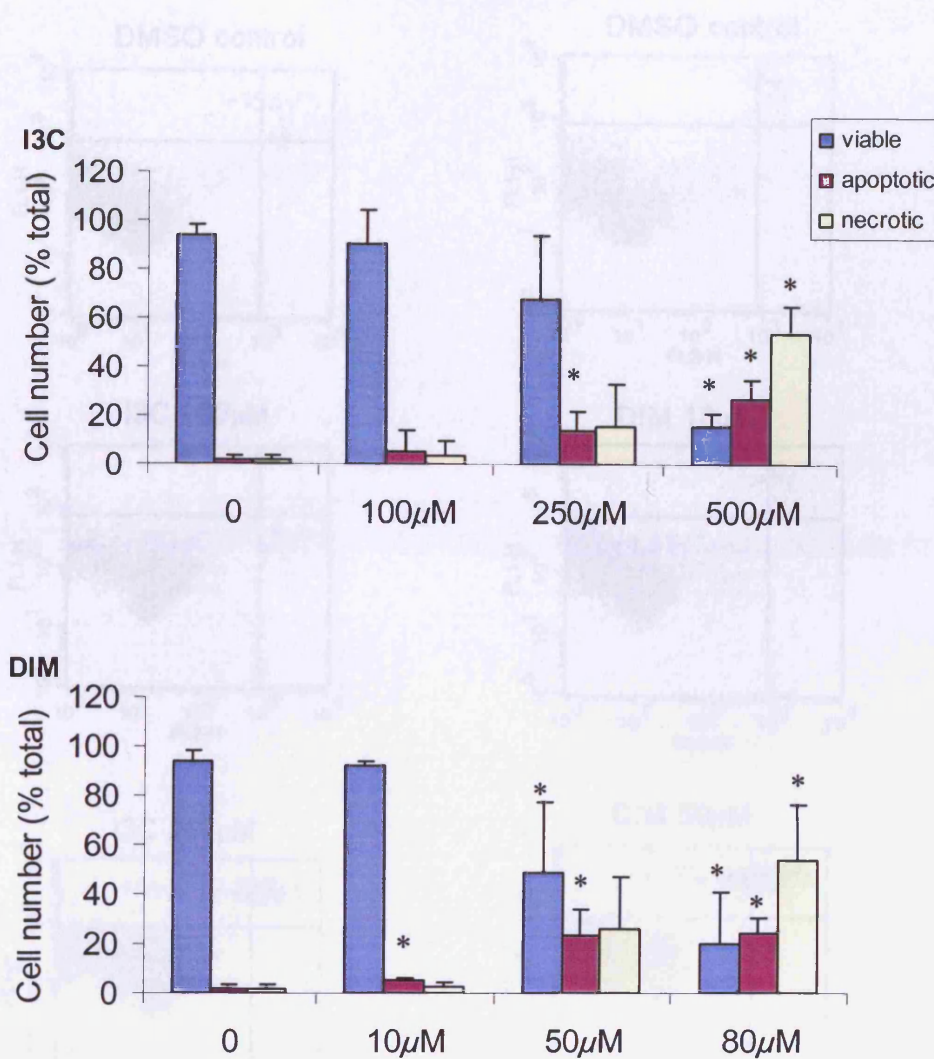


**Figure 5.12** Effect of I3C or DIM on apoptosis in J82 cells. Cells were treated with I3C (top) at 100, 250 or 500 $\mu$ M or DIM (lower) at 10, 50 or 80 $\mu$ M for 48 hours. Apoptosis and necrosis was assessed by annexin V and PI staining. \* denotes a significant difference from DMSO control ( $p < 0.05$ ,  $n = 5$ ,  $\pm$ SD) using oneway ANOVA followed by Scheffe's significant difference post hoc test and Student's t-test.

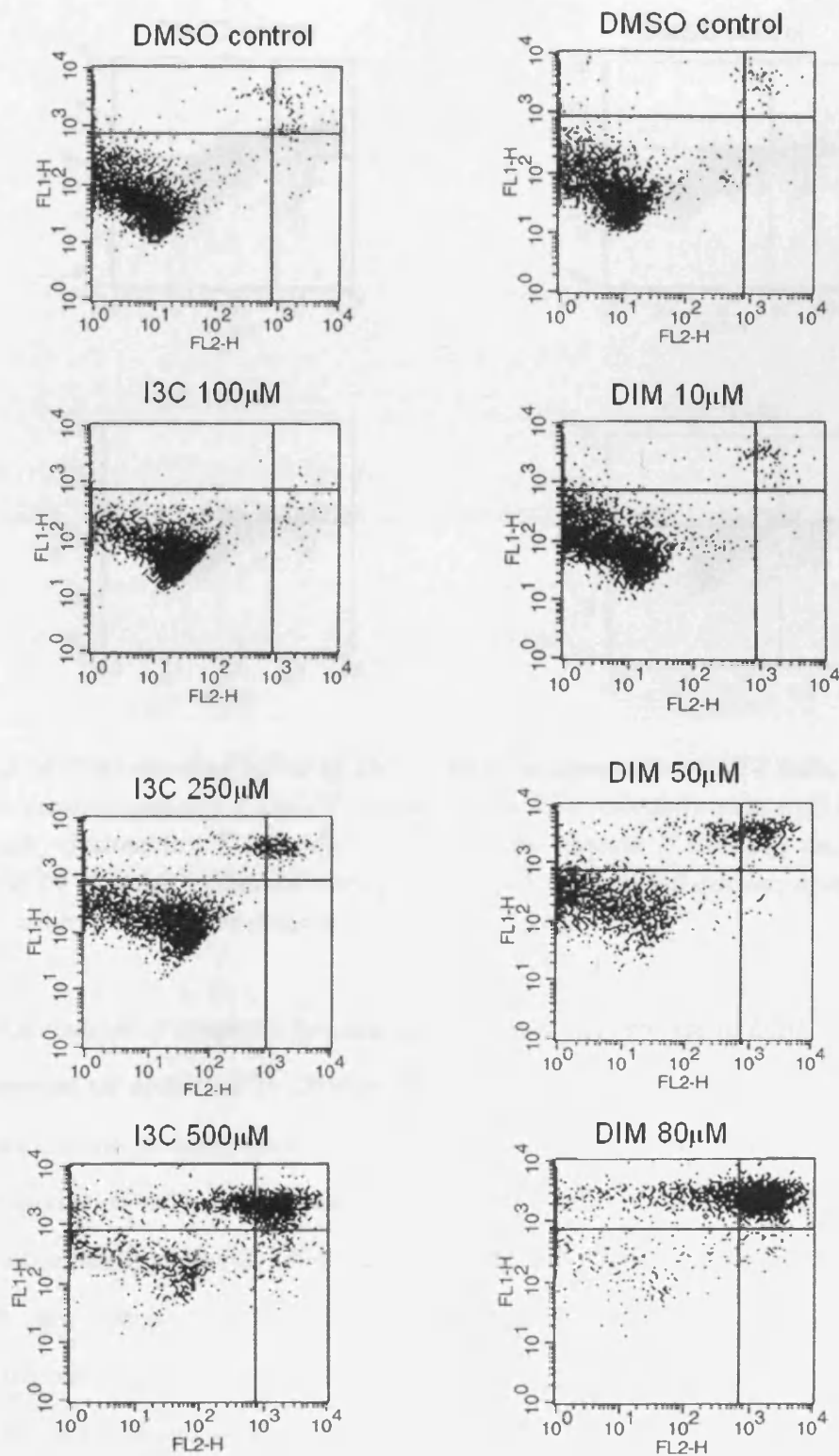


**Figure 5.13** Plots showing effect of I3C or DIM on apoptosis in J82 cells. Representative dot plots for figure 5.12, showing annexin V and PI staining in the J82 cells following a 48 hour I3C (left) or DIM (right) treatment. Y axis (FL1-H) represents annexin V staining, and X axis (FL2-H) represents PI staining. Live cells are present in the bottom left corner, apoptotic cells in the top left corner, and necrotic cells in the top right corner.

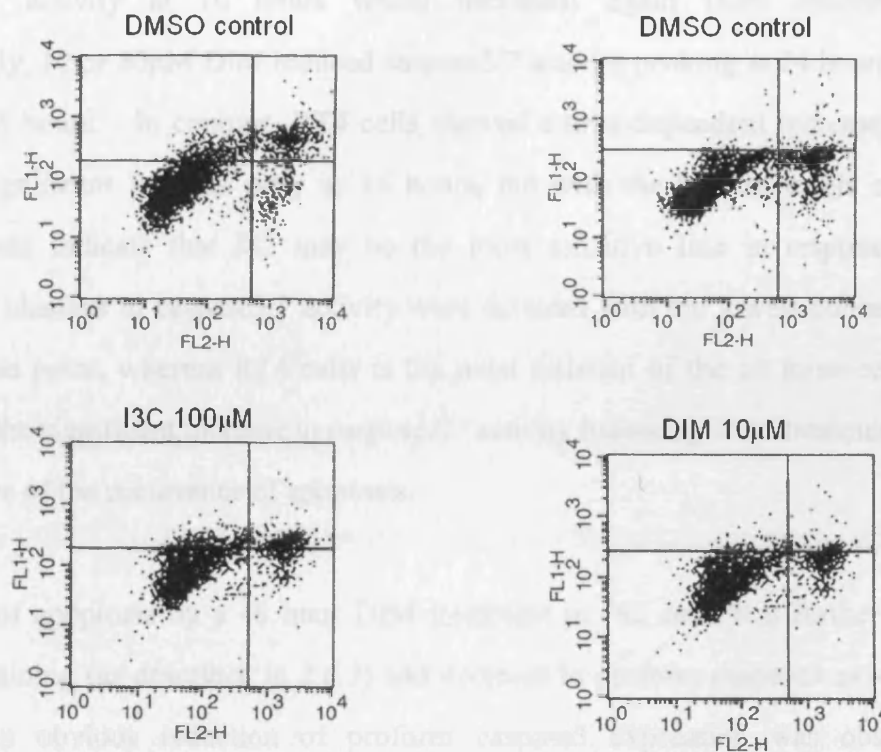


**Figure 5.14** Plots showing effect of I3C or DIM on apoptosis in RT4 cells. Representative dot plots showing annexin V and PI staining in the RT4 cells following a 48 hour I3C (left) or DIM (right) treatment. Y axis (FL1-H) represents annexin V staining, and X axis (FL2-H) represents PI staining. Live cells are present in the bottom left corner, apoptotic cells in the top left corner, and necrotic cells in the top right corner.

### 5.3.2.2 Assessment of apoptosis by caspase3/7 activity in response to DIM

The induction of apoptosis by DIM in RT4, J82 and RT112 cells was assessed or further confirmed by the measurement of caspase3/7 activity as described in 2.6.4 (figure 5.15). The sensitivity of cells in response to DIM was varied. Among all three cell lines, the lowest concentration (10µM) DIM induced the fastest increase in caspase3/7 activity in J82 cells, whereas a higher concentration (50µM) induced the fastest increase in RT112 cells. Overall the response in RT4 cells was the slowest, peaking at 48 hours, when caspase activity levels were falling again in the other two lines.

In the J82 cell line, a significant increase in caspase3/7 activity was observed following DIM treatment at 16hours, peaking at 24hours and decreasing again from 48hours at all concentrations. In RT112 cells treated with 80µM DIM, there was a dramatic increase in

caspase3/7 activity at 16 hours which decreased again from 24 hours in RT112. Interestingly, 10 or 50 $\mu$ M DIM induced caspase3/7 activity peaking at 24 hours and dropping down at 48 hours. In contrast, RT4 cells showed a time-dependent increase in caspase3/7 activity, significant from as early as 16 hours, but with the highest levels observed at 48 hours. Data indicate that J82 may be the most sensitive line in response to DIM, as significant changes in caspase3/7 activity were detected with the lowest concentration at the earliest time point, whereas RT4 cells is the most resistant of the all three cell lines tested. However, the significant increase in caspase3/7 activity following DIM treatment in RT4 cells is indicative of the occurrence of apoptosis.

Induction of apoptosis by a 48 hour DIM treatment in J82 cells was further confirmed by Hoechst staining (as described in 2.6.3) and decrease in proform caspase3 expression (*figure 5.16*). An obvious reduction of proform caspase3 expression was observed with a concentration as low as 10 $\mu$ M, consistent with annexin V data. Evidence from Hoechst staining, which shows increased fluorescence in apoptotic cells due to condensed chromatin, further supports the induction of apoptosis by DIM in J82 cells.

#### *5.3.2.3 Assessment of apoptosis by PARP cleavage in response to DIM*

Another measure of apoptosis is cleavage of the caspase3/7 substrate poly (ADP ribose) polymerase (PARP). *Figure 5.17* shows representative blots of PARP cleavage in J82, RT112 and RT4 cells following DIM treatment up to 48 hours.

In J82 cells, significant PARP cleavage was observed from as early as 16 hours with 80 $\mu$ M. At 10 $\mu$ M, PARP cleavage was detectable by 48 hours. Similarly, there was a dose- and time-dependent increase in PARP cleavage upon RT112 cells following DIM treatment. An increase in PARP cleavage was also found with 80 $\mu$ M DIM from 16 hours in RT4 cells, however no PARP cleavage was detectable at 10 $\mu$ M by 48 hours, suggesting that the most resistant line was RT4, in agreement with the caspase3/7 activity results (*figure 5.15*).

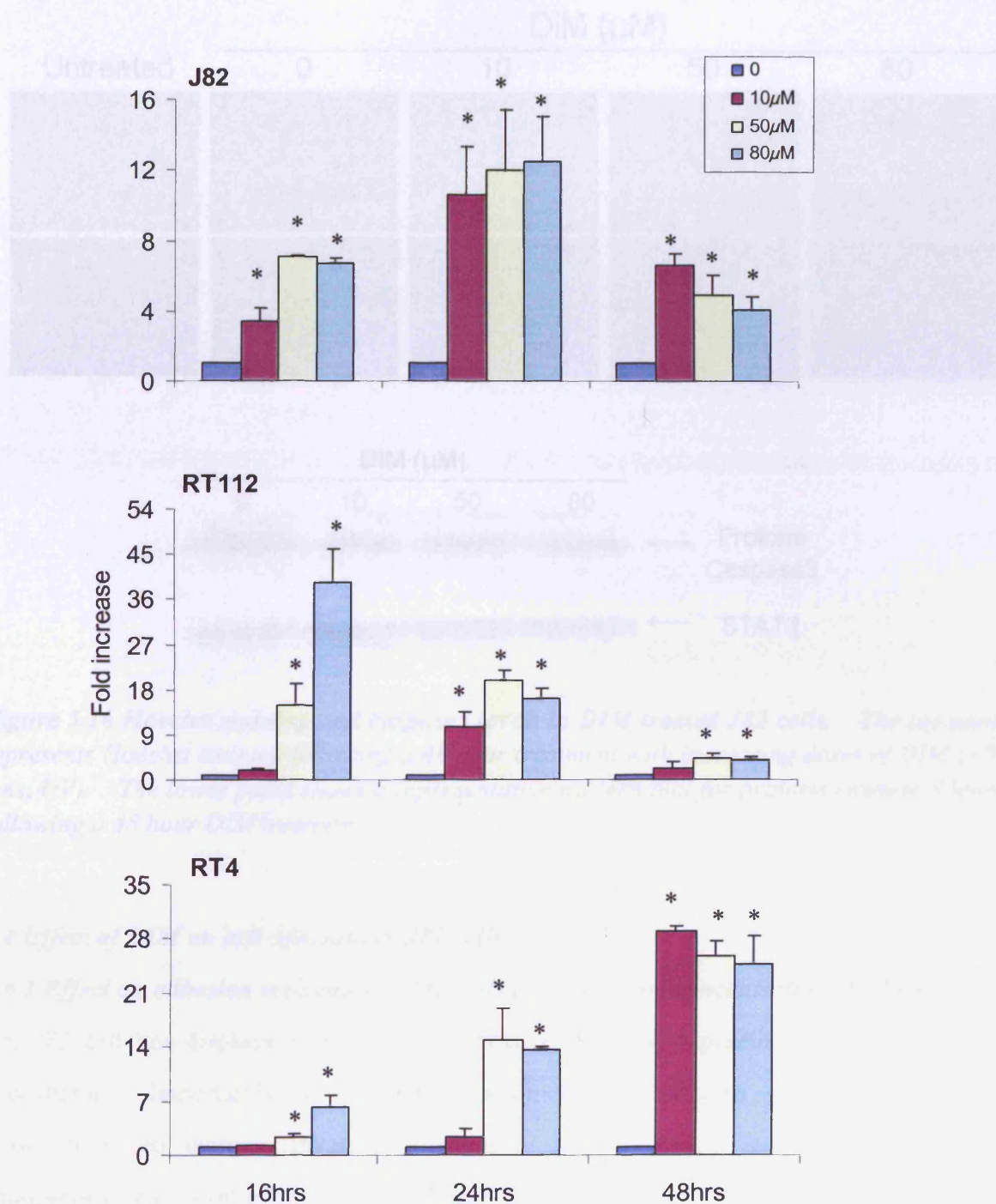


**Figure 5.15** Effect of DIM on caspase3/7 activity in J82, RT112 and RT4 cells. Cells were treated with DIM at 10, 50 or 80 $\mu$ M for 48 hours. Charts show levels of caspases3/7 activity, expressed as fold increase over DMSO control as determined by fluorescence measurement. \* denotes a significant difference from DMSO control ( $p < 0.05$ ,  $n = 3$ ,  $\pm SD$ ) using oneway ANOVA followed by Scheffe's significant difference post hoc test and Student's  $t$ -test.

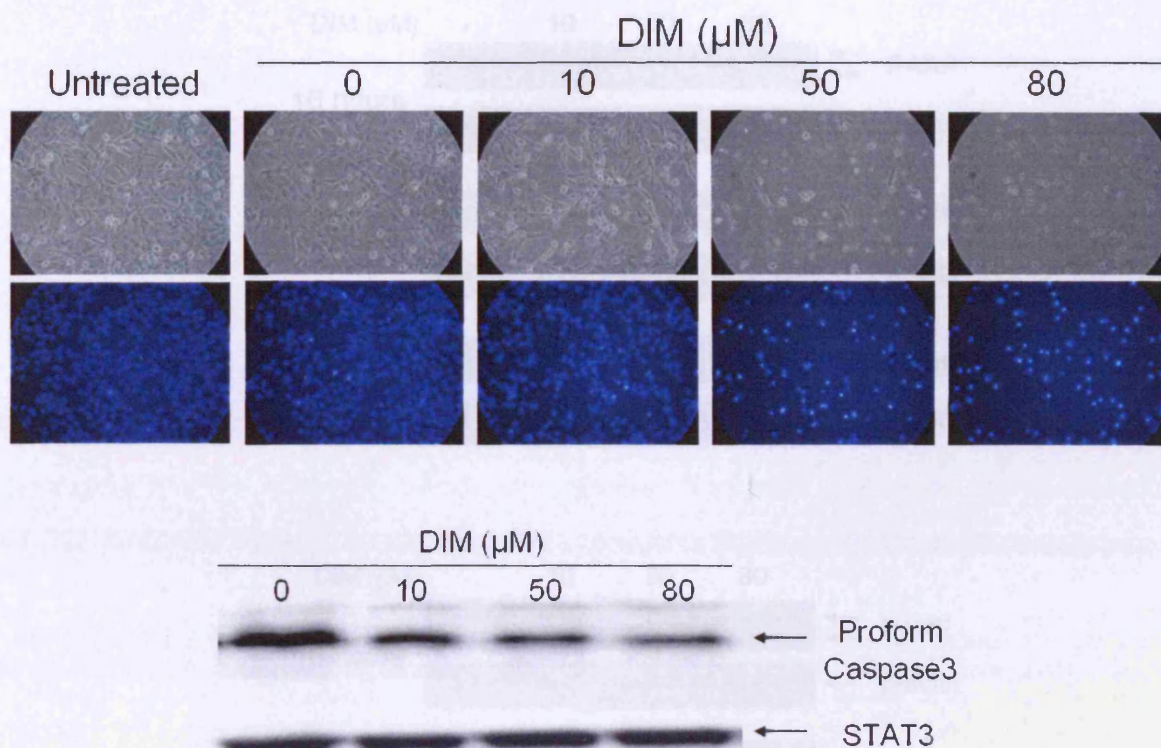


**Figure 5.16** Hoechst staining and caspase3 levels in DIM treated J82 cells. The top panel represents Hoechst staining following a 48 hour treatment with increasing doses of DIM ( $\times 20$  lens, UV). The lower panel shows a representative western blot for proform caspase 3 levels following a 48 hour DIM treatment.

#### 5.4 Effect of DIM on cell adhesion in J82 cells

##### 5.4.1 Effect on adhesion molecules in J82 cells following low concentration DIM treatment

The J82 cell line displays a high *in vitro* invasive capacity, expressing N-cadherin but no E-cadherin. Importantly, it has been shown that N-cadherin expression following transfection can increase invasive potential in human bladder cell lines which lack endogenous expression of N-cadherin (Rieger-Christ *et al.*, 2004). So, it was important to determine the effects of DIM upon cadherin/catenin system, in order to assess the potential for DIM to inhibit cell invasion.

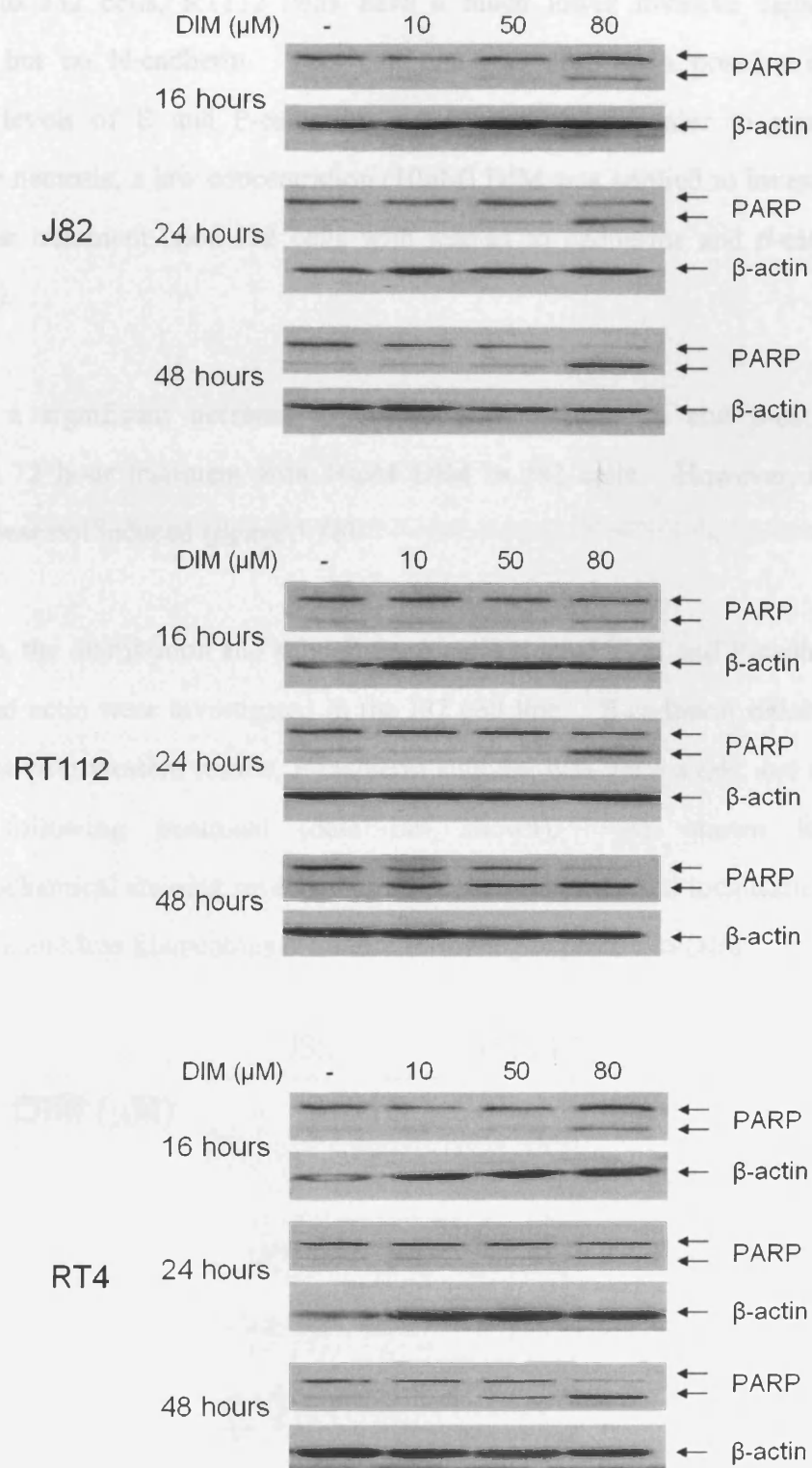


**Figure 5.17** Effect of DIM on PARP cleavage in J82, RT112 and RT4 cells. Representative western blots show the effect on PARP cleavage in three bladder lines following a DIM treatment up to 48 hours. Blots were performed on 2 separate occasions and also show actin protein-loading controls.

Compared to J82 cells, RT112 cells have a much lower invasive capacity, expressing E-cadherin but no N-cadherin. This cell line was used as a positive control to show expression levels of E and P-cadherin and  $\beta$ -catenin. In order to avoid induction of apoptosis or necrosis, a low concentration (10 $\mu$ M) DIM was applied to investigate the effects of a 72 hour treatment upon J82 cells with respect to cadherins and  $\beta$ -catenin expression (figure 5.18).

There was a significant decrease in N-Cadherin, P-Cadherin and  $\beta$ -catenin expression following a 72 hour treatment with 10 $\mu$ M DIM in J82 cells. However, re-expression of E-cadherin was not induced (figure 5.18).

Furthermore, the distribution and subcellular localisation of E, N and P-cadherins,  $\beta$ -catenin,  $\alpha$ -tubulin and actin were investigated in the J82 cell line. E-cadherin staining was negative in agreement with western results, P-cadherin staining was very weak, and actin showed no difference following treatment (data not shown). As shown in figure 5.19, immunocytochemical staining revealed some decrease and altered localisation of N-cadherin and  $\beta$ -catenin and less filamentous  $\alpha$ -tubulin following exposure to DIM.

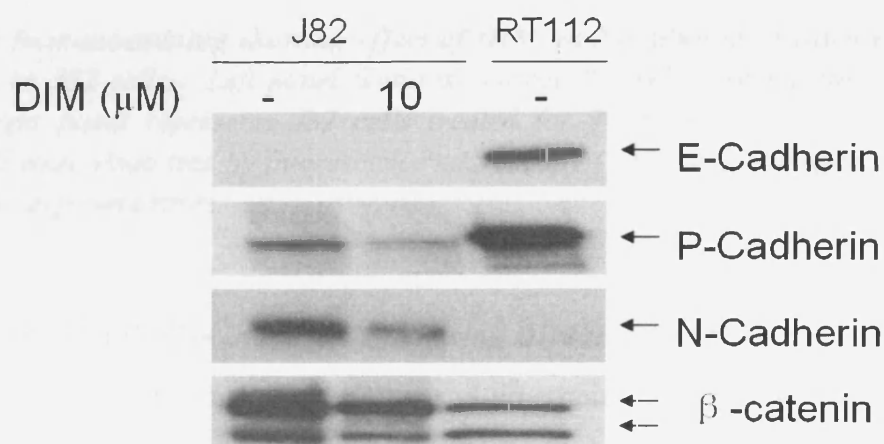


**Figure 5.18 Effect of DIM on cadherins and  $\beta$ -catenin levels in J82 cells.** J82 cells were treated with DIM at 10 $\mu$ M for 72 hours. RT112 was used as a positive control showing expression levels of E, P-cadherin and  $\beta$ -catenin and blots were performed on 2 separate occasions.

In order to determine whether cell adhesion to fibronectin and collagen I can be influenced following a short-term DIM treatment, assays were carried out in J82 cells, as shown in figure 5.20. As a 15 hour treatment was insufficient to increase cell adhesion to fibronectin in J82 cells (figure 5.13), in the adhesion assay, J82 cells were treated for 72 hours with DIM. As shown in figure 5.20, DIM-treated

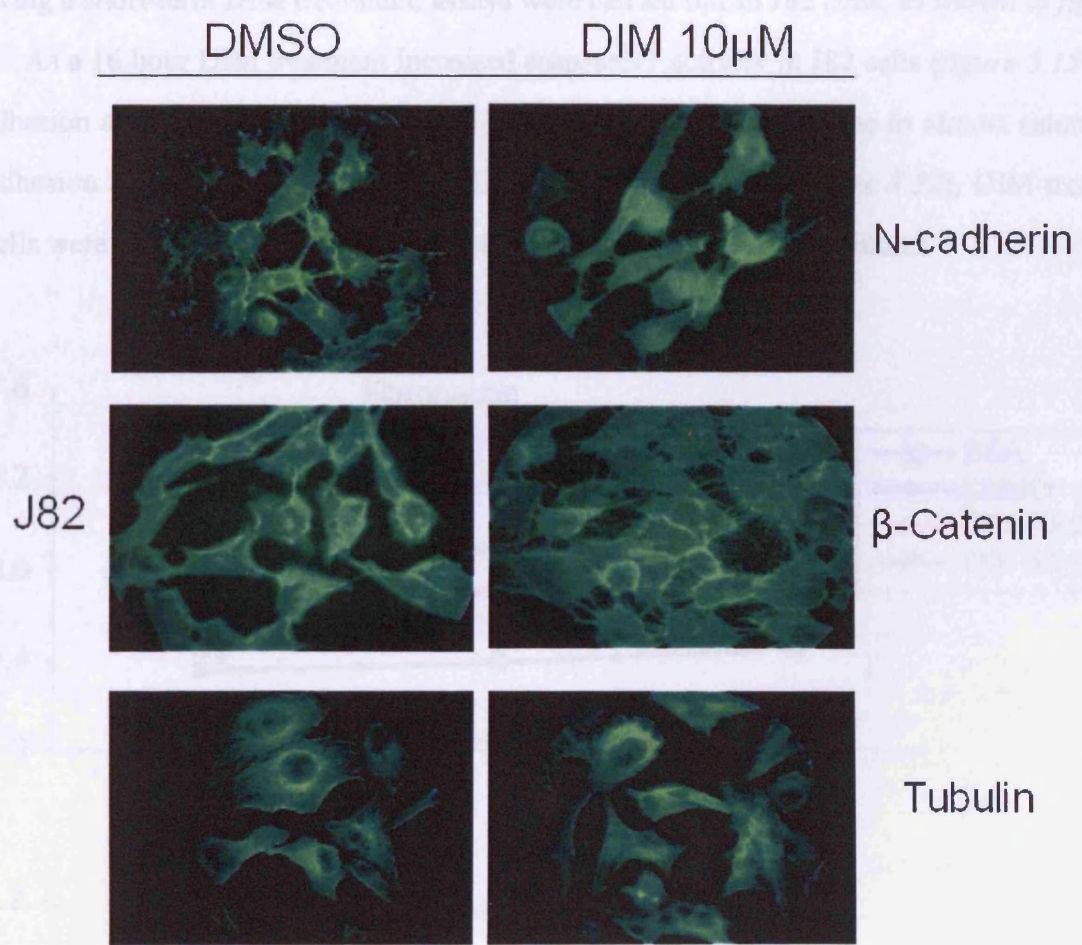


**Figure 5.19 Immunostaining showing effect of DIM on N-cadherin,  $\beta$ -catenin and tubulin distribution in J82 cells.** Left panel features control J82 cells, treated for 72 hours with DMSO. Right panel represents J82 cells treated for 72 hours with 10 $\mu$ M DIM. After staining, cell were visualised by fluorescence microscopy ( $\times 40$  lens). Images were captured with the same exposure times.

**5.4.2 Effect on cell adhesion in J82 cells following DIM treatment**

The appropriate concentrations of substrates and time points for adhesion assays have been established (refer to Chapter 4, figure 4.32), and the specificity of J82 cell adhesion to fibronectin and collagen I has been examined (refer to Chapter 4, figure 4.33).

In order to determine whether cell adhesion to fibronectin and collagen I can be influenced following a short-term DIM treatment, assays were carried out in J82 cells, as shown in *figure 5.20*. As a 16 hour DIM treatment increased caspase3/7 activity in J82 cells (*figure 5.15*), in the adhesion assay DIM treatment was no longer than 16 hours, and due to almost saturated cell adhesion to fibronectin (10 $\mu$ g/ml) at 120 minutes (*Chapter 4, figure 4.32*), DIM-treated J82 cells were allowed to attach to fibronectin-coated plates up to 120 minutes.

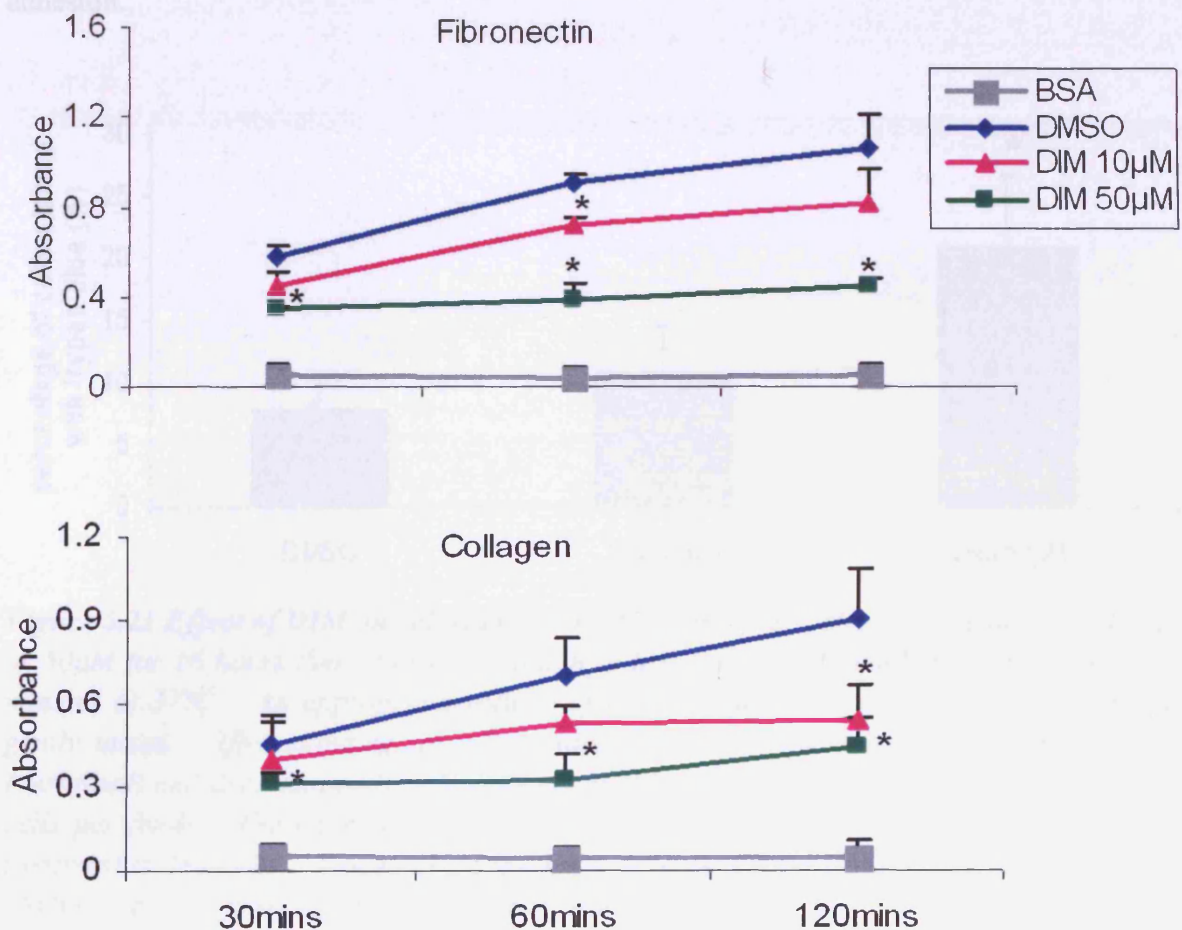


**Figure 5.20** Effect of DIM on J82 cell adhesion to fibronectin and collagen I. J82 cells were treated with DIM (10 or 50 $\mu$ M) for 16 hours then allowed to attach to fibronectin- (10 $\mu$ g/ml) or collagen I- (50 $\mu$ g/ml) coated surfaces for 30, 60 or 120 minutes at 37°C. Unattached cells were removed, and remaining cells were stained with crystal violet. Cell attachment was quantified by absorbance measured at 550nm. Each time point was done in triplicate and \* denotes a significant difference from DMSO control ( $p < 0.05$ ,  $n = 3$ ,  $\pm$ SD) using oneway ANOVA followed by Student's *t*-test.

There was a time-dependent inhibition of cell adhesion to fibronectin and collagen I following 10 $\mu$ M DIM treatment over 16 hours. Following 50 $\mu$ M, J82 cell adhesion to both ECM proteins was significantly slowed down in a time-dependent manner.

However, as a 10 $\mu$ M DIM treatment was sufficient to induce significant increase of caspase3/7 activity in J82 cells (figure 5.15), it was important to determine the percentage of viable cells following DIM treatment in order to rule out apoptosis as the cause of reduced adhesion.

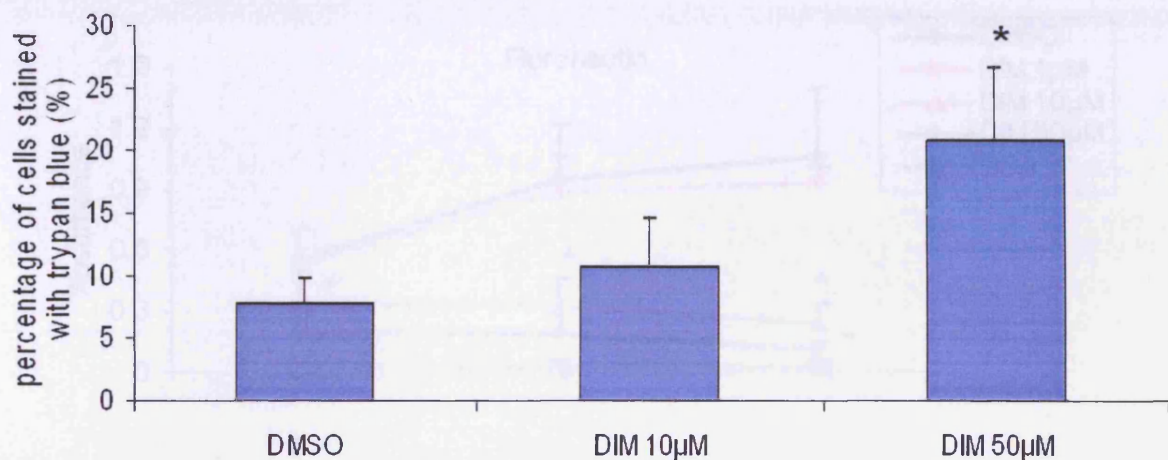


**Figure 5.21 Effect of DIM on cell viability in J82 cells.** J82 cells were treated with DIM 10 or 50 $\mu$ M for 16 hours then allowed to attach to fibronectin- (10 $\mu$ g/ml) coated plates for 120 minutes at 37°C. An appropriate volume of 0.4% Trypan blue was added into plates and gently mixed. After standing for 30 minutes at room temperature, the number of viable (unstained) and dead (stained) cells were counted in randomly chosen fields (minimum of 100 cells per field). The chart shows the percentage of dead cells following a 16 hour DIM treatment in J82 cells. \* denotes a significant difference from DMSO control ( $p < 0.05$ ,  $n = 5$ ,  $\pm$ SD) using an oneway ANOVA followed by Student's  $t$ -test.

Figure 5.21 shows the effect of a 16 hour DIM treatment upon J82 cells with respect to cell viability. There was no significant increase in the number of cells stained by trypan blue following a 10 $\mu$ M DIM treatment. However, a significant increase in the population of stained cells was observed at 50 $\mu$ M, suggesting that apoptosis may account, at least in part, for the decrease of cell adhesion shown in figure 5.20 at this concentration.

Possibilities were that DIM was binding to the substrate to block binding sites or to cell surface protein. To further investigate the effect on cell adhesion in response to DIM, J82 cells were seeded on to fibronectin or collagen I-coated plates in the continued presence of DIM. As shown in *figure 5.22*, at 1 $\mu$ M DIM did not affect cell-adhesion to either fibronectin or collagen I. There was, however, a significant and time-dependent inhibition of cell adhesion from 10 $\mu$ M DIM. Data so far suggest that the effect of DIM on cell adhesion may be due to the disruption of focal adhesion, either by binding to ECM proteins (fibronectin, collagen) or inactivating integrins.

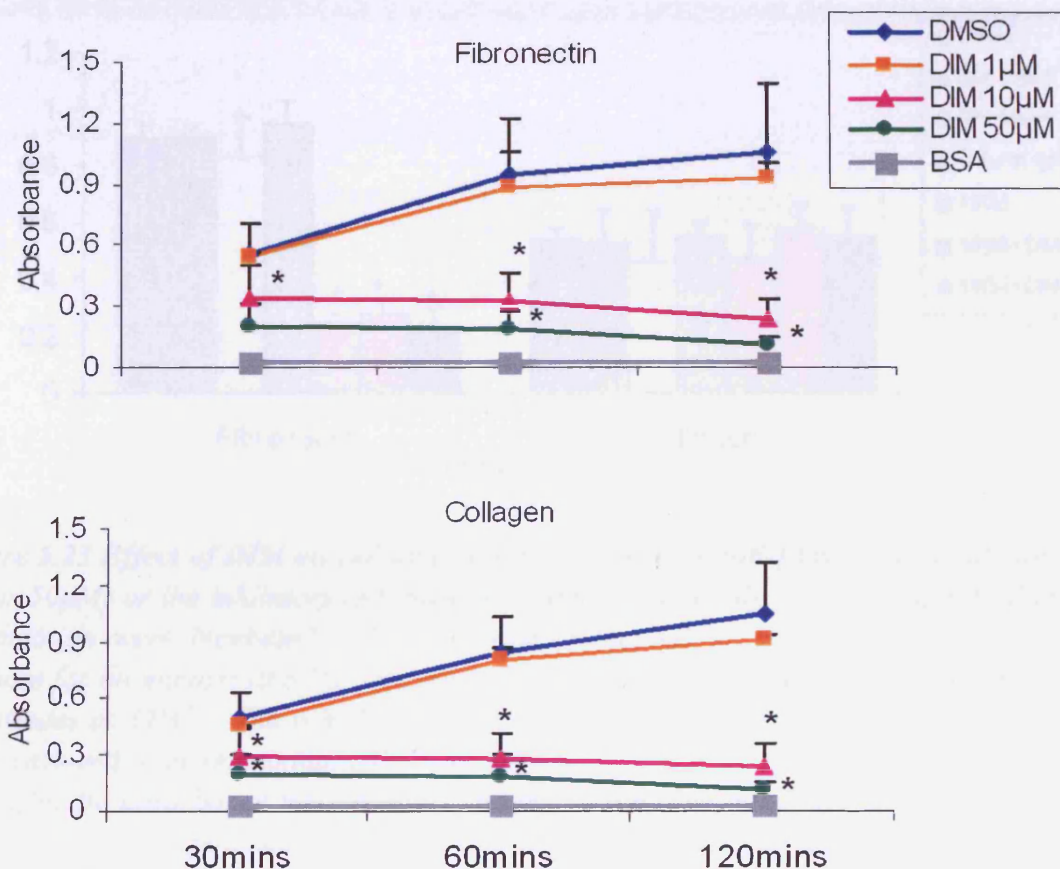


**Figure 5.22** Effect on cell adhesion to fibronectin and collagen I in the presence of DIM. J82 cells were plated in the presence of DIM (1, 10 or 50 $\mu$ M) onto fibronectin- (10 $\mu$ g/ml) or collagen I- (50 $\mu$ g/ml) coated surfaces for 30, 60 or 120 minutes at 37°C. Controls were incubated in the absence of any substrate (BSA). Unattached cells were removed, and remaining cells were stained with crystal violet. Cell attachment was quantified by absorbance measured at 550nm. Each time point was done in triplicate and \* denotes a significant difference from DMSO control ( $p < 0.05$ ,  $n = 4$ ,  $\pm$ SD) using oneway ANOVA followed by Student's *t*-test.

To address whether DIM exerts an effect on cell adhesion via binding to ECM proteins, an inhibitory anti-human fibronectin antibody, 16G3 was applied. The adhesion assays were carried out as described in 2.7.1, after DIM or 16G3 alone or in combination were pre-incubated on coated plates for 60 minutes at 37°C. *Figure 5.23* shows that DIM alone did not affect cell adhesion either to fibronectin or collagen I at either concentration. 16G3 alone or combined with DIM significantly decreased J82 cell adhesion on fibronectin but not collagen I. These results indicate that DIM does not bind to ECM proteins directly.

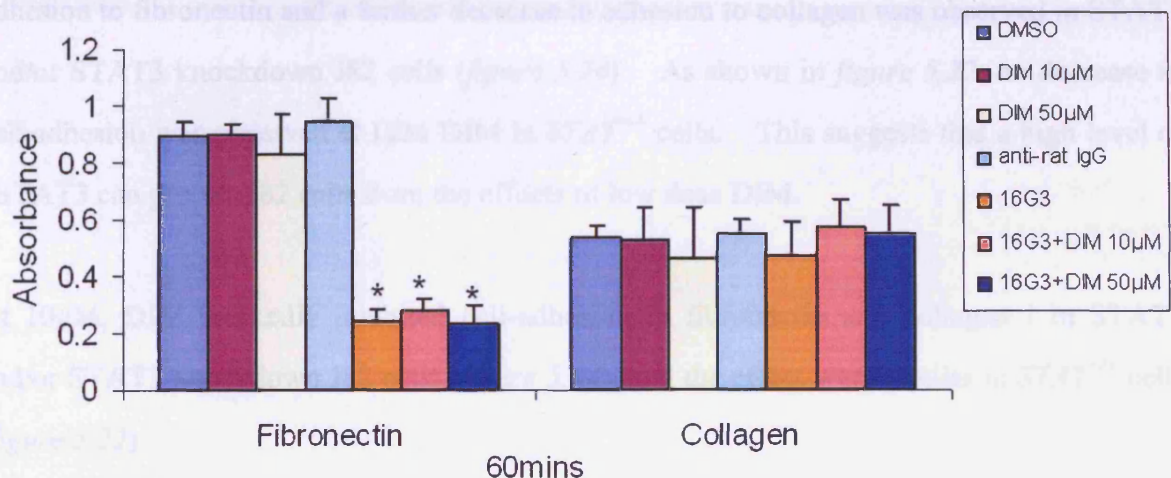


**Figure 5.23 Effect of DIM on cell adhesion in presence of anti-fibronectin antibody.** DIM (10 or 50µM) or the inhibitory anti-human fibronectin antibody (16G3, 20µg/ml) alone or in combination were incubated with fibronectin- (10µg/ml) or collagen I- (50µg/ml) coated surfaces for 60 minutes at 37°C before washing off. Then J82 cells were plated for another 60 minutes at 37°C. The vehicle for 16G3 was anti-rat IgG (10µg/ml). Unattached cells were removed, and remaining cells were stained with crystal violet. Cell attachment was quantified by absorbance measured at 550nm. Each time point was assessed in triplicate and \* denotes a significant difference from anti-rat IgG control ( $p < 0.05$ ,  $n = 3$ ,  $\pm SD$ ) using oneway ANOVA followed by Student's *t*-test.

#### ***5.4.3 Effect on cell adhesion in STAT1 and/or 3 knockdown J82 cells following DIM treatment***

As shown in *figure 4.34*, knockdown of STAT1 alone or STAT1 and 3 together results in a significant decrease in cell attachment to fibronectin or collagen, suggesting that STAT1 is important for J82 cell adhesion. Therefore, one of the essential questions to be addressed based upon the evidence presented so far, is whether DIM treatment in STAT1 or STAT3 knockdown J82 cells could further decrease cell-adhesion to the ECM proteins tested.

It appeared that a 1 $\mu$ M DIM treatment was responsible for a significant decrease in cell adhesion to fibronectin and a further decrease in adhesion to collagen was observed in STAT1 and/or STAT3 knockdown J82 cells (*figure 5.24*). As shown in *figure 5.22*, no decrease in cell adhesion was observed at 1 $\mu$ M DIM in *STAT<sup>+/+</sup>* cells. This suggests that a high level of pSTAT3 can protect J82 cells from the effects of low dose DIM.

At 10 $\mu$ M, DIM markedly inhibited cell-adhesion to fibronectin and collagen I in STAT1 and/or STAT3 knockdown J82 cells (*figure 5.24*), and the effect were similar in *STAT<sup>+/+</sup>* cells (*figure 5.22*).

Taken together, the data suggest that DIM may exert its inhibitory effect on cell adhesion, not only via STATs, but also via other molecules, such as cadherins and integrins. It possibly initiates the inhibition of adhesion through modulating STATs, and other pathways are involved to sustain or enhance this effect.

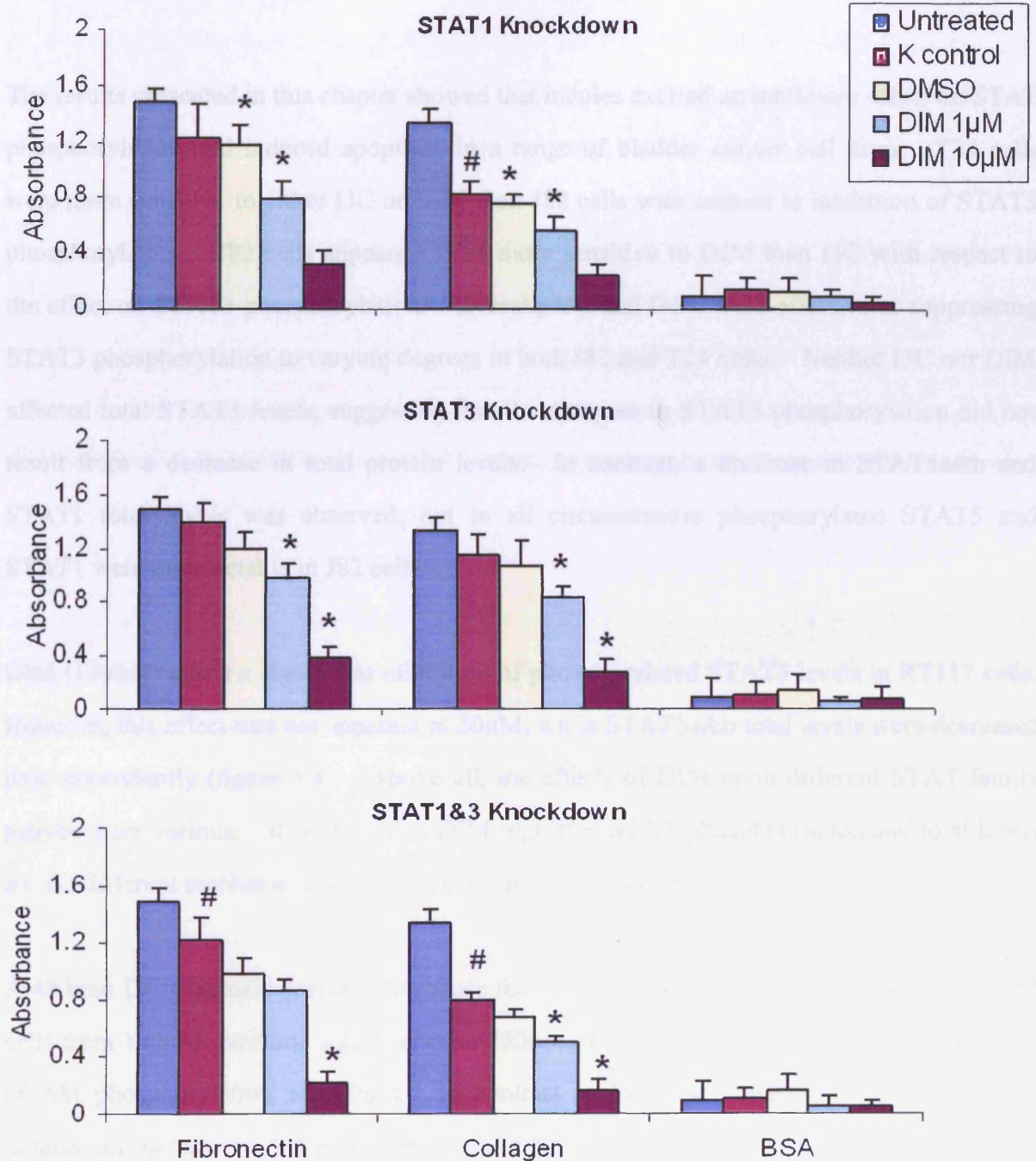


**Figure 5.24** Effect of DIM on cell adhesion in STAT1 and/or 3 knockdown J82 cells. STAT1 and/or 3 knockdown J82 cells were plated in the presence of DIM (1 or 10 µM) onto fibronectin- (10 µg/ml) or collagen I- (50 µg/ml) coated surfaces or in the absence of any substrate (BSA) for 60 mins at 37°C. Unattached cells were removed, and remaining cells were stained with crystal violet. Cell attachment was quantified by absorbance measured at 550nm. Each data point was done in triplicate. Untreated = J82 cells without transfection or DIM treatment; K control = J82 cells transfected with siRNA to STAT1 and/or STAT3. # denotes a significant difference from untreated cells, and \* denotes a significant difference from DMSO control ( $p < 0.05$ ,  $n = 4$ ,  $\pm SD$ ) using oneway ANOVA followed by Student's t-test.

## ***DISCUSSION***

The results presented in this chapter showed that indoles exerted an inhibitory effect on STAT phosphorylation and induced apoptosis in a range of bladder cancer cell lines. T24 cells were more sensitive to either I3C or DIM than J82 cells with respect to inhibition of STAT3 phosphorylation. J82 cells appeared to be more sensitive to DIM than I3C with respect to the effect on STAT3 phosphorylation. Overall, I3C and DIM were effective at suppressing STAT3 phosphorylation to varying degrees in both J82 and T24 cells. Neither I3C nor DIM affected total STAT3 levels, suggesting that the decrease in STAT3 phosphorylation did not result from a decrease in total protein levels. In contrast, a decrease in STAT5a&b and STAT1 total levels was observed, but in all circumstances phosphorylated STAT5 and STAT1 were undetectable in J82 cells.

DIM (10 $\mu$ M) caused a significant inhibition of phosphorylated STAT5 levels in RT112 cells. However, this effect was not apparent at 50 $\mu$ M, while STAT5a&b total levels were decreased dose dependently (*figure 5.4*). Above all, the effects of DIM upon different STAT family members are various. It is likely that DIM-regulated STAT phosphorylation and total levels are via different mechanisms which are unclear at the moment.

A 48 hour I3C treatment was able to reduce the levels of Akt phosphorylation (ser473) in J82 cells from 100 $\mu$ M, reaching significance at 250 $\mu$ M, but unable to sustain this downregulation of Akt phosphorylation at 500 $\mu$ M. In contrast to I3C, the condensation product, DIM induced an increase in Akt phosphorylation at 50 $\mu$ M, but this effect was reversed at 80 $\mu$ M. Following oral administration, I3C is rapidly absorbed and cleared from blood and tissues within an hour, while DIM peaks slightly later and is more persistent. After intake of I3C, both I3C and DIM are detectable in blood and multiple organs, and several studies have demonstrated distinct responses to I3C and DIM in animal models. Therefore, the *in vivo* activity of I3C can be attributed partially, but not completely, to the production of DIM (reviewed in Howells *et al.*, 2007). In breast carcinoma lines, I3C has an inconsistent effect upon both T47D and MCF7 cells, with a similar level of increased Akt phosphorylation (ser

473) at the higher concentration ( $\geq 500\mu\text{M}$ ). However, in MDA MB468 cells, a dose-dependent decrease in Akt phosphorylation (ser 473) was observed from  $100\mu\text{M}$  of I3C treatment (Howells 2003). Above all, data suggest that different doses of I3C and DIM may exert different effects on this pathway in bladder cancer cells.

From the data presented, the effects of either I3C or DIM upon Akt phosphorylation status are inconsistent, particularly at the higher concentrations. There is evidence in the literature to show that STAT3-induced overexpression of p53 and p50, the PI3K regulatory subunits can reduce the level of activated Akt (Abell K *et al.*, 2005). This suggested the possibility that to some extent DIM-modulated Akt phosphorylation could be mediated by the link between STAT3 and PI3K regulatory subunits in J82 cells.

I3C has previously been observed to have a stimulatory effect upon ERK phosphorylation in human breast cell lines (Howells, 2003), but in this study, there was no obvious change in phosphorylated ERK levels in J82 cells following treatment with any concentration of I3C. However, DIM induced a significant increase in ERK phosphorylation which was observed from  $50\mu\text{M}$ , suggesting that high concentrations of DIM may exert a stimulatory effect on this pathway in J82 cells.

A study by Okabe *et al.*, (2006) showed the phosphorylation of cyclin D1 at Thr286 was mediated by the activity of MAPK cascade, and cyclin D1 underwent increased degradation once its phosphorylation was enhanced. The effects of DIM upon cyclin D1 were investigated, in order to provide an insight as to how DIM may be inducing cell cycle arrest in the J82 cells. *Figure 5.9* shows an obvious decrease in cyclin D1 levels in response to  $50\mu\text{M}$  DIM at 24 hours in both J82 and RT112 cells. Consistently, DIM-induced downregulation of cyclin D1 levels has been observed in human breast cancer cells (Vanderlaag *et al.*, 2006) and prostate cancer cells (Garikapaty *et al.*, 2006). Treatment with  $50\mu\text{M}$  DIM results in activation of ERK phosphorylation from 18 hours (data not shown), so it may indicate that reduction of cyclin D1 expression is due to sustained activation of ERK.

Both I3C (Brandi *et al.*, 2003, Chinni *et al.*, 2001) and DIM (Hong *et al.*, 2002, Garikapaty *et al.*, 2006) have been previously shown to cause G<sub>1</sub> cell cycle arrest. In this study, there was an increase in the percentage of J82 cells in the G<sub>2</sub>/M phase and an increase of RT112 cells in the G<sub>0</sub>/G<sub>1</sub> phase at 50µM DIM at 24 hours (*table 5.1*). However, in J82 cells (*figure 5.8*) this effect switched to G<sub>0</sub>/G<sub>1</sub> phase with a 48 hour DIM treatment, indicating that at earlier time point, DIM slows down cell cycle via accumulation in G<sub>2</sub>/M phase then causes G<sub>1</sub> arrest at longer treatment. It is interesting to note that Tyagi *et al.*, (2004) found G<sub>2</sub>-M arrest was associated with the modulation in CDKI-CDK-cyclin cascade by silibinin (a natural flavonoid from milk thistle) in human bladder carcinoma cells. In this study, a decrease in cyclin D1 levels in response to DIM was observed in both cell lines, suggesting that DIM-induced G<sub>2</sub>/M arrest in J82 cells may be correlated with the downregulation of cyclin D1 expression.

In addition, *figure 5.9* shows that survivin expression was markedly downregulated by 50µM DIM with a 24 hour treatment in both cell lines. Consistently, a study by Takada *et al.*, (2005) showed that I3C causes downregulation of survivin in myeloid and leukaemia cells. It has also been shown that survivin expression is associated with cell cycle progression, including the acceleration of S phase and resistance to G<sub>1</sub> arrest (Suzuki *et al.*, 2000). It appears that the decrease of survivin expression possibly leads to the reduction in S phase and G<sub>0</sub>/G<sub>1</sub> phase arrest in both cell lines in response to DIM.

Data presented so far indicate that the modulation of cell cycle arrest by DIM may be due to the reduction of survivin expression which initiates cell cycle entry, or the decrease of cyclin D1 levels which is required for cell cycle progression.

In both cell lines, a reduction of cells in the S phase was observed in response to 50µM DIM at 24 hours or longer treatment, possibly indicating an inhibition of cell growth. The appearance of a sub G<sub>1</sub> peak with increasing DIM in both cell lines may be indicative of the occurrence of apoptosis which is in agreement with annexin V staining in J82 and RT112 cells showing a significant increase in apoptotic cells following a 48 hour DIM treatment (*figure 5.10 and 5.12*).

In contrast to J82 and RT112 cells, the apoptosis and necrosis in RT4 cells induced by DIM could not be measured properly via annexin V and PI staining (*figure 5.14*). However, RT4 cells were found to readily detach from flasks, to round up and float in medium following a 48 hour DIM treatment, suggesting that they may undergo apoptosis. This observation was confirmed by the assessment of caspase 3/7 activity and PARP cleavage. There was a time- and dose- dependent increase of caspase 3/7 activity with DIM treatment, and PARP cleavage was detected following a treatment up to 48 hours, providing evidence of induction of apoptosis in RT4 cells. A significant increase in caspase 3/7 activity and PARP cleavage was also observed in J82 and RT112 cells. Since RT4 was previously found to be the most resistant line to radiotherapy among several human bladder cell lines, including J82 and RT112 (Moneef *et al.*, 2003), it is encouraging that DIM could induce apoptosis in a panel of bladder cancer cells with different sensitivity to radiotherapy or chemotherapy, thus suggesting a novel potential agent for chemoprevention or an adjunct to chemo- or radiotherapy in bladder tumours.

J82 cells are E-cadherin<sup>-ve</sup> and N-cadherin<sup>+ve</sup>, whereas RT112 cells are E-cadherin<sup>+ve</sup> and N-cadherin<sup>-ve</sup>. In addition, J82 cells express more  $\beta$ -catenin compared with RT112 line (*table 5.2*). There is evidence to suggest that the high invasive capacity of J82 cell line is due to expression of N-cadherin (Rieger-Christ *et al.*, 2004) and enhanced  $\beta$ -catenin levels are correlated with increased tumorigenesis (Peifer 1997).

**Table 5.2 J82 and RT112 cell lines expressing different cadherin/catenin profiles**

	J82	RT112
<b>E-Cadherin</b>	-	+
<b>N-Cadherin</b>	+	-
<b>P-Cadherin</b>	+	++
<b><math>\beta</math>-Catenin</b>	++	+

There was a significant decrease (assessed by western blotting) in N-cadherin, P-cadherin and  $\beta$ -catenin expression following a 72 hour treatment with 10 $\mu$ M DIM in J82 cells (*figure 5.18*) and some decrease in N-cadherin and  $\beta$ -catenin by immuno-staining was also observed. In

J82 cells re-expression of E-cadherin was not induced by DIM, possibly due to the continued existence of E-cadherin repressors, such as Snail (Ohkubo and Ozawa, 2004), Slug (Bolos *et al.*, 2003), Zeb1 (Aigner *et al.*, 2007) or Sip1 (Vandewalle *et al.*, 2005), the methylation or the deletion of E-cadherin. Such modulation of cadherin/catenin system suggested that DIM may have an inhibitory effect on cell invasion.

This was further investigated using adhesion assays with fibronectin and collagen, two possible extracellular protein substrates. The specificity of binding of J82 cells to fibronectin or collagen was assessed by applying inhibitory antibody to  $\beta_1$ -integrin (*figure 4.33*). *Figure 5.20* shows a significant inhibition in cell adhesion to fibronectin and collagen I with 50 $\mu$ M DIM treatment over 16 hours. However, this effect was mainly due to an increased number of cells undergoing apoptosis or necrosis (*figure 5.21*).

In order to avoid the influence of cell death, the effect on cell adhesion by low dose DIM was investigated with shorter treatment. As shown in *figure 5.22*, in presence of DIM, a significant and time-dependent inhibition of cell adhesion to fibronectin and collagen I was observed from 10 $\mu$ M DIM. This suggested that the effect of DIM on suppression of cell adhesion may be due to its binding to fibronectin or collagen, or inactivation of integrins.

An inhibitory antibody to fibronectin (16G3) was applied in order to address whether the inhibitory effect of DIM on cell adhesion occurred via its binding to ECM proteins. *Figure 5.23* shows that in the absence of 16G3, DIM treatment of the substrate has no effect on cell adhesion, however, 16G3 significantly inhibited J82 cell adhesion to fibronectin, but not collagen I, in either the absence or the presence of DIM. This suggested that DIM was not binding directly ECM proteins.

As shown in *Chapter 4 (figure 4.34)*, there was a significant decrease of cell adhesion on fibronectin and collagen I in STAT1 knockdown J82 cells, indicating that STAT1 plays an important role in J82 cell adhesion. Data also showed an inhibitory effect of DIM on J82

cell adhesion, therefore it is important to further investigate whether this effect is altered by prior inhibition of STAT signalling pathway.

Treatment of normal J82 cells with 1  $\mu$ M DIM produced no effect on cell adhesion to either fibronectin or collagen (*figure 5.22*). However, at this concentration a significant additional decrease in cell adhesion to both ECM proteins was observed in either STAT1 or STAT3 knockdown J82 cells (*figure 5.24*). This suggests that the inhibitory effect of DIM on cell adhesion may involve the STAT pathway.

Compared with *STAT<sup>+/+</sup>* cells, it appeared that 10  $\mu$ M DIM can not induce further decrease of cell adhesion in STAT knockdown cells (*figure 5.24*). It leads to hypothesis that DIM may exert its inhibitory effect on cell adhesion not only via STATs but also via other molecules, such as cadherins and integrins. It possibly initiates the inhibition of adhesion through STATs, and other pathways are then involved to sustain or enhance this effect.

In a study by Rieger-Christ KM *et al.*, (2007) in invasive bladder carcinoma cells, reduction of N-cadherin expression was observed in a dose-dependent manner with concomitant inhibition of cell migration, in response to EGCG (the major phytochemical in green tea). In this study, DIM decreased N-cadherin, P-cadherin and  $\beta$ -catenin expression in J82 cells, suggesting that the inhibition of J82 cell-adhesion and migration by DIM may be partly via downregulation of these proteins.

Overall, DIM appears to be a promising agent with respect to inhibition of constitutive STAT signalling and its ability to cause cell cycle arrest, induce apoptosis and suppress cell adhesion, at least partly via STAT signalling pathway. However, it is still not clear that the STAT pathway is involved in DIM-induced cell cycle arrest and apoptosis, which will be investigated in the future work.

## **CHAPTER 6**

### **GENERAL DISCUSSION**

Overactive STATs have been reported in various human tumours, but data are lacking for bladder cancer. Thus the present study was designed to test the hypothesis that STATs are activated in human bladder tumours and their inhibition might be of benefit in treatment or prevention. The immunohistochemistry results obtained in tumour tissues strongly support this contention – STATs phosphorylation was observed in bladder tumours, but was essentially absent in normal epithelium. Increased STATs expression and activation suggested as an invasion-associated phenomenon, since phosphorylated STATs occurred in more than half of muscle invasive samples in cytoplasm or nuclei, whereas only 33% (3/9) of superficial tumours showed phosphorylated STAT3 which was confined to the cytoplasm.

As expected, STATs expression and phosphorylation was also observed in a range of human bladder cancer cell lines. STAT5 in epithelial lines (E-cadherin<sup>+</sup>) and STAT3 in mesenchymal lines were constitutively phosphorylated. This led to the hypothesis that phosphorylated STAT3 may be associated with high invasive capacity. In A431 cells following DOX-inducible expression of wide-type SIP1 (a repressor of E-cadherin expression), classic EMT (from a proliferative to an invasive type of cell behaviour) was induced, accompanied by downregulated E-cadherin and upregulated N-cadherin (Mejlvang *et al.*, 2007). In this model, expression of SIP1 (A431/Sip<sup>+</sup>) promoted STAT3 activation and decreased phosphorylated STAT5, providing further support for a role for active STAT3 in invasiveness of cancer cells. Consistently, significant inhibition of cell migration in STAT3-deficient J82 cells was observed. In addition, Debidda *et al.*, (2005) have reported that in STAT3 null MEFs (Mouse embryonic fibroblasts), STAT3 represents an essential effector pathway of Rho GTPases in regulating cell migration.

Besides switching of cadherin expression in A431/Sip<sup>+</sup> cells, SIP1 was reported to inhibit cell-cell adhesion and activate cell adhesion to collagen and fibronectin via increased formation of focal adhesions (Mejlvang *et al.*, 2007). Also, it has been shown that STAT1 activation was associated with FAK during cell adhesion (Xie *et al.*, 2001) and the deficiency of STAT3 caused loss of collagen production (Lim *et al.*, 2006), providing some explanation for data presented in this study that knockdown of STAT1, alone or in the combination with STAT3, significantly inhibited cell-matrix adhesion, possibly due to suppressed formation of focal adhesions or degradation/inactivation of matrix proteins.

In J82 cells, PP2 (src inhibitor) treatment appeared to promote cell-cell adhesions allowing cells to form large clusters. Nam *et al.*, (2002) have shown enhanced E-cadherin/catenin expression and suppressed metastasis in PP2-treated cancer cells. Consistently, upon src expression/activation, E-cadherin was actively degraded which facilitated the dissolution of adherens junctions (Palacios *et al.*, 2005). In melanoma cells, it has been found that expression of dominant-negative src prevented N-cadherin phosphorylation which was involved during cell transmigration (Qi *et al.*, 2006). Src is known to contribute to STATs phosphorylation: for example, src kinase activates IL-3-mediated STAT3 phosphorylation in myeloid cells (Chaturvedi *et al.*, 1998) and is also involved in IFN $\alpha$ -induced serine phosphorylation of STAT1 and STAT3 (Su and David 2000). A study by Sachsenmaier *et al.*, (1999) found that STAT activation by PDGF receptors does not require src tyrosine kinase activation. Similar to the observation in squamous carcinoma cells (Quadros *et al.*, 2004), src inhibitor (PP2) had only negligible effect on growth factor-independent STAT3 or STAT5 phosphorylation in bladder cancer cells tested, demonstrating that the kinase responsible for STAT3 (Tyr705) or STAT5 (Tyr694) phosphorylation may be not a src-like kinase and suggesting that STATs may not be involved in src-regulated expression of cadherins, leading to the mediation of cell-cell adhesions. By contrast, treatment with JAK2 inhibitor AG490 significantly reduced pSTAT3 (Tyr705) in J82 cells and pSTAT5 (Tyr694) in RT112 cells, although from data presented, its effect was transient and reversible. This suggests that JAK2 may act synergistically with other kinases, such as JAK1 to maintain this constitutive STAT phosphorylation. Identification of the kinase principally responsible for STAT phosphorylation in bladder cancer cells awaits future studies.

In J82 cells, knockdown of STAT1, STAT3 or STAT5 individually did not affect the overall transcriptional activity of STATs as assessed by reporter gene, which might be explained by the potential compensatory effects among different STAT family members. However, knockdown of STAT1, STAT3 and STAT5 together still only reduced STATs transactivation level by less than 40%, suggesting that either STATs possess low transcriptional activity in bladder cancer cells or STATs knockdown activates other pathways which can promote transcriptional activity of STATs. Bild *et al.*, (2002) and Quadros *et al.*, (2004) have demonstrated that STAT3 phosphorylation on both Tyr705 and Ser727 is insufficient to induce STAT3 DNA binding, and complexes with activated EGFR are a necessary prerequisite for nuclear import, DNA binding and transcriptional activity. In five bladder lines tested, EGF receptors were expressed in a reasonable level, but were not phosphorylated under normal

growth conditions which might be responsible for at least in part on the transactivation level of STATs, and suggesting that a complex between activated EGFR and phosphorylated STATs might also be crucial for STATs transactivation in bladder cancer cells.

Current therapies for bladder cancer are not satisfactory, and Moneef *et al.*, (2003) have shown that several bladder cancer cell lines are resistant to radiotherapy. Thus, chemoprevention, using natural or synthetic chemicals to reverse the onset, suppress or prevent the development of the carcinogenesis process (Gescher *et al.*, 1998) becomes a novel approach to cancer therapy. Indoles have been well-documented as chemopreventive agents, and several studies have demonstrated that STAT signalling is targeted by various dietary agents.

This was the first study to investigate the potential for indoles as effective agents in the chemoprevention of bladder cancer, by inhibiting the STAT pathway in bladder cells. It was interesting to observe that either I3C or its acid condensation product DIM significantly inhibited constitutive STAT3 activation in J82 and T24 cells. Also, in RT112 cells, STAT5 (a and b) expression and activity were significantly suppressed following DIM treatment, although the alteration in STAT5 phosphorylation was inconsistent. Further investigation showed that DIM induced a significant increase in caspase3/7 activity and PARP cleavage in three bladder lines (RT4, RT112 and J82) with different resistance to radiotherapy. FACS analysis indicated increased apoptosis and necrosis in J82 and RT112 cells in response to either I3C or DIM, providing further evidence that indoles induce apoptosis in bladder cancer cells of differing phenotype.

DIM have been previously shown to cause G<sub>1</sub> cell cycle arrest (Hong *et al.*, 2002, Garikapaty *et al.*, 2006). In the present study, an increase in the percentage of J82 cells in G<sub>0</sub>/G<sub>1</sub> phase was observed in response to a 48 hour DIM treatment, although an accumulation of cells in G<sub>2</sub>/M phase was induced at earlier time points. DIM also caused transient G<sub>0</sub>/G<sub>1</sub> phase arrest at 24 hour in RT112 cells.

It was rather unexpected that phosphorylated ERK was upregulated while the total ERK level was decreased in J82 cells following DIM treatment. It was also surprising that no significant alteration in total or phosphorylated Akt levels was observed in response to either I3C or DIM treatment, as both have been found to downregulate Akt and MAPK pathways in several

human cancers (Li *et al.*, 2003; Rahman and Sarkar, 2005). This may suggest that Akt and ERK do not contribute to indole-induced apoptosis in bladder cancer.

Another rather unexpected result of this study was that knockdown of STAT1, 3 or 5 did not alter the expression of cell cycle or apoptosis-related proteins, such as cyclin D1, survivin or pro-caspase3. However, DIM treatment of J82 and RT112 cells inhibited cyclin D1 and survivin expression significantly. This suggested that inhibition of STAT is not sufficient for DIM-induced cell cycle arrest and apoptosis. Although AG490 caused G<sub>0</sub>/G<sub>1</sub> arrest in J82 cells and S phase arrest in RT112 cells, it showed inconsistent inhibitory effects on STAT3 or STAT5 phosphorylation, also indicating that STATs are not crucial for cell cycle process.

Interestingly, at 1 $\mu$ M, DIM had no effect on cell-matrix adhesion to fibronectin and collagen. However, following knockdown of STAT1 and/or STAT3, 1 $\mu$ M DIM was observed to significantly further suppress J82 cell adhesion to fibronectin and collagen, suggesting the involvement of STAT in cell-matrix adhesion. In addition, a low concentration of DIM (10 $\mu$ M) suppressed N- and P-cadherin and  $\beta$ -catenin expression. In agreement with a recent study on EGCG (Rieger-Christ KM *et al.*, 2007), this suggested that cadherins may contribute to cell adhesion in bladder cancer, together with STATs activity.

Here, STATs have been shown to be potential target for indoles, possibly contributing to their inhibitory effect on cell adhesion and migration. Indoles also induce pro-apoptotic effects in a range of bladder cancer cells, again suggesting a positive role for their chemopreventive effects in human bladder cancer. Chemopreventive agents should have minimal toxicity to normal cells which is not always the case with current aggressive chemotherapy or radiotherapy treatment, so a normal urothelial line would ideally be included in future work to check for lack of unwanted toxicity.

This investigation into the STATs status *in vivo* and *in vitro* has provided an indication that active STATs may be a potential marker of invasiveness in human bladder cancer, and effects of indoles at a molecular level has given an insight as to how these dietary agents may be useful in the therapy and/or prevention of bladder tumours. Studies are continuing to further investigate how STATs fulfil a role in cell adhesion and migration, and how their inactivation contributes to the indole-mediated inhibition of cell-matrix adhesion in bladder cancer cells.

## **REFERENCES**

**Abdelrahim, M., Newman, K., Vanderlaag, K., Samudio, I. and Safe, S. (2006).** 3,3'-diindolylmethane (DIM) and its derivatives induce apoptosis in pancreatic cancer cells through endoplasmic reticulum stress-dependent upregulation of DR5. *Carcinogenesis* **27**, 717-728.

**Abell, K., Bilancio, A., Clarkson, R. W., Tiffen, P. G., Altaparmakov, A. I., Burdon, T. G., Asano, T., Vanhaesebroeck, B. and Watson, C. J. (2005).** Stat3-induced apoptosis requires a molecular switch in PI(3)K subunit composition. *Nat. Cell Biol.* **7**, 392-398.

**Aggarwal, B. B. and Shishodia, S. (2006).** Molecular targets of dietary agents for prevention and therapy of cancer. *Biochem. Pharmacol.* **71**, 1397-1421.

**Agrawal, R. C. and Kumar, S. (1999).** Prevention of chromosomal aberration in mouse bone marrow by indole-3-carbinol. *Toxicol. Lett.* **106**, 137-141.

**Aigner, K., Dampier, B., Descovich, L., Mikula, M., Sultan, A., Schreiber, M., Mikulits, W., Brabletz, T., Strand, D., Obrist, P. et al. (2007).** The transcription factor ZEB1 (deltaEF1) promotes tumour cell dedifferentiation by repressing master regulators of epithelial polarity. *Oncogene*. [Epub ahead of print]

**Akiyama, S. K., Yamada, S. S., Chen, W. T. and Yamada, K. M. (1989).** Analysis of fibronectin receptor function with monoclonal antibodies: Roles in cell adhesion, migration, matrix assembly, and cytoskeletal organization. *J. Cell Biol.* **109**, 863-875.

**Alexander, N. R., Tran, N. L., Rekapally, H., Summers, C. E., Glackin, C. and Heimark, R. L. (2006).** N-cadherin gene expression in prostate carcinoma is modulated by integrin-dependent nuclear translocation of Twist1. *Cancer Res.* **66**, 3365-3369.

**Anderton, M. J., Manson, M. M., Verschoyle, R., Gescher, A., Steward, W. P., Williams, M. L. and Mager, D. E. (2004a).** Physiological modeling of formulated and crystalline 3,3'-diindolylmethane pharmacokinetics following oral administration in mice. *Drug Metab. Dispos.* **32**, 632-638.

**Anderton, M. J., Manson, M. M., Verschoyle, R. D., Gescher, A., Lamb, J. H., Farmer, P. B., Steward, W. P. and Williams, M. L. (2004b).** Pharmacokinetics and tissue disposition of indole-3-carbinol and its acid condensation products after oral administration to mice. *Clin. Cancer Res.* **10**, 5233-5241.

**Aoki, Y., Feldman, G. M. and Tosato, G. (2003).** Inhibition of STAT3 signaling induces apoptosis and decreases survivin expression in primary effusion lymphoma. *Blood* **101**, 1535-1542.

**Arany, I., Chen, S. H., Megyesi, J. K., Adler-Storthz, K., Chen, Z., Rajaraman, S., Ember, I. A., Tying, S. K. and Brysk, M. M. (2003).** Differentiation-dependent expression of signal transducers and activators of transcription (STATs) might modify responses to growth factors in the cancers of the head and neck. *Cancer Lett.* **199**, 83-89.

**Arif, J. M., Gairola, C. G., Kelloff, G. J., Lubet, R. A. and Gupta, R. C. (2000).** Inhibition of cigarette smoke-related DNA adducts in rat tissues by indole-3-carbinol. *Mutat. Res.* **452**, 11-18.

**Avizienyte, E. and Frame, M. C. (2005).** Src and FAK signalling controls adhesion fate and the epithelial-to-mesenchymal transition. *Curr. Opin. Cell Biol.* **17**, 542-547.

**Bakkar, A. A., Wallerand, H., Radvanyi, F., Lahaye, J. B., Pissard, S., Lecerf, L., Kouyoumdjian, J. C., Abbou, C. C., Paireon, J. C., Jaurand, M. C. et al. (2003).** FGFR3 and TP53 gene mutations define two distinct pathways in urothelial cell carcinoma of the bladder. *Cancer Res.* **63**, 8108-8112.

**Baselga, J. (2000a).** Current and planned clinical trials with trastuzumab (herceptin). *Semin. Oncol.* **27**, 27-32.

**Baselga, J. (2000b).** New therapeutic agents targeting the epidermal growth factor receptor. *J. Clin. Oncol.* **18**, 54S-9S.

**Baselga, J. and Averbuch, S. D. (2000).** ZD1839 ('iressa') as an anticancer agent. *Drugs* **60 Suppl 1**, 33-40; discussion 41-2.

**Battle, T. E. and Frank, D. A. (2002).** The role of STATs in apoptosis. *Curr. Mol. Med.* **2**, 381-392.

**Beadling, C., Ng, J., Babbage, J. W. and Cantrell, D. A. (1996).** Interleukin-2 activation of STAT5 requires the convergent action of tyrosine kinases and a serine/threonine kinase pathway distinct from the Raf1/ERK2 MAP kinase pathway. *EMBO J.* **15**, 1902-1913.

**Betz, A., Lampen, N., Martinek, S., Young, M. W. and Darnell, J. E., Jr. (2001).** A *Drosophila* PIAS homologue negatively regulates *stat92E*. *Proc. Natl. Acad. Sci. U. S. A.* **98**, 9563-9568.

**Bharti, A. C., Donato, N. and Aggarwal, B. B. (2003).** Curcumin (diferuloylmethane) inhibits constitutive and IL-6-inducible STAT3 phosphorylation in human multiple myeloma cells. *J. Immunol.* **171**, 3863-3871.

**Bhuiyan, M. M., Li, Y., Banerjee, S., Ahmed, F., Wang, Z., Ali, S. and Sarkar, F. H. (2006).** Down-regulation of androgen receptor by 3,3'-diindolylmethane contributes to inhibition of cell proliferation and induction of apoptosis in both hormone-sensitive LNCaP and insensitive C4-2B prostate cancer cells. *Cancer Res.* **66**, 10064-10072.

**Bild, A. H., Turkson, J. and Jove, R. (2002).** Cytoplasmic transport of Stat3 by receptor-mediated endocytosis. *EMBO J.* **21**, 3255-3263.

**Billerey, C., Chopin, D., Aubriot-Lorton, M. H., Ricol, D., Gil Diez de Medina, S., Van Rhijn, B., Bralet, M. P., Lefrere-Belda, M. A., Lahaye, J. B., Abbou, C. C. et al. (2001).** Frequent FGFR3 mutations in papillary non-invasive bladder (pTa) tumors. *Am. J. Pathol.* **158**, 1955-1959.

**Bindels, E. M., Vermey, M., van den Beemd, R., Dinjens, W. N. and Van Der Kwast, T. H. (2000).** E-cadherin promotes intraepithelial expansion of bladder carcinoma cells in an in vitro model of carcinoma in situ. *Cancer Res.* **60**, 177-183.

**Birt, D. F., Pelling, J. C., Pour, P. M., Tibbels, M. G., Schweickert, L. and Bresnick, E. (1987).** Enhanced pancreatic and skin tumorigenesis in cabbage-fed hamsters and mice. *Carcinogenesis* **8**, 913-917.

**Bolos, V., Peinado, H., Perez-Moreno, M. A., Fraga, M. F., Esteller, M. and Cano, A.** (2003). The transcription factor slug represses E-cadherin expression and induces epithelial to mesenchymal transitions: A comparison with snail and E47 repressors. *J. Cell. Sci.* **116**, 499-511.

**Booth, C., Harnden, P., Trejdosiewicz, L. K., Scriven, S., Selby, P. J. and Southgate, J.** (1997). Stromal and vascular invasion in an human in vitro bladder cancer model. *Lab. Invest.* **76**, 843-857.

**Bornman, D. M., Mathew, S., Alsrue, J., Herman, J. G. and Gabrielson, E.** (2001). Methylation of the E-cadherin gene in bladder neoplasia and in normal urothelial epithelium from elderly individuals. *Am. J. Pathol.* **159**, 831-835.

**Bowman, T., Broome, M. A., Sinibaldi, D., Wharton, W., Pledger, W. J., Sedivy, J. M., Irby, R., Yeatman, T., Courtneidge, S. A. and Jove, R.** (2001). Stat3-mediated myc expression is required for src transformation and PDGF-induced mitogenesis. *Proc. Natl. Acad. Sci. U. S. A.* **98**, 7319-7324.

**Bowman, T., Garcia, R., Turkson, J. and Jove, R.** (2000). STATs in oncogenesis. *Oncogene* **19**, 2474-2488.

**Brandau, S. and Bohle, A.** (2001). Bladder cancer. I. molecular and genetic basis of carcinogenesis. *Eur. Urol.* **39**, 491-497.

**Brandi, G., Paiardini, M., Cervasi, B., Fiorucci, C., Filippone, P., De Marco, C., Zaffaroni, N. and Magnani, M.** (2003). A new indole-3-carbinol tetrameric derivative inhibits cyclin-dependent kinase 6 expression, and induces G1 cell cycle arrest in both estrogen-dependent and estrogen-independent breast cancer cell lines. *Cancer Res.* **63**, 4028-4036.

**Bratton, S. B., MacFarlane, M., Cain, K. and Cohen, G. M.** (2000). Protein complexes activate distinct caspase cascades in death receptor and stress-induced apoptosis. *Exp. Cell Res.* **256**, 27-33.

**Brew, C. T., Aronchik, I., Hsu, J. C., Sheen, J. H., Dickson, R. B., Bjeldanes, L. F. and Firestone, G. L. (2006).** Indole-3-carbinol activates the ATM signaling pathway independent of DNA damage to stabilize p53 and induce G1 arrest of human mammary epithelial cells. *Int. J. Cancer* **118**, 857-868.

**Bringuier, P. P., Umbas, R., Schaafsma, H. E., Karthaus, H. F., Debruyne, F. M. and Schalken, J. A. (1993).** Decreased E-cadherin immunoreactivity correlates with poor survival in patients with bladder tumors. *Cancer Res.* **53**, 3241-3245.

**Bromberg, J. (2002).** Stat proteins and oncogenesis. *J. Clin. Invest.* **109**, 1139-1142.

**Bromberg, J. F., Horvath, C. M., Besser, D., Lathem, W. W. and Darnell, J. E., Jr. (1998).** Stat3 activation is required for cellular transformation by v-src. *Mol. Cell. Biol.* **18**, 2553-2558.

**Bromberg, J. F., Horvath, C. M., Wen, Z., Schreiber, R. D. and Darnell, J. E., Jr. (1996).** Transcriptionally active Stat1 is required for the antiproliferative effects of both interferon alpha and interferon gamma. *Proc. Natl. Acad. Sci. U. S. A.* **93**, 7673-7678.

**Bromberg, J. F., Wrzeszczynska, M. H., Devgan, G., Zhao, Y., Pestell, R. G., Albanese, C. and Darnell, J. E., Jr. (1999).** Stat3 as an oncogene. *Cell* **98**, 295-303.

**Buettner, R., Mora, L. B. and Jove, R. (2002).** Activated STAT signaling in human tumors provides novel molecular targets for therapeutic intervention. *Clin. Cancer Res.* **8**, 945-954.

**Calo, V., Migliavacca, M., Bazan, V., Macaluso, M., Buscemi, M., Gebbia, N. and Russo, A. (2003).** STAT proteins: From normal control of cellular events to tumorigenesis. *J. Cell. Physiol.* **197**, 157-168.

**Cappellen, D., De Oliveira, C., Ricol, D., de Medina, S., Bourdin, J., Sastre-Garau, X., Chopin, D., Thiery, J. P. and Radvanyi, F. (1999).** Frequent activating mutations of FGFR3 in human bladder and cervix carcinomas. *Nat. Genet.* **23**, 18-20.

**Catlett-Falcone, R., Dalton, W. S. and Jove, R. (1999a).** STAT proteins as novel targets for cancer therapy. signal transducer and activator of transcription. *Curr. Opin. Oncol.* **11**, 490-496.

**Catlett-Falcone, R., Landowski, T. H., Oshiro, M. M., Turkson, J., Levitzki, A., Savino, R., Ciliberto, G., Moscinski, L., Fernandez-Luna, J. L., Nunez, G. et al. (1999b).** Constitutive activation of Stat3 signaling confers resistance to apoptosis in human U266 myeloma cells. *Immunity* **10**, 105-115.

**Chang, T. L., Peng, X. and Fu, X. Y. (2000).** Interleukin-4 mediates cell growth inhibition through activation of Stat1. *J. Biol. Chem.* **275**, 10212-10217.

**Chapman, R. S., Lourenco, P. C., Tonner, E., Flint, D. J., Selbert, S., Takeda, K., Akira, S., Clarke, A. R. and Watson, C. J. (1999).** Suppression of epithelial apoptosis and delayed mammary gland involution in mice with a conditional knockout of Stat3. *Genes Dev.* **13**, 2604-2616.

**Chatterjee, S. J., Datar, R., Youssefzadeh, D., George, B., Goebell, P. J., Stein, J. P., Young, L., Shi, S. R., Gee, C., Groshen, S. et al. (2004a).** Combined effects of p53, p21, and pRb expression in the progression of bladder transitional cell carcinoma. *J. Clin. Oncol.* **22**, 1007-1013.

**Chatterjee, S. J., George, B., Goebell, P. J., Alavi-Tafreshi, M., Shi, S. R., Fung, Y. K., Jones, P. A., Cordon-Cardo, C., Datar, R. H. and Cote, R. J. (2004b).** Hyperphosphorylation of pRb: A mechanism for RB tumour suppressor pathway inactivation in bladder cancer. *J. Pathol.* **203**, 762-770.

**Chaturvedi, P., Reddy, M. V. and Reddy, E. P. (1998).** Src kinases and not JAKs activate STATs during IL-3 induced myeloid cell proliferation. *Oncogene* **16**, 1749-1758.

**Chen, D. Z., Qi, M., Auburn, K. J. and Carter, T. H. (2001).** Indole-3-carbinol and diindolylmethane induce apoptosis of human cervical cancer cells and in murine HPV16-transgenic preneoplastic cervical epithelium. *J. Nutr.* **131**, 3294-3302.

**Chen, H., Ye, D., Xie, X., Chen, B. and Lu, W. (2004).** VEGF, VEGFRs expressions and activated STATs in ovarian epithelial carcinoma. *Gynecol. Oncol.* **94**, 630-635.

**Chen, M. and Wang, J.** (2002). Initiator caspases in apoptosis signaling pathways. *Apoptosis* 7, 313-319.

**Chen, W., Daines, M. O. and Khurana Hershey, G. K.** (2004). Turning off signal transducer and activator of transcription (STAT): The negative regulation of STAT signaling. *J. Allergy Clin. Immunol.* 114, 476-89; quiz 490.

**Chen, X. and Gumbiner, B. M.** (2006). Crosstalk between different adhesion molecules. *Curr. Opin. Cell Biol.* 18, 572-578.

**Chen, X. P., Losman, J. A. and Rothman, P.** (2000). SOCS proteins, regulators of intracellular signaling. *Immunity* 13, 287-290.

**Chiang, G. J., Billmeyer, B. R., Canes, D., Stoffel, J., Moinzadeh, A., Austin, C. A., Kosakowski, M., Rieger-Christ, K. M., Libertino, J. A. and Summerhayes, I. C.** (2005). The src-family kinase inhibitor PP2 suppresses the in vitro invasive phenotype of bladder carcinoma cells via modulation of akt. *BJU Int.* 96, 416-422.

**Chinni, S. R., Li, Y., Upadhyay, S., Koppolu, P. K. and Sarkar, F. H.** (2001). Indole-3-carbinol (I3C) induced cell growth inhibition, G1 cell cycle arrest and apoptosis in prostate cancer cells. *Oncogene* 20, 2927-2936.

**Chinni, S. R. and Sarkar, F. H.** (2002). Akt inactivation is a key event in indole-3-carbinol-induced apoptosis in PC-3 cells. *Clin. Cancer Res.* 8, 1228-1236.

**Cho, S. S., Bacon, C. M., Sudarshan, C., Rees, R. C., Finbloom, D., Pine, R. and O'Shea, J. J.** (1996). Activation of STAT4 by IL-12 and IFN-alpha: Evidence for the involvement of ligand-induced tyrosine and serine phosphorylation. *J. Immunol.* 157, 4781-4789.

**Christoph, F., Kempkensteffen, C., Weikert, S., Kollermann, J., Krause, H., Miller, K., Schostak, M. and Schrader, M.** (2006). Methylation of tumour suppressor genes APAF-1 and DAPK-1 and in vitro effects of demethylating agents in bladder and kidney cancer. *Br. J. Cancer* 95, 1701-1707.

**Cohen, G. M.** (1997). Caspases: The executioners of apoptosis. *Biochem. J.* **326** ( Pt 1), 1-16.

**Colquhoun, A. J. and Mellon, J. K.** (2002). Epidermal growth factor receptor and bladder cancer. *Postgrad. Med. J.* **78**, 584-589.

**Cooper, M. J., Haluschak, J. J., Johnson, D., Schwartz, S., Morrison, L. J., Lippa, M., Hatzivassiliou, G. and Tan, J.** (1994). P53 mutations in bladder carcinoma cell lines. *Oncol. Res.* **6**, 569-579.

**Copeland, N. G., Gilbert, D. J., Schindler, C., Zhong, Z., Wen, Z., Darnell, J. E., Jr, Mui, A. L., Miyajima, A., Quelle, F. W. and Ihle, J. N.** (1995). Distribution of the mammalian stat gene family in mouse chromosomes. *Genomics* **29**, 225-228.

**Cordon-Cardo, C., Dalbagni, G., Saez, G. T., Oliva, M. R., Zhang, Z. F., Rosai, J., Reuter, V. E. and Pellicer, A.** (1994). p53 mutations in human bladder cancer: Genotypic versus phenotypic patterns. *Int. J. Cancer* **56**, 347-353.

**Cotarla, I., Ren, S., Zhang, Y., Gehan, E., Singh, B. and Furth, P. A.** (2004). Stat5a is tyrosine phosphorylated and nuclear localized in a high proportion of human breast cancers. *Int. J. Cancer* **108**, 665-671.

**Cote, R. J. and Datar, R. H.** (2003). Therapeutic approaches to bladder cancer: Identifying targets and mechanisms. *Crit. Rev. Oncol. Hematol.* **46 Suppl**, S67-83.

**Cote, R. J., Dunn, M. D., Chatterjee, S. J., Stein, J. P., Shi, S. R., Tran, Q. C., Hu, S. X., Xu, H. J., Groshen, S., Taylor, C. R. et al.** (1998). Elevated and absent pRb expression is associated with bladder cancer progression and has cooperative effects with p53. *Cancer Res.* **58**, 1090-1094.

**Cousens, L. P., Goulette, F. A. and Darnowski, J. W.** (2005). JAK-mediated signaling inhibits fas ligand-induced apoptosis independent of de novo protein synthesis. *J. Immunol.* **174**, 320-327.

**Cover, C. M., Hsieh, S. J., Tran, S. H., Hallden, G., Kim, G. S., Bjeldanes, L. F. and Firestone, G. L. (1998).** Indole-3-carbinol inhibits the expression of cyclin-dependent kinase-6 and induces a G1 cell cycle arrest of human breast cancer cells independent of estrogen receptor signaling. *J. Biol. Chem.* **273**, 3838-3847.

**Dalton, W. S. and Jove, R. (1999).** Drug resistance in multiple myeloma: Approaches to circumvention. *Semin. Oncol.* **26**, 23-27.

**Darnell, J. E., Jr. (1997).** STATs and gene regulation. *Science* **277**, 1630-1635.

**Dashwood, R. H., Fong, A. T., Williams, D. E., Hendricks, J. D. and Bailey, G. S. (1991).** Promotion of aflatoxin B1 carcinogenesis by the natural tumor modulator indole-3-carbinol: Influence of dose, duration, and intermittent exposure on indole-3-carbinol promotional potency. *Cancer Res.* **51**, 2362-2365.

**de Groot, R. P., Raaijmakers, J. A., Lammers, J. W., Jove, R. and Koenderman, L. (1999).** STAT5 activation by BCR-abl contributes to transformation of K562 leukemia cells. *Blood* **94**, 1108-1112.

**de Rooij, J., Kerstens, A., Danuser, G., Schwartz, M. A. and Waterman-Storer, C. M. (2005).** Integrin-dependent actomyosin contraction regulates epithelial cell scattering. *J. Cell Biol.* **171**, 153-164.

**Debidda, M., Wang, L., Zang, H., Poli, V. and Zheng, Y. (2005).** A role of STAT3 in rho GTPase-regulated cell migration and proliferation. *J. Biol. Chem.* **280**, 17275-17285.

**Dechow, T. N., Pedranzini, L., Leitch, A., Leslie, K., Gerald, W. L., Linkov, I. and Bromberg, J. F. (2004).** Requirement of matrix metalloproteinase-9 for the transformation of human mammary epithelial cells by Stat3-C. *Proc. Natl. Acad. Sci. U. S. A.* **101**, 10602-10607.

**Decker, T. and Kovarik, P. (2000).** Serine phosphorylation of STATs. *Oncogene* **19**, 2628-2637.

**Dinney, C. P., McConkey, D. J., Millikan, R. E., Wu, X., Bar-Eli, M., Adam, L., Kamat, A. M., Siefker-Radtke, A. O., Tuziak, T., Sabichi, A. L. et al. (2004).** Focus on bladder cancer. *Cancer. Cell.* **6**, 111-116.

**Dowell, S. P., Wilson, P. O., Derias, N. W., Lane, D. P. and Hall, P. A. (1994).** Clinical utility of the immunocytochemical detection of p53 protein in cytological specimens. *Cancer Res.* **54**, 2914-2918.

**Duncan, S. A., Zhong, Z., Wen, Z. and Darnell, J. E., Jr. (1997).** STAT signaling is active during early mammalian development. *Dev. Dyn.* **208**, 190-198.

**Durbin, J. E., Hackenmiller, R., Simon, M. C. and Levy, D. E. (1996).** Targeted disruption of the mouse Stat1 gene results in compromised innate immunity to viral disease. *Cell* **84**, 443-450.

**Epling-Burnette, P. K., Liu, J. H., Catlett-Falcone, R., Turkson, J., Oshiro, M., Kothapalli, R., Li, Y., Wang, J. M., Yang-Yen, H. F., Karras, J. et al. (2001).** Inhibition of STAT3 signaling leads to apoptosis of leukemic large granular lymphocytes and decreased mcl-1 expression. *J. Clin. Invest.* **107**, 351-362.

**Esrig, D., Spruck, C. H., 3rd, Nichols, P. W., Chaiwun, B., Steven, K., Groshen, S., Chen, S. C., Skinner, D. G., Jones, P. A. and Cote, R. J. (1993).** p53 nuclear protein accumulation correlates with mutations in the p53 gene, tumor grade, and stage in bladder cancer. *Am. J. Pathol.* **143**, 1389-1397.

**Fabricant, R. N., De Larco, J. E. and Todaro, G. J. (1977).** Nerve growth factor receptors on human melanoma cells in culture. *Proc. Natl. Acad. Sci. U. S. A.* **74**, 565-569.

**Fan, S., Meng, Q., Auburn, K., Carter, T. and Rosen, E. M. (2006).** BRCA1 and BRCA2 as molecular targets for phytochemicals indole-3-carbinol and genistein in breast and prostate cancer cells. *Br. J. Cancer* **94**, 407-426.

**Feng, Z., Hu, W., Rom, W. N., Beland, F. A. and Tang, M. S. (2002).** 4-Aminobiphenyl is a major etiological agent of human bladder cancer: Evidence from its DNA binding spectrum in human p53 gene. *Carcinogenesis* **23**, 1721-1727.

**Fidler, I. J.** (2003). The pathogenesis of cancer metastasis: The 'seed and soil' hypothesis revisited. *Nat. Rev. Cancer.* **3**, 453-458.

**Firestone, G. L. and Bjeldanes, L. F.** (2003). Indole-3-carbinol and 3,3'-diindolylmethane antiproliferative signaling pathways control cell-cycle gene transcription in human breast cancer cells by regulating promoter-Spl transcription factor interactions. *J. Nutr.* **133**, 2448S-2455S.

**Friedl, P. and Wolf, K.** (2003). Tumour-cell invasion and migration: Diversity and escape mechanisms. *Nat. Rev. Cancer.* **3**, 362-374.

**Gao, J., Huang, H. Y., Pak, J., Cheng, J., Zhang, Z. T., Shapiro, E., Pellicer, A., Sun, T. T. and Wu, X. R.** (2004). p53 deficiency provokes urothelial proliferation and synergizes with activated ha-ras in promoting urothelial tumorigenesis. *Oncogene* **23**, 687-696.

**Garcia, H. H., Brar, G. A., Nguyen, D. H., Bjeldanes, L. F. and Firestone, G. L.** (2005). Indole-3-carbinol (I3C) inhibits cyclin-dependent kinase-2 function in human breast cancer cells by regulating the size distribution, associated cyclin E forms, and subcellular localization of the CDK2 protein complex. *J. Biol. Chem.* **280**, 8756-8764.

**Garcia, R., Bowman, T. L., Niu, G., Yu, H., Minton, S., Muro-Cacho, C. A., Cox, C. E., Falcone, R., Fairclough, R., Parsons, S. et al.** (2001). Constitutive activation of Stat3 by the src and JAK tyrosine kinases participates in growth regulation of human breast carcinoma cells. *Oncogene* **20**, 2499-2513.

**Garcia, R., Yu, C. L., Hudnall, A., Catlett, R., Nelson, K. L., Smithgall, T., Fujita, D. J., Ethier, S. P. and Jove, R.** (1997). Constitutive activation of Stat3 in fibroblasts transformed by diverse oncoproteins and in breast carcinoma cells. *Cell Growth Differ.* **8**, 1267-1276.

**Garikapaty, V. P., Ashok, B. T., Tadi, K., Mittelman, A. and Tiwari, R. K.** (2006a). 3,3'-diindolylmethane downregulates pro-survival pathway in hormone independent prostate cancer. *Biochem. Biophys. Res. Commun.* **340**, 718-725.

**Garikapaty, V. P., Ashok, B. T., Tadi, K., Mittelman, A. and Tiwari, R. K.** (2006b). 3,3'-diindolylmethane downregulates pro-survival pathway in hormone independent prostate cancer. *Biochem. Biophys. Res. Commun.* **340**, 718-725.

**Gescher, A., Pastorino, U., Plummer, S. M. and Manson, M. M. (1998).** Suppression of tumour development by substances derived from the diet--mechanisms and clinical implications. *Br. J. Clin. Pharmacol.* **45**, 1-12.

**Gioldi, L. A., Bringuier, P. P., Shimazui, T., Jansen, K. and Schalken, J. A. (1999).** Changes in cadherin-catenin complexes in the progression of human bladder carcinoma. *Int. J. Cancer* **82**, 70-76.

**Gong, Y., Firestone, G. L. and Bjeldanes, L. F. (2006).** 3,3'-diindolylmethane is a novel topoisomerase II $\alpha$  catalytic inhibitor that induces S-phase retardation and mitotic delay in human hepatoma HepG2 cells. *Mol. Pharmacol.* **69**, 1320-1327.

**Gouilleux-Gruart, V., Gouilleux, F., Desaint, C., Claisse, J. F., Capiod, J. C., Delobel, J., Weber-Nordt, R., Dusanter-Fourt, I., Dreyfus, F., Groner, B. et al. (1996).** STAT-related transcription factors are constitutively activated in peripheral blood cells from acute leukemia patients. *Blood* **87**, 1692-1697.

**Grandis, J. R., Drenning, S. D., Chakraborty, A., Zhou, M. Y., Zeng, Q., Pitt, A. S. and Tweardy, D. J. (1998).** Requirement of Stat3 but not Stat1 activation for epidermal growth factor receptor- mediated cell growth in vitro. *J. Clin. Invest.* **102**, 1385-1392.

**Greenhalgh, C. J. and Hilton, D. J. (2001).** Negative regulation of cytokine signaling. *J. Leukoc. Biol.* **70**, 348-356.

**Grossman, H. B., Lee, C., Bromberg, J. and Liebert, M. (2000).** Expression of the  $\alpha 6 \beta 4$  integrin provides prognostic information in bladder cancer. *Oncol. Rep.* **7**, 13-16.

**Grubbs, C. J., Steele, V. E., Casebolt, T., Juliana, M. M., Eto, I., Whitaker, L. M., Dragnev, K. H., Kelloff, G. J. and Lubet, R. L. (1995).** Chemoprevention of chemically-induced mammary carcinogenesis by indole-3-carbinol. *Anticancer Res.* **15**, 709-716.

**Gumbiner, B. M. (2005).** Regulation of cadherin-mediated adhesion in morphogenesis. *Nat. Rev. Mol. Cell Biol.* **6**, 622-634.

**Gupta, G. P. and Massague, J. (2006).** Cancer metastasis: Building a framework. *Cell* **127**, 679-695.

**Harabayashi, T., Kanai, Y., Yamada, T., Sakamoto, M., Ochiai, A., Kakizoe, T., Koyanagi, T. and Hirohashi, S. (1999).** Reduction of integrin beta4 and enhanced migration on laminin in association with intraepithelial spreading of urinary bladder carcinomas. *J. Urol.* **161**, 1364-1371.

**Hardy, R. G., Tselepis, C., Hoyland, J., Wallis, Y., Pretlow, T. P., Talbot, I., Sanders, D. S., Matthews, G., Morton, D. and Jankowski, J. A. (2002).** Aberrant P-cadherin expression is an early event in hyperplastic and dysplastic transformation in the colon. *Gut* **50**, 513-519.

**Hartmann, A., Schlake, G., Zaak, D., Hungerhuber, E., Hofstetter, A., Hofstaedter, F. and Knuechel, R. (2002).** Occurrence of chromosome 9 and p53 alterations in multifocal dysplasia and carcinoma in situ of human urinary bladder. *Cancer Res.* **62**, 809-818.

**Hayat, M. J., Howlader, N., Reichman, M. E. and Edwards, B. K. (2007).** Cancer statistics, trends, and multiple primary cancer analyses from the surveillance, epidemiology, and end results (SEER) program. *Oncologist* **12**, 20-37.

**Heaney, R. K. and Fenwick, G. R. (1995).** Natural toxins and protective factors in brassica species, including rapeseed. *Nat. Toxins* **3**, 233-7; discussion 242.

**Heyder, C., Gloria-Maercker, E., Hatzmann, W., Niggemann, B., Zanker, K. S. and Dittmar, T. (2005).** Role of the beta1-integrin subunit in the adhesion, extravasation and migration of T24 human bladder carcinoma cells. *Clin. Exp. Metastasis* **22**, 99-106.

**Hickman, E. S., Moroni, M. C. and Helin, K. (2002).** The role of p53 and pRB in apoptosis and cancer. *Curr. Opin. Genet. Dev.* **12**, 60-66.

**Hodge, D. R., Xiao, W., Wang, L. H., Li, D. and Farrar, W. L. (2004).** Activating mutations in STAT3 and STAT5 differentially affect cellular proliferation and apoptotic resistance in multiple myeloma cells. *Cancer. Biol. Ther.* **3**, 188-194.

**Hollstein, M., Sidransky, D., Vogelstein, B. and Harris, C. C. (1991).** P53 mutations in human cancers. *Science* **253**, 49-53.

**Hong, C., Kim, H. A., Firestone, G. L. and Bjeldanes, L. F. (2002).** 3,3'-diindolylmethane (DIM) induces a G(1) cell cycle arrest in human breast cancer cells that is accompanied by Sp1-mediated activation of p21(WAF1/CIP1) expression. *Carcinogenesis* **23**, 1297-1305.

**Hong, S. J., Lee, T., Park, Y. S., Lee, K. O., Chung, B. H. and Lee, S. H. (1996).** A PCR-RFLP method for the detection of activated H-ras oncogene with a point mutation at codon 12 and 61. *Yonsei Med. J.* **37**, 371-379.

**Hou, J., Schindler, U., Henzel, W. J., Ho, T. C., Brasseur, M. and McKnight, S. L. (1994).** An interleukin-4-induced transcription factor: IL-4 stat. *Science* **265**, 1701-1706.

**Howells, L. M. (2003).** Mechanisms of action of the chemopreventive agent indole-3-carbinol in breast cell lines. PhD thesis. *University of Leicester, Leicester.*

**Howells, L. M., Gallacher-Horley, B., Houghton, C. E., Manson, M. M. and Hudson, E. A. (2002).** Indole-3-carbinol inhibits protein kinase B/Akt and induces apoptosis in the human breast tumor cell line MDA MB468 but not in the nontumorigenic HBL100 line. *Mol. Cancer. Ther.* **1**, 1161-1172.

**Howells, L. M., Moiseeva, E. P., Neal, C. P., Foreman, B. E., Andreadi, C. K., Sun, Y. Y., Hudson, E. A. and Manson, M. M. (2007).** Predicting the physiological relevance of in vitro cancer preventive activities of phytochemicals. *Acta Pharmacol. Sin.* **28**, 1274-1304.

**Hsiao, J. R., Jin, Y. T., Tsai, S. T., Shiau, A. L., Wu, C. L. and Su, W. C. (2003).** Constitutive activation of STAT3 and STAT5 is present in the majority of nasopharyngeal carcinoma and correlates with better prognosis. *Br. J. Cancer* **89**, 344-349.

**Hsu, J. C., Dev, A., Wing, A., Brew, C. T., Bjeldanes, L. F. and Firestone, G. L. (2006).** Indole-3-carbinol mediated cell cycle arrest of LNCaP human prostate cancer cells requires the induced production of activated p53 tumor suppressor protein. *Biochem. Pharmacol.* **72**, 1714-1723.

**Hsu, J. C., Zhang, J., Dev, A., Wing, A., Bjeldanes, L. F. and Firestone, G. L. (2005).** Indole-3-carbinol inhibition of androgen receptor expression and downregulation of androgen responsiveness in human prostate cancer cells. *Carcinogenesis* **26**, 1896-1904.

**Hung, W. and Elliott, B. (2001).** Co-operative effect of c-src tyrosine kinase and Stat3 in activation of hepatocyte growth factor expression in mammary carcinoma cells. *J. Biol. Chem.* **276**, 12395-12403.

**Hynes, R. O. (2002).** Integrins: Bidirectional, allosteric signaling machines. *Cell* **110**, 673-687.

**Imada, K., Bloom, E. T., Nakajima, H., Horvath-Arcidiacono, J. A., Udy, G. B., Davey, H. W. and Leonard, W. J. (1998).** Stat5b is essential for natural killer cell-mediated proliferation and cytolytic activity. *J. Exp. Med.* **188**, 2067-2074.

**Imao, T., Koshida, K., Endo, Y., Uchibayashi, T., Sasaki, T. and Namiki, M. (1999).** Dominant role of E-cadherin in the progression of bladder cancer. *J. Urol.* **161**, 692-698.

**Ito, N., Tatematsu, M., Hasegawa, R. and Tsuda, H. (1989).** Medium-term bioassay system for detection of carcinogens and modifiers of hepatocarcinogenesis utilizing the GST-P positive liver cell focus as an endpoint marker. *Toxicol. Pathol.* **17**, 630-641.

**Itoh, M., Murata, T., Suzuki, T., Shindoh, M., Nakajima, K., Imai, K. and Yoshida, K. (2006).** Requirement of STAT3 activation for maximal collagenase-1 (MMP-1) induction by epidermal growth factor and malignant characteristics in T24 bladder cancer cells. *Oncogene* **25**, 1195-1204.

**Ivashkiv, L. B. and Hu, X. (2004).** Signaling by STATs. *Arthritis Res. Ther.* **6**, 159-168.

**Jebar, A. H., Hurst, C. D., Tomlinson, D. C., Johnston, C., Taylor, C. F. and Knowles, M. A. (2005).** FGFR3 and ras gene mutations are mutually exclusive genetic events in urothelial cell carcinoma. *Oncogene* **24**, 5218-5225.

**Jiao, H., Berrada, K., Yang, W., Tabrizi, M., Plataniias, L. C. and Yi, T. (1996).** Direct association with and dephosphorylation of Jak2 kinase by the SH2-domain-containing protein tyrosine phosphatase SHP-1. *Mol. Cell. Biol.* **16**, 6985-6992.

**Jones, S. M. and Kazlauskas, A. (2001).** Growth factor-dependent signaling and cell cycle progression. *Chem. Rev.* **101**, 2413-2423.

**Kadler, K. E., Baldock, C., Bella, J. and Boot-Handford, R. P. (2007).** Collagens at a glance. *J. Cell. Sci.* **120**, 1955-1958.

**Kamat, A. M. and Lamm, D. L. (1999).** Chemoprevention of urological cancer. *J. Urol.* **161**, 1748-1760.

**Kang, Y. and Massague, J. (2004).** Epithelial-mesenchymal transitions: Twist in development and metastasis. *Cell* **118**, 277-279.

**Kaplan, D. H., Shankaran, V., Dighe, A. S., Stockert, E., Aguet, M., Old, L. J. and Schreiber, R. D. (1998).** Demonstration of an interferon gamma-dependent tumor surveillance system in immunocompetent mice. *Proc. Natl. Acad. Sci. U. S. A.* **95**, 7556-7561.

**Kaplan, M. H., Sun, Y. L., Hoey, T. and Grusby, M. J. (1996).** Impaired IL-12 responses and enhanced development of Th2 cells in Stat4-deficient mice. *Nature* **382**, 174-177.

**Kassie, F., Uhl, M., Rabot, S., Grasl-Kraupp, B., Verkerk, R., Kundi, M., Chabicovsky, M., Schulte-Hermann, R. and Knasmüller, S. (2003).** Chemoprevention of 2-amino-3-methylimidazo[4,5-f]quinoline (IQ)-induced colonic and hepatic preneoplastic lesions in the F344 rat by cruciferous vegetables administered simultaneously with the carcinogen. *Carcinogenesis* **24**, 255-261.

**Kawamata, H., Hattori, K., Omotehara, F., Uchida, D., Hino, S., Sato, M. and Oyasu, R. (1999).** Balance between activated-STAT and MAP kinase regulates the growth of human bladder cell lines after treatment with epidermal growth factor. *Int. J. Oncol.* **15**, 661-667.

**Kawamoto, K., Enokida, H., Gotanda, T., Kubo, H., Nishiyama, K., Kawahara, M. and Nakagawa, M. (2006).** p16INK4a and p14ARF methylation as a potential biomarker for human bladder cancer. *Biochem. Biophys. Res. Commun.* **339**, 790-796.

**Kawasaki, T., Tomita, Y., Bilim, V., Takeda, M., Takahashi, K. and Kumanishi, T. (1996).** Abrogation of apoptosis induced by DNA-damaging agents in human bladder-cancer cell lines with p21/WAF1/CIP1 and/or p53 gene alterations. *Int. J. Cancer* **68**, 501-505.

**Kedrin, D., van Rheenen, J., Hernandez, L., Condeelis, J. and Segall, J. E. (2007).** Cell motility and cytoskeletal regulation in invasion and metastasis. *J. Mammary Gland Biol. Neoplasia*. [Epub ahead of print]

**Kim, D. J., Han, B. S., Ahn, B., Hasegawa, R., Shirai, T., Ito, N. and Tsuda, H. (1997).** Enhancement by indole-3-carbinol of liver and thyroid gland neoplastic development in a rat medium-term multiorgan carcinogenesis model. *Carcinogenesis* **18**, 377-381.

**Kim, D. S., Jeong, Y. M., Moon, S. I., Kim, S. Y., Kwon, S. B., Park, E. S., Youn, S. W. and Park, K. C. (2006).** Indole-3-carbinol enhances ultraviolet B-induced apoptosis by sensitizing human melanoma cells. *Cell Mol. Life Sci.* **63**, 2661-2668.

**Kim, E. J., Park, S. Y., Shin, H. K., Kwon, D. Y., Surh, Y. J. and Park, J. H. (2007).** Activation of caspase-8 contributes to 3,3'-diindolylmethane-induced apoptosis in colon cancer cells. *J. Nutr.* **137**, 31-36.

**Kim, S. O., Sheikh, H. I., Ha, S. D., Martins, A. and Reid, G. (2006).** G-CSF-mediated inhibition of JNK is a key mechanism for *Lactobacillus rhamnosus*-induced suppression of TNF production in macrophages. *Cell. Microbiol.* **8**, 1958-1971.

**Knowles, M. A. (2001).** What we could do now: Molecular pathology of bladder cancer. *Mol. Pathol.* **54**, 215-221.

**Koenig, A., Mueller, C., Hasel, C., Adler, G. and Menke, A. (2006).** Collagen type I induces disruption of E-cadherin-mediated cell-cell contacts and promotes proliferation of pancreatic carcinoma cells. *Cancer Res.* **66**, 4662-4671.

**Koksal, I. T., Ates, M., Danisman, A., Sezer, C., Ciftcioglu, A., Karpuzoglu, G. and Sevuk, M. (2006).** Reduced E-cadherin and alpha-catenin expressions have no prognostic role in bladder carcinoma. *Pathol. Oncol. Res.* **12**, 13-19.

**Kong, D., Li, Y., Wang, Z., Banerjee, S. and Sarkar, F. H. (2007).** Inhibition of angiogenesis and invasion by 3,3'-diindolylmethane is mediated by the nuclear factor-kappaB downstream target genes MMP-9 and uPA that regulated bioavailability of vascular endothelial growth factor in prostate cancer. *Cancer Res.* **67**, 3310-3319.

**Kovacs, A., Dhillon, J. and Walker, R. A. (2003).** Expression of P-cadherin, but not E-cadherin or N-cadherin, relates to pathological and functional differentiation of breast carcinomas. *Mol. Pathol.* **56**, 318-322.

**Kroemer, G., Dallaporta, B. and Resche-Rigon, M. (1998).** The mitochondrial death/life regulator in apoptosis and necrosis. *Annu. Rev. Physiol.* **60**, 619-642.

**Kusaba, T., Nakayama, T., Yamazumi, K., Yakata, Y., Yoshizaki, A., Inoue, K., Nagayasu, T. and Sekine, I. (2006).** Activation of STAT3 is a marker of poor prognosis in human colorectal cancer. *Oncol. Rep.* **15**, 1445-1451.

**Kusaba, T., Nakayama, T., Yamazumi, K., Yakata, Y., Yoshizaki, A., Nagayasu, T. and Sekine, I. (2005).** Expression of p-STAT3 in human colorectal adenocarcinoma and adenoma; correlation with clinicopathological factors. *J. Clin. Pathol.* **58**, 833-838.

**Larue, L. and Bellacosa, A. (2005).** Epithelial-mesenchymal transition in development and cancer: Role of phosphatidylinositol 3' kinase/AKT pathways. *Oncogene* **24**, 7443-7454.

**Lascombe, I., Clairotte, A., Fauconnet, S., Bernardini, S., Wallerand, H., Kantelip, B. and Bittard, H. (2006).** N-cadherin as a novel prognostic marker of progression in superficial urothelial tumors. *Clin. Cancer Res.* **12**, 2780-2787.

**Lauffenburger, D. A. and Horwitz, A. F. (1996).** Cell migration: A physically integrated molecular process. *Cell* **84**, 359-369.

**Lee, C. K., Raz, R., Gimeno, R., Gertner, R., Wistinghausen, B., Takeshita, K., DePinho, R. A. and Levy, D. E. (2002).** STAT3 is a negative regulator of granulopoiesis but is not required for G-CSF-dependent differentiation. *Immunity* **17**, 63-72.

**Lee, C. K., Smith, E., Gimeno, R., Gertner, R. and Levy, D. E. (2000).** STAT1 affects lymphocyte survival and proliferation partially independent of its role downstream of IFN-gamma. *J. Immunol.* **164**, 1286-1292.

**Lee, N. P., Mruk, D., Lee, W. M. and Cheng, C. Y. (2003).** Is the cadherin/catenin complex a functional unit of cell-cell actin-based adherens junctions in the rat testis? *Biol. Reprod.* **68**, 489-508.

**Leibelt, D. A., Hedstrom, O. R., Fischer, K. A., Pereira, C. B. and Williams, D. E. (2003).** Evaluation of chronic dietary exposure to indole-3-carbinol and absorption-enhanced 3,3'-diindolylmethane in sprague-dawley rats. *Toxicol. Sci.* **74**, 10-21.

**Leslie, K., Lang, C., Devgan, G., Azare, J., Berishaj, M., Gerald, W., Kim, Y. B., Paz, K., Darnell, J. E., Albanese, C. et al. (2006).** Cyclin D1 is transcriptionally regulated by and required for transformation by activated signal transducer and activator of transcription 3. *Cancer Res.* **66**, 2544-2552.

**Levitzki, A. (1999).** Protein tyrosine kinase inhibitors as novel therapeutic agents. *Pharmacol. Ther.* **82**, 231-239.

**Li, C., Teng, R. H., Tsai, Y. C., Ke, H. S., Huang, J. Y., Chen, C. C., Kao, Y. L., Kuo, C. C., Bell, W. R. and Shieh, B. (2005).** H-ras oncogene counteracts the growth-inhibitory effect of genistein in T24 bladder carcinoma cells. *Br. J. Cancer* **92**, 80-88.

**Li, F., Ambrosini, G., Chu, E. Y., Plescia, J., Tognin, S., Marchisio, P. C. and Altieri, D. C. (1998).** Control of apoptosis and mitotic spindle checkpoint by survivin. *Nature* **396**, 580-584.

**Li, M., Song, T., Yin, Z. F. and Na, Y. Q. (2007).** XIAP as a prognostic marker of early recurrence of nonmuscular invasive bladder cancer. *Chin. Med. J. (Engl)* **120**, 469-473.

**Li, Y., Li, X. and Sarkar, F. H. (2003).** Gene expression profiles of I3C- and DIM-treated PC3 human prostate cancer cells determined by cDNA microarray analysis. *J. Nutr.* **133**, 1011-1019.

**Li, Y., Wang, Z., Kong, D., Murthy, S., Dou, Q. P., Sheng, S., Reddy, G. P. and Sarkar, F. H. (2007).** Regulation of FOXO3a/beta-catenin/GSK-3beta signaling by 3,3'-diindolylmethane contributes to inhibition of cell proliferation and induction of apoptosis in prostate cancer cells. *J. Biol. Chem.* [Epub ahead of print]

**Lian, J. P., Word, B., Taylor, S., Hammons, G. J. and Lyn-Cook, B. D. (2004).** Modulation of the constitutive activated STAT3 transcription factor in pancreatic cancer prevention: Effects of indole-3-carbinol (I3C) and genistein. *Anticancer Res.* **24**, 133-137.

**Liby, K., Voong, N., Williams, C. R., Risingsong, R., Royce, D. B., Honda, T., Gribble, G. W., Sporn, M. B. and Letterio, J. J. (2006).** The synthetic triterpenoid CDDO-imidazolide suppresses STAT phosphorylation and induces apoptosis in myeloma and lung cancer cells. *Clin. Cancer Res.* **12**, 4288-4293.

**Lim, C. P., Phan, T. T., Lim, I. J. and Cao, X. (2006).** Stat3 contributes to keloid pathogenesis via promoting collagen production, cell proliferation and migration. *Oncogene* **25**, 5416-5425.

**Liu, R. Y., Fan, C., Garcia, R., Jove, R. and Zuckerman, K. S. (1999).** Constitutive activation of the JAK2/STAT5 signal transduction pathway correlates with growth factor independence of megakaryocytic leukemic cell lines. *Blood* **93**, 2369-2379.

**Liu, X., Robinson, G. W., Wagner, K. U., Garrett, L., Wynshaw-Boris, A. and Hennighausen, L. (1997).** Stat5a is mandatory for adult mammary gland development and lactogenesis. *Genes Dev.* **11**, 179-186.

**Lopez-Beltran, A., Requena, M. J., Luque, R. J., Alvarez-Kindelan, J., Quintero, A., Blanca, A. M., Rodriguez, M. E., Siendones, E. and Montironi, R. (2006).** Cyclin D3 expression in primary Ta/T1 bladder cancer. *J. Pathol.* **209**, 106-113.

**Luckow, B. and Schutz, G. (1987).** CAT constructions with multiple unique restriction sites for the functional analysis of eukaryotic promoters and regulatory elements. *Nucleic Acids Res.* **15**, 5490.

**Lund, T. C., Prator, P. C., Medveczky, M. M. and Medveczky, P. G. (1999).** The lck binding domain of herpesvirus saimiri tip-484 constitutively activates lck and STAT3 in T cells. *J. Virol.* **73**, 1689-1694.

**Lutzeyer, W., Rubben, H. and Dahm, H. (1982).** Prognostic parameters in superficial bladder cancer: An analysis of 315 cases. *J. Urol.* **127**, 250-252.

**Ma, X. T., Wang, S., Ye, Y. J., Du, R. Y., Cui, Z. R. and Somsouk, M. (2004).** Constitutive activation of Stat3 signaling pathway in human colorectal carcinoma. *World J. Gastroenterol.* **10**, 1569-1573.

**Maluf, F. C., Cordon-Cardo, C., Verbel, D. A., Satagopan, J. M., Boyle, M. G., Herr, H. and Bajorin, D. F. (2006).** Assessing interactions between mdm-2, p53, and bcl-2 as prognostic variables in muscle-invasive bladder cancer treated with neo-adjuvant chemotherapy followed by locoregional surgical treatment. *Ann. Oncol.* **17**, 1677-1686.

**Manson, M. M. (2003).** Cancer prevention -- the potential for diet to modulate molecular signalling. *Trends Mol. Med.* **9**, 11-18.

**Manson, M. M. (2005).** Inhibition of survival signalling by dietary polyphenols and indole-3-carbinol. *Eur. J. Cancer* **41**, 1842-1853.

**Manson, M. M., Gescher, A., Hudson, E. A., Plummer, S. M., Squires, M. S. and Prigent, S. A. (2000).** Blocking and suppressing mechanisms of chemoprevention by dietary constituents. *Toxicol. Lett.* **112-113**, 499-505.

**Manson, M. M., Hudson, E. A., Ball, H. W., Barrett, M. C., Clark, H. L., Judah, D. J., Verschoyle, R. D. and Neal, G. E. (1998).** Chemoprevention of aflatoxin B1-induced carcinogenesis by indole-3-carbinol in rat liver--predicting the outcome using early biomarkers. *Carcinogenesis* **19**, 1829-1836.

**Martino, A., Holmes, J. H., 4th, Lord, J. D., Moon, J. J. and Nelson, B. H. (2001).** Stat5 and Sp1 regulate transcription of the cyclin D2 gene in response to IL-2. *J. Immunol.* **166**, 1723-1729.

**Masters, J. R., Hepburn, P. J., Walker, L., Highman, W. J., Trejdosiewicz, L. K., Povey, S., Parkar, M., Hill, B. T., Riddle, P. R. and Franks, L. M. (1986).** Tissue culture model of transitional cell carcinoma: Characterization of twenty-two human urothelial cell lines. *Cancer Res.* **46**, 3630-3636.

**Masuda, M., Suzui, M. and Weinstein, I. B. (2001).** Effects of epigallocatechin-3-gallate on growth, epidermal growth factor receptor signaling pathways, gene expression, and chemosensitivity in human head and neck squamous cell carcinoma cell lines. *Clin. Cancer Res.* **7**, 4220-4229.

**Masuda, M., Suzui, M., Yasumatu, R., Nakashima, T., Kuratomi, Y., Azuma, K., Tomita, K., Komiyama, S. and Weinstein, I. B. (2002).** Constitutive activation of signal transducers and activators of transcription 3 correlates with cyclin D1 overexpression and may provide a novel prognostic marker in head and neck squamous cell carcinoma. *Cancer Res.* **62**, 3351-3355.

**Matsumoto, A., Masuhara, M., Mitsui, K., Yokouchi, M., Ohtsubo, M., Misawa, H., Miyajima, A. and Yoshimura, A. (1997).** CIS, a cytokine inducible SH2 protein, is a target of the JAK-STAT5 pathway and modulates STAT5 activation. *Blood* **89**, 3148-3154.

**McDonald, E. R., 3rd and El-Deiry, W. S. (2000).** Cell cycle control as a basis for cancer drug development (review). *Int. J. Oncol.* **16**, 871-886.

**Mejlvang, J., Kriajevska, M., Vandewalle, C., Chernova, T., Sayan, A. E., Berx, G., Mellon, J. K. and Tulchinsky, E. (2007).** Direct repression of cyclin D1 by SIP1 attenuates cell cycle progression in cells undergoing an epithelial mesenchymal transition. *Mol. Biol. Cell.* [Epub ahead of print]

**Meng, Q., Yuan, F., Goldberg, I. D., Rosen, E. M., Auburn, K. and Fan, S. (2000).** Indole-3-carbinol is a negative regulator of estrogen receptor-alpha signaling in human tumor cells. *J. Nutr.* **130**, 2927-2931.

**Meraz, M. A., White, J. M., Sheehan, K. C., Bach, E. A., Rodig, S. J., Dighe, A. S., Kaplan, D. H., Riley, J. K., Greenlund, A. C., Campbell, D. et al. (1996).** Targeted disruption of the Stat1 gene in mice reveals unexpected physiologic specificity in the JAK-STAT signaling pathway. *Cell* **84**, 431-442.

**Meydan, N., Grunberger, T., Dadi, H., Shahar, M., Arpaia, E., Lapidot, Z., Leeder, J. S., Freedman, M., Cohen, A., Gazit, A. et al. (1996).** Inhibition of acute lymphoblastic leukaemia by a jak-2 inhibitor. *Nature* **379**, 645-648.

**Migone, T. S., Lin, J. X., Cereseto, A., Mulloy, J. C., O'Shea, J. J., Franchini, G. and Leonard, W. J. (1995).** Constitutively activated jak-STAT pathway in T cells transformed with HTLV-I. *Science* **269**, 79-81.

**Miranti, C. K. and Brugge, J. S. (2002).** Sensing the environment: A historical perspective on integrin signal transduction. *Nat. Cell Biol.* **4**, E83-90.

**Mo, L., Zheng, X., Huang, H. Y., Shapiro, E., Lepor, H., Cordon-Cardo, C., Sun, T. T. and Wu, X. R. (2007).** Hyperactivation of ha-ras oncogene, but not Ink4a/Arf deficiency, triggers bladder tumorigenesis. *J. Clin. Invest.* **117**, 314-325.

**Moiseeva, E. P., Heukers, R. and Manson, M. M. (2007).** EGFR and src are involved in indole-3-carbinol-induced death and cell cycle arrest of human breast cancer cells. *Carcinogenesis* **28**, 435-445.

**Moneef, M. A., Sherwood, B. T., Bowman, K. J., Kockelbergh, R. C., Symonds, R. P., Steward, W. P., Mellon, J. K. and Jones, G. D. (2003).** Measurements using the alkaline comet assay predict bladder cancer cell radiosensitivity. *Br. J. Cancer* **89**, 2271-2276.

**Mora, L. B., Buettner, R., Seigne, J., Diaz, J., Ahmad, N., Garcia, R., Bowman, T., Falcone, R., Fairclough, R., Cantor, A. et al. (2002).** Constitutive activation of Stat3 in human prostate tumors and cell lines: Direct inhibition of Stat3 signaling induces apoptosis of prostate cancer cells. *Cancer Res.* **62**, 6659-6666.

**Moran, D. M., Mattocks, M. A., Cahill, P. A., Koniaris, L. G. and McKillop, I. H. (2007).** Interleukin-6 mediates G(0)/G(1) growth arrest in hepatocellular carcinoma through a STAT 3-dependent pathway. *J. Surg. Res.* [Epub ahead of print]

**Moss, M. L. and Lambert, M. H. (2002).** Shedding of membrane proteins by ADAM family proteases. *Essays Biochem.* **38**, 141-153.

**Murakami, Y., Nakano, S., Niho, Y., Hamasaki, N. and Izuhara, K. (1998).** Constitutive activation of jak-2 and tyk-2 in a v-src-transformed human gallbladder adenocarcinoma cell line. *J. Cell. Physiol.* **175**, 220-228.

**Murillo, G. and Mehta, R. G. (2001).** Cruciferous vegetables and cancer prevention. *Nutr. Cancer* **41**, 17-28.

**Nachshon-Kedmi, M., Fares, F. A. and Yannai, S. (2004a).** Therapeutic activity of 3,3'-diindolylmethane on prostate cancer in an in vivo model. *Prostate* **61**, 153-160.

**Nachshon-Kedmi, M., Yannai, S. and Fares, F. A. (2004b).** Induction of apoptosis in human prostate cancer cell line, PC3, by 3,3'-diindolylmethane through the mitochondrial pathway. *Br. J. Cancer* **91**, 1358-1363.

**Nagai, T., Yamakawa, N., Aota, S., Yamada, S. S., Akiyama, S. K., Olden, K. and Yamada, K. M. (1991).** Monoclonal antibody characterization of two distant sites required for function of the central cell-binding domain of fibronectin in cell adhesion, cell migration, and matrix assembly. *J. Cell Biol.* **114**, 1295-1305.

**Nam, J. S., Ino, Y., Sakamoto, M. and Hirohashi, S. (2002).** Src family kinase inhibitor PP2 restores the E-cadherin/catenin cell adhesion system in human cancer cells and reduces cancer metastasis. *Clin. Cancer Res.* **8**, 2430-2436.

**Ni, Z., Lou, W., Lee, S. O., Dhir, R., DeMiguel, F., Grandis, J. R. and Gao, A. C. (2002).** Selective activation of members of the signal transducers and activators of transcription family in prostate carcinoma. *J. Urol.* **167**, 1859-1862.

**Nicholson, R. I., Gee, J. M. and Harper, M. E. (2001).** EGFR and cancer prognosis. *Eur. J. Cancer* **37 Suppl 4**, S9-15.

**Niu, G., Wright, K. L., Huang, M., Song, L., Haura, E., Turkson, J., Zhang, S., Wang, T., Sinibaldi, D., Coppola, D. et al. (2002).** Constitutive Stat3 activity up-regulates VEGF expression and tumor angiogenesis. *Oncogene* **21**, 2000-2008.

**Niu, G., Wright, K. L., Ma, Y., Wright, G. M., Huang, M., Irby, R., Briggs, J., Karras, J., Cress, W. D., Pardoll, D. et al. (2005).** Role of Stat3 in regulating p53 expression and function. *Mol. Cell. Biol.* **25**, 7432-7440.

**Niwa, Y., Kanda, H., Shikauchi, Y., Saiura, A., Matsubara, K., Kitagawa, T., Yamamoto, J., Kubo, T. and Yoshikawa, H. (2005).** Methylation silencing of SOCS-3 promotes cell growth and migration by enhancing JAK/STAT and FAK signalings in human hepatocellular carcinoma. *Oncogene* **24**, 6406-6417.

**Norbury, C. and Nurse, P. (1992).** Animal cell cycles and their control. *Annu. Rev. Biochem.* **61**, 441-470.

**Oganesian, A., Hendricks, J. D. and Williams, D. E. (1997).** Long term dietary indole-3-carbinol inhibits diethylnitrosamine-initiated hepatocarcinogenesis in the infant mouse model. *Cancer Lett.* **118**, 87-94.

**Ohkubo, T. and Ozawa, M. (2004).** The transcription factor snail downregulates the tight junction components independently of E-cadherin downregulation. *J. Cell. Sci.* **117**, 1675-1685.

**Okabe, H., Lee, S. H., Phuchareon, J., Albertson, D. G., McCormick, F. and Tetsu, O. (2006).** A critical role for FBXW8 and MAPK in cyclin D1 degradation and cancer cell proliferation. *PLoS ONE* **1**, e128.

**Orlow, I., LaRue, H., Osman, I., Lacombe, L., Moore, L., Rabbani, F., Meyer, F., Fradet, Y. and Cordon-Cardo, C. (1999).** Deletions of the INK4A gene in superficial bladder tumors. association with recurrence. *Am. J. Pathol.* **155**, 105-113.

**Palacios, F., Tushir, J. S., Fujita, Y. and D'Souza-Schorey, C. (2005).** Lysosomal targeting of E-cadherin: A unique mechanism for the down-regulation of cell-cell adhesion during epithelial to mesenchymal transitions. *Mol. Cell. Biol.* **25**, 389-402.

**Pankov, R. and Yamada, K. M. (2002).** Fibronectin at a glance. *J. Cell. Sci.* **115**, 3861-3863.

**Park, C., Li, S., Cha, E. and Schindler, C. (2000).** Immune response in Stat2 knockout mice. *Immunity* **13**, 795-804.

**Peifer, M. (1997).** Beta-catenin as oncogene: The smoking gun. *Science* **275**, 1752-1753.

**Pence, B. C., Buddingh, F. and Yang, S. P. (1986).** Multiple dietary factors in the enhancement of dimethylhydrazine carcinogenesis: Main effect of indole-3-carbinol. *J. Natl. Cancer Inst.* **77**, 269-276.

**Pierce, J. P., Stefanick, M. L., Flatt, S. W., Natarajan, L., Sternfeld, B., Madlensky, L., Al-Delaimy, W. K., Thomson, C. A., Kealey, S., Hajek, R. et al. (2007).** Greater survival after breast cancer in physically active women with high vegetable-fruit intake regardless of obesity. *J. Clin. Oncol.* **25**, 2345-2351.

**Pines, J. (1995).** Cyclins and cyclin-dependent kinases: Theme and variations. *Adv. Cancer Res.* **66**, 181-212.

**Plate, K. H., Breier, G., Weich, H. A. and Risau, W. (1992).** Vascular endothelial growth factor is a potential tumour angiogenesis factor in human gliomas in vivo. *Nature* **359**, 845-848.

**Popov, Z., Gil-Diez de Medina, S., Lefrere-Belda, M. A., Hoznek, A., Bastuji-Garin, S., Abbou, C. C., Thiery, J. P., Radvanyi, F. and Chopin, D. K. (2000).** Low E-cadherin expression in bladder cancer at the transcriptional and protein level provides prognostic information. *Br. J. Cancer* **83**, 209-214.

**Przybojewska, B., Jagiello, A. and Jalmuzna, P. (2000).** H-RAS, K-RAS, and N-RAS gene activation in human bladder cancers. *Cancer Genet. Cytogenet.* **121**, 73-77.

**Qi, J., Wang, J., Romanyuk, O. and Siu, C. H. (2006).** Involvement of src family kinases in N-cadherin phosphorylation and beta-catenin dissociation during transendothelial migration of melanoma cells. *Mol. Biol. Cell* **17**, 1261-1272.

**Quadros, M. R., Peruzzi, F., Kari, C. and Rodeck, U. (2004).** Complex regulation of signal transducers and activators of transcription 3 activation in normal and malignant keratinocytes. *Cancer Res.* **64**, 3934-3939.

**Rahman, K. M., Li, Y. and Sarkar, F. H. (2004).** Inactivation of akt and NF-kappaB play important roles during indole-3-carbinol-induced apoptosis in breast cancer cells. *Nutr. Cancer* **48**, 84-94.

**Rahman, K. W., Li, Y., Wang, Z., Sarkar, S. H. and Sarkar, F. H. (2006).** Gene expression profiling revealed survivin as a target of 3,3'-diindolylmethane-induced cell growth inhibition and apoptosis in breast cancer cells. *Cancer Res.* **66**, 4952-4960.

**Rahman, K. W. and Sarkar, F. H. (2005).** Inhibition of nuclear translocation of nuclear factor- $\kappa$ B contributes to 3,3'-diindolylmethane-induced apoptosis in breast cancer cells. *Cancer Res.* **65**, 364-371.

**Ramana, C. V., Grammatikakis, N., Chernov, M., Nguyen, H., Goh, K. C., Williams, B. R. and Stark, G. R. (2000).** Regulation of c-myc expression by IFN-gamma through Stat1-dependent and -independent pathways. *EMBO J.* **19**, 263-272.

**Raspollini, M. R., Nesi, G., Baroni, G., Girardi, L. R. and Taddei, G. L. (2006).** p16(INK4a) expression in urinary bladder carcinoma. *Arch. Ital. Urol. Androl.* **78**, 97-100.

**Reddy, L., Odhav, B. and Bhoola, K. D. (2003).** Natural products for cancer prevention: A global perspective. *Pharmacol. Ther.* **99**, 1-13.

**Rieger, K. M., Little, A. F., Swart, J. M., Kastrinakis, W. V., Fitzgerald, J. M., Hess, D. T., Libertino, J. A. and Summerhayes, I. C. (1995).** Human bladder carcinoma cell lines as indicators of oncogenic change relevant to urothelial neoplastic progression. *Br. J. Cancer* **72**, 683-690.

**Rieger-Christ, K. M., Cain, J. W., Braasch, J. W., Dugan, J. M., Silverman, M. L., Bouyounes, B., Libertino, J. A. and Summerhayes, I. C. (2001).** Expression of classic cadherins type I in urothelial neoplastic progression. *Hum. Pathol.* **32**, 18-23.

**Rieger-Christ, K. M., Hanley, R., Lodowsky, C., Bernier, T., Vemulapalli, P., Roth, M., Kim, J., Yee, A. S., Le, S. M., Marie, P. J. et al. (2007).** The green tea compound, (-)-epigallocatechin-3-gallate downregulates N-cadherin and suppresses migration of bladder carcinoma cells. *J. Cell. Biochem.* [Epub ahead of print]

**Rieger-Christ, K. M., Lee, P., Zaghera, R., Kosakowski, M., Moinzadeh, A., Stoffel, J., Ben-Ze'ev, A., Libertino, J. A. and Summerhayes, I. C. (2004).** Novel expression of N-cadherin elicits in vitro bladder cell invasion via the akt signaling pathway. *Oncogene* **23**, 4745-4753.

**Rivat, C., De Wever, O., Bruyneel, E., Mareel, M., Gespach, C. and Attoub, S. (2004).** Disruption of STAT3 signaling leads to tumor cell invasion through alterations of homotypic cell-cell adhesion complexes. *Oncogene* **23**, 3317-3327.

**Rosen, D. G., Mercado-Uribe, I., Yang, G., Bast, R. C., Jr, Amin, H. M., Lai, R. and Liu, J. (2006).** The role of constitutively active signal transducer and activator of transcription 3 in ovarian tumorigenesis and prognosis. *Cancer* **107**, 2730-2740.

**Russo, G. L. (2007).** Ins and outs of dietary phytochemicals in cancer chemoprevention. *Biochem. Pharmacol.* [Epub ahead of print]

**Sachsenmaier, C., Sadowski, H. B. and Cooper, J. A. (1999).** STAT activation by the PDGF receptor requires juxtamembrane phosphorylation sites but not src tyrosine kinase activation. *Oncogene* **18**, 3583-3592.

**Saito, S., Hata, M., Fukuyama, R., Sakai, K., Kudoh, J., Tazaki, H. and Shimizu, N. (1997).** Screening of H-ras gene point mutations in 50 cases of bladder carcinoma. *Int. J. Urol.* **4**, 178-185.

**Sakamoto, E., Hato, F., Kato, T., Sakamoto, C., Akahori, M., Hino, M. and Kitagawa, S. (2005).** Type I and type II interferons delay human neutrophil apoptosis via activation of STAT3 and up-regulation of cellular inhibitor of apoptosis 2. *J. Leukoc. Biol.* **78**, 301-309.

**Sambrook J and Russell D.W. (2001).** *Molecular Cloning (Edition 3)*: Cold Spring Harbor Laboratory Press.

**Sartor, C. I., Dziubinski, M. L., Yu, C. L., Jove, R. and Ethier, S. P. (1997).** Role of epidermal growth factor receptor and STAT-3 activation in autonomous proliferation of SUM-102PT human breast cancer cells. *Cancer Res.* **57**, 978-987.

**Schaefer, L. K., Ren, Z., Fuller, G. N. and Schaefer, T. S. (2002).** Constitutive activation of Stat3alpha in brain tumors: Localization to tumor endothelial cells and activation by the endothelial tyrosine kinase receptor (VEGFR-2). *Oncogene* **21**, 2058-2065.

**Schatzmann, F., Marlow, R. and Streuli, C. H. (2003).** Integrin signaling and mammary cell function. *J. Mammary Gland Biol. Neoplasia* **8**, 395-408.

**Schindler, C. and Darnell, J. E., Jr. (1995).** Transcriptional responses to polypeptide ligands: The JAK-STAT pathway. *Annu. Rev. Biochem.* **64**, 621-651.

**Schindler, C., Shuai, K., Prezioso, V. R. and Darnell, J. E., Jr. (1992).** Interferon-dependent tyrosine phosphorylation of a latent cytoplasmic transcription factor. *Science* **257**, 809-813.

**Schwaller, J., Frantsve, J., Aster, J., Williams, I. R., Tomasson, M. H., Ross, T. S., Peeters, P., Van Rompaey, L., Van Etten, R. A., Ilaria, R., Jr et al. (1998).** Transformation of hematopoietic cell lines to growth-factor independence and induction of a fatal myelo- and lymphoproliferative disease in mice by retrovirally transduced TEL/JAK2 fusion genes. *EMBO J.* **17**, 5321-5333.

**Serra, S., Salahshor, S., Fagih, M., Niakosari, F., Radhi, J. M. and Chetty, R. (2007).** Nuclear expression of E-cadherin in solid pseudopapillary tumors of the pancreas. *JOP* **8**, 296-303.

**Shan, Y., Sun, C., Zhao, X., Wu, K., Cassidy, A. and Bao, Y. (2006).** Effect of sulforaphane on cell growth, G(0)/G(1) phase cell progression and apoptosis in human bladder cancer T24 cells. *Int. J. Oncol.* **29**, 883-888.

**Shankaran, V., Ikeda, H., Bruce, A. T., White, J. M., Swanson, P. E., Old, L. J. and Schreiber, R. D. (2001).** IFN $\gamma$  and lymphocytes prevent primary tumour development and shape tumour immunogenicity. *Nature* **410**, 1107-1111.

**Shapiro, G. I. (2006).** Cyclin-dependent kinase pathways as targets for cancer treatment. *J. Clin. Oncol.* **24**, 1770-1783.

**Shariat, S. F., Ashfaq, R., Sagalowsky, A. I. and Lotan, Y. (2006).** Correlation of cyclin D1 and E1 expression with bladder cancer presence, invasion, progression, and metastasis. *Hum. Pathol.* **37**, 1568-1576.

**Shariat, S. F., Ashfaq, R., Sagalowsky, A. I. and Lotan, Y. (2007a).** Predictive value of cell cycle biomarkers in nonmuscle invasive bladder transitional cell carcinoma. *J. Urol.* **177**, 481-7; discussion 487.

**Shariat, S. F., Zlotta, A. R., Ashfaq, R., Sagalowsky, A. I. and Lotan, Y. (2007b).** Cooperative effect of cell-cycle regulators expression on bladder cancer development and biologic aggressiveness. *Mod. Pathol.* **20**, 445-459.

**Shehata, M. F. (2005).** Rel/Nuclear factor-kappa B apoptosis pathways in human cervical cancer cells. *Cancer. Cell. Int.* **5**, 10-22.

**Shertzer, H. G. and Sainsbury, M. (1991).** Intrinsic acute toxicity and hepatic enzyme inducing properties of the chemoprotectants indole-3-carbinol and 5,10-dihydroindeno[1,2-b]indole in mice. *Food Chem. Toxicol.* **29**, 237-242.

**Shimoda, K., Feng, J., Murakami, H., Nagata, S., Watling, D., Rogers, N. C., Stark, G. R., Kerr, I. M. and Ihle, J. N. (1997).** Jak1 plays an essential role for receptor phosphorylation and stat activation in response to granulocyte colony-stimulating factor. *Blood* **90**, 597-604.

**Shimoda, K., van Deursen, J., Sangster, M. Y., Sarawar, S. R., Carson, R. T., Tripp, R. A., Chu, C., Quelle, F. W., Nosaka, T., Vignali, D. A. et al. (1996).** Lack of IL-4-induced Th2 response and IgE class switching in mice with disrupted Stat6 gene. *Nature* **380**, 630-633.

**Shimoyama, Y., Hirohashi, S., Hirano, S., Noguchi, M., Shimosato, Y., Takeichi, M. and Abe, O. (1989).** Cadherin cell-adhesion molecules in human epithelial tissues and carcinomas. *Cancer Res.* **49**, 2128-2133.

**Shuai, K., Halpern, J., ten Hoeve, J., Rao, X. and Sawyers, C. L. (1996).** Constitutive activation of STAT5 by the BCR-ABL oncogene in chronic myelogenous leukemia. *Oncogene* **13**, 247-254.

**Silver, D. L., Naora, H., Liu, J., Cheng, W. and Montell, D. J. (2004).** Activated signal transducer and activator of transcription (STAT) 3: Localization in focal adhesions and function in ovarian cancer cell motility. *Cancer Res.* **64**, 3550-3558.

**Singh, A. V., Franke, A. A., Blackburn, G. L. and Zhou, J. R. (2006).** Soy phytochemicals prevent orthotopic growth and metastasis of bladder cancer in mice by alterations of cancer cell proliferation and apoptosis and tumor angiogenesis. *Cancer Res.* **66**, 1851-1858.

**Smith, P. D. and Crompton, M. R. (1998).** Expression of v-src in mammary epithelial cells induces transcription via STAT3. *Biochem. J.* **331 ( Pt 2)**, 381-385.

**Spruck, C. H., 3rd, Ohneseit, P. F., Gonzalez-Zulueta, M., Esrig, D., Miyao, N., Tsai, Y. C., Lerner, S. P., Schmutte, C., Yang, A. S. and Cote, R. (1994).** Two molecular pathways to transitional cell carcinoma of the bladder. *Cancer Res.* **54**, 784-788.

**Srivastava, B. and Shukla, Y. (1998).** Antitumour promoting activity of indole-3-carbinol in mouse skin carcinogenesis. *Cancer Lett.* **134**, 91-95.

**Stoner, G., Casto, B., Ralston, S., Roebuck, B., Pereira, C. and Bailey, G. (2002).** Development of a multi-organ rat model for evaluating chemopreventive agents: Efficacy of indole-3-carbinol. *Carcinogenesis* **23**, 265-272.

**Su, L. and David, M. (2000).** Distinct mechanisms of STAT phosphorylation via the interferon-alpha/beta receptor. selective inhibition of STAT3 and STAT5 by piceatannol. *J. Biol. Chem.* **275**, 12661-12666.

**Sun, W. and Herrera, G. A. (2004).** E-cadherin expression in invasive urothelial carcinoma. *Ann. Diagn. Pathol.* **8**, 17-22.

**Surh, Y. J. (2003).** Cancer chemoprevention with dietary phytochemicals. *Nat. Rev. Cancer.* **3**, 768-780.

**Suzuki, A., Hayashida, M., Ito, T., Kawano, H., Nakano, T., Miura, M., Akahane, K. and Shiraki, K. (2000).** Survivin initiates cell cycle entry by the competitive interaction with Cdk4/p16(INK4a) and Cdk2/cyclin E complex activation. *Oncogene* **19**, 3225-3234.

**Syrigos, K. N., Harrington, K., Waxman, J., Krausz, T. and Pignatelli, M. (1998).** Altered gamma-catenin expression correlates with poor survival in patients with bladder cancer. *J. Urol.* **160**, 1889-1893.

**Szekely, E., Torok, V., Szekely, T., Riesz, P. and Romics, I. (2006).** E-cadherin expression in transitional cell carcinomas. *Pathol. Oncol. Res.* **12**, 73-77.

**Tadi, K., Chang, Y., Ashok, B. T., Chen, Y., Moscatello, A., Schaefer, S. D., Schantz, S. P., Policastro, A. J., Geliebter, J. and Tiwari, R. K. (2005).** 3,3'-diindolylmethane, a cruciferous vegetable derived synthetic anti-proliferative compound in thyroid disease. *Biochem. Biophys. Res. Commun.* **337**, 1019-1025.

**Takada, Y., Andreeff, M. and Aggarwal, B. B. (2005).** Indole-3-carbinol suppresses NF-kappaB and I kappa Balpha kinase activation, causing inhibition of expression of NF-kappaB-regulated antiapoptotic and metastatic gene products and enhancement of apoptosis in myeloid and leukemia cells. *Blood* **106**, 641-649.

**Takeda, K., Clausen, B. E., Kaisho, T., Tsujimura, T., Terada, N., Forster, I. and Akira, S. (1999).** Enhanced Th1 activity and development of chronic enterocolitis in mice devoid of Stat3 in macrophages and neutrophils. *Immunity* **10**, 39-49.

**Takeda, K., Kaisho, T., Yoshida, N., Takeda, J., Kishimoto, T. and Akira, S. (1998).** Stat3 activation is responsible for IL-6-dependent T cell proliferation through preventing apoptosis: Generation and characterization of T cell-specific Stat3-deficient mice. *J. Immunol.* **161**, 4652-4660.

**Takeda, K., Noguchi, K., Shi, W., Tanaka, T., Matsumoto, M., Yoshida, N., Kishimoto, T. and Akira, S. (1997).** Targeted disruption of the mouse Stat3 gene leads to early embryonic lethality. *Proc. Natl. Acad. Sci. U. S. A.* **94**, 3801-3804.

**Thomson, C. A., Rock, C. L., Caan, B. J., Flatt, S. W., Al-Delaimy, W. A., Newman, V. A., Hajek, R. A., Chilton, J. A. and Pierce, J. P. (2007).** Increase in cruciferous vegetable intake in women previously treated for breast cancer participating in a dietary intervention trial. *Nutr. Cancer* **57**, 11-19.

**Tong, Q. S., Zheng, L. D., Lu, P., Jiang, F. C., Chen, F. M., Zeng, F. Q., Wang, L. and Dong, J. H. (2006).** Apoptosis-inducing effects of curcumin derivatives in human bladder cancer cells. *Anticancer Drugs* **17**, 279-287.

**Townsend, P. A., Scarabelli, T. M., Davidson, S. M., Knight, R. A., Latchman, D. S. and Stephanou, A. (2004).** STAT-1 interacts with p53 to enhance DNA damage-induced apoptosis. *J. Biol. Chem.* **279**, 5811-5820.

**Trovato, M., Grosso, M., Vitarelli, E., Ruggeri, R. M., Alesci, S., Trimarchi, F., Barresi, G. and Benvenga, S. (2003).** Distinctive expression of STAT3 in papillary thyroid carcinomas and a subset of follicular adenomas. *Histol. Histopathol.* **18**, 393-399.

**Tsugane, S. and Sasazuki, S. (2007).** Diet and the risk of gastric cancer: Review of epidemiological evidence. *Gastric Cancer.* **10**, 75-83.

**Turkson, J., Bowman, T., Garcia, R., Caldenhoven, E., De Groot, R. P. and Jove, R. (1998).** Stat3 activation by src induces specific gene regulation and is required for cell transformation. *Mol. Cell. Biol.* **18**, 2545-2552.

**Turkson, J. and Jove, R. (2000).** STAT proteins: Novel molecular targets for cancer drug discovery. *Oncogene* **19**, 6613-6626.

**Turkson, J., Ryan, D., Kim, J. S., Zhang, Y., Chen, Z., Haura, E., Laudano, A., Sebt, S., Hamilton, A. D. and Jove, R. (2001).** Phosphotyrosyl peptides block Stat3-mediated DNA binding activity, gene regulation, and cell transformation. *J. Biol. Chem.* **276**, 45443-45455.

**Tyagi, A., Agarwal, C., Harrison, G., Glode, L. M. and Agarwal, R. (2004).** Silibinin causes cell cycle arrest and apoptosis in human bladder transitional cell carcinoma cells by regulating CDKI-CDK-cyclin cascade, and caspase 3 and PARP cleavages. *Carcinogenesis* **25**, 1711-1720.

**Udy, G. B., Towers, R. P., Snell, R. G., Wilkins, R. J., Park, S. H., Ram, P. A., Waxman, D. J. and Davey, H. W. (1997).** Requirement of STAT5b for sexual dimorphism of body growth rates and liver gene expression. *Proc. Natl. Acad. Sci. U. S. A.* **94**, 7239-7244.

**Vageli, D., Kiaris, H., Delakas, D., Anezinis, P., Cranidis, A. and Spandidos, D. A. (1996).** Transcriptional activation of H-ras, K-ras and N-ras proto-oncogenes in human bladder tumors. *Cancer Lett.* **107**, 241-247.

**van der Heijden, A. G., Jansen, C. F., Verhaegh, G., O'donnell, M. A., Schalken, J. A. and Witjes, J. A. (2004).** The effect of hyperthermia on mitomycin-C induced cytotoxicity in four human bladder cancer cell lines. *Eur. Urol.* **46**, 670-674.

**van Rhijn, B. W., van der Kwast, T. H., Vis, A. N., Kirkels, W. J., Boeve, E. R., Jobsis, A. C. and Zwarthoff, E. C. (2004).** FGFR3 and P53 characterize alternative genetic pathways in the pathogenesis of urothelial cell carcinoma. *Cancer Res.* **64**, 1911-1914.

**Vanderlaag, K., Samudio, I., Burghardt, R., Barhoumi, R. and Safe, S. (2006).** Inhibition of breast cancer cell growth and induction of cell death by 1,1-bis(3'-indolyl)methane (DIM) and 5,5'-dibromoDIM. *Cancer Lett.* **236**, 198-212.

**Vandewalle, C., Comijn, J., De Craene, B., Vermassen, P., Bruyneel, E., Andersen, H., Tulchinsky, E., Van Roy, F. and Berx, G. (2005).** SIP1/ZEB2 induces EMT by repressing genes of different epithelial cell-cell junctions. *Nucleic Acids Res.* **33**, 6566-6578.

**Veikkola, T., Karkkainen, M., Claesson-Welsh, L. and Alitalo, K. (2000).** Regulation of angiogenesis via vascular endothelial growth factor receptors. *Cancer Res.* **60**, 203-212.

**Verhoeven, D. T., Verhagen, H., Goldbohm, R. A., van den Brandt, P. A. and van Poppel, G. (1997).** A review of mechanisms underlying anticarcinogenicity by brassica vegetables. *Chem. Biol. Interact.* **103**, 79-129.

**Vermes, I., Haanen, C., Steffens-Nakken, H. and Reutelingsperger, C. (1995).** A novel assay for apoptosis. flow cytometric detection of phosphatidylserine expression on early apoptotic cells using fluorescein labelled annexin V. *J. Immunol. Methods* **184**, 39-51.

**Vermeulen, K., Van Bockstaele, D. R. and Berneman, Z. N. (2003).** The cell cycle: A review of regulation, deregulation and therapeutic targets in cancer. *Cell Prolif.* **36**, 131-149.

**Wahl, J. K., 3rd, Kim, Y. J., Cullen, J. M., Johnson, K. R. and Wheelock, M. J. (2003).** N-cadherin-catenin complexes form prior to cleavage of the proregion and transport to the plasma membrane. *J. Biol. Chem.* **278**, 17269-17276.

**Walz, C., Crowley, B. J., Hudon, H. E., Gramlich, J. L., Neuberger, D. S., Podar, K., Griffin, J. D. and Sattler, M. (2006).** Activated Jak2 with the V617F point mutation promotes G1/S phase transition. *J. Biol. Chem.* **281**, 18177-18183.

**Wang, T., Niu, G., Kortylewski, M., Burdelya, L., Shain, K., Zhang, S., Bhattacharya, R., Gabrilovich, D., Heller, R., Coppola, D. et al. (2004).** Regulation of the innate and adaptive immune responses by stat-3 signaling in tumor cells. *Nat. Med.* **10**, 48-54.

**Wargovich, M. J., Chen, C. D., Jimenez, A., Steele, V. E., Velasco, M., Stephens, L. C., Price, R., Gray, K. and Kelloff, G. J. (1996).** Aberrant crypts as a biomarker for colon cancer: Evaluation of potential chemopreventive agents in the rat. *Cancer Epidemiol. Biomarkers Prev.* **5**, 355-360.

**Watson, C. J. and Miller, W. R. (1995).** Elevated levels of members of the STAT family of transcription factors in breast carcinoma nuclear extracts. *Br. J. Cancer* **71**, 840-844.

**Weber-Nordt, R. M., Egen, C., Wehinger, J., Ludwig, W., Gouilleux-Gruart, V., Mertelsmann, R. and Finke, J. (1996).** Constitutive activation of STAT proteins in primary lymphoid and myeloid leukemia cells and in Epstein-Barr virus (EBV)-related lymphoma cell lines. *Blood* **88**, 809-816.

**Welte, T., Zhang, S. S., Wang, T., Zhang, Z., Hesslein, D. G., Yin, Z., Kano, A., Iwamoto, Y., Li, E., Craft, J. E. et al. (2003).** STAT3 deletion during hematopoiesis causes Crohn's disease-like pathogenesis and lethality: A critical role of STAT3 in innate immunity. *Proc. Natl. Acad. Sci. U. S. A.* **100**, 1879-1884.

**Wen, Z., Zhong, Z. and Darnell, J. E., Jr.** (1995). Maximal activation of transcription by Stat1 and Stat3 requires both tyrosine and serine phosphorylation. *Cell* **82**, 241-250.

**Williams, S. G. and Stein, J. P.** (2004). Molecular pathways in bladder cancer. *Urol. Res.* **32**, 373-385.

**Wolff, E. M., Liang, G. and Jones, P. A.** (2005). Mechanisms of disease: Genetic and epigenetic alterations that drive bladder cancer. *Nat. Clin. Pract. Urol.* **2**, 502-510.

**Xie, B., Zhao, J., Kitagawa, M., Durbin, J., Madri, J. A., Guan, J. L. and Fu, X. Y.** (2001). Focal adhesion kinase activates Stat1 in integrin-mediated cell migration and adhesion. *J. Biol. Chem.* **276**, 19512-19523.

**Xu, M., Bailey, A. C., Hernaez, J. F., Taoka, C. R., Schut, H. A. and Dashwood, R. H.** (1996). Protection by green tea, black tea, and indole-3-carbinol against 2-amino-3-methylimidazo[4,5-f]quinoline-induced DNA adducts and colonic aberrant crypts in the F344 rat. *Carcinogenesis* **17**, 1429-1434.

**Yahata, Y., Shirakata, Y., Tokumaru, S., Yamasaki, K., Sayama, K., Hanakawa, Y., Detmar, M. and Hashimoto, K.** (2003). Nuclear translocation of phosphorylated STAT3 is essential for vascular endothelial growth factor-induced human dermal microvascular endothelial cell migration and tube formation. *J. Biol. Chem.* **278**, 40026-40031.

**Yakata, Y., Nakayama, T., Yoshizaki, A., Kusaba, T., Inoue, K. and Sekine, I.** (2007). Expression of p-STAT3 in human gastric carcinoma: Significant correlation in tumour invasion and prognosis. *Int. J. Oncol.* **30**, 437-442.

**Yano, H., Mazaki, Y., Kurokawa, K., Hanks, S. K., Matsuda, M. and Sabe, H.** (2004). Roles played by a subset of integrin signaling molecules in cadherin-based cell-cell adhesion. *J. Cell Biol.* **166**, 283-295.

**Yu, C. L., Jove, R. and Burakoff, S. J.** (1997). Constitutive activation of the janus kinase-STAT pathway in T lymphoma overexpressing the lck protein tyrosine kinase. *J. Immunol.* **159**, 5206-5210.

**Yu, H. and Jove, R.** (2004). The STATs of cancer--new molecular targets come of age. *Nat. Rev. Cancer.* **4**, 97-105.

**Zamir, E. and Geiger, B.** (2001). Molecular complexity and dynamics of cell-matrix adhesions. *J. Cell. Sci.* **114**, 3583-3590.

**Zhang, J., Hsu, B. A. J. C., Kinseth, B. A. M. A., Bjeldanes, L. F. and Firestone, G. L.** (2003). Indole-3-carbinol induces a G1 cell cycle arrest and inhibits prostate-specific antigen production in human LNCaP prostate carcinoma cells. *Cancer* **98**, 2511-2520.

**Zhang, Y., Turkson, J., Carter-Su, C., Smithgall, T., Levitzki, A., Kraker, A., Krolewski, J. J., Medveczky, P. and Jove, R.** (2000). Activation of Stat3 in v-src-transformed fibroblasts requires cooperation of Jak1 kinase activity. *J. Biol. Chem.* **275**, 24935-24944.

**Zhivotovsky, B., Samali, A., Gahm, A. and Orrenius, S.** (1999). Caspases: Their intracellular localization and translocation during apoptosis. *Cell Death Differ.* **6**, 644-651.

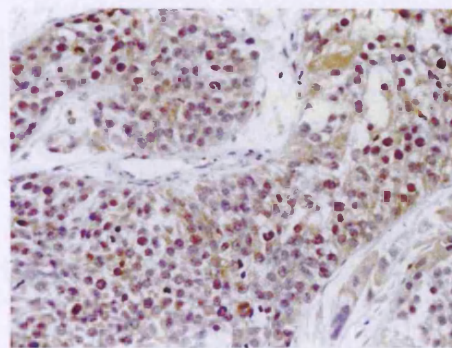
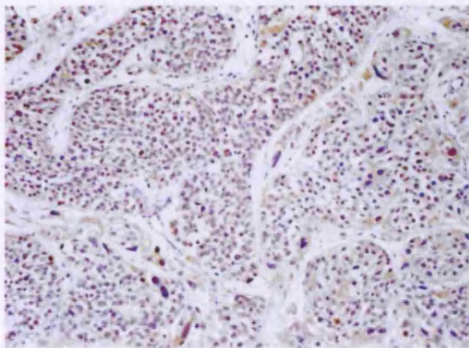
**Zushi, S., Shinomura, Y., Kiyohara, T., Miyazaki, Y., Kondo, S., Sugimachi, M., Higashimoto, Y., Kanayama, S. and Matsuzawa, Y.** (1998). STAT3 mediates the survival signal in oncogenic ras-transfected intestinal epithelial cells. *Int. J. Cancer* **78**, 326-330.

## **APPENDICES**

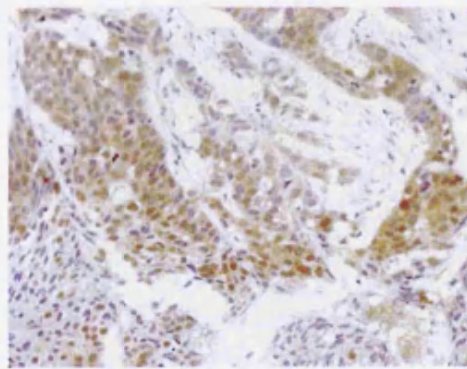
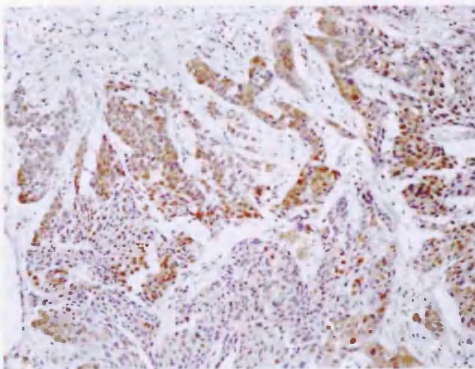
### ***Appendix 1 Immunohistochemistry of bladder cancers***

Further experiments of IHC of superficial and muscle invasive tumours are presented. Images in the left hand column were photographed using a x20 microscope lens. An enlarged area photographed using a x40 lens lens is shown in the right hand column.

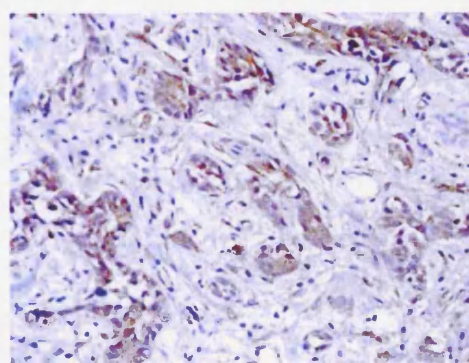
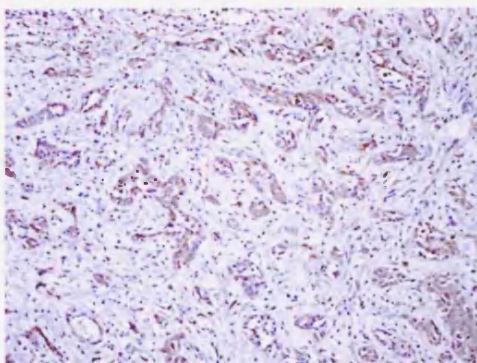
#### **Superficial bladder tumours**



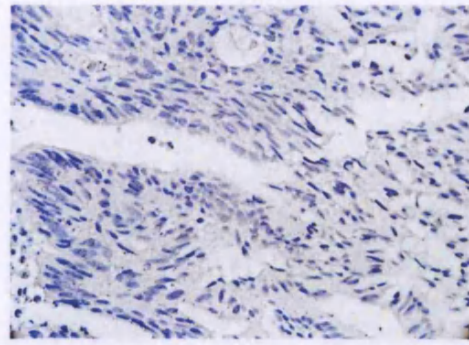
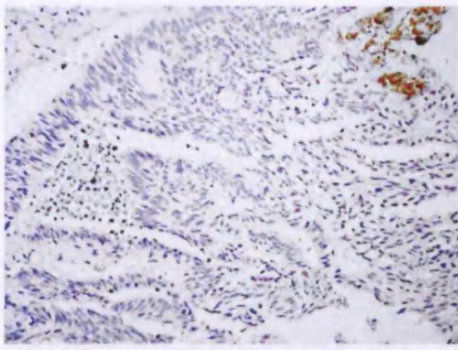
Cytoplasmic and some nuclear STAT3 (Block 1)



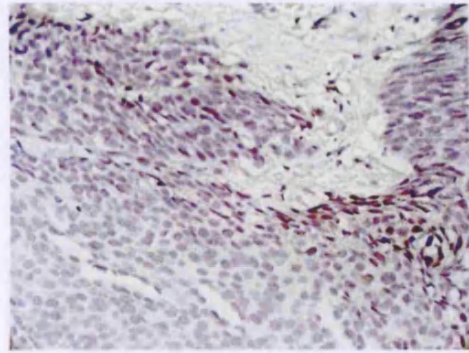
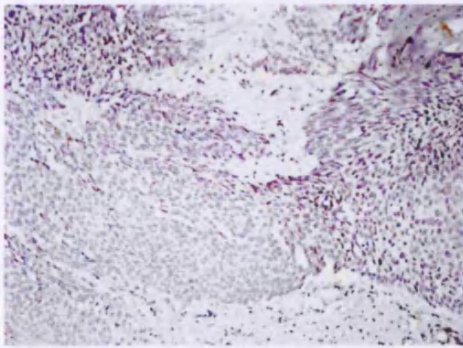
Cytoplasmic and nuclear STAT3 (Block 2)



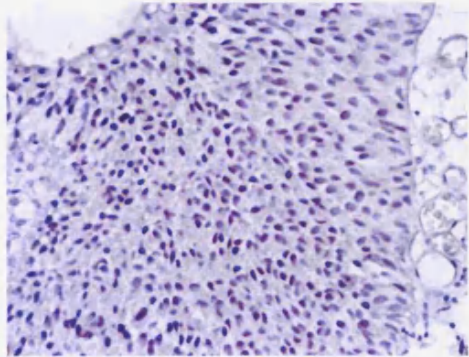
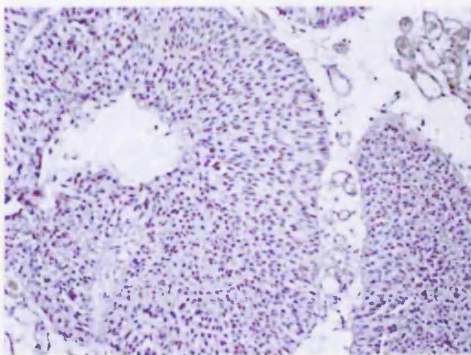
Cytoplasmic STAT3 (Block 3)



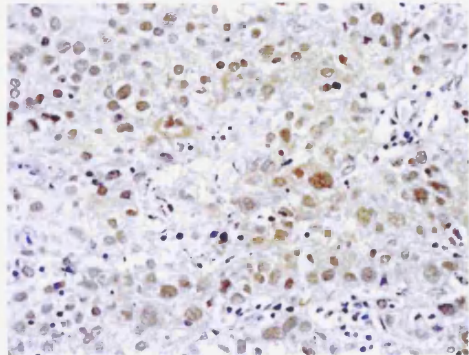
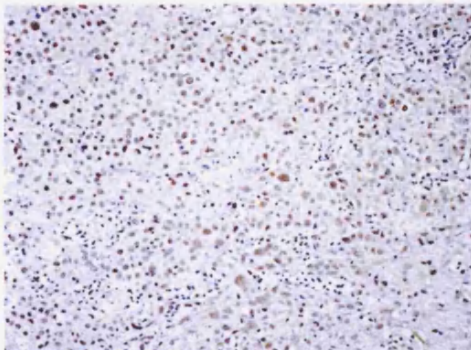
Negative for pSTAT3 (Block 7)



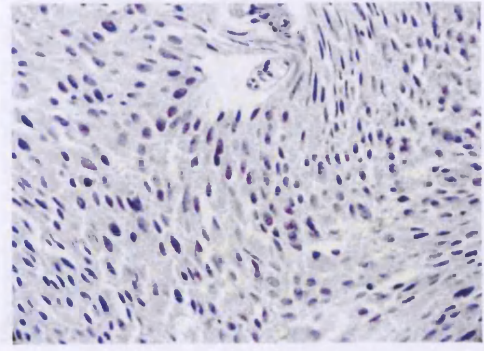
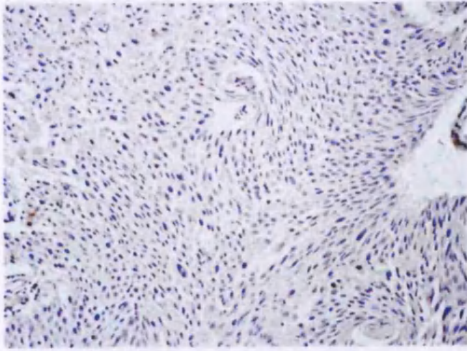
Negative for pSTAT3 (Block 2)



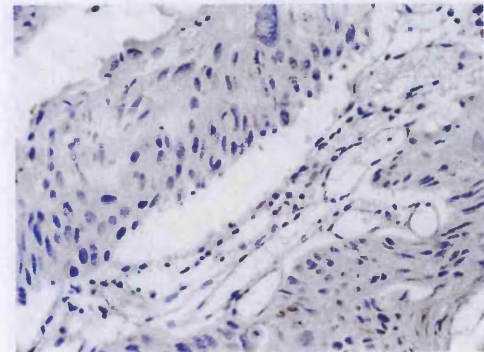
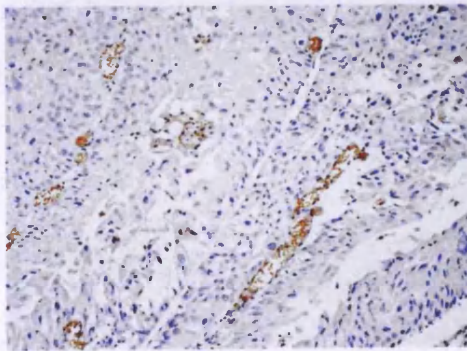
Negative for STAT5a (Block 8)



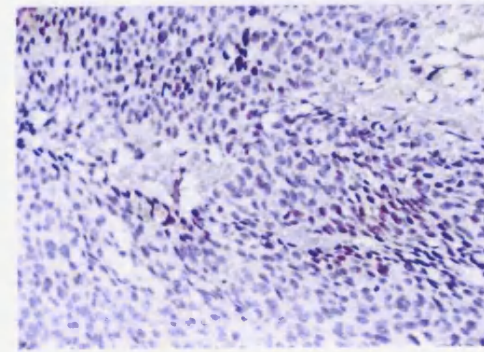
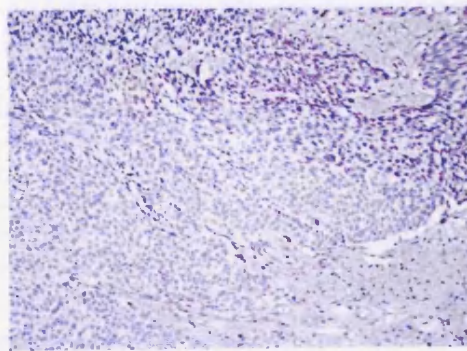
Cytoplasmic and nuclear STAT5b (Block 6)



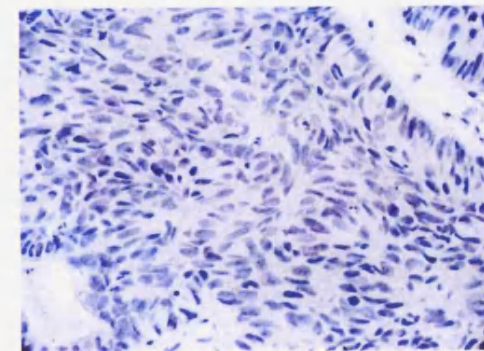
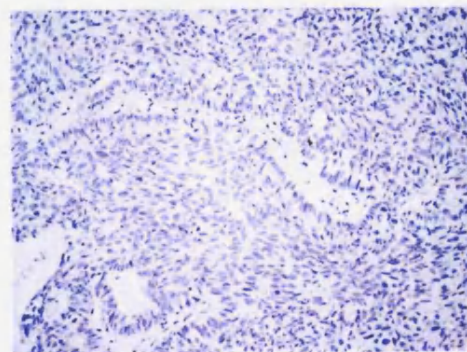
Negative for pSTAT5 (Block 9)



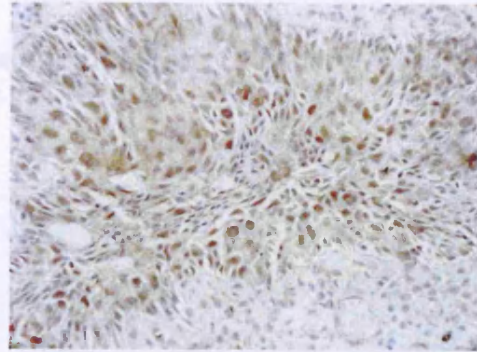
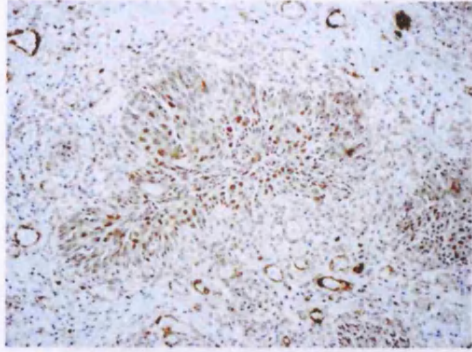
Negative for STAT1 (Block 9)



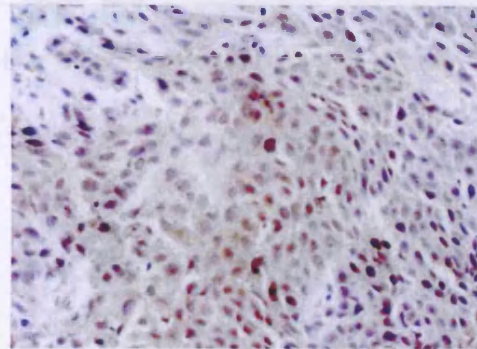
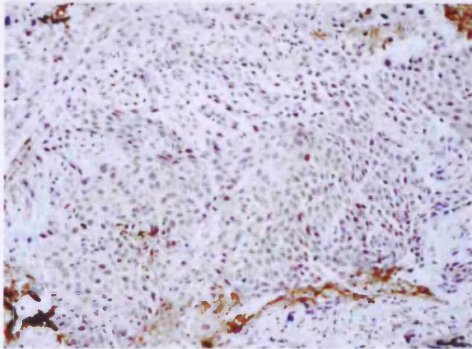
Negative for pSTAT1 (Block 2)



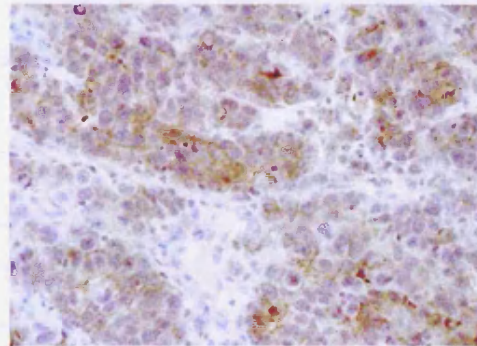
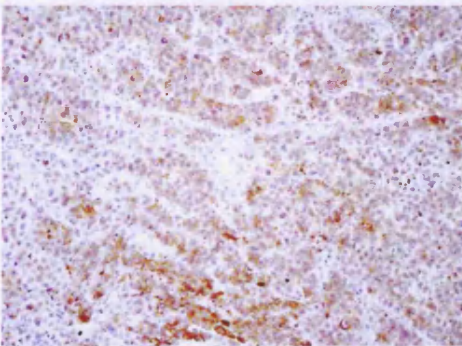
Negative for pSTAT1 (Block 7)



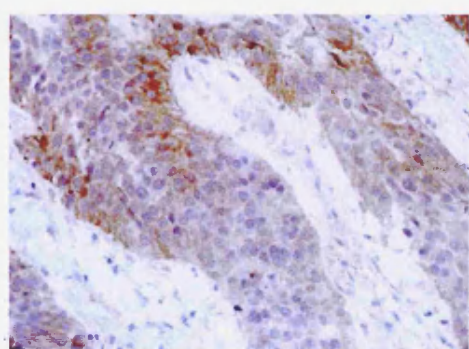
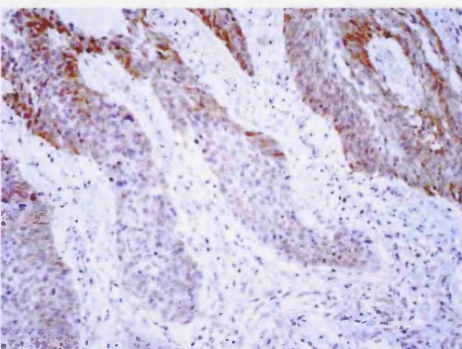
Nuclear N-cadherin (Block 3)



Nuclear N-cadherin (Block 2)

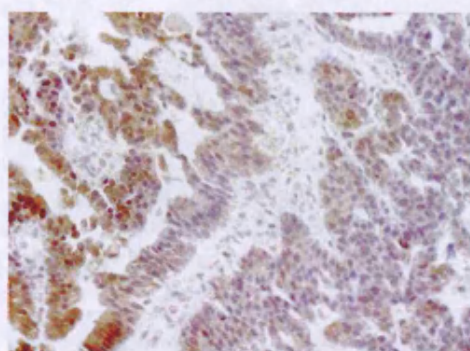
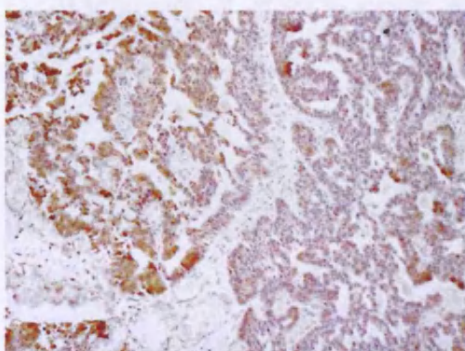


Cytoplasmic and membranous P-cadherin (Block 4)

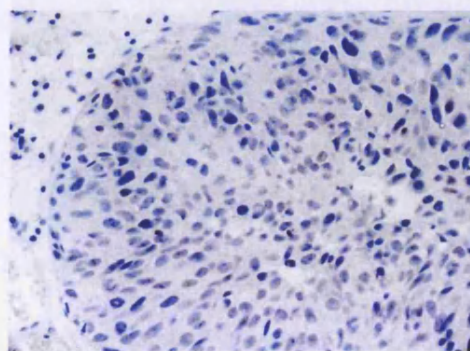
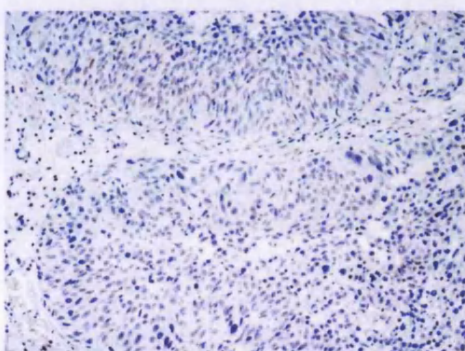


Membranous P-cadherin (Block 5)

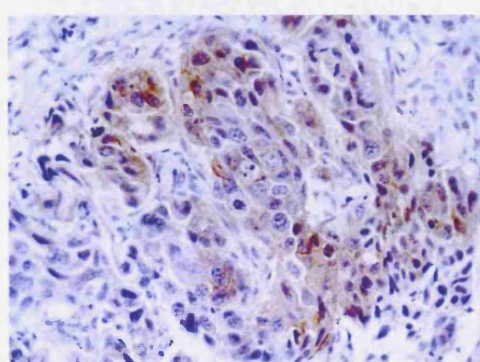
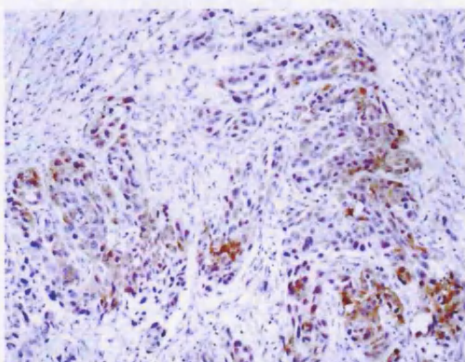
### Muscle invasive bladder tumours



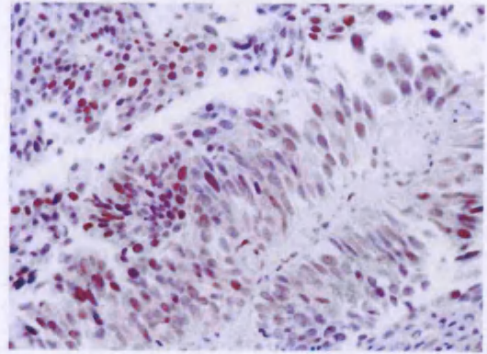
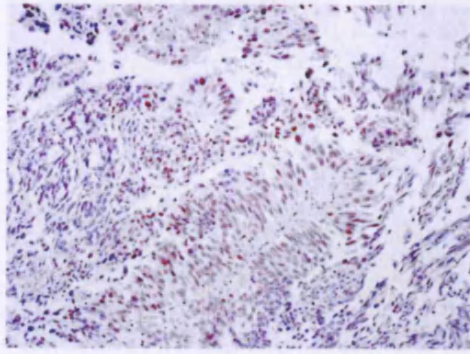
Cytoplasmic and occasional nuclear STAT3 (Block 14)



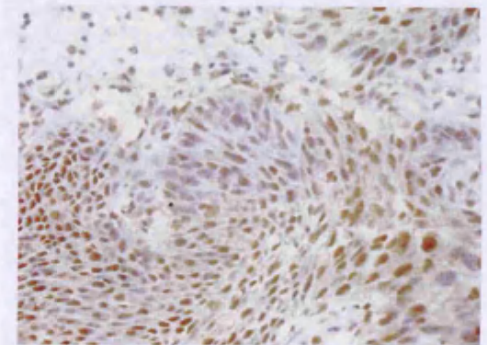
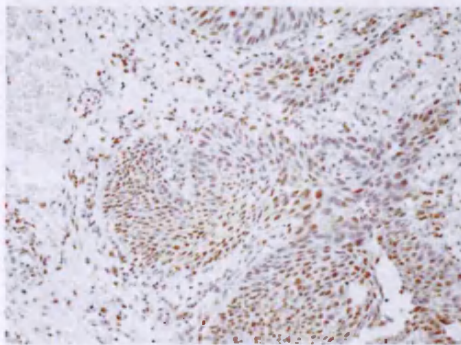
Negative for pSTAT3 (Block 2)



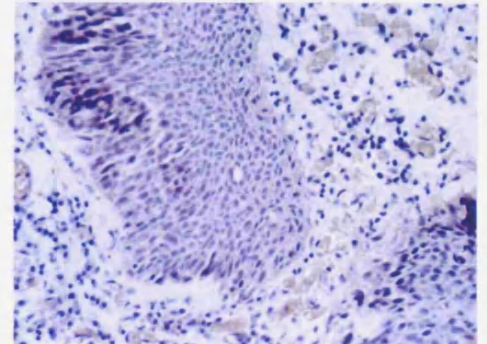
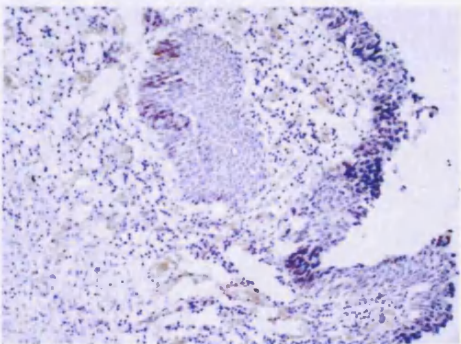
Membranous pSTAT3 (Block 5)



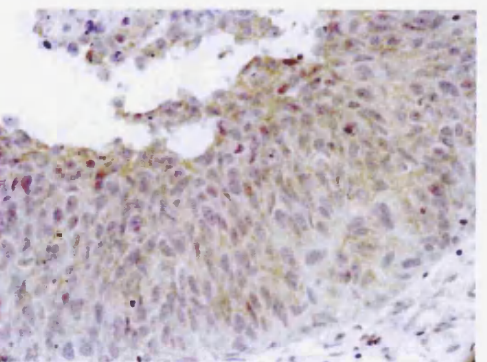
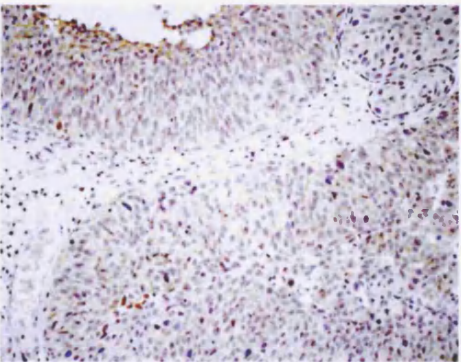
Patchy nuclear pSTAT3 (Block 14)



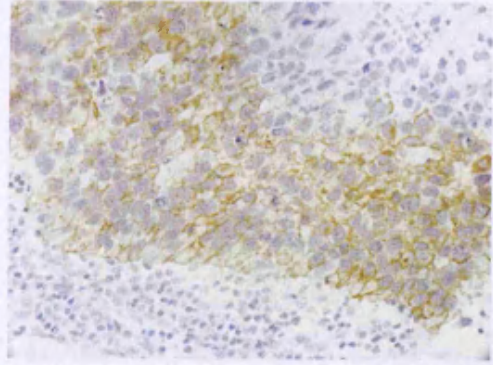
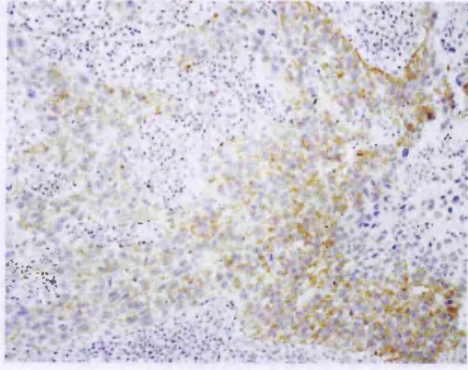
Nuclear STAT5a (Block 3)



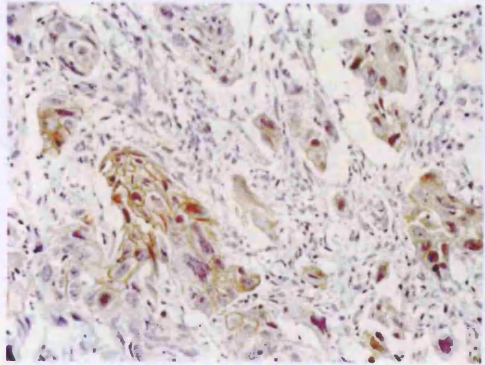
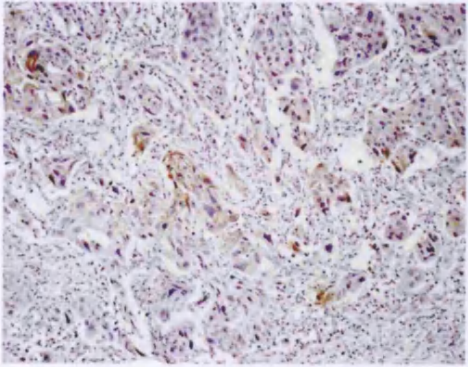
Negative for pSTAT5 (Block 14)



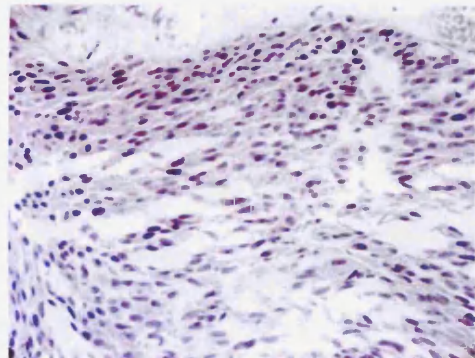
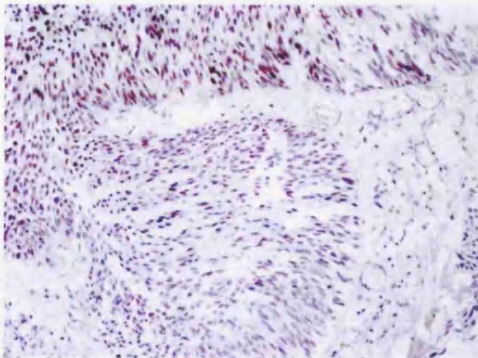
Membranous pSTAT5 (Block 2)



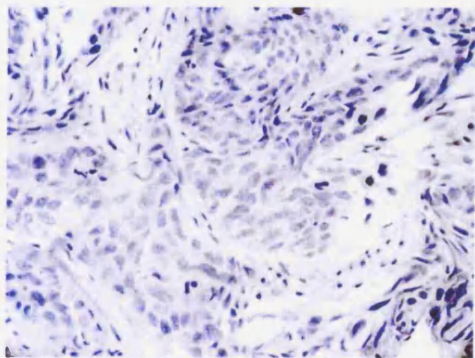
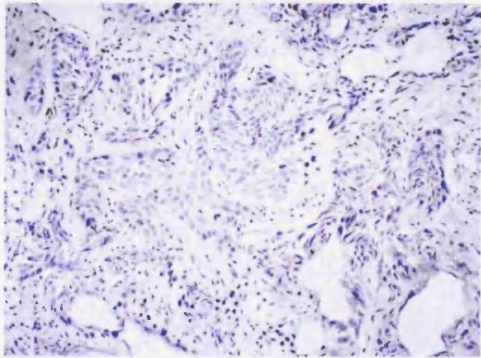
Membranous pSTAT5 (Block 4)



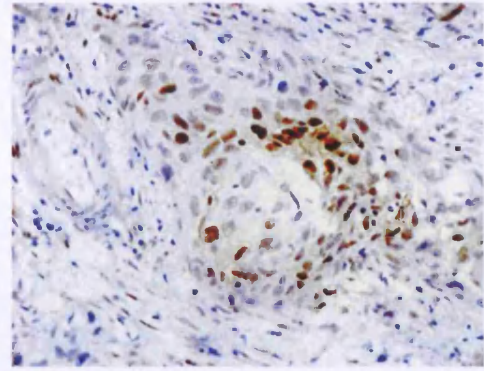
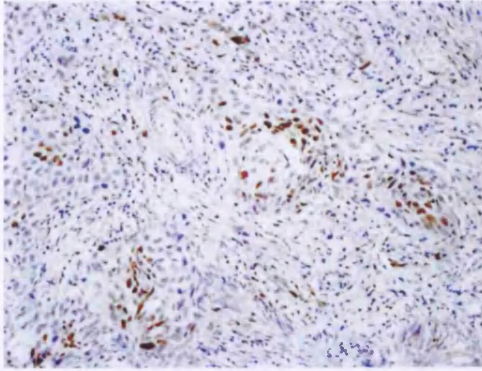
Membranous and nuclear pSTAT5 (Block 5)



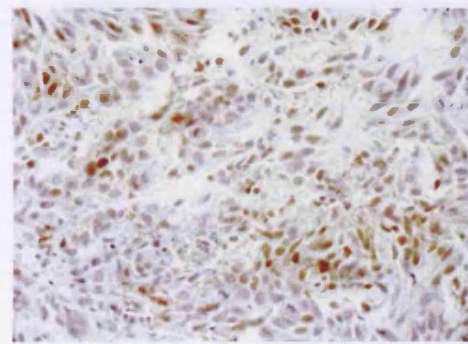
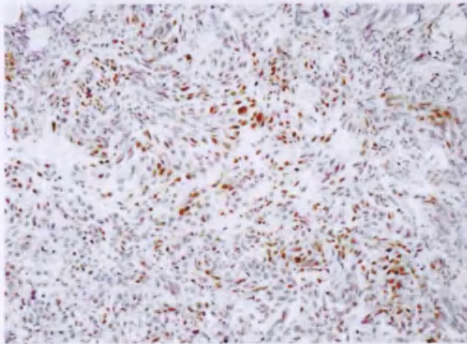
Negative for pSTAT1 (Block 7)



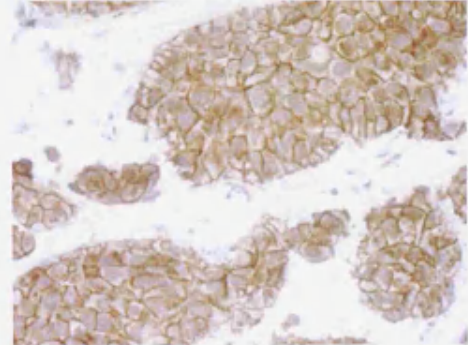
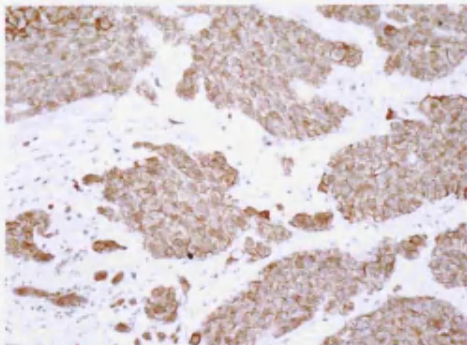
Negative for pSTAT1 (Block 13)



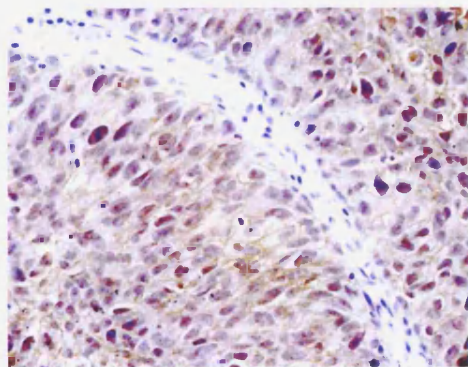
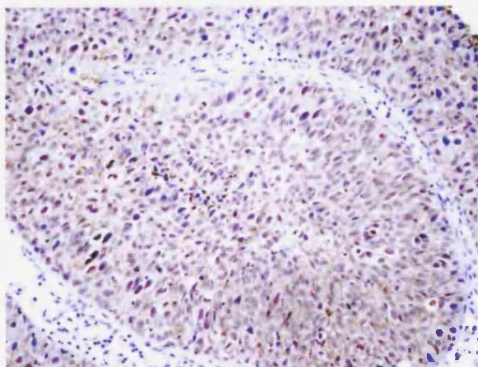
Pathcy nuclear pSTAT1 (Block 2)



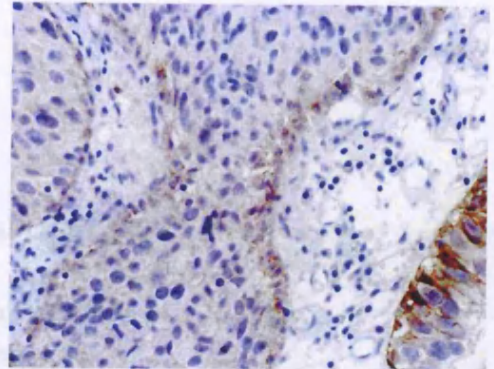
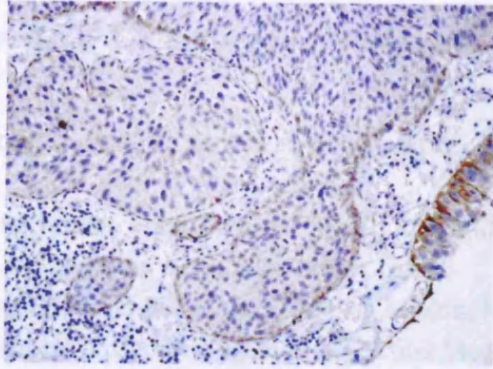
Nuclear pSTAT1 (Block 16)



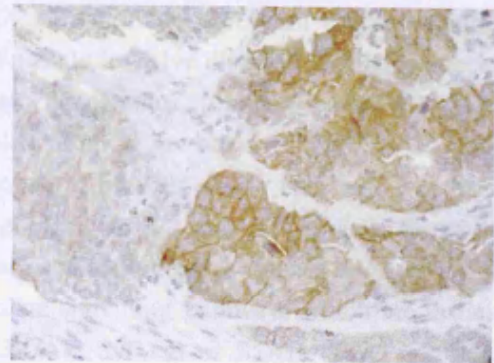
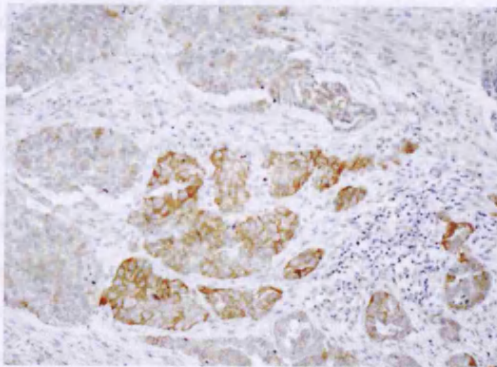
Membranous E-cadherin (Block 10)



Membranous E-cadherin (Block 2)



Occasional membranous P-cadherin (Block 2)



Membranous P-cadherin (Block 13)

## ***Appendix 2 Meeting presentation***

Abstract AACR annual meeting, April 2007

### **Indoles induce apoptosis and modify upregulated signal transducers and activators of transcription (STAT) signalling in bladder cancer cells**

Yiyang Sun, Mai-Kim Cheng, J Kilian Mellon, Marina Kriaievska, Margaret M Manson

Department of Cancer Studies & Molecular Medicine, Leicester University, UK

Bladder cancer is one of the most common cancers in the UK. Most cases (~90%) present as transitional cell carcinoma, of which ~75% are superficial tumours. Approximately 60% of those patients with invasive disease develop metastases. Current treatment of muscle-invasive disease has limited success, so new therapies are of crucial importance. The dietary molecules, indole-3-carbinol (I3C) and diindolylmethane (DIM), derived from cruciferous vegetables, promote growth arrest and induce apoptosis in different cancer cell lines. Their role in repressing growth of bladder cancer cell lines was therefore examined. I3C ( $\geq 100 \mu\text{M}$ ) or DIM ( $\geq 50 \mu\text{M}$ ) induced apoptosis in J82 and RT112 cells by 48 hours, determined by annexin V staining and supported by other assays (increased caspase 3/7 activity, PARP cleavage and Hoechst nuclear staining). Indoles can modulate signalling pathways which are critical for tumour cell survival, such as those involving MAPK, PI3K/Akt, NF- $\kappa$ B or STATs. STAT transcription factors are aberrantly activated in a number of human tumours and cancer cell lines, but have not been studied in bladder cancer. Bladder cancer cell lines of epithelial (RT112, RT4, HT1376) or mesenchymal (J82, T24, UMUC3) phenotype were screened for STAT expression. The three epithelial lines, which are E-cadherin<sup>+</sup>, have constitutive activation of STAT5, while the three mesenchymal lines (E-cadherin<sup>-</sup>) have activated STAT3. In all six lines total STAT1, 3 and 5b were expressed at similar levels. DIM-induced apoptosis in J82 cells was accompanied by downregulation of STAT1, 5a and 5b and inhibition of phospho-STAT1 and phospho-STAT3. Upregulation of phospho-STAT5 was observed when DIM was added at concentrations of 10 or 50  $\mu\text{M}$ . In RT112 cells, DIM inhibited STAT5b and phospho-STAT5, but had no effect on STAT3. Downregulation of STAT3 in J82 cells with siRNA was accompanied by upregulation of phospho-STAT1 and did not induce apoptosis. In patient tissues we observed STAT3 and STAT5 staining in normal bladder epithelium, while expression of the phosphorylated proteins was essentially absent. On the other hand, 9 out of 13 muscle invasive tumours contained nuclear phospho-STAT3, while one had nuclear phospho-STAT5 suggesting that STAT3 is likely to be implicated in bladder cancer. In conclusion, nuclear phospho-STAT3 is present in some human bladder tumours, but not in normal epithelium. Indoles induce apoptosis in bladder cancer cell lines of different phenotype, with concomitant downregulation of STATs and phospho-STATs. The role of STAT proteins in bladder tumour cells and the mechanism of indole-induced apoptosis are now the focus of our studies.

This work was supported by the UK MRC

# DIM induces apoptosis and modifies upregulated STAT signalling in bladder cancer cells



Yiyang Sun, Mai-Kim Cheng, J Kilian Mellon, Marina Kriajevska, Margaret M Manson  
Department of Cancer Studies & Molecular Medicine, Leicester University, UK



## Introduction

Bladder cancer is a relatively common cancer in the UK. Most cases (~90%) present as transitional cell carcinoma, of which ~75% are superficial tumours. Approximately 60% of those patients with invasive disease develop metastases. Current treatment of muscle-invasive disease has limited success, so new therapies are of crucial importance. The dietary molecule, diindolylmethane (DIM), derived from cruciferous vegetables, promotes growth arrest and induces apoptosis in different cancer cell lines. DIM can modulate signalling pathways which are critical for tumour cell survival, such as those involving MAPK, PI3K/Akt, NF- $\kappa$ B or STATs. STAT transcription factors are aberrantly activated in a number of human tumours and cancer cell lines, but have not been studied in bladder cancer.



## Aims

To investigate 1) STATs signalling in bladder cancer, 2) the effect of DIM in bladder cell lines, and further explore the link between STATs and the effect of DIM in human bladder cancer cells.

## Results 1 Expression of STAT3 & 5 in human bladder tumours

Staining for STAT3 and stronger staining for STAT5 was observed in normal bladder epithelium. However, expression of phosphorylated proteins was essentially absent. In contrast, 11 out of 15 tumours had nuclear staining for phosphoSTAT3, while one had nuclear phosphoSTAT5, which suggests that activated STAT3 in particular was expressed in a significant proportion of bladder tumours.

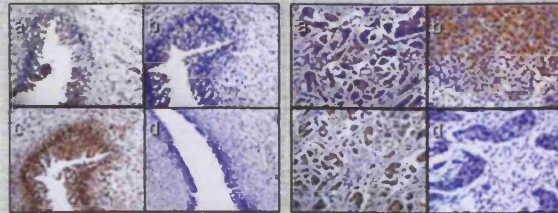


Fig.1 Representative immunohistochemistry staining of STATs expression in (1) human normal bladder tissues and (2) human muscle-invasive bladder tumours. (a) STAT3; (b) pSTAT3; (c) STAT5b; (d) pSTAT5 (a&b)

## Results 2 STATs expression in human bladder cancer cells

Six bladder cancer cell lines of epithelial (RT4, RT112, HT1376) or mesenchymal (J82, T24, UMUC3) phenotype were screened for STAT expression. The three epithelial lines expressed phosphorylated STAT5, while the three mesenchymal lines expressed phosphorylated STAT3. In all six cell lines, total STAT1, 3, 5 were expressed at similar levels (Fig.2).



Fig.2 STATs expression in a panel of human bladder cancer cell lines. All six cell lines express similar low level of phosphorylated STAT1 (data not shown).

## Results 3 Modification of STATs expression by DIM in human bladder cancer cells

In J82 cells, downregulation of phosphoSTAT3 was detected following DIM treatment with a concentration as low as 20 $\mu$ M at 16 hours (Fig.3). This effect was dose and time-dependent. Furthermore, inhibition of phosphoSTAT3 in J82 and phosphoSTAT5 in RT112 cells, and downregulation of STAT1 and STAT5 were observed after a 48 hour DIM treatment (Fig.4).

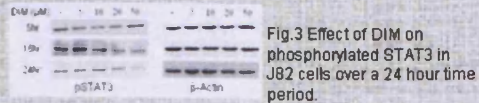


Fig.3 Effect of DIM on phosphorylated STAT3 in J82 cells over a 24 hour time period.

